(NASA-TM-78226) DEVELOPMENT OF MINING GUIDANCE AND CONTROL SYSTEMS Annual Report, Oct. 1976 - Sep. 1977 (NASA) 225 p
HC A10/MF A01 CSCL 08I

N80-13601

Unclas
G3/43 46235

DOE/NASA TECHNICAL MEMORANDUM

DOE/NASA TM-78226

May 1979

DEVELOPMENT OF MINING GUIDANCE AND CONTROL SYSTEMS

Prepared by

National Aeronautics and Space Administration
George C. Marshall Space Flight Center, Alabama 35812
Program Development Directorate

Annual Report, No. ALW-11, October 1976 through September 1977

For The U. S. Department of the Interior, Bureau of Mines

and

The U. S. Department of Energy

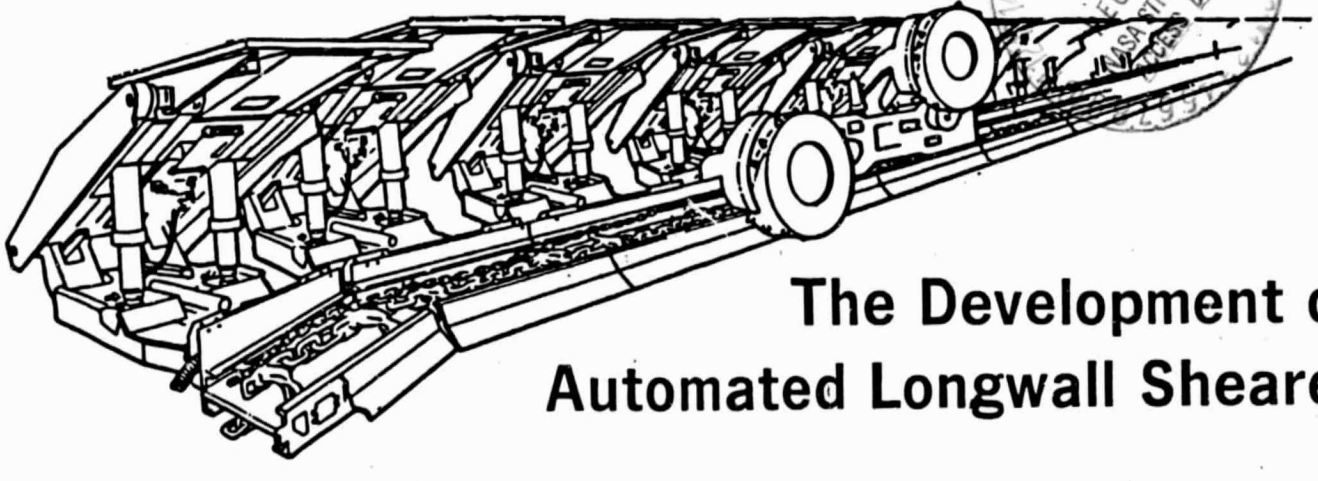

The Development of Automated Longwall Shearer

George C. Marshall Space Flight Center
Marshall Space Flight Center, Alabama 35812

Prepared for
U. S. Department of Energy

Report No. ALW-11

DEVELOPMENT OF MINING GUIDANCE AND CONTROL SYSTEMS

ANNUAL REPORT

October 1976 through September 1977

Bureau of Mines Agreement No. H0155092
NASA RTOP No. 776-41-11

APPROVALS:

James T. Murphy
Director, Program Development

R. E. Pease
Manager,
Mineral Extraction Task Team

Richard A. Campbell
Task Leader, S&E
Automated Longwall Shearer

FOREWORD

In accordance with established national goals, the Department of the Interior (DOI) and the National Aeronautics and Space Administration (NASA) entered into an agreement* in January 1974 for joint participation in a program of "Advanced Mineral Extraction Technology." It was stated that coal mining was to be the first priority of these efforts. Under this agreement, NASA has been utilizing its capabilities to assist the DOI's Bureau of Mines in achieving advanced mineral extraction goals. The advancement of longwall mining technology was given a high priority in this program. NASA's George C. Marshall Space Flight Center is currently engaged in selected research, development, and studies of mining guidance and control systems principally in support of the longwall program. As of October 1, 1977, the longwall program management was transferred from the Bureau of Mines to the newly created Department of Energy (DOE). The guidance and control work is now continuing in support of the DOE.

This document is the annual report for the period October 1, 1976, through September 30, 1977, covering the work authorized under Bureau of Mines working fund agreement number H0155092 and NASA RTOP number 776-41-11, entitled "Development of Mining Guidance and Control Systems."

---

* NASA NMI 1052.187 dated January 17, 1975.

TABLE OF CONTENTS

TABLE OF CONTENTS (Concluded)

LIST OF ILLUSTRATIONS

LIST OF ILLUSTRATIONS (Continued)

LIST OF ILLUSTRATIONS (Continued)

LIST OF ILLUSTRATIONS (Continued)

LIST OF ILLUSTRATIONS (Continued)

LIST OF ILLUSTRATIONS (Continued)

LIST OF ILLUSTRATIONS (Concluded)

LIST OF TABLES

LIST OF TABLES (Concluded)

1.0 INTRODUCTION

This report describes the work performed by the National Aeronautics and Space Administration's (NASA) Marshall Space Flight Center (MSFC) for the Bureau of Mines during the 12 month period ending October 1, 1977. The work has been organized into two principal divisions, fundamental sensor research and development of a longwall shearer guidance and control system, as described in NASA RTOP 776-41-11 dated November 22, 1976.

The addition of the fundamental sensor research activity during this past year reflected the Bureau of Mines desire to broaden the scope of investigation of the application of certain scientific principles to the problem of residual coal thickness measurement, independent of their potential use in the longwall shearer guidance and control system.

Research and development for a longwall guidance and control system continued in FY77 as the area of primary emphasis, expanding upon sensor and control system concept investigations performed in FY76 [1]. These longwall guidance and control system studies are scheduled for completion at the end of 1978, and are expected to lead to final decisions by the Bureau of Mines[1] as to development of a prototype hardware system suitable for mine demonstration. Development of a practical guidance and control system longwall automation is expected to:

(a) Remove more coal with less rock cut

(b) Speed up cutting operations

(c) Decrease equipment breakdowns and reduce downtime

(d) Reduce hazards, improve personnel health, and create safer working conditions.

The Management Summary (Section 2.0) presents the project objectives, approach, results and conclusions, resources status, and recommendations for future development work. Following this, a comprehensive report on technical results and special studies is presented in Sections 3.0 through 6.0. Description and data are given for the analytical, laboratory, and mine test work performed, including a summary of significant technical results.

---

1. Program responsibility transferred to Department of Energy as of October 1, 1977.

During the reporting period, field tests were conducted by MSFC personnel at the Bureau of Mines experimental coal mine, Bruceton, Pennsylvania, and in coal mines of the Warrior Basin, Alabama. These field tests were made possible by the excellent cooperation of the Bureau of Mines personnel at the Pittsburgh Mining and Research Center and the Mining Enforcement and Safety Administration (MESA) field office located in Birmingham, Alabama.

The project was conducted under the direction of MSFC's Mineral Extraction Task Team. Project management and technical staff responsibilities are as follows:

Manager	Robert E. Pease
Project Engineer — Control Systems	Peter H. Broussard
Project Engineer — Sensors	Richard J. Stein
Project Secretary	Betty T. Carlin/Marie Woolbright
Program Planning and Control	Donald F. Bishop

Science and Engineering:

Task Leader	Dr. R. A. Campbell
Nucleonic CID	Stephen D. Rose/Dr. E. W. Jones*
Radar CID	Thomas A. Barr
Sensitized Pick	John L. Burch
Surface Recognition	Harry Reid/Joe E. Zimmerman
CID Dynamic Simulator	Fred D. Roe
Systems Engineering	E. T. Deaton
Vertical Control System	John E. Farmer/Ralph R. Kissel
Special Test Engineer	Paul Fisher
Yaw/Roll Control	James R. Currie/Dr. E. W. Jones*

* Mississippi State — Visiting Professor

2.0 MANAGEMENT SUMMARY

2.1 Objectives

The objectives for fundamental sensor work during the FY77 reporting period were as follows:

(a) Categorize performance criteria and application potential for specific sensor concepts

(b) Identify and investigate scientific principles potentially applicable to coal thickness measuring.

The objectives for longwall shearer guidance and control work were as follows:

(a) Refine and test laboratory type coal interface detectors (CID's)

(b) Develop refinements for the vertical control system simulation model

(c) Determine whether there are promising alternate vertical control concepts

(d) Determine yaw and roll guidance and control concepts

(e) Design an experimental yaw and roll measuring device which can be integrated into the longwall shearer machine

(f) Assist the Bureau of Mines as required in initiating development of prototype hardware.

2.2 Approach

The previous studies and experiments of interface detection sensors were purposely limited to the geological environment of the Pittsburgh Coal Seam and application to the longwall miner. The Bureau of Mines had indicated a desire to broaden sensor research to consider performance under a number of geological conditions, sensor application to a broader range of mining equipment, and to investigate the applicability of other scientific phenomena to sensors for interface detection. This year MSFC initiated work to identify and investigate new fundamental interface sensor concepts, including tabulation of the physical and performance characteristics of any new interface detector concept shown to be

feasible. These investigations also considered such data as were provided from Bureau of Mines field surveys (e.g. geology of the coal interface, mining strategies, or other conditions applicable to underground coal mines).

Studies of guidance and control techniques for the longwall miner have identified three basic systems for use in automated/remote controlled longwall mining, described as follows:

(a) Vertical Control System (VCS) — The VCS consists of CID's, last cut height sensors, shearer position/velocity sensors, a digital controller, operation and display panels, and interface connections to the drum arm actuators and controls. The VCS provides continuous adjustment of the vertical position of the shearer cutting drums as the machine proceeds along the face, extracting the desired portion of the coal seam, while minimizing the amount of rock mined.

(b) Face Advancement System (FAS) — The FAS consists of a coal face alignment measuring device (for yaw), display panels, a digital controller, an inclinometer (for roll), and interface connections to the roof support and shearer tilt actuators.

(c) Master Control Station (MCS) — The MCS consists of the necessary controls and information displays to permit operators to control the longwall operation from the main gate location. The MCS also serves to integrate automated and nonautomated functions, and their control.

Previously MSFC had identified several promising laboratory type CID's, conducted analytical simulations, and defined preliminary concepts and requirements for the VCS. Based on the results of this work, efforts continued this past year with the primary emphasis on the CID's, including additional improvements and evaluation, use of signal averaging to improve CID measuring accuracies, and the study of the effects of CID accuracy on the VCS performance. Studies of the previously reported VCS concept (for control of the drum in "real-time" with roof and floor CID's) were continued. Alternate VCS concepts, utilizing data from past cuts to predict the new cut interface, were also evaluated. For face alignment (yaw/roll), an experimental yaw angle measuring device which could be shearer mounted was studied, and fabrication plans were initiated. An off-the-shelf roll inclinometer was tested, and alternate alignment measuring approaches were also considered.

A system study which will more completely define the longwall guidance and control system design concepts, integration of the various control functions (vertical, yaw and roll), and hardware technical requirements was initiated. Further objectives of these system studies are to determine the practical degree

of automation, use and limits, considering such factors as interaction with the operators, safety, current equipment utilization, operational limitations, and the potential effect on face production and the cost of coal.

It is planned that the system definition study, which will be completed in 1978, will provide sufficient technical requirements (preliminary designs, specifications, etc.) and other data necessary to support a decision and RFP for procurement of a prototype mine demonstration system.

It should also be noted that planning was initiated during the fourth quarter FY77 for guidance and control testing scheduled in 1978 at the longwall surface test facility, Bruceton, Pennsylvania.

The schedule of the major activities performed and milestones completed in FY77 and planned for FY78 is shown in Figure 1.

2.3 Results and Conclusions

During the initial phase of the fundamental sensor development, eight scientific principles were identified that were believed to have some promise for use in coal thickness measurements (Table 1). These principles were investigated and the relative suitability of each was presented to the Bureau of Mines, together with suitable recommendations by NASA/MSFC, for a decision of which ones to continue and which ones to eliminate. Those selected for continued development were natural background radiation, magnetic spin resonance, hydraulic drill, and acoustics. The progress on each of these concepts are summarized as follows:

(a) Natural Background Radiation — Utilizing available laboratory instruments, natural background radiation measurements from overlying roof shale strata with various coal thickness residuals were made at two locations, Bruceton, Pennsylvania, and Graysville, Alabama. Radioactive potassium in the shale is the primary source of radiation measured. A significant amount of radiation was also detected from the floor at the Bruceton site (approximately 80 percent of the roof value). The data, to date, indicate a high potential of utilizing this concept as a viable coal depth measuring CID. Although measured deviations experienced were large, increased detector surface area and/or longer count times can be utilized to bring the measuring accuracy within acceptable tolerances. Results obtained at the two locations were quite similar; however, tests at additional locations are planned to increase confidence in this concept.

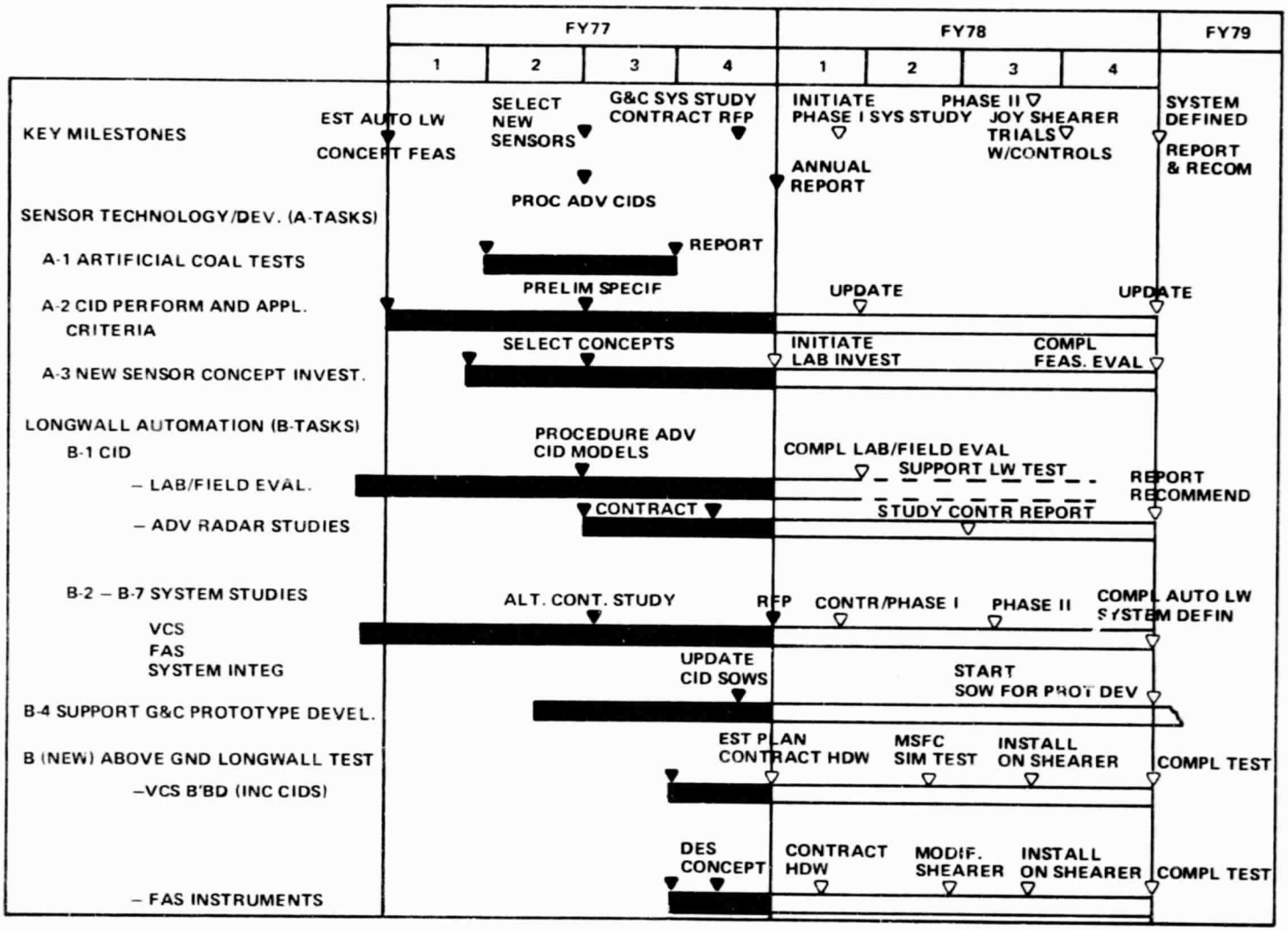

Figure 1. Mining guidance and control schedule (RTOP 776-41-11).

TABLE 1. FUNDAMENTAL SENSOR CONCEPTS

Technique	Measuring Principle
Natural Background Radiation	Measures the natural radiation flux emanating from shale. Coal thickness determined by attenuation of the radiation.
Magnetic Spin Resonance	Depends upon the presence of free electrons in coal but not in shale. Interacting an RF and magnetic field normal to each other. At the shale/coal interface, the signal amplitude drops; this is used as the interface locator.
Acoustics	The measurement is based upon detecting the reflection of an ultrasonic echo from the coal/share boundary.
Hydraulic Drill	Based upon the water jet cutting through coal but not roof rock. Coal thickness determined by mechanically measuring depth of cut.
Electronic Capacitance	Based upon the principle that coal is a mixture of dielectric materials.
Electrical Conductance	Based upon the electrical conductance of coal and possible changes in conductance properties arising from layered characteristics of coal seams.
Infrared	Possible differences in infrared radiation characteristics of coal and shale.
Thermally Sensitized Pick	Possible existence of thermal gradient when cutting coal and shale.

(b) Magnetic Spin Resonance — The presence of free electrons in coal and their absence in shale can be used to discriminate between these two materials. The discriminator is the absorption of measurable RF energy by the free electrons in coal. Laboratory experiments conducted by Southwest Research Institute have substantuated this postulation by demonstrating an abrupt

change in amplitude at the shale/coal interface, with average values of coal measured at 85.5 dB as compared to shale values of 13.2 dB, a ratio of approximately 6:1. Preliminary experiments have therefore proved encouraging, indicating that this technique is promising as a coal/shale interface sensor.

(c) Hydraulic Drill — The concept of penetrating coal and not penetrating shale by adjusting the angle of incidence of a high pressure water jet appears to offer a promising interface sensor technique, whereby the depth of penetration can be measured mechanically to locate the interface. The University of Missouri has been contracted to perform appropriate laboratory experiments to investigate this method.

(d) Acoustics — Initial laboratory investigations of acoustics indicated that the coal was highly attenuative to an acoustic signal (more attenuative the higher the frequency); however, data indicate that it would be possible to discriminate thin coal layers (1 to 2 in.) if a suitable coupling device could be devised. Thus far, only a water column has been identified as a possible method to couple the signal into the coal. Further investigations are planned to more broadly categorize acoustic properties of coal, to expand signal processing techniques, and to assess coupling techniques.

CID's identified for development as part of the longwall VCS [1] were subjected to extensive laboratory and field tests; the data were analyzed and problems contributing to measurement inaccuracy or uncertainty were identified. Techniques which offered a means to overcome those problems through redesign of the hardware were investigated and evaluated. Progress on these CID's is summarized as follows:

(a) Nucleonic CID — The initial nucleonic sensors configured with a rigid frame have been redesigned. The new design is based upon the concept of independently mounting the transmitter and receiver in separate housings which should follow the coal surface contour more precisely than does the rigid frame model. The problems of "air gaps" disrupting the accuracy of the measurements should be reduced to an acceptable level, if not eliminated altogether. Fabrication of this design will be completed during the first quarter FY78, followed by laboratory and field tests to verify performance expectations.

A mine permissible data display module was designed and fabricated during the reporting period. It will be used in conjunction with the new sensor.

(b) Radar CID — The radar has demonstrated its ability to penetrate from 2 to 6 in. of coal. However, it has been found that moisture in the coal, as well as certain characteristics of the CW/FM configuration used, restricted

the radar's ability to measure greater depths of coal repeatedly and reliably. Evaluation of the test conditions and the radar itself led to the conclusion that wider bandwidth systems as well as certain signal processing techniques offered possibilities to extend the depth measuring range. Currently a 0.7 to 4.3 GHz CW/FM radar configuration has been designed, components ordered, and assembly scheduled for completion early in the second quarter of FY78. To assess the relationship between frequency and coal depth measuring capability, more advanced radar operating over a frequency range of 0.7 to 8 GHz is also in design and will be fabricated for use during the third quarter FY78. Signal processing involves subtraction of the front reflection and correlation of the remaining signal to identify the interface signal. Algorithms for this purpose are currently under intensive study with the intent of selecting one that is simple and reliable to the extent that 60 percent of the measurements recorded will accurately identify the interface.

(c) Sensitized Pick — The sensitized pick has been designed and fabricated to be compatible with the Joy Longwall Shearer as well as for mine permissibility. It is anticipated that underground tests will be performed using an operating longwall shearer at the Rochester and Pittsburgh Coal Company's Jane mine during the first quarter of FY78 to obtain characteristic data for evaluation.

(d) Surface Recognition Sensor — Early evaluation of the performance of the penetrometer and the reflectometer indicated that a more flexible instrument was necessary for satisfactory surface identification. The desired flexibility was accomplished by integrating these two devices into a single module, which was designated a surface recognition sensor. Recognition is indicated by a voting logic circuit of the combined measurements of two reflectometers and one penetrometer. Two of three compatible measurements is used, therefore, to identify the surface. Fabrication of this instrument, designated as a surface recognition sensor, is scheduled for completion during the first quarter FY78. It will then be subjected to laboratory and field testing to assess its performance.

Studies of the VCS continued with refinement of the baseline mathematical model. Field tests were conducted to measure the dynamic responses of the Joy Longwall Shearer at Bruceton, and test data were gathered on the vibrational characteristics of the shearer drum arm on an operating longwall shearer. Dynamic data, CID error effects, drum filtering effects, and shearer configuration changes have been incorporated into the computer model. The model continues to predict stable operation over multiple cutting passes, and performances above 95 percent coal removal and less than two percent rock taken, even where fairly large CID errors were assumed. Alternate VCS concepts

which included the storing of CID measurements from previous cuts for prediction of the interface for the cut were studied. Guidance accuracy and stability were found to be marginal when using previous cut data only; however, when used in conjunction with real-time CID data on the current cut, stability was indicated with some gain in cutting accuracy attained at the largest CID error cases. Multiple combinations of the CID's have been considered. Although not always necessary, it was shown that for some mining conditions two or more CID's would improve reliability and accuracy (e.g., sensitized pick and trailing depth sensor). An investigation was initiated to determine whether automatic vertical control of the rear (or floor) cutting drum could be achieved without the the use of a "floor" CID, which is at present difficult to mount and protect. A promising approach has been identified using the roof as a reference (see Section 4.0). Several variations of this concept, using mechanical and remote electronic sensors for referencing drum location, will be studied for practicality and accuracy.

Studies of the FAS have, to date, been directed primarily toward face profile measuring in two axes, yaw and roll. The roof support and advance and face alignment sequence will be a function of the manner in which the shearer is used to shear the face. However, the current concept envisions utilizing data from face alignment sensors, together with pre-established computer programs for the advance sequence, to automatically control the forward movement of the roof supports and conveyor sections after a cut has been made by the shearer. Programmable roof support systems currently exist but lack only the addition of face alignment sensors to provide closed-loop control. Present studies indicate that the yaw angle measuring instrument (which describes conveyor path when mounted on the shearer) could provide the location of the conveyor within ±1 ft accuracy (if such accuracy is required). Alternate methods of face alignment measuring (yaw), such as the "lost rope" (or buried cable) method tried in Europe, have been reviewed and may have potential. This technique measures total distance traveled by the chocks. When employed to locate chocks on face ends, this concept together with yaw angle profile measuring appears to be one of the most promising systems for ascertaining the position of the face. Roll measuring by use of an inclinometer offers a feasible approach to shearer roll control, but this must be tied in with the VCS, because the two functions (VCS and roll) are interdependent in achieving proper control of the longwall's forward advance through the seam.

An RFP was coordinated with Bureau of Mines and released in September 1977 for the conduct of guidance and control system studies. These studies are to be performed in two phases. Initially only phase I will be contracted which will expand the depth of analysis for the VCS and FAS system and define the

overall system concept (VCS, FAS, and MCS as an integrated system). Subsequent to the approval of the system concept in phase I, it is anticipated that phase II will be initiated to provide a preliminary design and definition of technical requirements for a "prototype system."

In the category of special studies, a limited analysis was performed to determine the extent of potential benefits that might be possible as a result of automating the longwall shearer. Although the improvements to the safety and health of the operators are fairly obvious by lowering their exposure to dust and other face hazards, the effect on production and cost was of considerable interest. Using data published by the Bureau of Mines on longwall mining costs, data supplied by the Jet Propulsion Lab, and results of MSFC's guidance and control studies, the analysis resulted in several preliminary conclusions, summarized as follows:

(a) Automating the shearer would remove man-limiting factors, making it possible to attain shearer haulage speeds in the range of 30 to 40 ft/min and corresponding face production rates in the vicinity of 2500 to 3000 tons/shift. This is contrasted with 8 to 12 ft/min and 700 to 1200 tons/shift presently attained on a regular basis.[2]

(b) However, current face conveyor capacities would limit shearer haulage speed to approximately 20 ft/min and face production to approximately 2500 tons/shift (for 6 ft seam, 500 ft face, and 50 percent longwall utilization factor).

(c) With the higher production rates and conditions of paragraph (b), the number of operating longwall faces in a given mine can be reduced. Also the quality of the product (less rock, etc.) improves with an automated VCS. The analysis indicates that this will result in approximately a 20 percent reduction in the cost of coal after preparation (or approximately 15 percent with run-of-the-mine product). This factor appeared to be quite consistent for mine sizes considered ranging from 1.3 to 3.3 million tons/year.

(d) The effect of increased cost of the longwall due to automation was also considered. For this analysis, a 25 percent increase in longwall face equipment cost resulted in only a 1.1 percent[3] increase in coal cost, with longwall

---

2. Rates obtainable during an operating shift, not annual averages.

3. This relationship does not hold true for other shift production rates or mine sizes (e.g., at lower production rates the effect on coal price is greater, see Fig. 102).

production rates of 2500 tons/shift/unit for a 3.3 million ton/year mine. This suggests that additional expenditures for improvements to significantly increase face production rates (e.g., for automation, reliability, lower maintenance, etc.) would be quite cost effective. For any given mine situation, a detailed analysis would be required.

(e) Finally it was noted that the reduction in cost of coal, possible with increasing shift production rates, is not linear and begins to taper off or flatten out significantly at rates above 2500 tons/shift (discussed in Section 5.0). This suggests that the capacities of available longwall equipment are adequate to take advantage of most of the cost benefits from higher face production rates. The implication of the foregoing to the guidance and control system requirement is that (1) particular attention should be given to rock avoidance and producing clean coal, (2) good stability and cutting accuracy must be maintained at shearer speeds in the 20 to 40 ft/min range, and (3) guidance and control equipment must be very reliable, require low maintenance, and be simple to operate.

2.4 Summary and Recommendations

The work conducted in FY77 continues to support the initial conclusions reached at the end of FY76, which indicated the technical feasibility of developing a practical guidance and control system for automating the longwall process. In addition, the studies indicate there is a high probability of attaining substantial economic as well as miner health and safety benefits.

The fundamental sensor investigations conducted have produced two new promising interface detector concepts: (1) the natural background radiation and (2) magnetic spin resonance. Both concepts are extremely attractive in that measuring coal depths up to 8 in. or more may be possible without requiring direct contact with the coal surface. More emphasis is recommended for development of these concepts. Two other concepts using acoustics and hydraulic drilling appear to offer limited depth sensing possibilities and may be useful in specialized application. These investigations should continue, however, at a low level of effort.

The results of the VCS simulations (mathematical model) and alternate concept studies show that good performance can be obtained at anticipated operating and seam conditions. The VCS will also accept a number of different CID inputs and should perform satisfactorily within a broad range of CID accuracies. Providing satisfactory operation of a floor CID for the rear drum poses a very difficult problem of installation and consistent performance (due to

floor debris). Therefore, it is recommended that an alternate control concept be studied further which would automatically maintain the floor cut a consistent distance from the roof. It is believed that this would be a more practical approach (not requiring a floor CID) if satisfactory performance can be obtained.

For the previously identified longwall CID candidates (i.e., nucleonic, radar, surface recognition, sensitized pick, and vibration sensing CID's), it is recommended that as many as possible of these CID's be tested in conjunction with "breadboard" VCS tests using simulated coal/rock materials on the longwall surface test facility at Bruceton, Pennsylvania. Laboratory CID's with suitable longwall operational configurations (in some cases that are not yet mine-permissible) are to be available by June 1978 for these tests. It should be possible to calibrate most of these CID's for operation with the simulated face materials at Bruceton, providing certain specifications[4] are followed. In addition, serious consideration should be given to establishing a test program for mine evaluation of each of the candidate CID's on a longwall machine. This is an extremely important step which is necessary to identify any mine operating problems affecting the final selection, the final design requirement, limits of use, or practicality of each CID type.

Regarding the FAS, it is recommended that the yaw and roll face alignment measuring sensors to be used in this system be evaluated on the Bruceton Surface Test Facility. Before selection of the final concept, other concepts under investigation in Europe (i.e., buried cable and optical alignment) should also be studied.

A point has been reached now where more detailed system studies are required to better define and bring together the primary elements of the guidance and control system, namely the VCS, FAS, and MSC. The interrelationship and interaction of these elements must be fully understood. Action to initiate these studies began in FY77. It was decided to conduct these studies in two phases. The first phase would define and select the final system concepts and requirements, and the second phase would establish preliminary system designs (not detailed hardware design) and the necessary specifications for development and procurement of a mine prototype system. Agreement to initiate phase I was reached between NASA and Bureau of Mines in August 1977. A further decision to initiate phase II will be required at the completion of phase I.

Further detailed technical recommendations are embodied in subsequent sections of the report.

---

4. These will be provided separately.

2.5 Resources

2.5.1 General. Research and development funds made available for the coal extraction project at MSFC and utilized during the period October 1976 to October 1977 were augmented by the carryover of $180 000.00 of FY76 funds.

Funding authority for FY77, supporting the project plan (see RTOP 776-41-11), arrived in two transmittals: $250 000.00 in January 1977 followed by $670 000.00 in April. The budgetary breakdown of these funds is shown on Table 2.

TABLE 2. FY77 BUDGET ALLOCATION

Budget Item	Allocation
Research and Development	$470 000.00
Research and Program Management (Salaries)	$440 000.00
(Travel)	$ 10 000.00
Total FY77 Funds	$920 000.00

2.5.2 Research and Development Funds. Table 3 summarizes obligation of the remaining FY76 funds. The obligation on status of FY77 funds is summarized in Table 4.

TABLE 3. OBLIGATION OF FY76 CARRYOVER RESEARCH AND DEVELOPMENT FUNDS

Contracted Studies	$ 76 000.00
Components and Parts for Sensors	31 000.00
Fabrication Nuclear Sensor	27 000.00
Fabrication Nuclear Sensor Display Module	5 000.00
Fabrication Surface Recognization Sensor	17 100.00
Special Test Equipment	23 537.00
Computer Services	5 000.00
Shipping and Miscellaneous Charges	2 904.00
Total FY76 Carryover	$188 000.00

TABLE 4. FISCAL STATUS FY77 FUNDS

Obligated for Contracted Studies	$ 88 146.00
Components and Parts (Sensors)	$ 22 394.00
Nuclear Sensor (Fabrication)	$ 12 015.00
Radar (CW/FM) Housing	$ 4 000.00
Special Test Equipment	$ 1 690.00
Computer Services	$ 23 801.00
Institutional and Management Support	$ 14 496.00
Subtotal FY77 Obligations	$166 522.00
Procurement Actions Initiated	$302 787.00[a]
Initiated Funds	$ 691.00
FY77 Research and Development Allocation	$470 000.00

a. These funds have been initiated for: the Guidance and Control Study Contract, advanced radar component purchases, modifications to the MSFC simulator, and a minicomputer to be developed as the radar signal processor.

2.5.3 Research and Project Management Funds. The estimate of the required manpower per RTOP 776-11-11 was $440 000.00. Cost of manpower actually utilized was $433 467.00. The balance, $6533.00, will be carried over and applied to October 1977 manpower charges. Travel expenditures during the year amounted to $9664.00 of which $1196.00 of FY77 funds were obligated, leaving a balance of $8904.00 to be applied to FY78 travel requirements.

3.0 FUNDAMENTAL SENSOR DEVELOPMENT

3.1 General

Fundamental sensor developments (Task A of RTOP 776-41-11) have proceeded with initial laboratory investigations, followed by more concentrated development work with the more promising candidate sensors. The follow-on developments were the product of a review held on April 11, 1977, with Bureau of Mines personnel who approved the MSFC findings and recommendations (Table 5). To fully explore the potential of magnetic spin resonance and hydraulic drill concepts, Southwest Research Institute and the University of Missouri's School of Mines were granted laboratory investigative and demonstration contracts.

3.2 Fundamental Concepts Discontinued

As mentioned previously, certain fundamental concepts were recommended for discontinuance, and agreed to by Bureau of Mines representatives. These concepts are summarized in the following paragraphs.

3.2.1 Electrical Resistance. The resistance between two needle point probes spaced 1 in. apart and held against coal and shale samples were measured using a Communications Measurements Laboratory Model 1515 ohm meter. The meter has a range of 0.4 to 100 000 ohms and operates on 500 V.

Samples used consisted of five 4 $in.^2$ blocks of coal with 13/16, 1, 2, 2 1/2, and 4 in. thicknesses. The samples of shale were irregular, but were approximately 3, 5, and 1 in. thicknesses. The measurements were taken at the center and at the corners of the samples. Results of these tests are shown in Table 6 where it will be noted that due to changes in the resistivity of the samples (between those that were dry and those that were wet) and the overlapping values of resistivity measurements of the coal and shale samples, discrimination between coal and shale in a mine environment does not appear feasible.

3.2.2 Electrical Capacitance. A capacitance probe in which a housing shielded each of two plates was constructed. Coupling between the plates was through the material to be measured, on which the housing was placed. A probe was connected by coaxial cables to a General Radio Type 1620-A capacitance measuring assembly consisting of a 1615-A capacitance bridge, a Type 1311-A audio oscillator, a Type 1232-A tuned amplifier, and null detector. The audio oscillator was operated at 10 kHz to obtain sufficient sensitivity. Two different

TABLE 5. SUMMARY OF RESULTS WITH RECOMMENDATIONS
(FUNDAMENTAL SENSOR CONCEPTS)

Fundamental Concept	Evaluation Summary	Recommendation
Acoustic	Measuring capacity 2 in. of coal severe signal attenuation encountered	Basic research and signal processing studies
Hydraulic Drill	Concept theoretically feasible	Perform laboratory testing for performance evaluation
Mechanical Drill	Concept feasible for depth measuring (stationary measuring)	Evaluate test data supplied by Bureau of Mines
Electrical Resistance	No discrimination	Discontinue effort
Electrical Capacitance	Feasible	Obtain mine data (Bureau of Mines decided to discontinue)
Infrared	No discrimination between wet coal and wet shale	Discontinue effort
Natural Radiation	Demonstrated feasible — depth measuring	Continue field testing, increase counting rate of detectors
Magnetic Resonance	Theoretically feasible for depth measuring	Perform analysis and laboratory test for performance evaluation
Thermal Sensitized Pick	Theoretically not feasible	Discontinue effort

TABLE 6. RESISTIVITY VALUES OF COAL AND SHALE SAMPLES
(VALUES IN MEGOHMS)

	Sample Thickness (in.)	Location of Measurement				
		Center	Corner 1	Corner 2	Corner 3	Corner 4
Dry Coal Samples	13/16		Greater than 100 000 megohms (all samples tested)			
	1					
	2					
	2 1/2					
	3					
Wet Coal Samples	13/16	0.6	1.5	0.4	5	5
	1	1.6	<0.4	3.5	5	0.55
	2	<0.4	<0.4	5	3	0.55
	2 1/2	2	0.4	<0.4	>100 000	5
	3	2	1	1000	1	5
Dry Shale	1	50	100	40	30	70
Wet Shale	1	<0.4	<0.4	<0.4	<0.4	<0.4

readings were made on the dry coal samples, one with the longitudinal axis of the instrument parallel to the coal grain and the second normal to the coal grain. The data in Table 7 show that variations in readings do not correlate with the direction of the coal grain. The randomness of the measurements recorded may relate to the roughness of the coal surface (Table 7).

TABLE 7. CAPACITANCE MEASUREMENT OF COAL AND SHALE SAMPLES

Thickness of Sample (in.)	Measurements Normal to Grain		Measurements Parallel to Grain
	Dry Sample	Wet Sample	Dry Sample
13/16	0.55 pF (0.004)	0.08 pF (0.005)	0.25 pF (0.009)
1	0.26 pF (0.001)	0.07 pF (0.003)	0.42 pF (0.002)
2	0.52 pF (0.003)	0.07 pF (0.003)	0.29 pF (0.001)
2 1/2	0.41 pF (0.003)	0.061 pF (0.06)	0.48 pF (0.002)
3	0.25 pF (0.001)	0.08 pF (0.004)	0.41 pF (0.003)
Shale Sample 1	0.16 pF (0.005)	0.0231 pF (0.000)	

Note: (1) The measured value for air: 0.11 pF (0.000).

Samples used were those used for the electrical resistivity measurements. Both dry and wet samples were tested. Based on an evaluation of the laboratory measurements, use of this technique is not feasible as discriminator between coal and shale for the following reasons:

(a) Measurements are sensitive to spacing between the surfaces of the material to be measured and the plates of the measuring instrument.

(b) Large variations between readings on wet and dry coal and overlapping values for shale were recorded.

3.2.3 Thermal Sensitized Pick. This concept consists of mounting a thermistor in the tip of a cutting bit, which could possibly detect the variations in rock cutting and coal cutting due to temperature gradients caused by resistance of rock to the cutting action.

The operating conditions of the longwall shearer cause the temperature characteristics of the cutting bits to be dominated by the water spray utilized for dust control. An analysis of this technique is as follows:

(a) The pick area exposed to water cooling is at least five times greater than the pick cutting surfaces where abrasive action causes heating.

(b) Nominally, the rotating pick is exposed to the water 50 percent of the time and to coal 50 percent of the time, thereby establishing an equilibrium pick temperature. As the picks pass through the rock/coal interface, the dwell time in the rock (for the addition of heat to the pick) is small. For example, assuming a 45° arc, the time available for the pick to deviate from its equilibrium temperature is only 45°/360° or 12.5 percent. For the remaining 87.5 percent of the time, the pick is experiencing conditions which tend to maintain its equilibrium temperature. Even when cutting solid rock, it appears that the pick is still exposed to the thermally dominant water spray 50 percent of the time.

Consequently, in view of the problematic nature of the principle of measuring thermal gradients recorded by a pick when encountering rock (as indicated by the subjective rationale previously outlined), the availability of more promising methods, and the resources required to conduct a detailed laboratory investigation, this technique is eliminated from further considerations.

3.2.4 Infrared Radiation. The amount and spectral distribution of radiation received from an object is dependent on its temperature, emissivity, and reflectance as well as the temperature emissivity and reflectance of surrounding objects. Under controlled conditions and knowing the temperature, the material in an object can be inferred by measuring the radiation from it and calculating its emissivity and reflectance.

These parameters are related analytically by the Boltzmann equation:

$$R = \sigma B T^4 ,$$

where

σ = emissivity of the surface material

B = Boltzmann constant

T = Black body temperature

R = magnitude of radiation .

This equation essentially states that the radiation levels for two bodies, both at the same temperature, will be proportional to their respective emissivities. Measurements of wavelengths between 8 to 12 correspond to black body temperatures between 10° to 45°C.

Thus, the natural black body infrared radiation appears as a large amplitude broadband noise from 8 to 12 wavelengths. Also, surface water temperature dominates the measurement at 12 Å. For these reasons, the concept is not a promising approach to the problem of differentiating between a surface of shale and that of coal.

3.3 Fundamental Sensors Selected for Continuance

The fundamental sensor concepts selected for continuance are (a) spin resonance, (b) hydraulic drill, and (c) the natural radiation. The acoustic sensor decision is to be subjected to a further, more thorough review to evaluate signal processing problems and coupling problems, especially in view of the existence of sensors whose operability offers advantages of simplicity in obtaining comparable measurements.

3.3.1 Natural Background Radiation.

3.3.1.1 Background Investigation (Preliminary Testing). Measurement of the attenuation by coal of natural radiation found in rock was evaluated in FY76 as a technique for coal interface detection. The results of the early laboratory investigations were reported in the year-end report for FY76, which indicated that it is possible to measure the interface location, given sufficient counts to produce good statistical results. The instrument used in those tests is depicted in Fig. 2. A 3 in. by 3 in. sodium iodide, NaI (Tl), crystal optically coupled to a 3 in. diameter photomultiplier was used to detect gamma ray photons from the rock. A lead annulus 1-3/4 in. thick and 9 in. high was used to provide shielding and collimation for the crystal and phototube. Including the shielding, the sensor weighed approximately 107 lb (96.29 lb shield plus 10 lb scintillator).

Tests were initially conducted with and without shielding.

The results from an unshielded detector were not satisfactory, differing from a shielded crystal considerably from that obtained (Fig. 3). This lead to

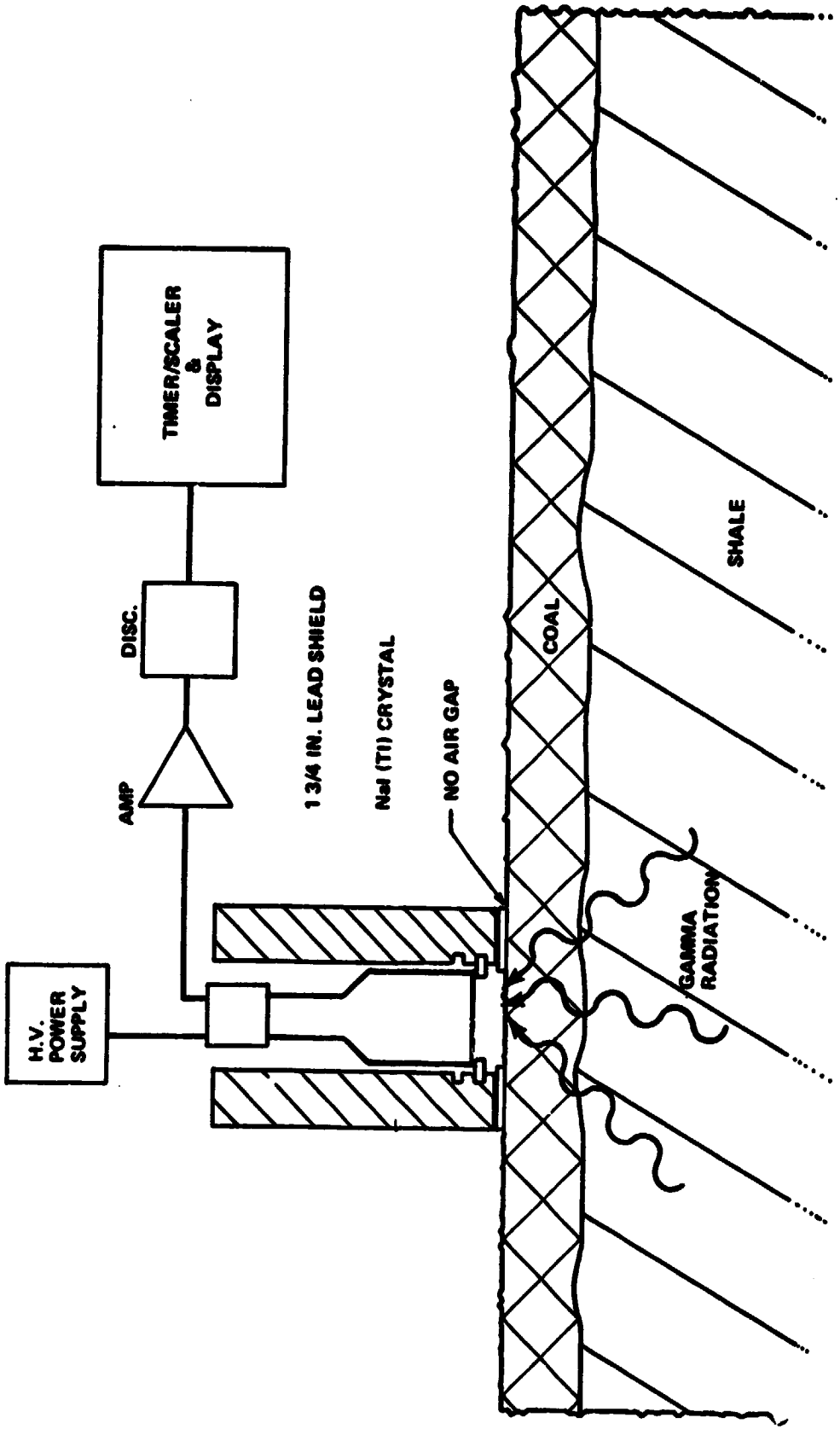

Figure 2. Natural radiation detector.

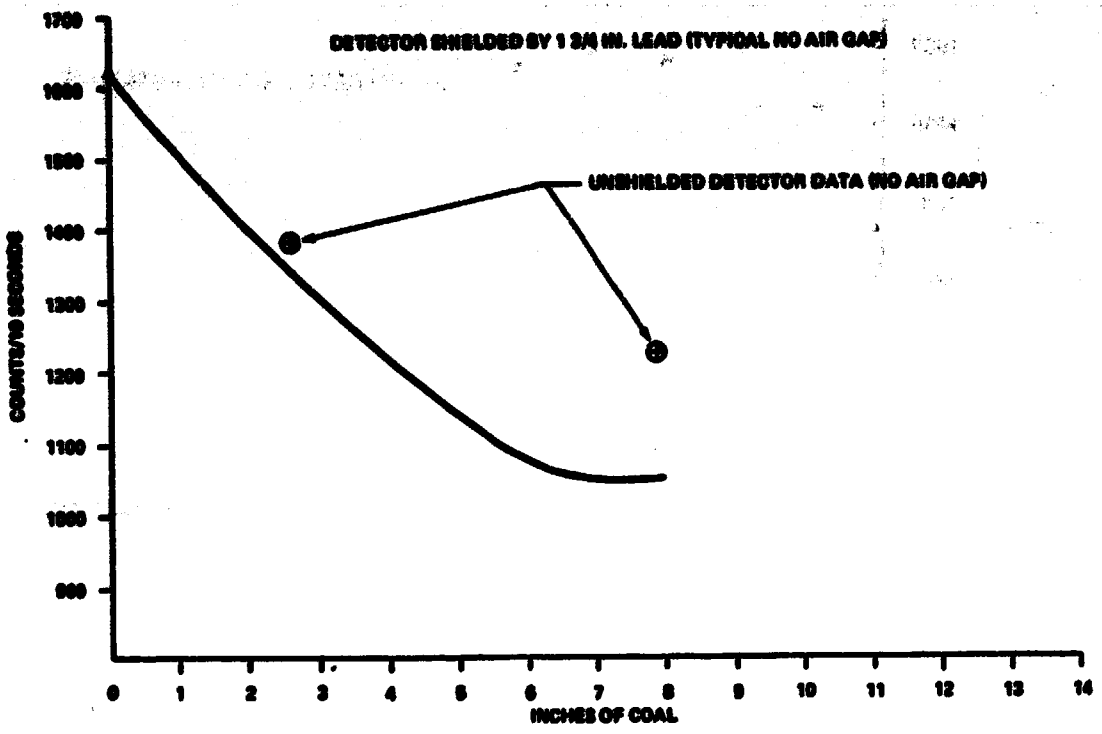

Figure 3. Natural radiation of shale through coal.

the conclusion, which was validated by later tests, that all future tests should be made with shielding around the crystal to prevent distorting the attenuation curve with uncontrolled background radiation. The early tests also indicated that an air gap up to 6 in. does not affect the radiation measurement from rock if the detector field of view was collimated by the lead shield (Fig. 4). To obtain a maximum number of counts and be able to operate with an air gap between the detector and the coal, it was found that recessing the crystal 1/4 in., collimation, was a good compromise.

To answer questions about the intensity and distribution of the radioactive materials in shale, a literature survey was conducted to determine if any background radiation measurements had been made in the U.S. It was found that during the late 1940's and 1950's the Department of Interior's Geological Survey conducted a study for the Atomic Energy Commission to determine the amount of uranium in black marine shale. Part of this work included radiation measurements of shale across the country using Geiger counters and scintillators. Mr. Vernon E. Swanson, Geologist, Branch of Coal Resources, Geological Survey, Denver, Colorado, reported that background radiation measurements could be expected in eastern coal beds while in western beds, having different

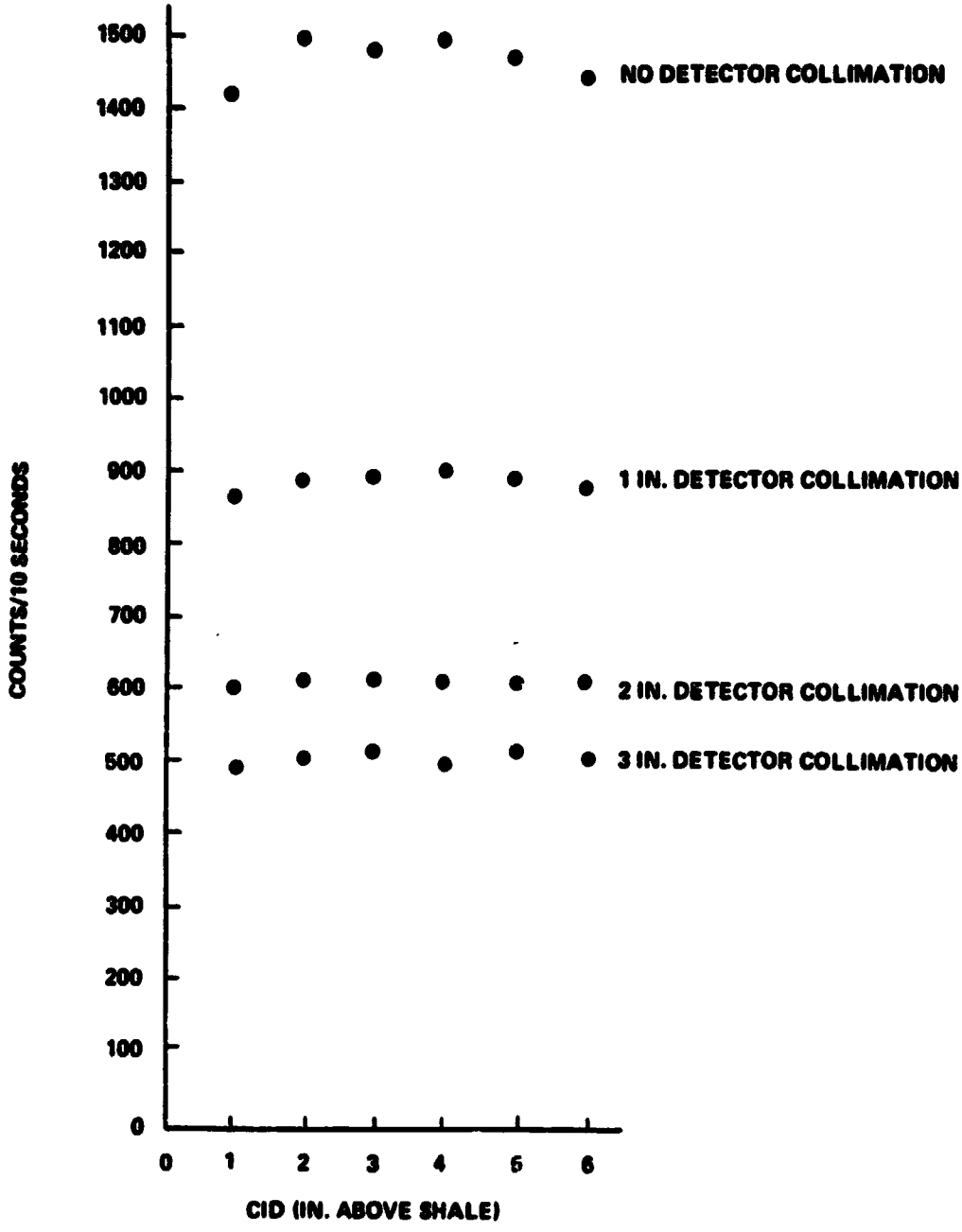

Figure 4. Natural radiation from shale.

overlying and underlying strata, consistent radiation measurements could not be expected. In a 100 square mile area in the East, the radiation levels would probably be fairly consistent; so, based on this reasonably encouraging information, it was decided to take field measurements at various coal miners in the eastern U.S. to test this prediction.

3.3.1.2 Description of Instrument Use in Tests. A portable detector and readout electronics (Fig. 5) were designed and fabricated specifically for use in a wide geographical diversity of coal mines to measure background radiation as function of coal thickness. The same 3 by 3 in. NaI (T1) crystal scintillator was used with a 3/4 in. lead annulus shield 6 in. high around the crystal and photomultiplier. A 1/4 in. aluminum spacer at the bottom of the shield (Fig. 5) creates sufficient collimation of the detector field of view to prevent any effect from small air gaps. In operation, the electronics amplify each pulse from the photomultiplier, register the event in a scaler, and at the end of a preselected counting interval automatically displays the total count on the digital light emitting diode (LED) readout. The count interval can be varied from 1 to 100 sec in the automatic mode or in the manual mode any time the interval can be obtained by throwing a switch for starts and stops. A built-in calibrator can be used to check the system prior to taking data. Power is supplied by batteries contained in the electronics box. The scintillator/detector housing is 7 by 16 in. and weighs approximately 30 lb. The electronics box is 17 by 12 by 6 in. and weighs 10 lb.

3.3.1.3 Field Tests. Field tests of this instrument were arranged in the Birmingham, Alabama, area with the cooperation and assistance of Mr. William H. Meadows and Mr. Harlan E. Blanton, Sr. from the MESA Office in Birmingham and the Jim Walters Company. The first test was conducted in April 1977 at the Bessie Mine in Graysville, Jefferson County, Alabama. Three test areas were selected for measurement where sufficient coal remained on the roof to obtain data from 0 to 12 in. thickness. The location of test points is illustrated in Figure 6, and the test data are shown in Figure 7. Each data point is the average of five 1 sec counts. The probable error of each data point is approximately one standard deviation, taken as the square root of the average, $\bar{x}$, where $\bar{x} \cong m$. The second field test occurred in July 1977 at the Nebo Mine in Jefferson County, Alabama. Figure 8 shows the test locations and Table 8 is a listing of the data points. Each point is the average of five 1 sec counts. The error is the standard deviation:

$$\sigma = \frac{\sqrt{\sum_{1}^{n} (\bar{x} - x_i)^2}}{N - 1} ,$$

where

$\bar{x}$ = Average

x_i = ith count

N = Number of count intervals

m = population mean .

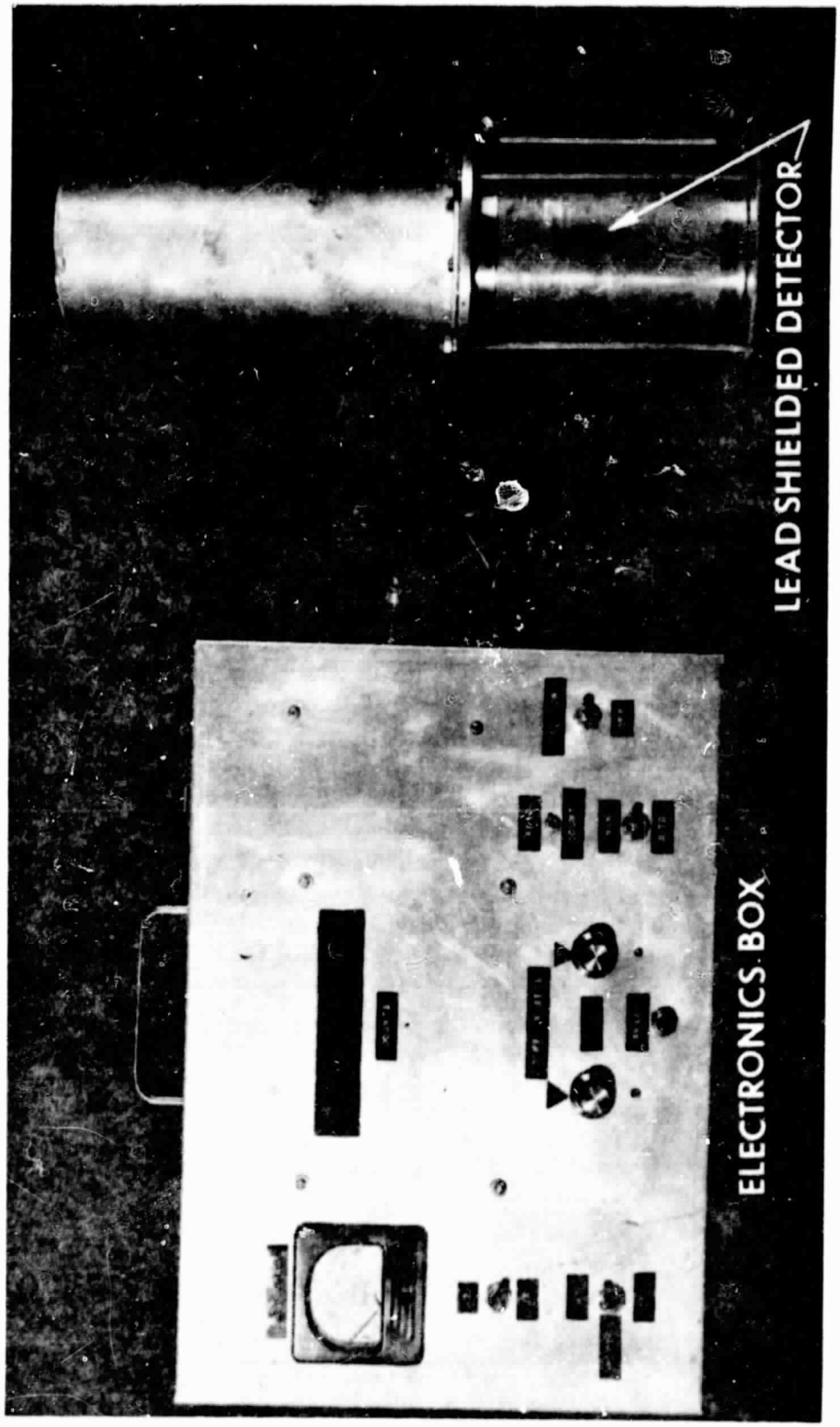

Figure 5. Natural radiation detector.

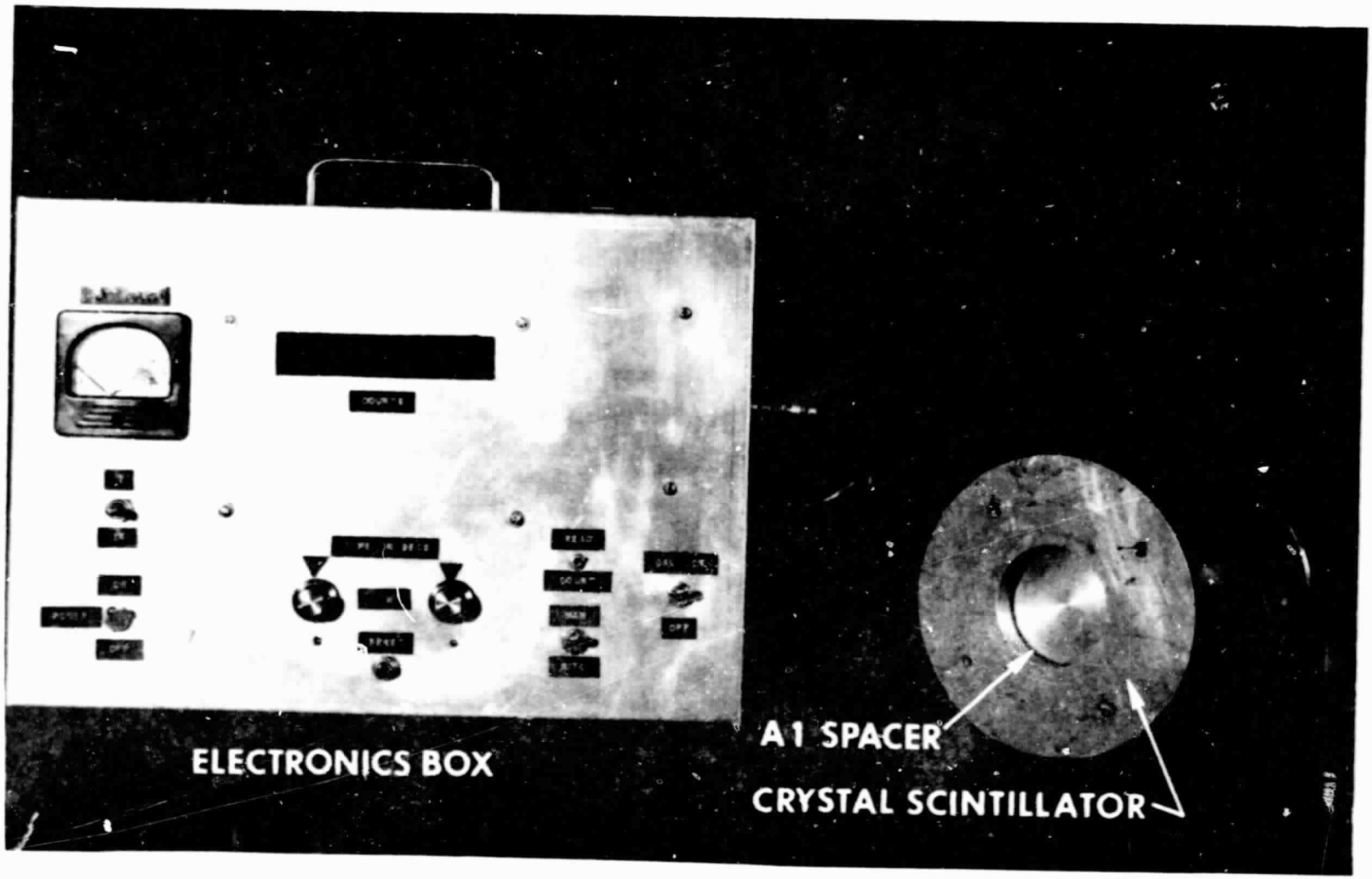

Figure 5. (Concluded).

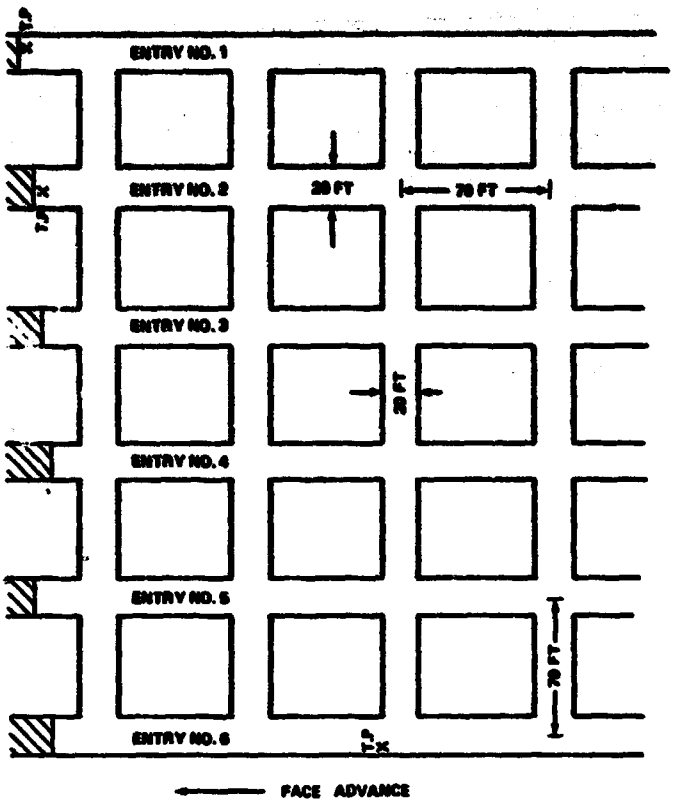

Figure 6. Bessie Mine, Graysville, Alabama, section No. 3.

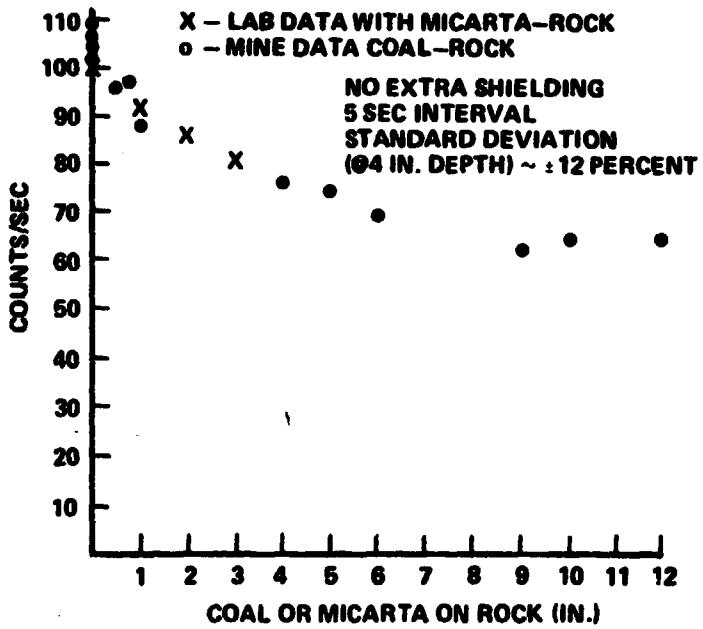

Figure 7. Natural radiation CID combined tests.

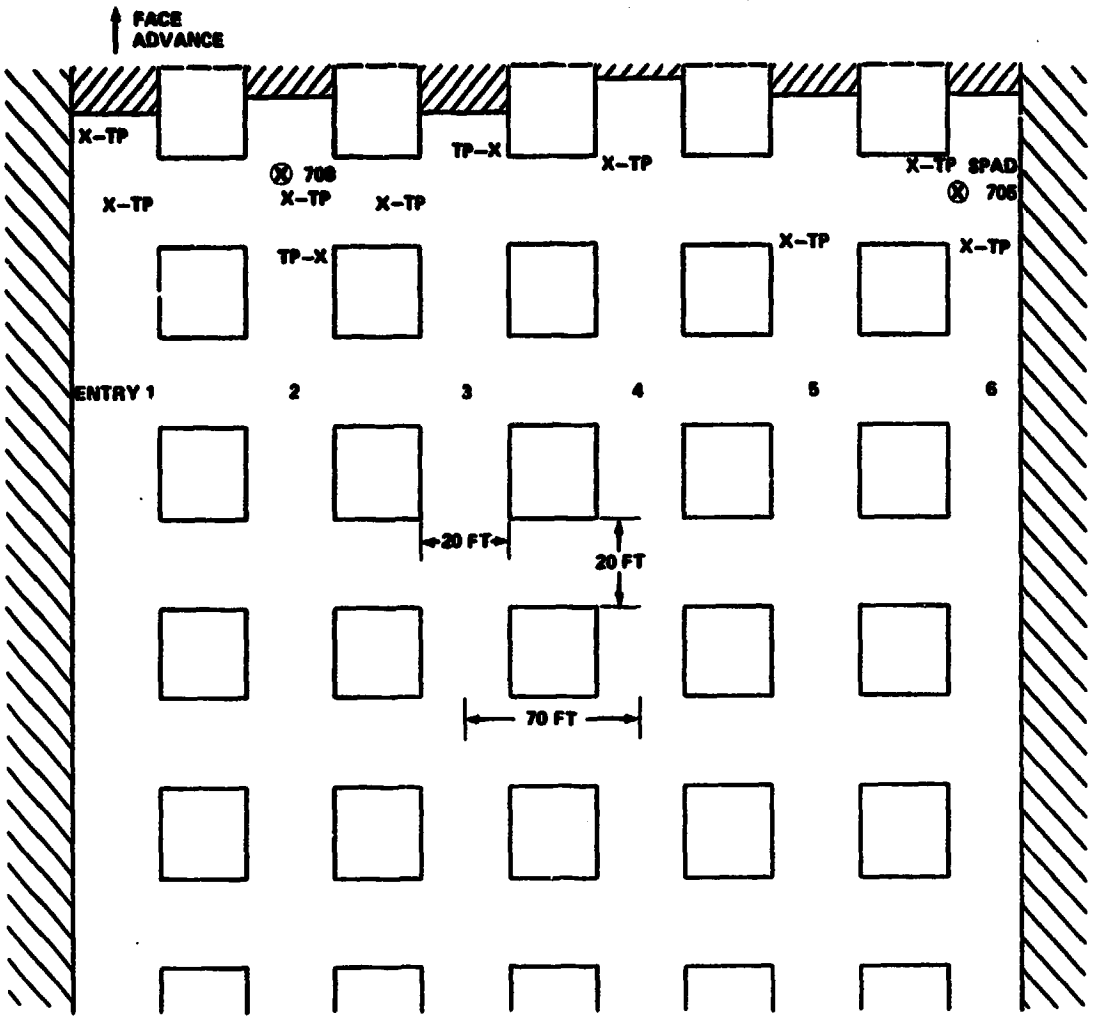

Figure 8. Nebo Mine, Jefferson County, Alabama, section No. 1.

Several measurements were taken in each entry as can be seen from Figure 8. In Figure 9 the data points are plotted as counts/second versus inches of roof coal. The magnitude of the uncertainty in any given measurement for these tests is considerably, with statistical fluctuations of individual readings ranging from ±10 to ±15 percent about the average; therefore, no attempt was made to fit the data from the Bessie and Nebo mines to an exponential curve. In the mine area available for these tests, it was not possible to find coal of any thickness with an area sufficient to shield nearby bare rock. Consequently, it is certain that many photons entering the detector came through the lead shield from bare rock. Further, since the patches of coal of approximately the same depth had

TABLE 8. NEBO MINE TEST DATA (AUGUST 21, 1977)

Section No. 1	Entry No.					
Coal Depth (in.)	1	2	3	4	5	6
	Counts/sec	Counts/sec	Counts/sec	Counts/sec	Counts/sec	Counts/sec
0	121.4 ± 5.9	109.4 ± 15.7	119.2 ± 9.8	128.8 ± 14.4	118.8 ± 15.8	121.0 ± 8.0
0	126.0 ± 10.6	123.0 ± 5.7	126.4 ± 7.0	116.0 ± 11.0	119.8 ± 16.5	115.4 ± 9.0
0	128.8 ± 8.2				116.8 ± 9.5	115.4 ± 9.0
0						116.6 ± 9.0
1/2	115.8 ± 7.9	121.0 ± 10.4				119.4 ± 11.0
1/2						
1/2						
1			93.4 ± 6.2	123.8 ± 16.7		109.0 ± 15.2
1			116.8 ± 14.2			
1						
2	86.4 ± 9.6					
2						
2						
3		88.0 ± 6.6	77.8 ± 8.5	97.6 ± 9.4		
3						
3						
4						86.2 ± 7.0
4						
4						
5	79.0 ± 10.5					83.4 ± 8.0
5						
5						
6		69.0 ± 9.3				69.0 ± 5.0
6						
6						
7 1/2					65.8 ± 4.5	
7 1/2						
7 1/2						
12		81.8 ± 13.6		80.4 ± 9.4		
12						
12						
11					72.0 ± 9.8	
11						
11						

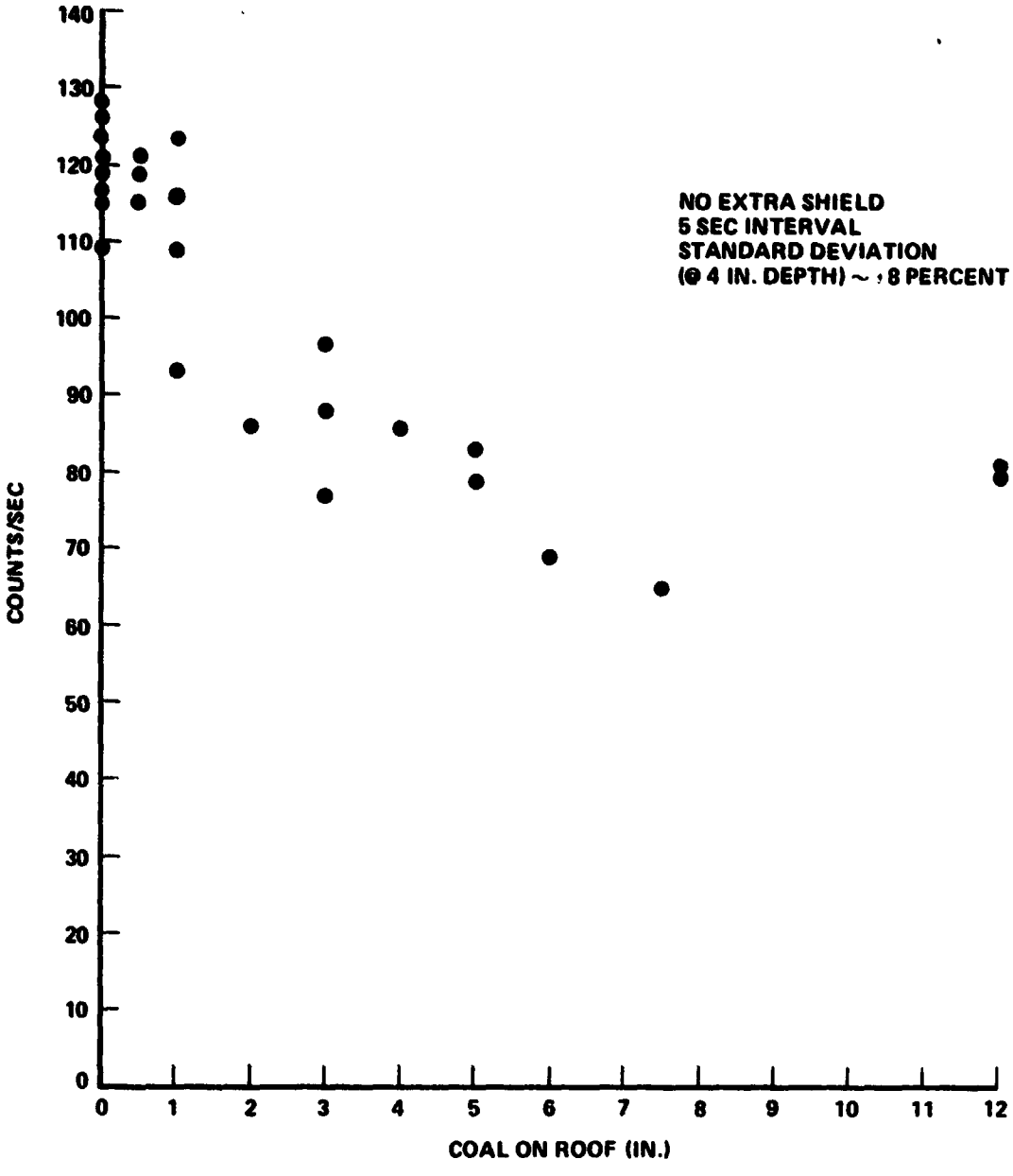

Figure 9. Natural radiation detector, Nebo Mine Test, Jefferson County, Alabama.

different areas, it is likely that the nearby bare rock contributed to some extent for each different measurement. It was noted that the 12 in. coal depth reading deviated from the expected exponential decline in counts due to attenuation. This was attributed to the presence of an 18 in. thick shale layer in the middle of the coal seam, which was located approximately 10 in. from the unshielded back of the scintillator/photomultiplier. When in the measuring position, the rock added

counts on top of the attenuation flux. The real significance of the data is that it shows a general trend of exponentially decreasing counts with increasing coal depth as predicted by theory.

Since the conditions previously described introduced an element of uncertainty, a third field test was conducted in August 1977 at the Bureau's Bruceton Experimental Mine to collect data under more controlled conditions (Fig. 10). Several different count intervals were used and measurements were taken with the 3/4 in. thick lead shield and with an added 2 in. thick lead shield around the scintillator/photomultiplier (PM) tube. The shielding was positioned around the detector as shown by Figure 11. The data collected at time intervals of 1, 5, 10, and 60 sec are shown in Figures 12 through 15. Further investigation of these type conditions is required.

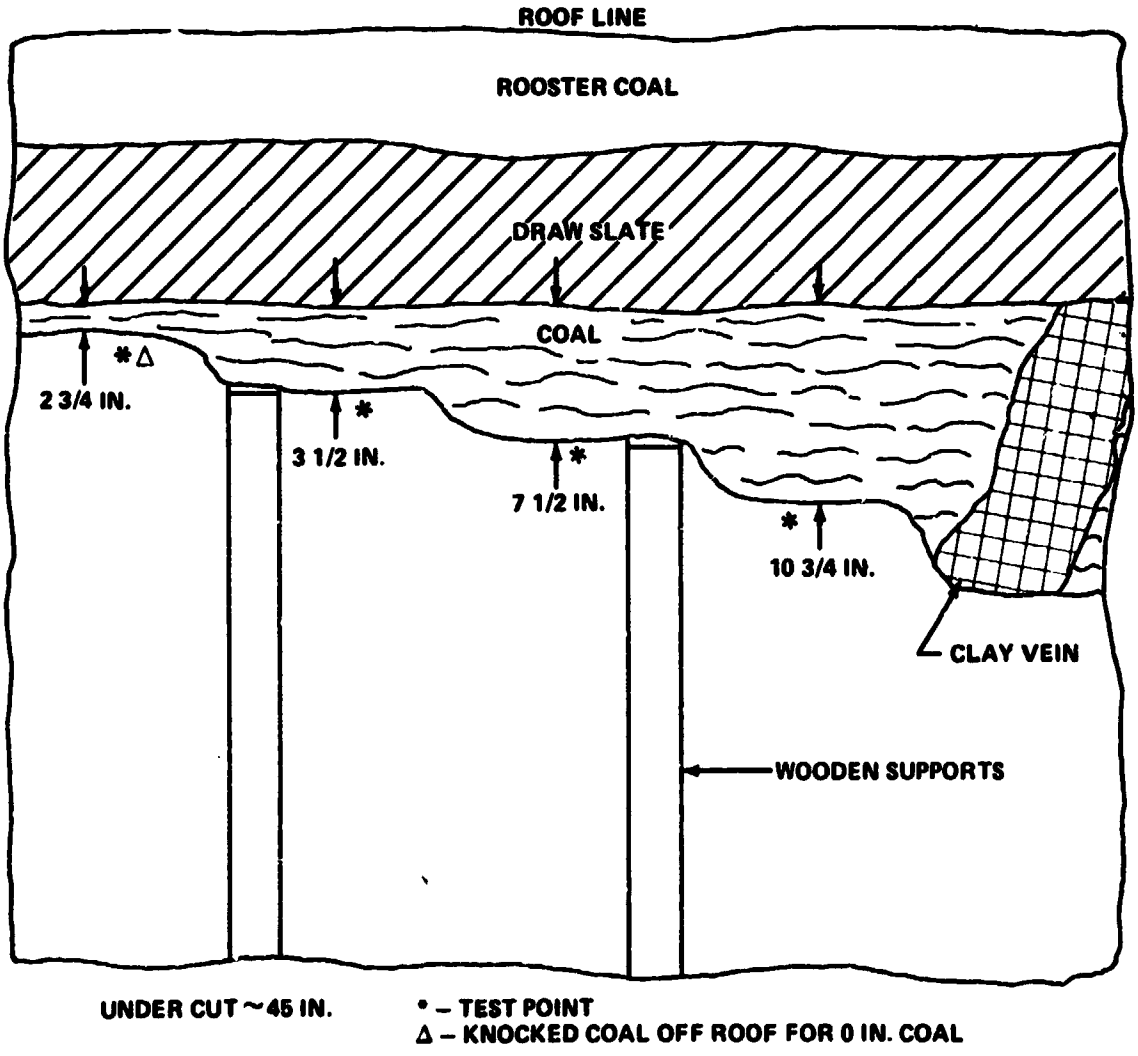

Figure 10. Bruceton experimental coal mine test area.

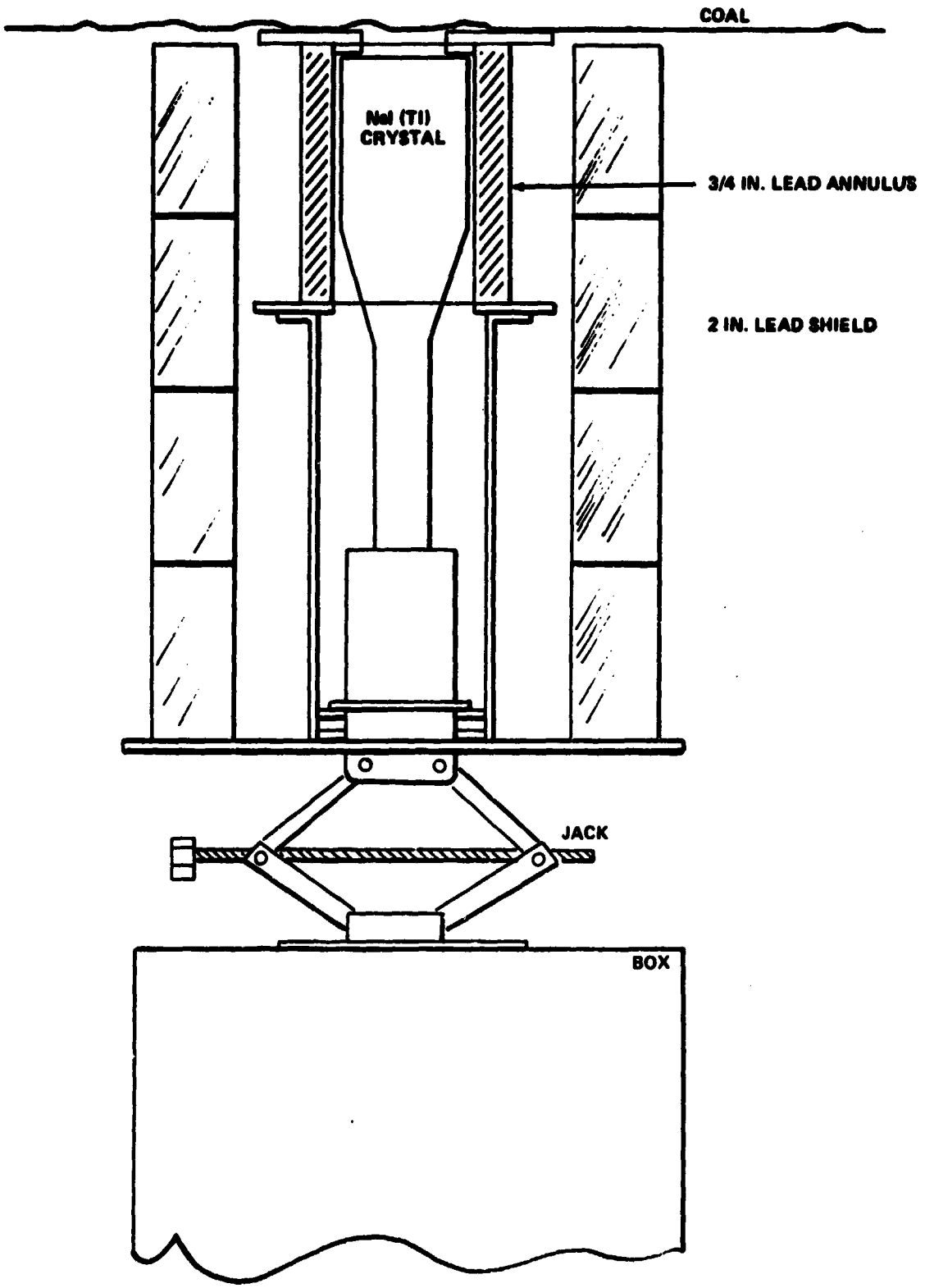

Figure 11. Extra shielding around detector.

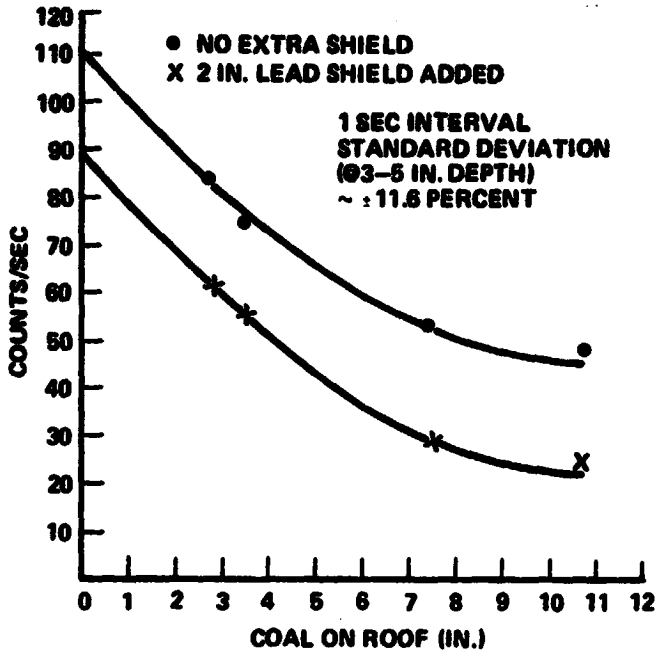

Figure 12. Bruceton test results (1 sec intervals).

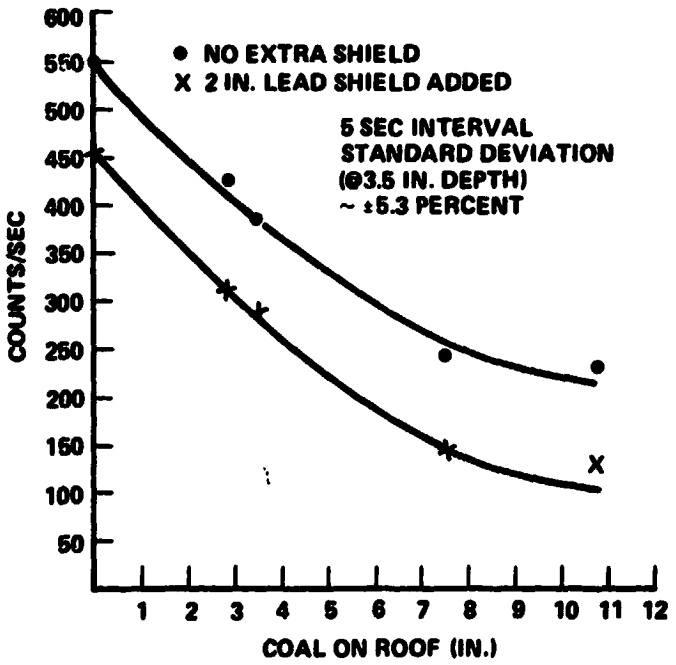

Figure 13. Bruceton test results (5 sec intervals).

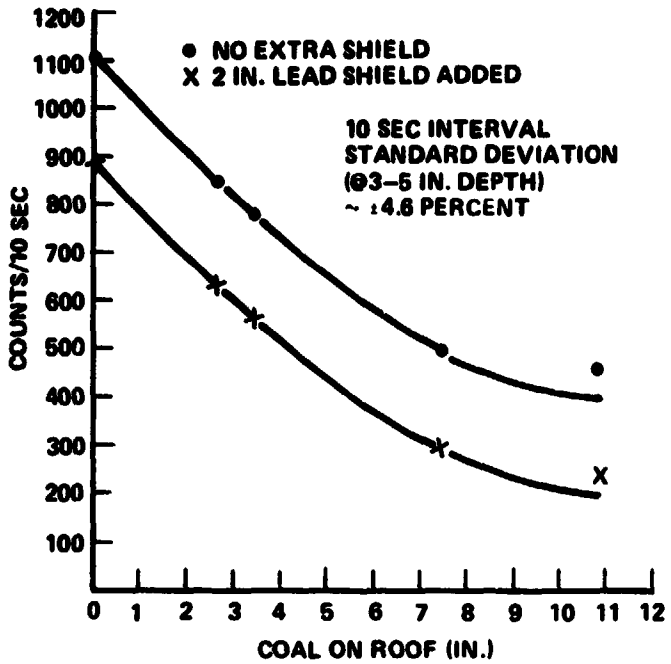

Figure 14. Bruceton test results (10 sec intervals).

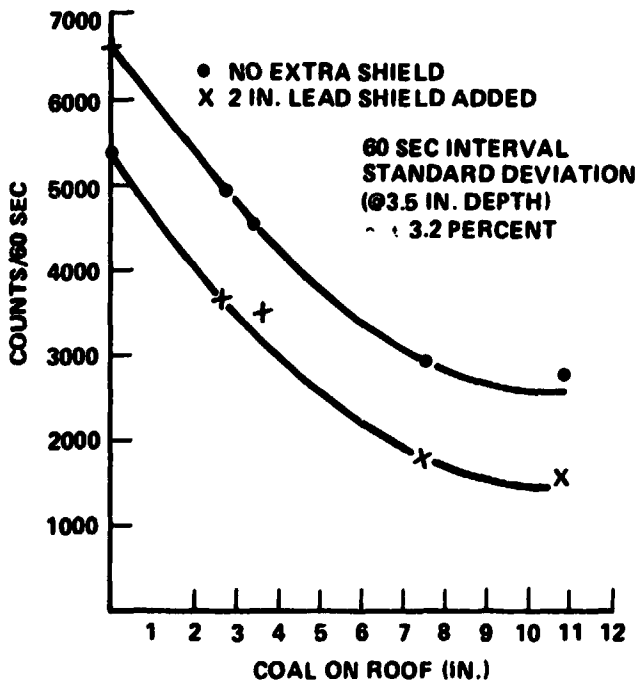

Figure 15. Bruceton test results (60 sec intervals).

Test results were considered satisfactory and characterized the performance and measuring capability of the sensor. It demonstrates that increasing the counting time improves the depth measurement statistics and that the addition of lead shielding around the NaI (T1) crystal/photomultiplier reduces the background radiation. The analysis of the amount and kind of shielding to optimize performance is still in process.

A second test at Bruceton was conducted in late September 1977 to obtain more data to provide a base for a more rigorous statistical analysis. Three-hundred readings were taken at each point on the roof and floor (Fig. 16). A least square quadratic was fitted to the data points. A detailed explanation of the statistical treatment of the data can be found in Appendix A.

3.3.1.4 Accuracy Improvement (Use of a Larger Crystal). Decreasing the dispersion for this particular 3 in. diameter crystal can be accomplished by counting for longer time intervals as shown in Figures 12 through 17. However, more counts in the same intervals from the rock source would also reduce the dispersion. Given the fixed nature of the intensity of radioactivity in shale, the only possible approach to increasing the counting rate is to increase the cross sectional area of detector exposed to the gamma flux. This can be done by adding more detectors of the same area (as discussed in Appendix C of Quarterly Report No. ALW-9, January - March 1977) or by increasing the cross sectional area of one single crystal. Since flux, ϕ, can be expressed as

$$\phi = \frac{C}{At} \frac{\text{photons}}{\text{in.}^2 \text{ sec}} ,$$

where

C = Counts

A = Cross section area (in.)

t = Time (sec) .

It can be seen that counts can be written as

$$C = A t \phi .$$

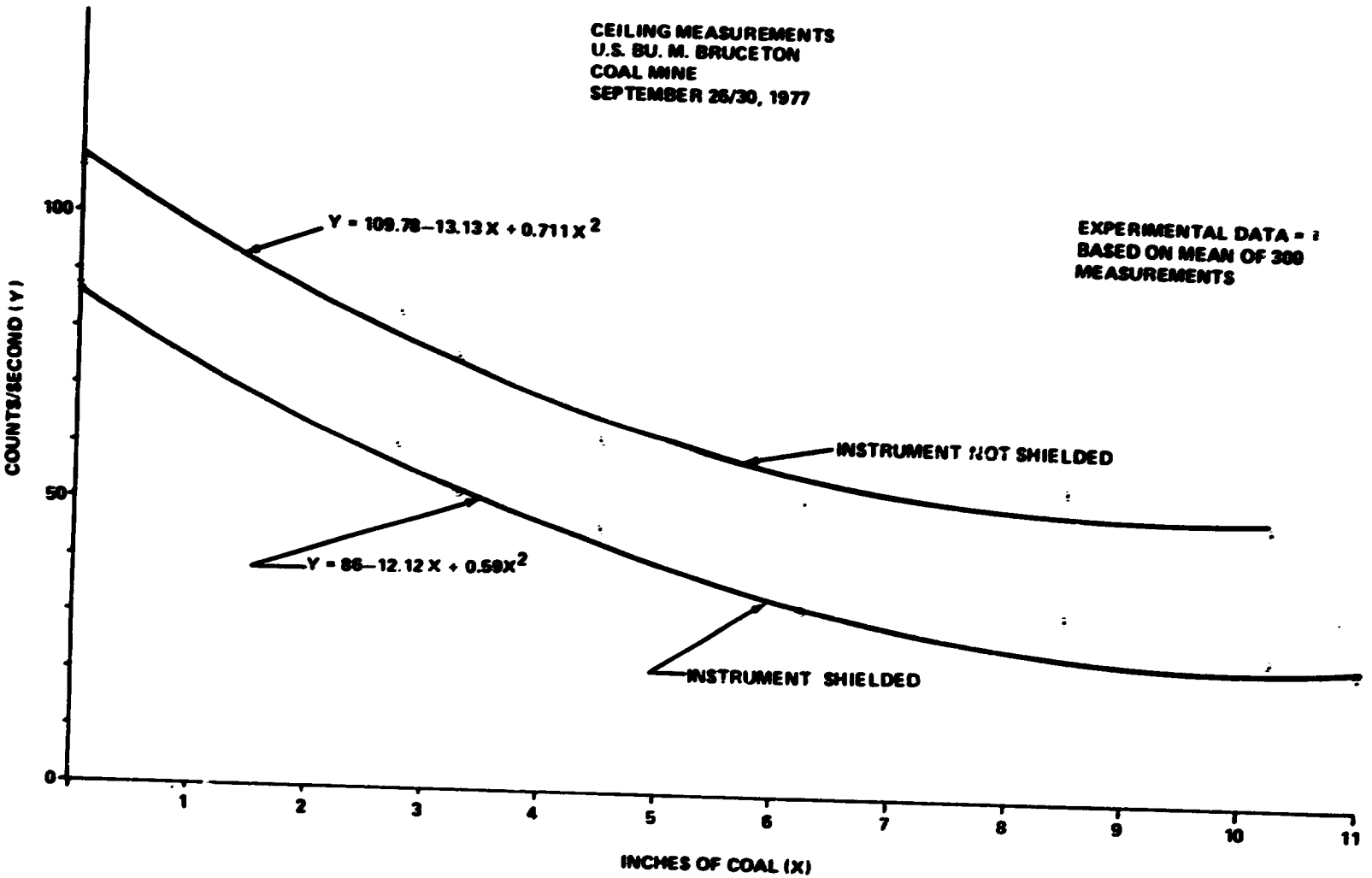

Figure 16. Natural radiation (ceiling measurements).

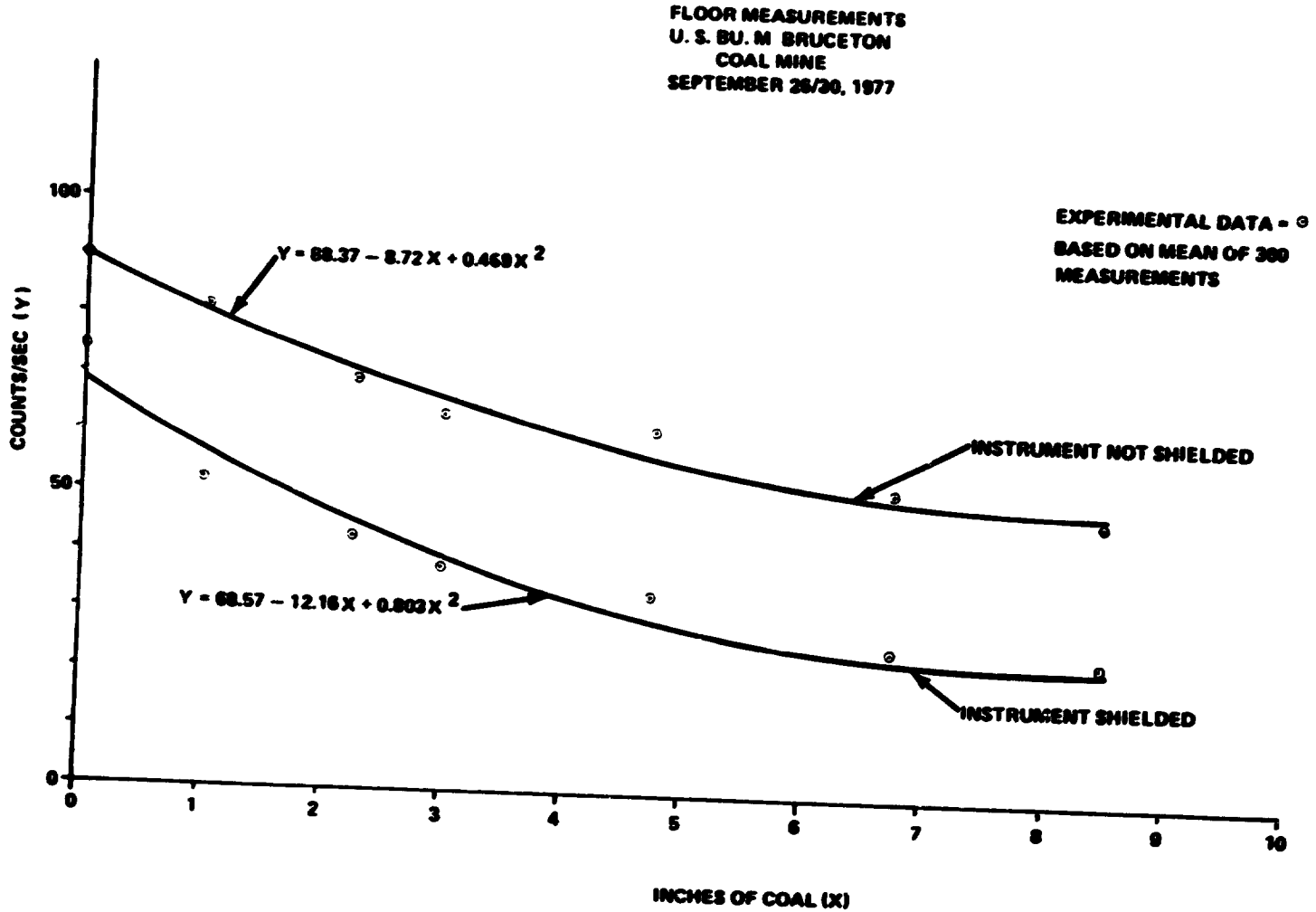

Figure 17. Natural radiation (floor measurements).

The radioactive intensity of the rock fixes ϕ and if t is held constant, then only A can be varied to increase the total counts. Because $A = \pi r^2$ for a cylindrical crystal where r is the radius, the ratio

$$\frac{A_2}{A_1} = \frac{r_2^2}{r_1}$$

can be used to predict the increase in counts by increasing r. For example if we increase the radius, r = d/2, from 1.5 to 2.5 in. the ratio is

$$\frac{r_2^2}{r_1^2} = \frac{(2.5)^2}{(1.5)^2} = \frac{6.25}{2.25} = 2.78 \quad .$$

Therefore, increasing the crystal diameter from 3 to 5 in. would yield 2.78 times the 3 in. count in a given time interval. For 110 counts/sec at zero inches of coal with the 3 in. diameter crystal, one would expect approximately 305 counts/sec with a 5 in. diameter crystal. Considering that an estimate of the standard deviation is given by the square root of the count for a Poisson, the fractional deviation can be computed:

$$\text{Standard Deviation} = \frac{\sigma}{\bar{x}} = \frac{\sqrt{\bar{x}}}{\bar{x}} = \frac{1}{\sqrt{\bar{x}}} \quad .$$

Therefore, for X = 110 counts/sec the Standard Deviation = 0.095 or 9.5 percent, and for Y = 350 counts/sec, the Standard Deviation = 0.057 or 5.7 percent.

A 5 in. diameter crystal is available as a standard item and at reasonable cost. Improvement of the detector shielding while maintaining a manageable weight for a portable unit could be accomplished by surrounding the detector with a NaI (Tl) crystal annulus to provide anti-coincidence signals at the scaler.

It is now planned to buy an unshielded and shielded 5 in. diameter crystal during the next year and incorporate the appropriate signal processing to achieve 1/2 in. or better coal depth resolution. Additional underground mine tests using the crystal shielded 5 in. scintillator will be conducted to verify this design approach.

3.3.1.5 Conclusions. Test results from the Warrior Basin (Nebo and Bessie Mines) show agreement within the margins of experimental error, which indicates that the radioactive content of the overlying strata is probably uniform within the Basin.

In comparing the results of the Bruceton test data with that of the Warrior tests, acceptable agreement was found in the magnitude of the radioactive contents measured.

These tests indicate that there is a good probability of using natural radiation measurements for coal depth sensing in coal mines of the Eastern US. More field tests in wider geographical locations will have to be performed before firm recommendations can be made. Analysis of the extensive test data (gathered at Bruceton during September 26-30, 1977) establishes that the data follow a Poisson distribution; a characteristic of the Poisson distribution is that the standard deviation equals the square root of the mean. The deviation of each group of readings for a specific coal depth measurement can then vary as much as 1 in. from the true measurement. This accuracy problem can be solved by running averages of a multiple number of separate counts reducing the measurement accuracy to 1/2 in. or less (Appendix A) or by use of a larger crystal (paragraph 3.3.1.4).

Improvements in the instruments performance, i.e., to decrease the weight of the shielding and thus the weight of the instrument, require redesign as well as the use of a larger crystal to increase the total number of event counts.

Preliminary results indicate this instrument is potentially feasible for use as a noncontacting coal depth sensor (for depths up to 6 in.) in coal seams overlayed and underlayed by shale or clay whose constituents contain a radioactive element.

3.3.2 Hydraulic Drill CID. Preliminary investigations of interface detection using hydraulic drilling principles have been completed. The concept appears feasible and a contract in the form of a grant has been let to the University of Missouri-Rolla. Term of performance is August 1977 to May 1978.

3.3.2.1 Detector Configuration. Hydraulic cutting techniques suggest an instrument consisting of a high pressure nozzle, a follower, and a sensing device such as a limit switch or potentiometer as shown in Figure 18. Conceptually, the nozzle would be mounted to project a cutting stream of high pressure water to impinge at a characteristic angle upon the coal. The angle of impingement of

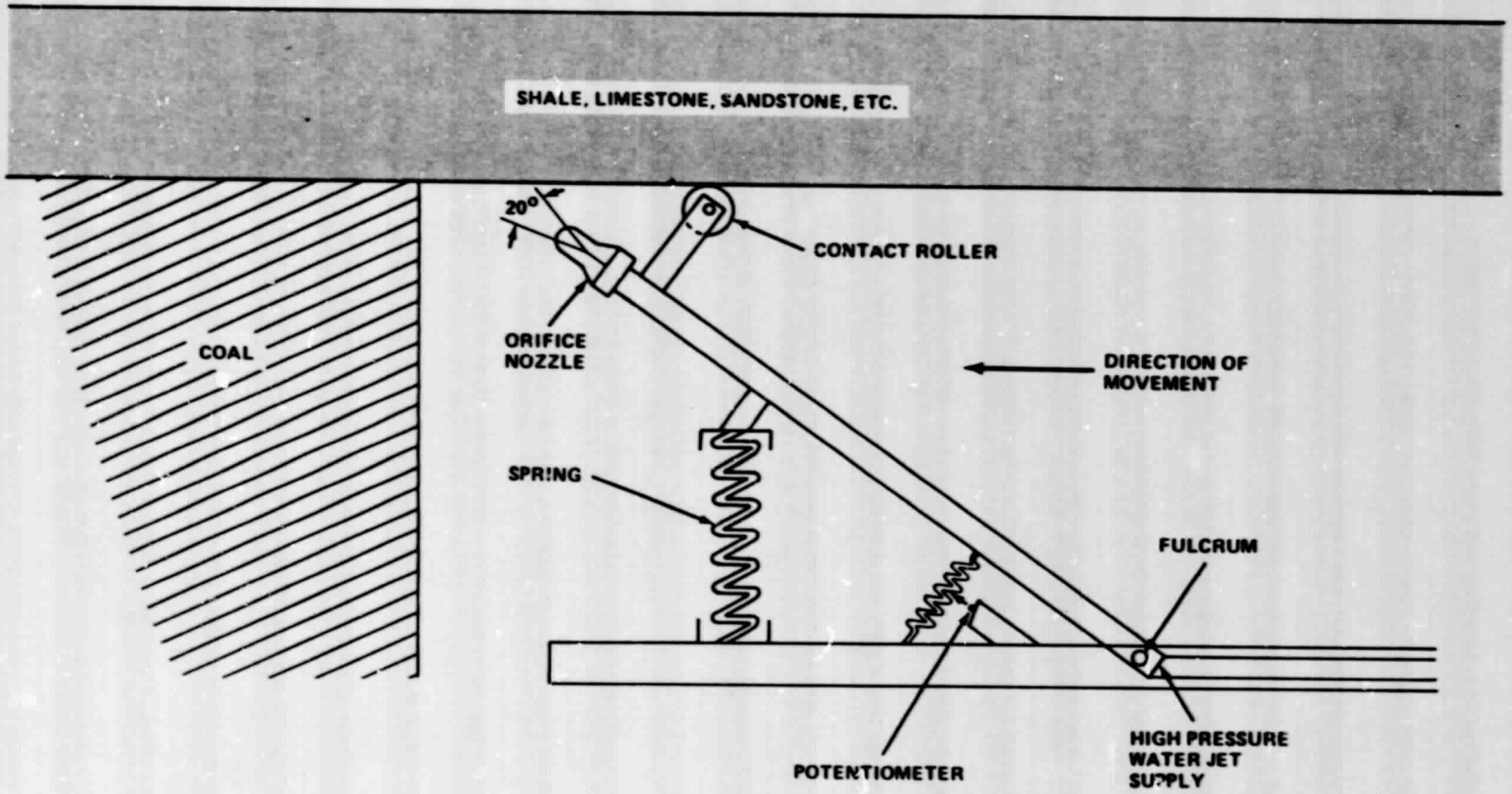

Figure 18. High pressure jet concept for coal interface detection.

the water would be selected to cut coal but not cut shale. The jet will cut the coal approximately 8 in. ahead of the nozzle. The follower, a contact roller, will follow the cut made by the water jet until the jet cutting action reaches the interface and penetration stops. The roller will then be depressed by the noncoal interface, compressing the spring-loaded acute angle formed by the nozzle's supporting boom on the base of the instrument, actuating a limit switch or potentiometer. The resultant signal can be used for control purposes.

A laboratory model of this instrument will be fabricated and tested. If laboratory tests are promising, arrangements will be made for more experimental tests in underground coal mines.

3.3.3 Acoustic CID Concept. Coal interface detection using an acoustic transducer is achieved by measuring the lapsed time required for an ultrasonic pulse, generated by the transmitter, to propagate through the coal, strike the rock interface, and return to the receiver. The loss of energy experienced by the transmitter signal is a function of the attenuation properties of the coal, the acoustical impedance mismatch occurring at material interfaces, and the incident angle of the wave as it strikes the rock interface.

The work which has been performed has been in two principal areas: (1) experimental determination of the attenuation of the transmitted acoustic signal in coal, under ideal signal coupling conditions and (2) development of a signal processing algorithm.

3.3.3.1 Acoustic Attenuation Test. A series of laboratory tests were conducted to determine the attenuation of the acoustic signal through coal. These tests were conducted using Bruceton mine coal which had been cut into rectangular sections. The test configuration is shown in Figure 19 together with the recorded data which have been plotted as signal attenuations (dB) versus inches of coal. These attenuation curves were obtained using transmitter frequencies of 0.10 MHz and 0.25 MHz with slopes of 10 dB/in. and 20 dB/in., respectively. The transmitter/receivers are Model 5055 PR by Panametric, Inc.

The curves intersection with the horizontal axis is indicative of the losses incurred as the acoustic signal enters and leaves the coal specimen. Notice that the data presented represent the loss of signal for transmission in one direction only. In actuality, the losses incurred in the acoustic CID would be twice as much because the transmitter signal would be reflected back by the rock interface through same coal thickness.

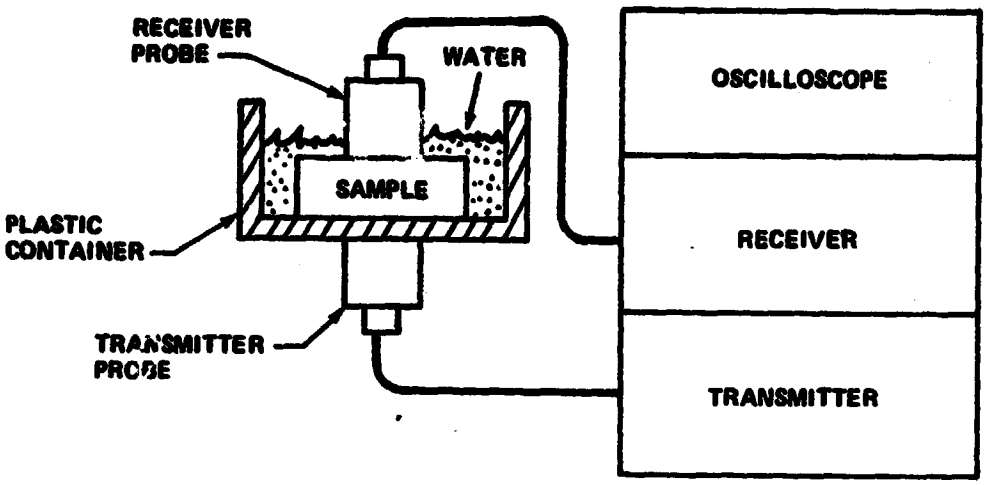

Figure 19. Acoustic experiment test setup.

3.3.3.2 Acoustic CID. Laboratory tests performed under ideal conditions with the 0.10 and 0.25 MHz ultrasonic transmitter/receivers have shown (Fig. 20) that the signal attenuation in coal is 10 and 20 dB/in. respectively. This value is 3 to 7 times greater than radar signal attenuation. The present theoretical depth measuring capability of an acoustic CID is 2.0 in. Plans for FY78 include investigating lower frequency transducer to improve the instrument's depth measuring capabilities.

3.3.3.3 FY78 Effort. Discussions with the Bureau have established that there is a need in the mining industry for a CID having 0 to 2 in. measuring capabilities. Therefore, work will continue in FY78 toward demonstrating this capability.

3.3.3.4 Conclusions. Preliminary investigations indicate that at the frequencies studied, the acoustic techniques can successfully measure approximately 1 1/4 in. of coal. The low signal levels of echos are a serious problem in measuring coal thicknesses (attenuation) and require good dynamic range of input converters; 10 bits give approximately 1000:1 range.

High peak signal levels are required for adequate penetration, which implies high peak-power levels and low duty cycles: desirable signals are short bursts or impulses.

A more comprehensive investigation is necessary which evaluates hardware characteristics (transducers, signal generators, amplifiers, filters, etc.) techniques of signal synthesis (to produce the most effective wave form) methods of coupling the signals to the coal, and signal processing methods compatible with low cost, reliable hardware to perform the processing function.

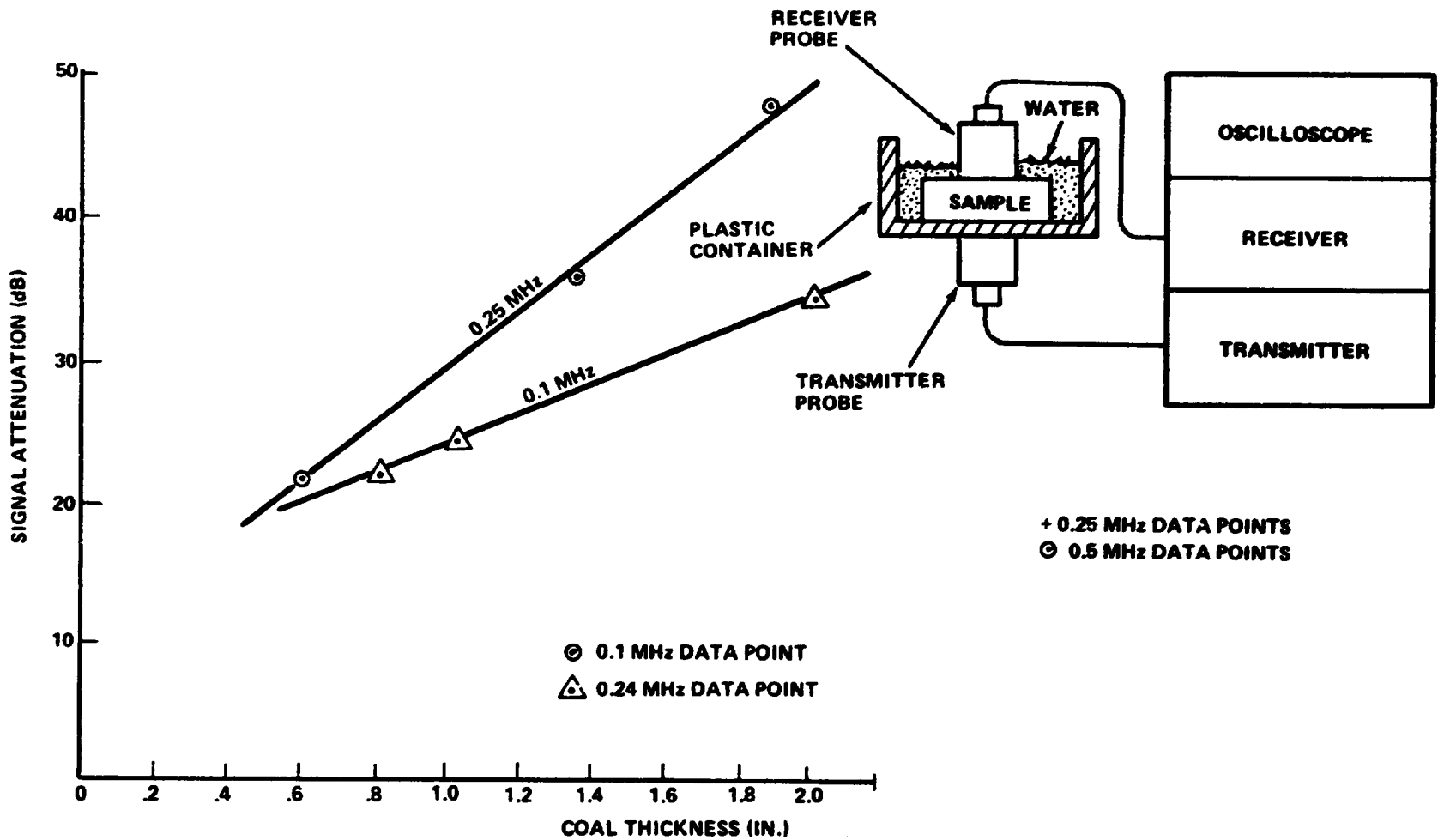

Figure 20. Acoustic attenuation test data.

3.3.4 Magnetic Spin Resonance. On August 20, 1977, contract (NAS8-32606) was let to Southwest Research Institute to investigate a system to measure coal thickness using RF resonance techniques. The process which is called RFRAS (Radio Frequency Resonance Absorption Spectroscopy) is made up of four techniques:

(a) Nuclear Magnetic Resonance (NMR)

(b) Nuclear Quadrupole Resonance (NQR)

(c) Electron Magnetic Resonance (EMR), also called Electron Spin Resonance (ESR)

(d) Microwave Molecular Resonance (MMR).

The contract objective is to study and measure the nuclear resonance properties of coal and shale and determine whether an RFRAS system can be built which will result in a new coal thickness measuring instrument.

Work to date has been concentrated on the EMR method. In EMR the potential detection technique would work as follows. Certain materials, such as coal, have a concentration of free electrons in them that have magnetic moments associated with the free electrons. These magnetic moments, when placed in a magnetic field, will align themselves either with or against the magnetic field in such a manner that they will be in one of two quantum mechanical energy states. If now an RF electromagnetic field is appropriately applied to these electrons, some of the electrons in the lower energy state can be excited to the higher energy state and the absorption of RF energy can be detected in an electron's circuit if the energy absorption is sufficiently high. The prime requirement for this detection is that there be a sufficiently high concentration of "free electron spin." Instrumentation has been developed that can precisely measure the free electron concentration in small samples.

For this technique to measure coal thickness there must be a substantial difference in electron spin concentration in the coal and shale. If there is a difference, it is possible to build a device that measures total spin concentration in the vicinity of the instrument, and as the coal gets thinner the spin total concentration that is measured will decrease in a well calibrated way.

For this reason one of the first tasks in this study was to send samples of coal and adjacent shale from several coal mine locations to Southwest Research Institute. The results to date are based on samples of coal and shale from a coal mine in Jefferson County, Alabama, and are preliminary but encouraging.

The instrument used for test was a Varian Model EM-500 Spin Resonance Spectrometer. Twenty-two samples were measured and plotted on a graph (Fig. 21) showing the peak to peak amplitude of the EMR response in arbitrary units. Figure 21 shows an abrupt change at the interface. The average value from the coal side is 85.3 where the average value of the rock side is 13.2 for change ratio of 6.48. The colors, black, gray, and brown, shown on Figure 21, are the colors of the test samples used in the laboratory experiments.

Samples from a coal mine in Bruceton, Pennsylvania, have also been sent to Southwest Research Institute for Analysis.

The next critical phase of this contract is to design a system and determine analytically whether it has the sensitivity to detect the coal thickness with sufficient accuracy.

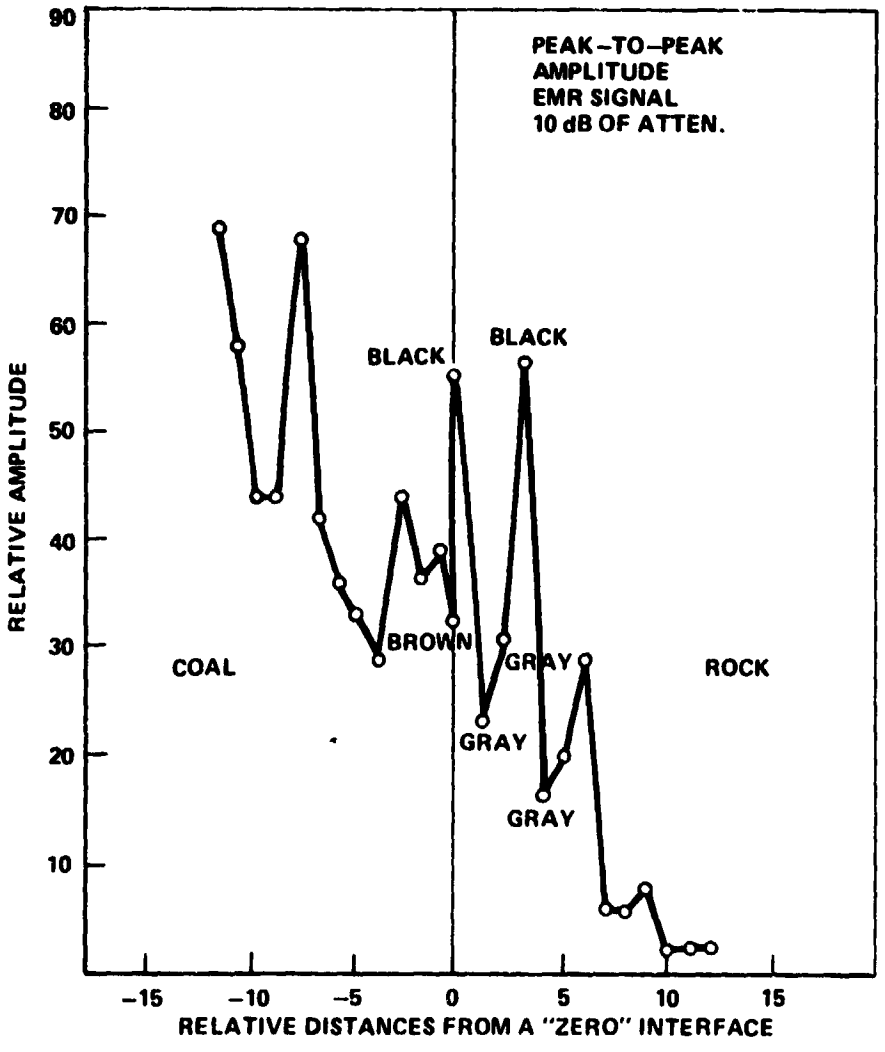

Figure 21. Sample of electron magnetic resonance response from coal and shale.

4.0 LONGWALL SHEARER GUIDANCE AND CONTROL

The work performed during the fiscal year ending September 31, 1977, on the research and development effort for a guidance and control system to be used on the longwall shearer consists of CID development and guidance and control studies (See Task B. RTOP 776-41-11).

4.1 Coal Interface Detectors (CID)

The primary effort during this reporting period was the analysis of laboratory and field test data that resulted in the identification of problems which affected the accuracy and use of the CID's. Based on these results, the emphasis has been on redesign and fabrication of second generation hardware for further test and evaluation.

4.1.1 Nucleonic Backscatter.

4.1.1.1 Test Results. During the week of August 30, 1976, the nucleonic CID was tested by U.S. Bureau of Mines Safety Research Coal Mine at Bruceton, Pennsylvania. The objective of this test was to compare the performance of the CID in the mine with that in the laboratory and with data obtained during in-mine tests in April 1976.

A test site was prepared by Bureau of Mines personnel, as illustrated by Figure 22. The numbers indicate reference points on 1 ft centers. It was intended that the two thicknesses on the roof and floor should be 3 in. and 6 in. Actual measurements of coal depth at selected points are shown in Figure 22. These depths were obtained by drilling holes into the roof and floor. The roof was undercut to a depth of approximately 67 in. and supported by wooden posts. An aluminum track was placed under the roof to provide support for a small cart on which the CID could be rolled back and forth. As is shown in Figure 20, the CID mounted on the cart was positioned against the roof by a scissors jack.

The data for each measurement were recorded in tabular form together with a visual description of the roof surface and test point numbers locating the center of the CID. Additionally, roof profile information was recorded on a tape recorder during the testing of the reflectometer CID as position along the track was recorded from a slide potentiometer on another parallel channel.

Two nucleonic units were tested: one with a 20 in. source-detector separation and a depth sensitivity of 7 in., and the other with a 7 in. source-detector separation and a low energy radiation source and a depth sensitivity of 3-1/2 to 4 in.

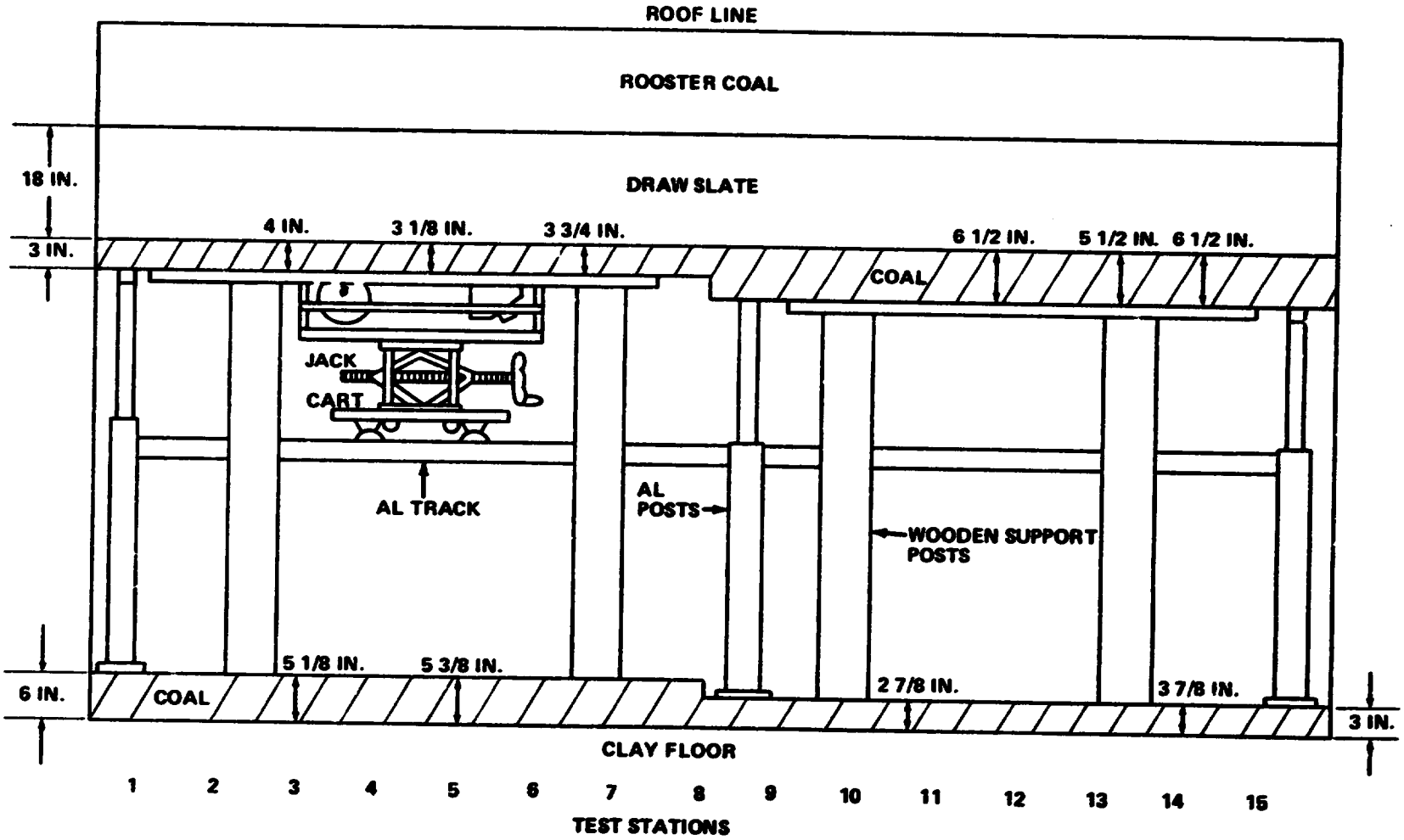

Figure 22. Test site.

The 20 in. CID was a two point contact model (Fig. 23). Its detector housing was not rigidly attached to the frame, allowing small movement so that the surfaces could more nearly conform to an irregular profile.

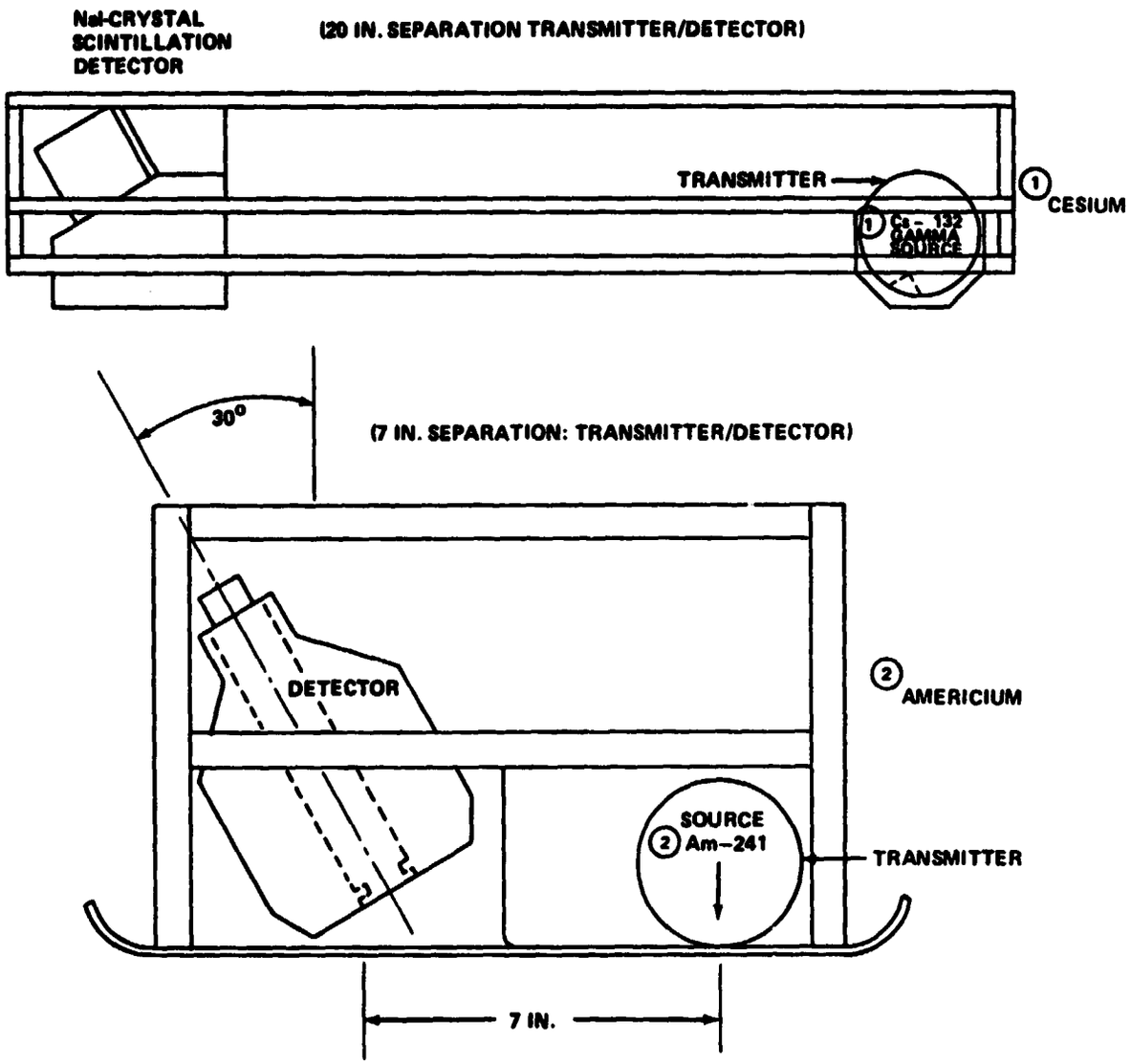

Figure 23. Experimental nucleonic CID.

The 7 in. CID had a flat bottom which made it more susceptible to air gap distortions from any single high point over the area of contact (Fig. 23).

Evaluation of the measurements of roof and floor coal depth taken with the 20 in. CID was accomplished by plotting the micarta bed. A corrected calibration curve was generated to reflect the difference in density of micarta and coal. This curve is shown as a dashed line in Figure 24. The specific gravity of the micarta is approximately 1.4 and the reported specific gravity of coal from the Bruceton mine is 1.5; an approximate calibration curve for coal was obtained by reducing the micarta counts by 7 percent.

One systematic source of error was built into the CID because the detector housing was not rigidly fixed in the CID frame. It was possible for the detector housing, which shields the detector from the source, to tilt forward, putting more lead in the path of back-scattered photons (Fig. 25) which resulted in a lower counting rate. This situation could have occurred if the CID was on a surface sloping upward (on the roof) in a way that yielded a low region of coal toward the CID center. Such a case may have occurred for tests Nos. 4 and 5 in Figure 22. Similarly, the detector housing could have tilted back when positioned over a bump, increasing the counting rate as in test No. 7.

The failure of the point in test No. 9 to fall on or closer to the curve is attributed to the accumulation of water on the floor from the cutting machine. Water quickly filled a hole drilled at station 10.5 when the actual coal depth was determined. The addition of water to cracks in the coal should increase the density of the material. Another contributing factor could have been due to the detector housing tilting forward (Fig. 23). All references to air gap in the figure are taken from visual observation of the interface. Very low accuracy of actual air gap size was obtained in this manner. It was anticipated that the profile information obtained from the reflectometer test could be used to verify visual observation; however, this information was unusable because of a recorder malfunction.

Laboratory analysis of the 20 in. CID reading when air gaps were present between the source and detector indicated that higher readings occurred as the position of the air gaps was moved toward the detector. This appears to be substantiated by the in-mine readings; i.e., when the air gap was observed under or close to the detector, the reading deviated most from the calibration value as in tests Nos. 6 and 7 of Figure 24.

The data from the 7 in. CID in-mine tests are plotted in Figure 26. Again, the laboratory calibration curve was corrected to reflect the difference in density between Micarta and Pittsburgh coal. As with the 20 in. CID, the air gap reference was taken by visual inspection. This unit responds in the same way to air gaps as does the 20 in. CID. However, when the air gap is located directly opposite the detector position and if it is small compared to the source detector separation, the deviation from the expected reading is smaller than for the case where the air gap location is between the detector and CID center.

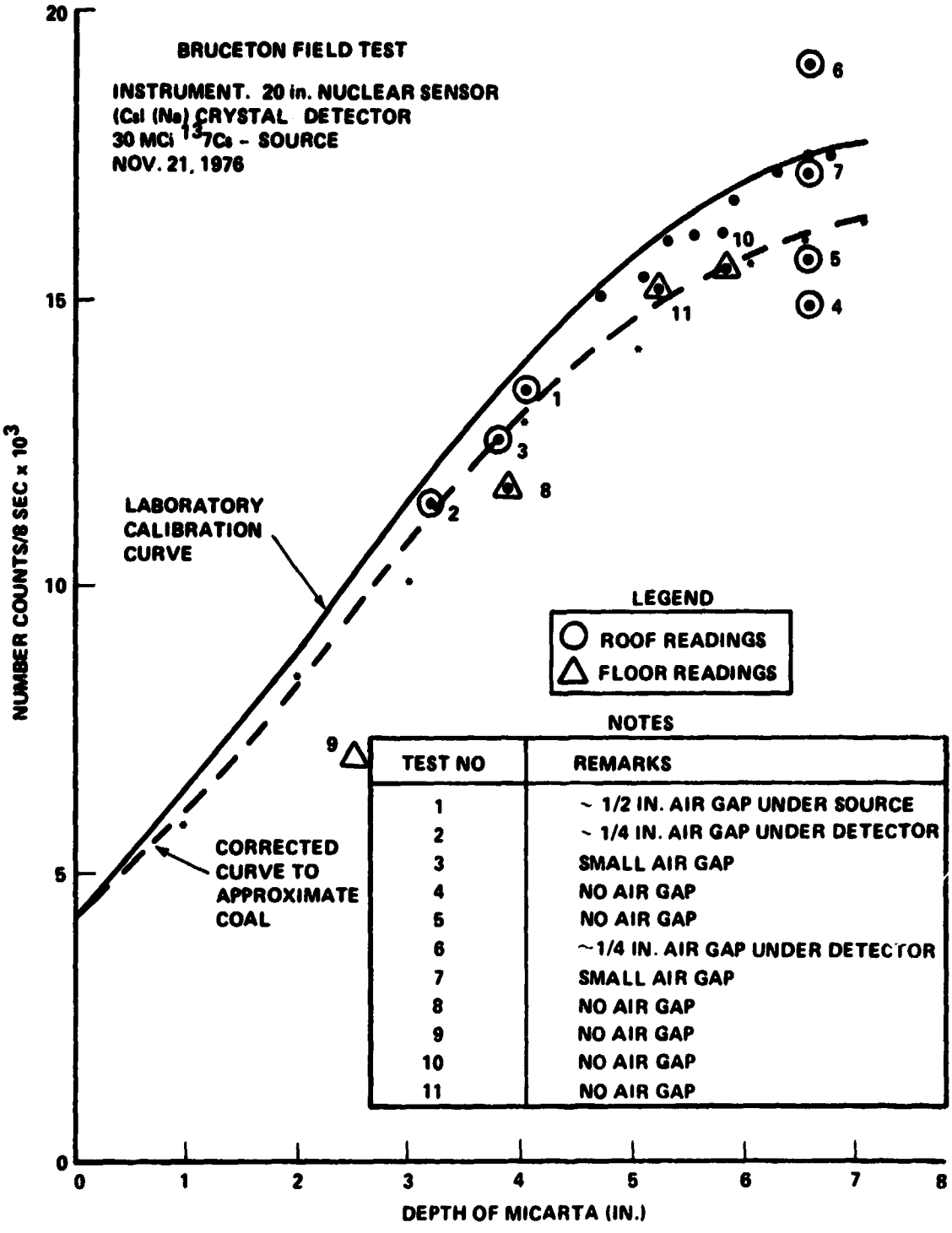

TEST NO	REMARKS
1	~ 1/2 IN. AIR GAP UNDER SOURCE
2	~ 1/4 IN. AIR GAP UNDER DETECTOR
3	SMALL AIR GAP
4	NO AIR GAP
5	NO AIR GAP
6	~1/4 IN. AIR GAP UNDER DETECTOR
7	SMALL AIR GAP
8	NO AIR GAP
9	NO AIR GAP
10	NO AIR GAP
11	NO AIR GAP

Figure 24. Corrected calibration curve showing the difference in density of micarta and coal.

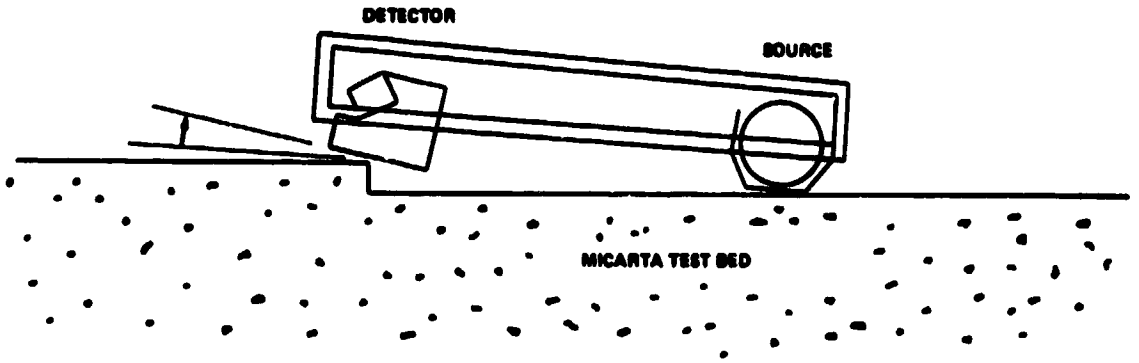

Figure 25. Nucleonic CID.

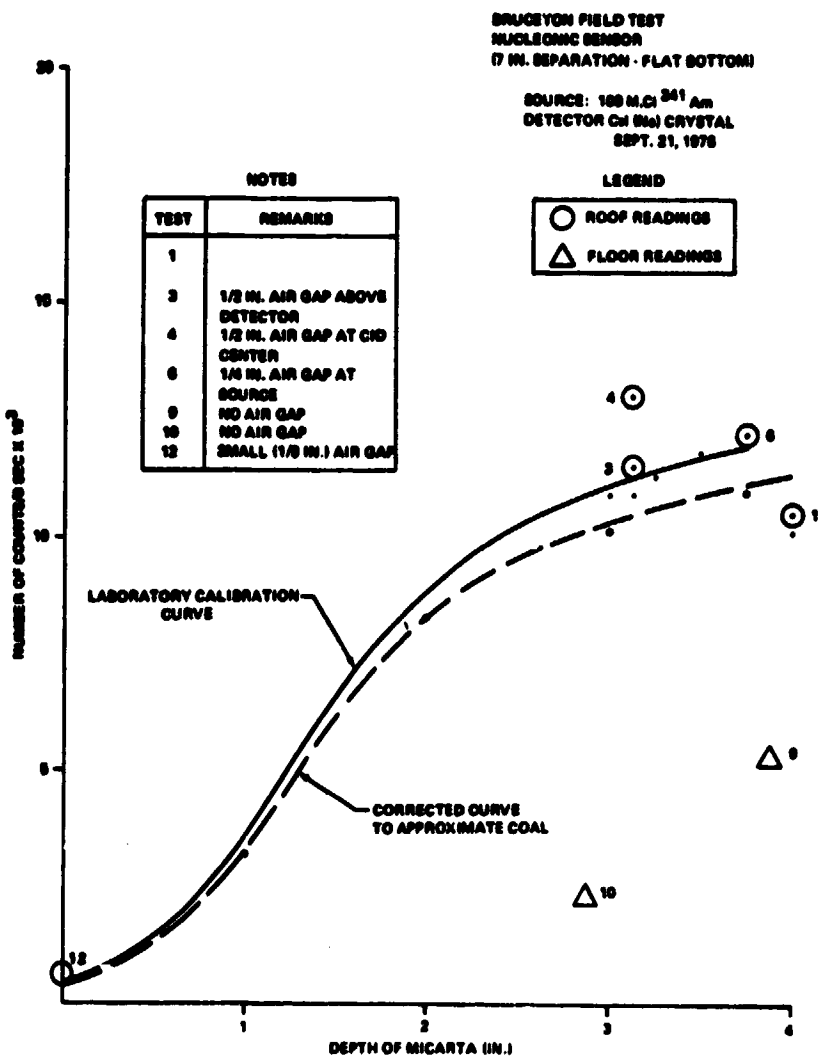

Figure 26. Data from the 7 in. CID in-mine tests.

4.1.1.2 Design of a Two-Point Contact Configuration. Design of a two-point contact fixed frame CID, similar to the laboratory version tested in the Bruceton Experimental Mine, was begun in the summer of 1976 and continued into early 1977, when a completed conceptual design evolved. In parallel, a floating head configuration (Figs. 27, 28, and 29) was developed using the design concepts of the fixed frame version but incorporating independent suspension for the detector and source modules.

Figure 27 presents a top view of the positioning of independently suspended modules for the detector and source on the mounting bar. Only the detector module is movable along the mounting bar. Figure 28 presents some details of the source housing. A portion of the hydropneumatic spring suspension is shown in the right view of Figure 28, and parts of the mechanical source activation mechanism are shown in Figure 29.

Figure 30 presents a few details of the detector module including the positioning of the scintillator detector, collimating, shielding surrounding the crystal scintillator, and the urethane dust cover above it.

Part of the design effort involved establishing requirements for mine permissibility to allow field testing in an underground coal mine. Consequently, a meeting between MSFC and MESA personnel was held in Pittsburgh in February 1977. At that meeting, the design of the CID and the display box (Fig. 31) were reviewed, and the following decisions were made:

(a) The display box contained nonintrinsically safe electronics and must be explosion proof. The box including cables would be purchased from supplies of explosion proof battery boxes.

(b) Power for the mine permissible CID should be from a battery rather than from the longwall machine during the field test phase.

(c) All electronics in the nucleonic sensor are probably intrinsically safe; however, the photomultiplier tube will have to be tested to verify safety.

(d) Cabling should be purchased from suppliers of mine permissible cables, and the lead entrances between the battery box, the display panel, and the CID must be packaged in an approved stuffing box (would be supplied by box manufacturer).

Funding delays prevented the release of a fabrication contract for the fixed frame version CID until the independent suspension configuration concept

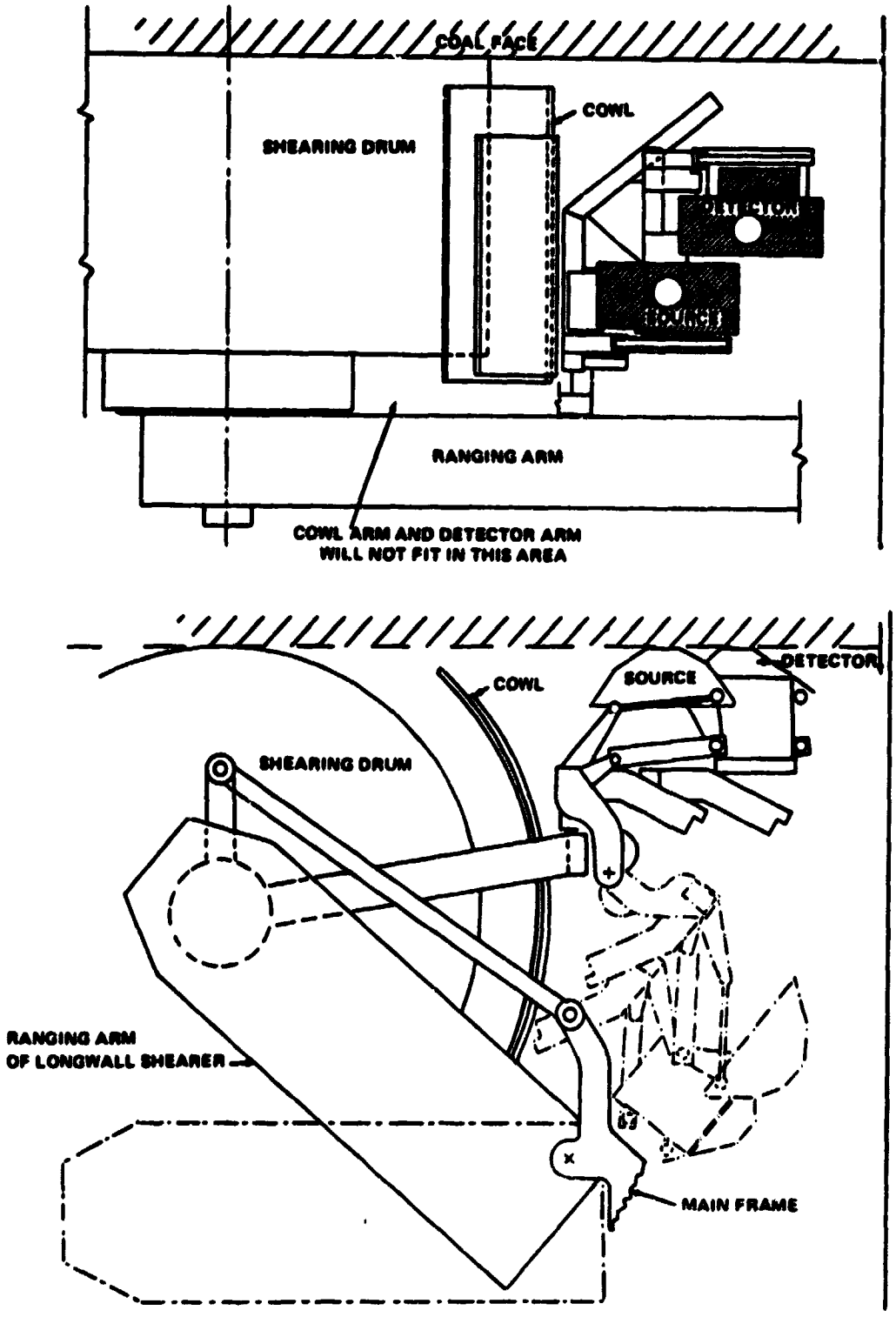

Figure 27. CID positioned on longwall shearer.

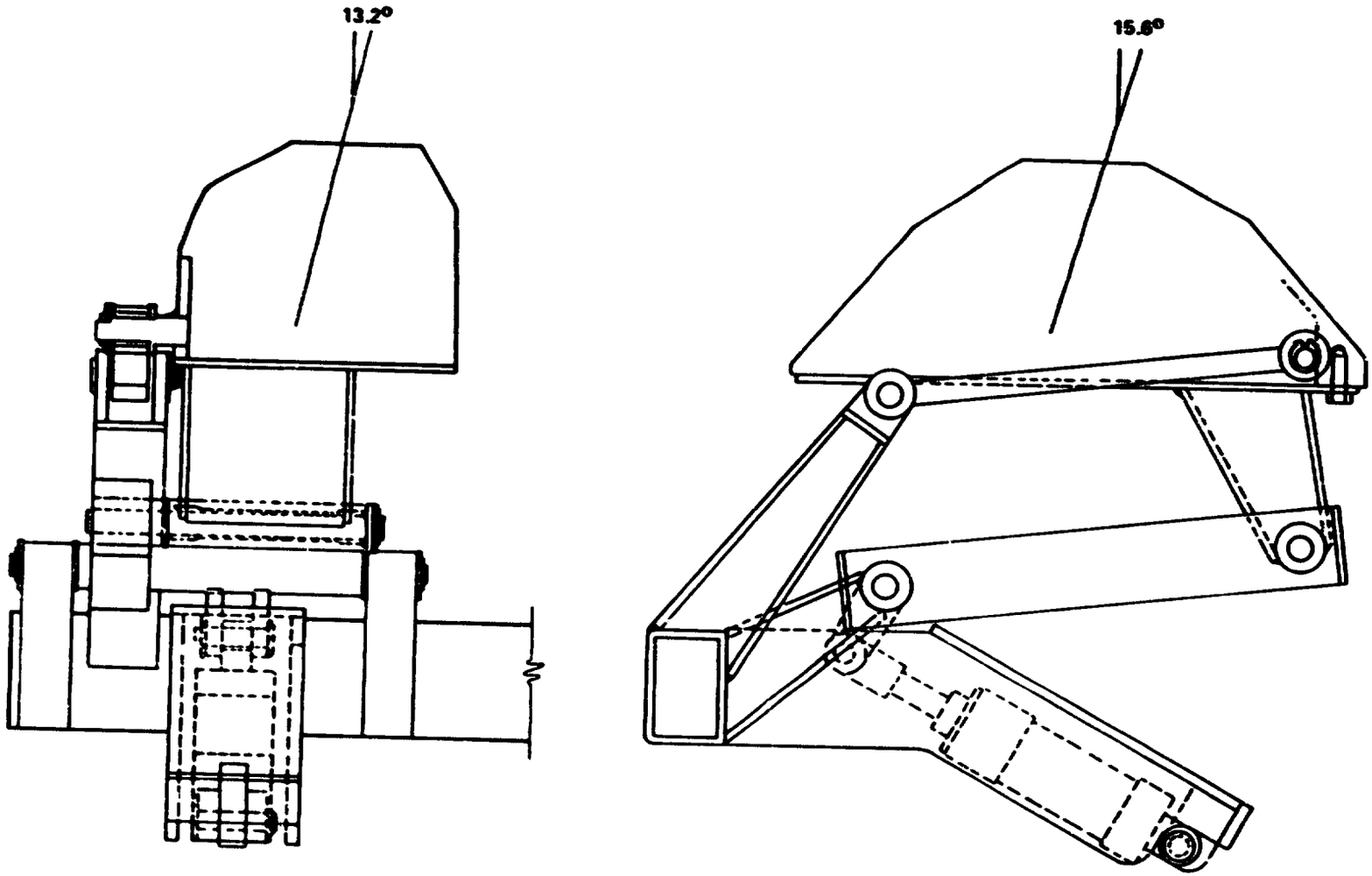

Figure 28. Coal interface detector.

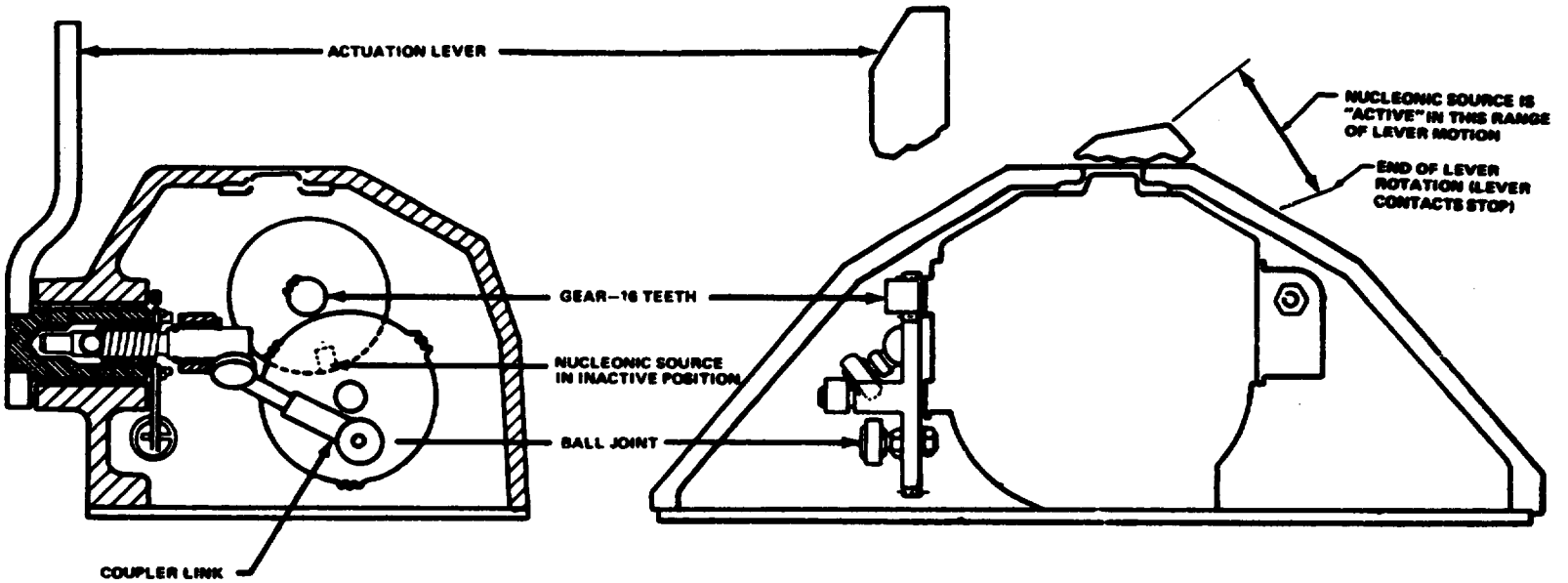

Figure 29. Nucleonic source, housing and spatial 4-bar linkage, actuation mechanism.

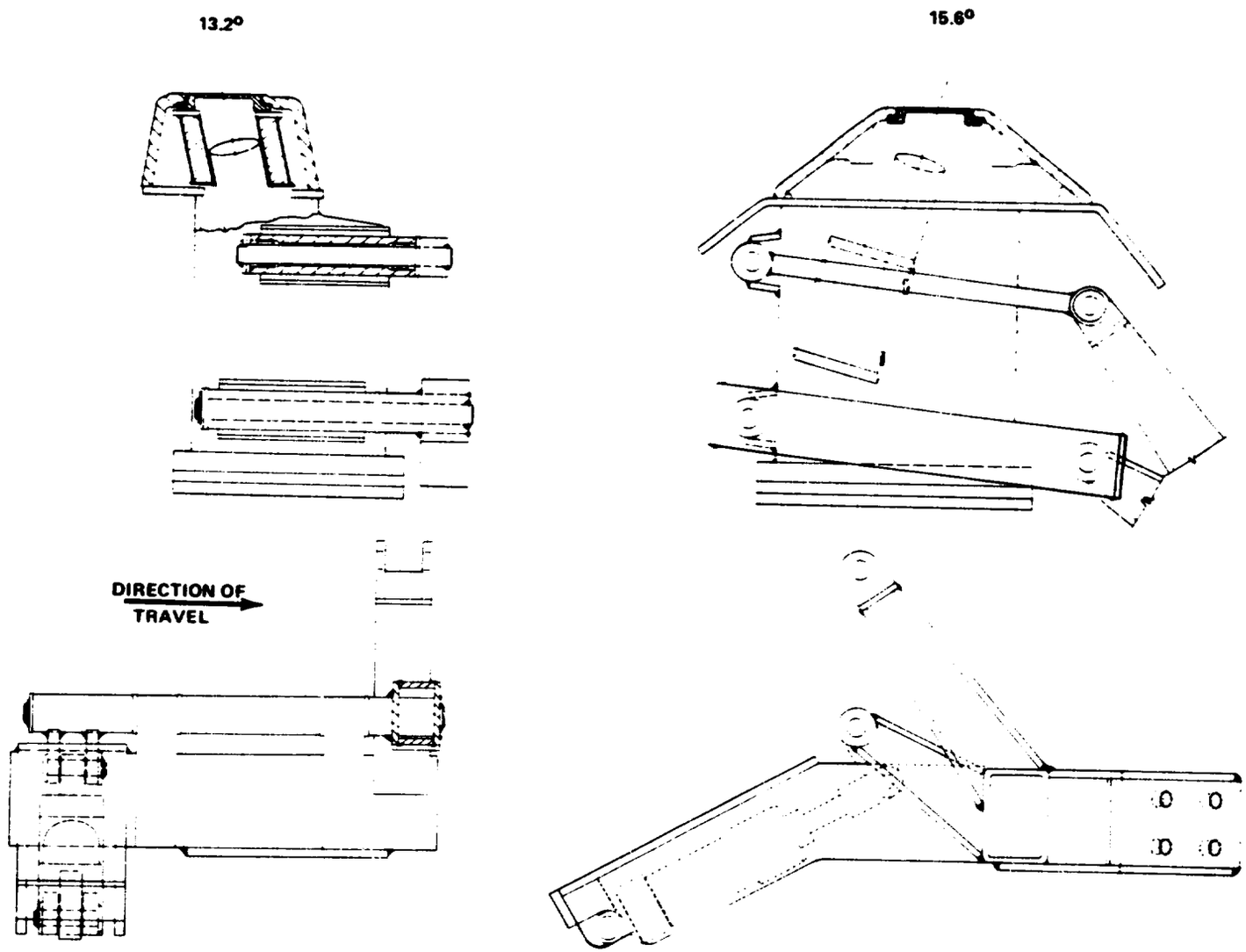

Figure 30. Coal interface detector.

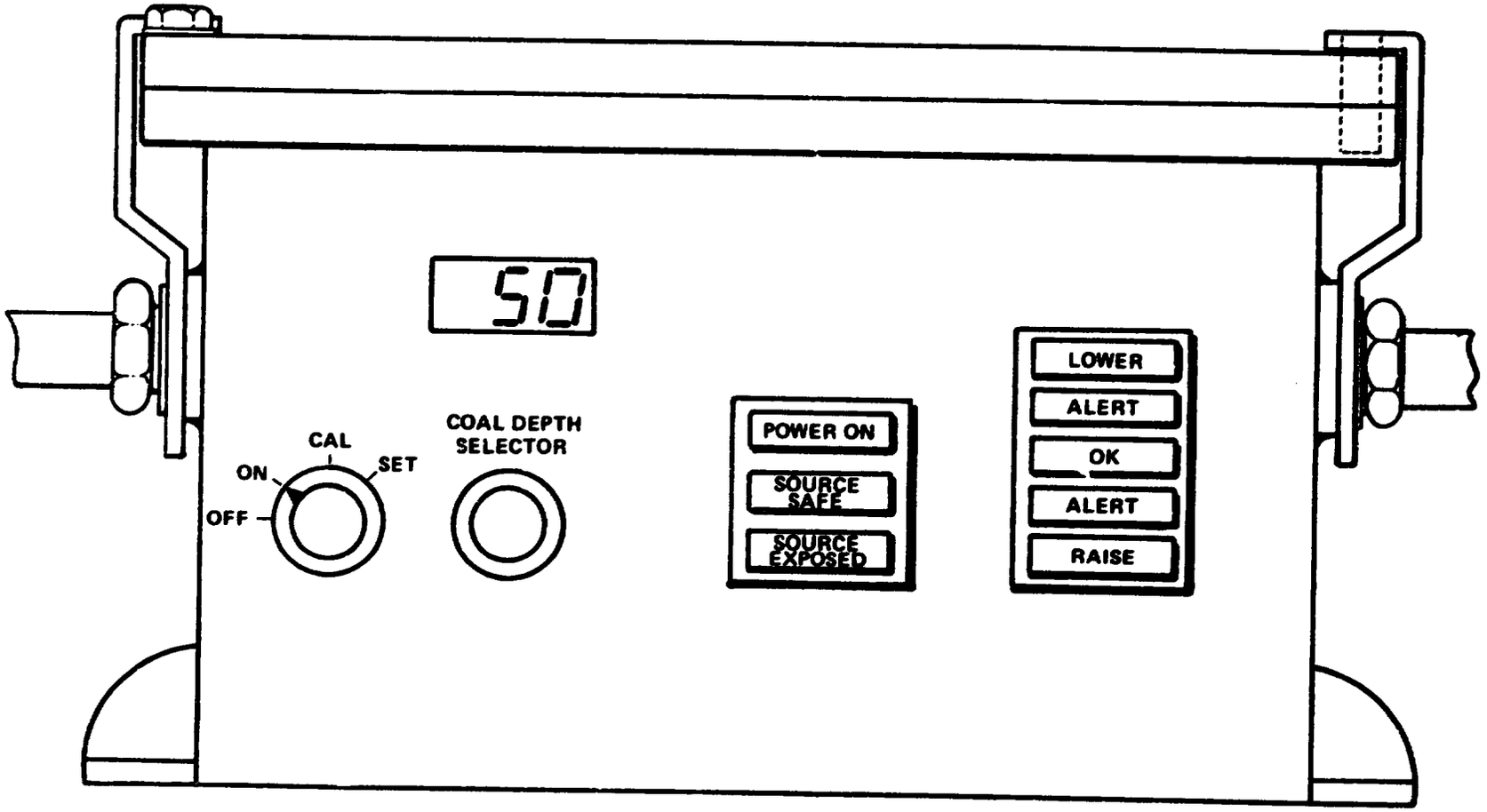

Figure 31. Gamma backscatter CID display box.

was completed and in March 1977; a design review was held at MSFC to evaluate this floating head design. A decision was made to build the floating head design because it offered many advantages over the fixed frame version. Further discussion of floating head design can be found in Contract NAS8-32214 Final Report [3].

4.1.1.2.1 Floating Head Configuration. In April 1977, procurement actions were prepared for design and manufacturing services required to build a floating head CID and the associated display box (Fig. 31). A contract for the display box was awarded to the Huntsville Division of Sperry-Rand on June 1, 1977, for the total cost of $5000. The unit was delivered in September 1977. MSFC will install the decimal digit display and a signal processor printed circuit board, and will provide the power source which can be either an ac-dc converter or a battery. The ac-dc power supplies, decimal display, and processor circuit have been purchased, assembled, and tested on the bench. All are performing satisfactorily and are ready to interface with the display box.

The procurement action for the design completion and manufacture of two CID units was awarded to Sperry-Rand on July 1, 1977, for $38 651 with delivery expected in November 1977. MSFC separately purchased the radiation sources, the scintillator detectors, amplifier circuit boards, and dust covers to be fitted to the mechanical assembly when delivered.

The MSFC purchased items have been delivered except for the scintillation detectors which have a delivery date of December 1977. All of the electronics including the amplifier, processor, ac-dc power supply, and a previously purchased scintillator detector have been integrated in the laboratory. Several interface problems have been corrected and the components are ready for installation.

4.1.1.2.2 Signal Processing. Signal processing for this experimental model has been simplified intentionally. Specifically, the calibration curve was linearized by taking the best straight line fit to data points from 0 to 6 in. coal depth as shown in Figure 32. The sample data points of Figure 32 are taken from the two-point contact 20 in. separation CID. The processor electronics in Figures 33 and 34 store pulses from the detector in a binary counter for 1 sec integration time. At the end of this period, the digital count is transferred to the holding register and converted to an analog voltage. This voltage is compared to the calibration curve in the region of interest through the voltage comparitors (Fig. 34).

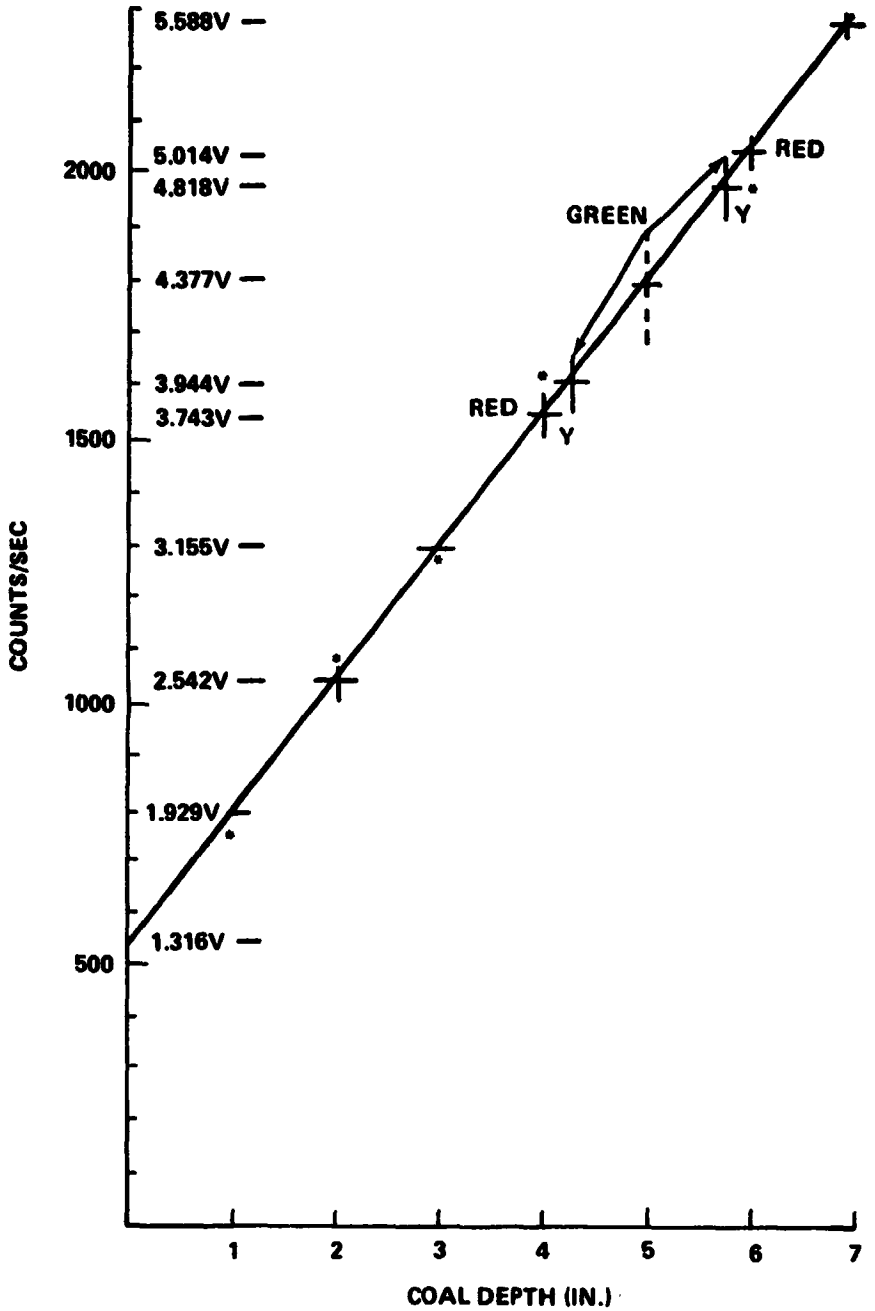

Figure 32. Nucleonic backscatter CID linearized calibration curve.

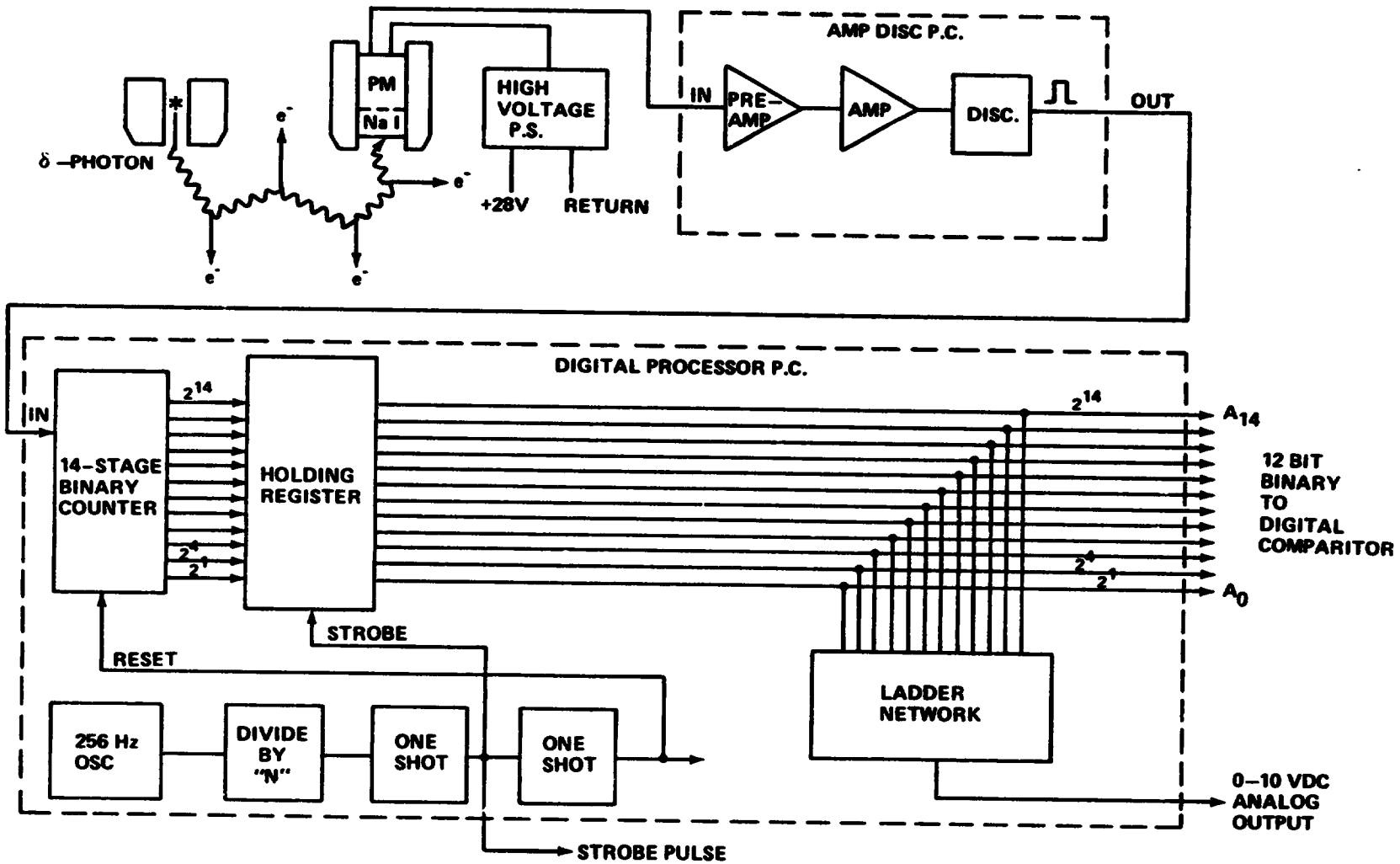

Figure 33. Nucleonic CID investigation.

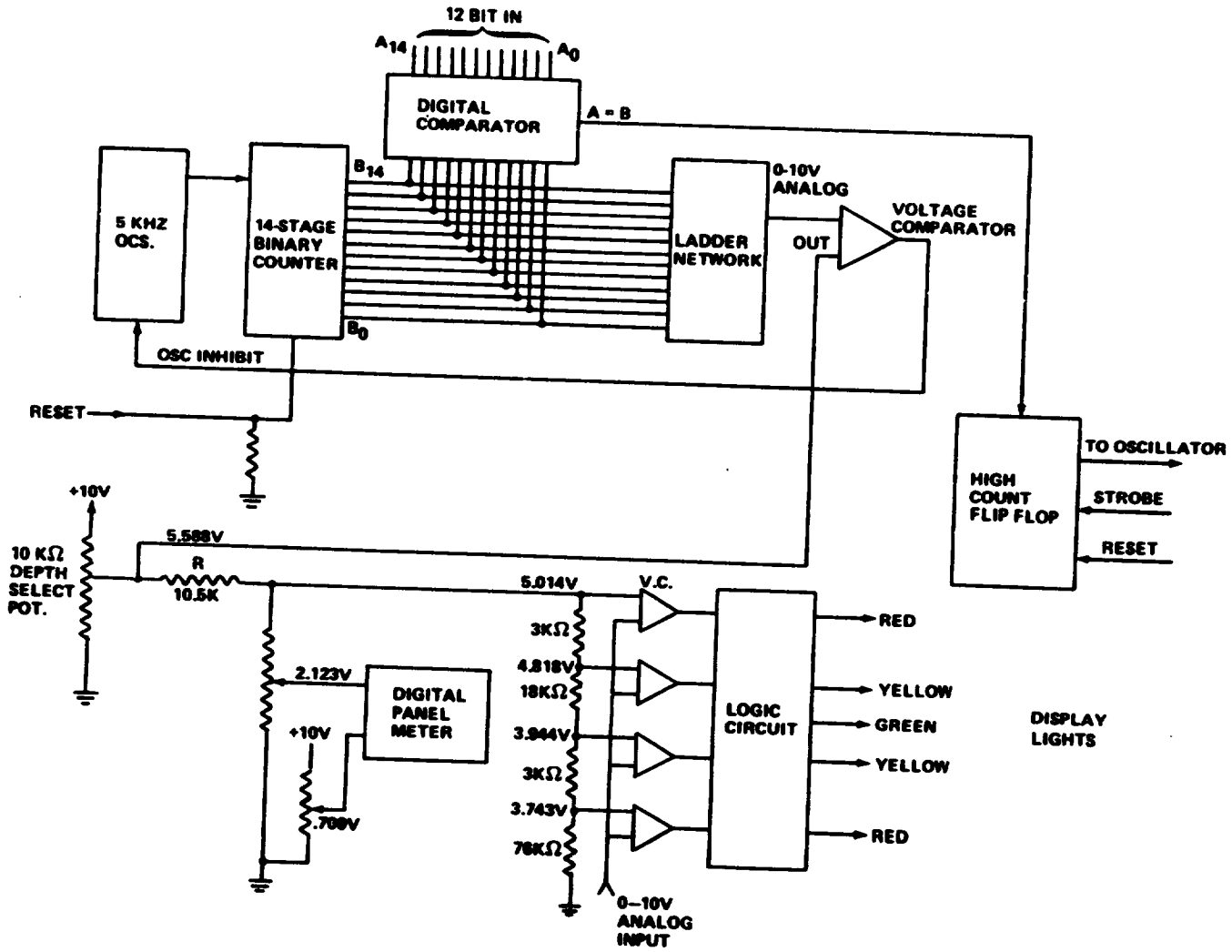

Figure 34. Nucleonic signal processor.

In Figure 32, for example, 5 in. is the selected operating point and +1 in. is allowed as an error band. If $3.944 \leq V \leq 4.818$ then the green light marked "OK" will light up on the display, Figure 31. However, when $4.818 \leq V \leq 5.014$ or $3.743 \leq V \leq 3.944$ one of the yellow lights marked "ALERT" will come on. Above 6 in. or below 4 in., one of the red lights marked "DOWN" or "UP" will light up. By adjusting the depth select potentiometer on the display box, the region of interest can be moved down the calibration curve with the new operating point display on the readout. An added option can be utilized by turning the mode switch one position clockwise from "SET". In this position the reading on the digital panel meter will be a real-time coal depth. When the count rate reaches that for 7 in. of coal in Figure 32, the true count determined from the data in Figure 24 is really greater than 2180 counts/sec. At this point the processor electronics will activate an oscillator in the message light driver circuit which will cause the red light marked "UP" to blink, indicating that an air gap is probably present and the action indicated should be ignored.

The visual indicators in the display are intended to be used by the machine operator or for laboratory tests of the CID. Signals to the visual indicators could just as easily be routed to a VCS.

4.1.2 Sensitized Pick. The Shaker Research Corporation under contract to MSFC has undertaken the task to design, fabricate and mine test on a longwall machine various configurations of the "Sensitized Pick" CID. Data will be obtained on pick forces and accelerations under various cutting conditions (i.e., coal only, roof rock, and floor). These data will be analyzed in the MSFC laboratories to establish a suitable signal processing technique for distinguishing the cutting of coal versus non-coal materials. Hardware has been fabricated, MESA and state permits have been made, and tests are expected to begin in the last quarter of 1978 at the Rochester and Pittsburgh Coal Company's Jane Mine.

4.1.2.1 Concept. The basis for application of a sensitized pick CID is the significant difference between the force required to fracture coal compared to that required to fracture rock or soft clay. Because coal is a pre-fractured material it tends to break away along strata planes in relatively large chunks, while rock is homogeneous and breaks up into smaller pieces. Clay is sheared easily. Compressive and shear strengths are greatest for rock, moderate for coal, and lowest for clay; therefore, a transducer which can measure the difference in bit cutting force between these materials can be used to provide cutting drum position control to automate that portion of mining machine operation.

Application of bit cutting force to machine control has a few unique problems which make the application of this technique rather interesting. First of all, the cutting action of the drum type cutter provides a variation in cutting depth which is a minimum at top and bottom (ceiling and floor) and maximum at the centerline height of the drum. A depth-of-cut diagram generated for typical conditions is shown in Figure 35. These conditions are:

(a) Drum speed = 60 rpm

(b) Drum diameter = 56 in.

(c) Machine haul speed = 15 fpm

(d) Double laced drum = 180° between corresponding bits.

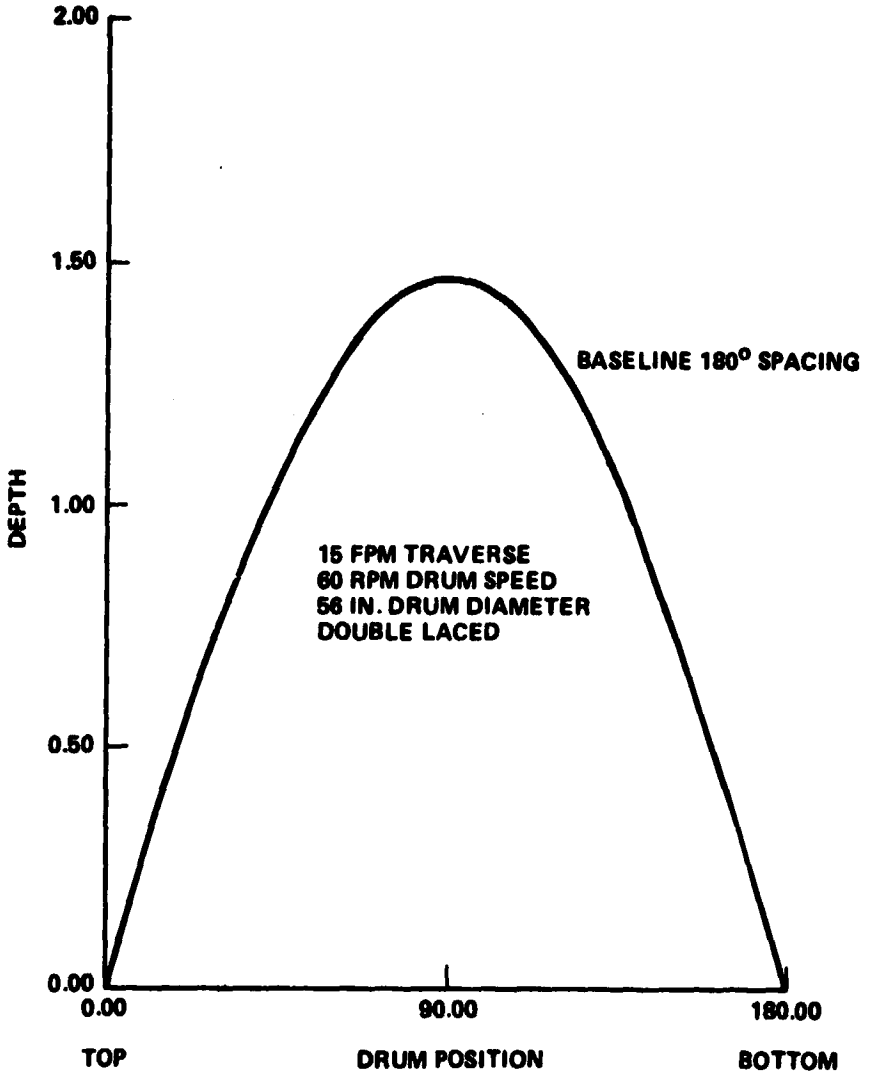

Figure 35. Drum position versus cutting depth.

It is reasonable to assume that bit cutting force varies with cutting depth, although the relationship depends upon coal hardness and the sharpness of the instrumented cutting bit. It can be seen from Figure 35 that the forces of concern at the ceiling and/or at the floor are only a small percentage of the maximum force condition at 90°; however, the cutting of rock or clay instead of coal at these locations may only double or halve the cutting force, and this amount of variation might easily escape detection in the presence of the much greater loads experienced at the maximum cutting thickness condition. As the drum cutting bits wear and dull, the cutting force for the same depth of cut will increase; therefore, it seems that some normalizing will be necessary to permit the control system to recognize and compensate for such changes.

A measurement system developed in Britain under a National Coal Board Contract [4] used a cutter bit mounted on an elastic cantilever beam with a displacement transducer to detect loads proportional to beam deflection. The instrumented bit was mounted directly behind and somewhat higher than a normal cutting bit so it could be cutting rock while all other bits were still in the coal seam. A drum position sensor was used so that the ceiling and floor cutting locations could be readily identified. It was reported that the system was used successfully to guide the machine drum position in extended mine usage, but the concept was apparently not advanced because of successes with other measurement techniques. Comments by a machinery manufacturer representative, familiar with the British tests, indicated that reliability problems were more likely the reason for discontinued use. Typical data from Reference 4 is shown as Figure 36, and these were the only published data found which represented bit dynamic loads in any realistic form.

In application, the sensitized pick output is processed by an analysis system which can recognize differences in output for normal coal cutting and for various rock or soft clay material cutting. The control for the leading drum of a double drum ranging shearer would move the cutting drum upward in small increments until rock was detected, then back off a small amount so that only coal was being cut. After a number of drum revolutions, the system would again range upward until the seam boundary was reached and then back off, so that the ceiling cut would end up a series of undulations. At the same time, the trailing drum would be driven down toward the lower seam boundary and then brought back as clay or rock was detected. Compensation would be necessary for variations in cutter bit sharpness, machine traversing speed, and coal strength properties.

The system would probably have to include logic which could recognize pass-to-pass variations and insure that subsequent cuts did not leave holes and

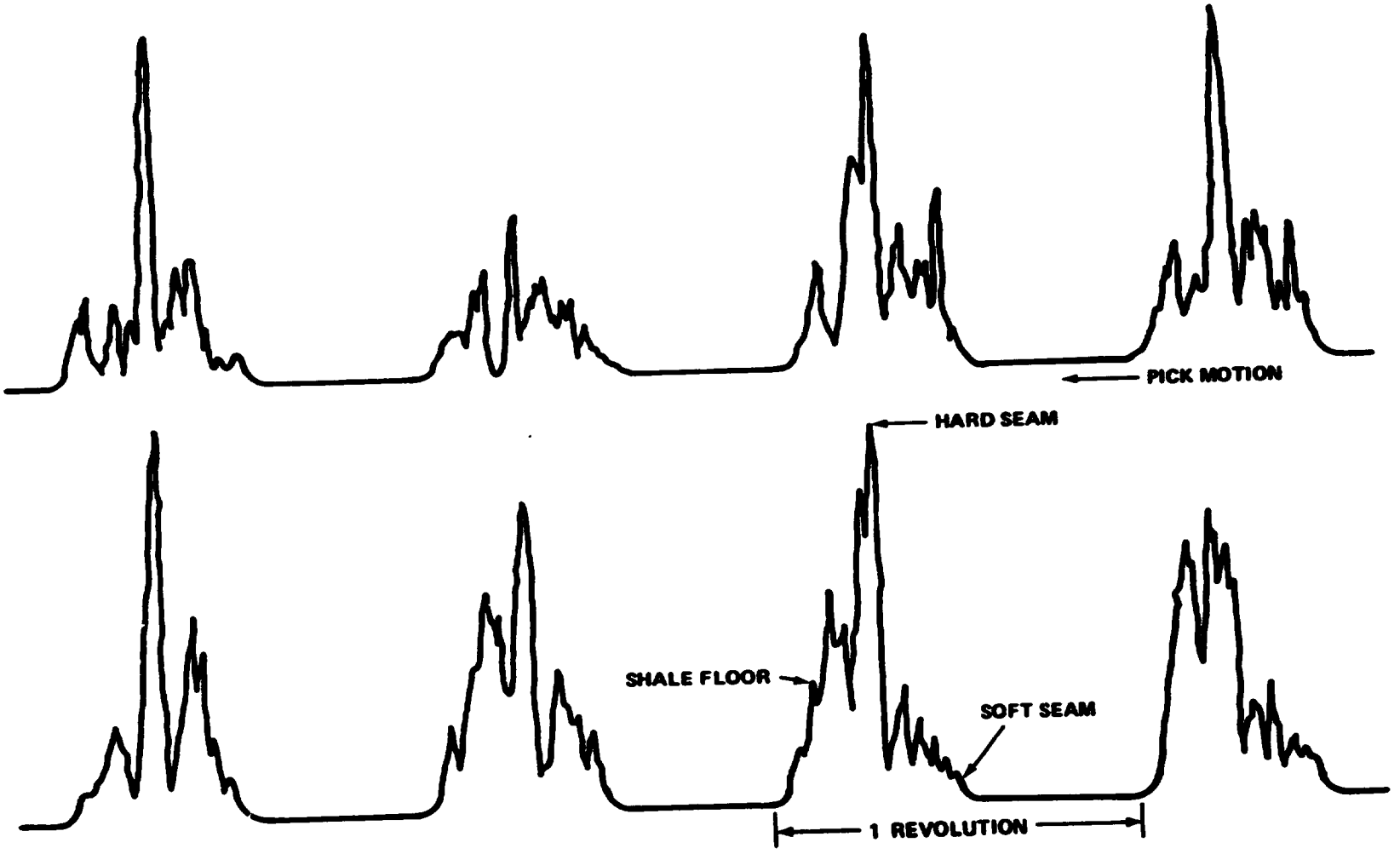

Figure 36. Example of typical signals from instrumented pick.

ridges which would jeopardize the integrity of the ceiling support system. This may mean that some rock would be cut and some coal would be left to provide overall mining system optimization at the expense of ash production, tool wear, and overall recovery.

4.1.2.1.1 Mine Review and Machine Selection. The initial phase of this program was to visit a number of operating mines to identify, if possible, a prospective test site and mining machine from which a workable data transmission system could be designed. It was felt that a system designed for a specific machine and mine situation would be much more cost effective and efficient than one required to meet universal installation requirements with only general guidelines. Several tool manufacturers were visited to obtain background on bit design criteria and an overview of current tool philosophy. Facilities and individuals visited are as follows:

(a) Appalachian Fuel Company, Huntington, West Virginia (Mr. Ken Winters)

(b) Consolidation Coal Company, Itmann No. 3, Itmann, West Virginia, Pocohontas Division (Mr. Frank Beard)

(c) Rochester and Pittsburgh Coal Company, Jane Mine, Indiana, Pennsylvania (Mr. Gene Jones)

(d) Consolidation Coal Company, Mountaineer No. 95, Shinnston, West Virginia, Fairmont Division (Mr. Tony Gemondo)

(e) Carmet Company, Mine Tool Division, Shinnston, West Virginia (Mr. Bill Walker)

(f) Kennametal Inc., Mining Tool Group, Bedford, Pennsylvania (Mr. Dough Evans)

(g) Chas. Philips Tool Company, Mannington, West Virginia, Mining Machine Rebuild Facility (Mr. Ken Phillips)

(h) Eickhoff-National Mine Company, Pittsburgh, Pennsylvania (Mr. Mike Schmidt)

(i) Mining Engineering Department, West Virginia University, Morgantown, West Virginia (Prof. E. Sandy).

Mines visited had coal seams ranging in height from 39 to 90 in., and it was concluded that working heights of less than 50 in. were very difficult with the equipment packages assembled for data recording. An agreement was reached with two mine operations for them to consider a proposal to evaluate the sensitized pick concept in their mines. Obviously neither could guarantee cooperation with only a very limited outline of what would be required of the selected site, but both felt that the potential for information return on their investment of mining crew time was well worthwhile.

The primary site selected was the Jane Mine of Rochester and Pittsburgh Coal Company at Indiana, Pennsylvania. Their Eickhoff 150 single drum mining machine operating in 56 in. of coal should provide realistic mining test conditions.

The back-up site is one longwall face of the Fairmont Division of Consolidated Coal Company, near Shinnston, West Virginia. There are several Eickhoff EDW 300 double drum machines operating in seams of 78 to 92 in. in this division which could be available for testing.

A third possible site for sensitized pick CID testing is at the Bureau of Mines' Bruceton Facility using the Joy double drum mining machine which was purchased for automated miner demonstration tests. This unit is to be set up outdoors for limited cutting of synthesized coal, and it provides a unique opportunity to evaluate background noise and data transmission requirements without the restrictions of mine permissibility and production schedules.

An early goal of this design study was to produce as universal and general a data system as possible so that application could be made to a maximum percentage of the longwall population. This means that two basic cutting bit systems need be considered — the blade type bit and the conical or "plumb-bob" type bit. The blade type bit was chosen for the evaluation when it became apparent that a single measurement device could not be readily designed that would fulfill the specialized needs of both bit designs. Some of the reasons for elimination of the conical bit were as follows:

(a) The requirement that the bit rotate in service to equalize wear eliminated a zero clearance retainer which is deemed necessary for maximum measurement accuracy and frequency response.

(b) The cutting action of the conical bit results in a combined compressive and bending load on the bit shank which complicates load sensor design.

(c) Recent studies by the Bureau of Mines [5] indicate that the conical bit produces a greater amount of airborne dust than other bit types because of the high specific energy characteristic for this bit design. (The Bureau has determined that airborne respirable dust generated per unit mass cut increases monotonically with increasing specific energy.)

All three candidate mining machine locations make use of the blade-type cutting bit; therefore, the design concepts are at least similar for each. The Bureau machine and the Rochester and Pittsburgh Coal Company machine use a 3 in. long bit with 3/4 by 1 1/4 in. rectangular shank, while the Consolidation machines are using the newer coarse laced 4 1/2 in. long heavy duty bits by Carmet with 1 9/16 in. diameter round shanks. Discussions with mine operators and bit manufacturers have indicated a very strong preference toward a measurement system which would allow simple replacement of a standard bit because cutter bit life in some circumstances is as short as 2 hr, although normal life is more like 2 to 4 days. A design goal then was to separate the load measurement element from the bit to avoid the necessity of throwing away an expensive part of the system.

4.1.2.1.2 Telemetry System Requirements. This program was begun with a goal of producing the better of two possible data telemetry systems:

(a) A distributed component system with sensing element, transmitter, and antenna located for maximum protection and optimum data transmission.

(b) A consolidated drum element containing the instrumented cutting bit, transmitter, battery pack, and antenna.

Either system would transmit to a chassis-mounted pick-up antenna and battery powered (MESA permitted) receiver, and the test data would be recorded on magnetic tape. It was concluded that a full frequency range of test data from dc (static) to at least 20 kHz need be evaluated; therefore, telemetry requirements were very stringent. A basic performance specification was established and distributed to a cross section of telemetry system manufacturers requesting information.

Standard production systems meeting major requirements were indicated by two suppliers: Acurex Corporation of Mountain View, California, and Inmet, Incorporated, of Indian Harbour Beach, Florida. Several other companies expressed an interest in developing suitable equipment, but did not have production devices available. The basic conclusions from this market survey were:

(a) Transmission of static (dc) strain data is possible using a FM-FM transmitter. Dynamic data to 2000 Hz (Inmet) or 1000 Hz (Acurex) are practical with this technique.

(b) Transmission of dynamic strain data is possible using a FM transmitter over a frequency range of 10 Hz to 90 kHz (Inmet) or 10 Hz to 20 kHz (Acurex).

(c) Up to 12 transmitters can be used simultaneously in an array without interference by separating carrier frequencies by 1.5 MHz.

(d) Temperature and acceleration signals may be transmitted over the same frequency spans as static and dynamic strain using suitable interchangeable transmitters.

(e) Two basic antenna systems are generally applied for short range data transmission: capacitive coupling using circular antenna elements 1 in. or less apart (Acurex) or electromagnetic coupling with whip antennas 3 to 20 ft apart.

(f) Normal FM telemetry techniques operate in the frequency range of 88 to 108 MHz. The carrier wavelength for this band is from 9 to 11 ft.

(g) The radio controls for remote operation of mining machine typically operate at higher carrier frequencies than the range specified here to improve data transmission in narrow tunnels. The Joy mining machine purchased by the Bureau of Mines for automation demonstrations operates at a center frequency of 460 MHz [6]. No interference between the two information transmission systems is expected.

For use in gaseous coal mines, all components must be reviewed by MESA for intrinsic safety, and because of the limited quantities involved a permit will be requested for the final system. Throwaway batteries with current-limiting resistors will be mounted on the drum to provide transmitter power while rechargeable batteries will be applied for receiver power. Designs goals are for a minimum of 100 hr operation for the transmitter battery and 5 hr operation of the receiver package between recharge cycles.

4.1.2.1.3 Instrumented Pick Design. The first phase of design for the sensitized pick installation was an attempt to find any test measurements of forces present at the bit when cutting coal and when cutting rock. Discussions with mine operators, manufacturers, and mining machine company representatives indicated that while these data may have been taken at some time, no one

knew of any published data presenting that information. Based upon the knowledge that, on occasion, the bits could be fractured by severe cutting requirements, an ultimate load was computed to give a reasonable starting point for a load measurement system. For 100 000 psi maximum bending stress in the 3 in. shearer bits used in the selected mine sites, a 4100 lb tip load is required, and the reaction force at the lower plane of the bit shank would be 4920 lb. Application is as follows:

(a) A standard cutting bit is inserted into the broached pick mount cavity by driving it past the pick retaining plug.

(b) The zero load strain output of the strain gaged load sensor is read out on the telemetry receiver output meter on the machine base.

(c) The preload bolt is tightened until a static strain of approximately one-third of the pick allowable strain is indicated. The lock nut jams the preload bolt in place.

(d) Static and dynamic changes in cutting bit load are indicated by load sensor strain outputs. The preloaded beam insures that the load sensor stays in intimate contact with the cutting bit.

(e) When necessary, the cutting bit may be removed and discarded by releasing the lock nut and preload bolt, and pulling the bit using a standard pry tool.

This special bit block is mounted in place of a standard block on the longwall cutting drum. A metal tube directs the transducer leads to transmitter/battery assembly mounted in the web of the drum. All electronic components and lead wires are installed after the support components are welded in place.

The spiral web of the cutting drum "pumps" the cut coal onto the face conveyor as it turns, but the outer (machine side) edge does only minimal work; therefore, this mounting location is acceptable. The details of construction of the telemetry transmitter assembly are shown in Figure 37. Major elements are: (a) strain gage FM-FM telemetry transmitter for dc to 2 kHz strain response, (b) a 12 V current-limited battery pack,) accelerometer FM telemetry transmitter for 10 Hz to 90 kHz acceleration response, and (d) two 75 ohm resistor transmitting antennas radiating through nonmetallic antenna covers. The accelerometer transmitter is an alternate to a FM dynamic transmitter which would be used if high frequency strain is the preferred measurement technique. The concept includes the alternate of pick shock response as

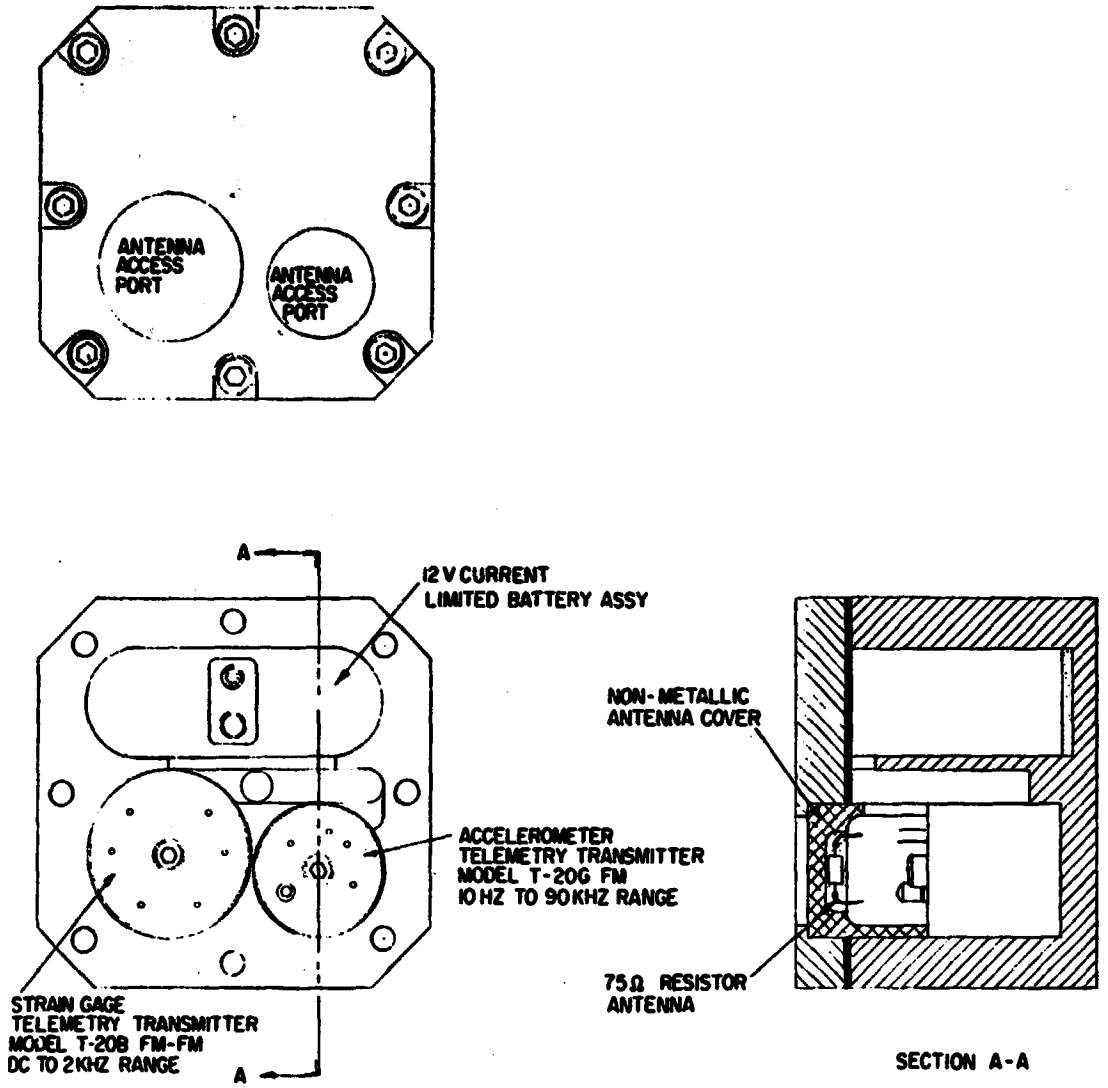

Figure 37. Telemetry transmitter assembly.

well as pick load as a measure of the cutting character of the material at the bit. It is assumed that shock energy levels for the bit striking rock or clay will be dramatically different from those for normal coal cutting operation. The impacts of cutting will cause the pick to vibrate at a number of its cantilever beam resonant frequencies, with the amplitude of response proportional to the impact energy and to system damping. Lower order modes are moderated significantly by damping as displacement amplitudes are large, but higher mode responses tend to be very pure as damping becomes less of an influence. High frequency vibration response techniques have been applied to a variety of machine element problem detection tasks, and it has been found that impact

characterization in the frequency range of 15 to 50 kHz is an extremely useful way of monitoring performance differences. Ball bearing rolling contact difficulties, gear train surface faults, pump fluid cavitation conditions, and machinery rub problems have been detected using the structural ringing of machine elements as a carrier of information to areas outside the direct fault site. The concept is implemented by attaching a suitable high frequency response accelerometer to the end of the compression member which is loaded against the bottom of the bit so that the minute shock response amplitudes of the exposed end of the pick might be measured.

The complete telemetry data transmission system is shown in Figure 38. It is assumed that two sensitized pick CID's are applied either to evaluate alternate arrangements for more definition of the same configuration 180° apart on one drum, or for ceiling and floor cut drums on a double drum mining machine. A decision was made to use 75 ohm resistor transmitting antennas and whip receiving antennas (dual whips with co-phased lead-in cable) with electromagnetic signal transmission. The close-coupled capacitive data transmission system was rejected because of installation space requirements in the drum hub area. The swinging cowl assemblies of double drum machines use up the required axial length needed for this type of radio wave transmission. The whip antennas are located as far away from each other as practical to take advantage of alternate data transmission paths from each transmitting antenna. One advantage of using the standard FM carrier bands is that blockage of carrier waves requires an obstacle that is one half wave length or greater in dimension, a span of 5 ft or more. There are few such obstacles around a longwall machine, and by taking advantage of reflections and multiple paths the widely spaced whips will be able to pick up continuous signals from all four transmitters. The lower dashed envelope shown in Figure 38 defines the contents of a receiver case which is mounted on the mining machine frame. The whip antenna signals pass through an adjustable antenna matching resistor which can be tuned to maximize antenna gain. A passive signal coupler splits the signal to each of four receivers so that the individual transmitter outputs are separated and made available for recording on four channels of a seven channel tape recorder which will be used to make a permanent record of test data outputs. A solid-state 12 V current-limited battery pack has been designed to permit operation of all four receivers for 6 hr or more before recharging is necessary. Figure 39 shows the general configuration of the proposed receiver package. It contains two FM receivers and two FM-FM receivers (all by Inmet, Inc.) so that two complete CID systems can be monitored over a frequency range from dc to 90 kHz with accurate determination of pick parameter output amplitudes. The unit is packaged in an aluminum case suitable for airline shipment and weighs approximately 65 lb. The size and weight are reasonable for handling by one person and can be mounted on a longwall mining machine without great difficulty.

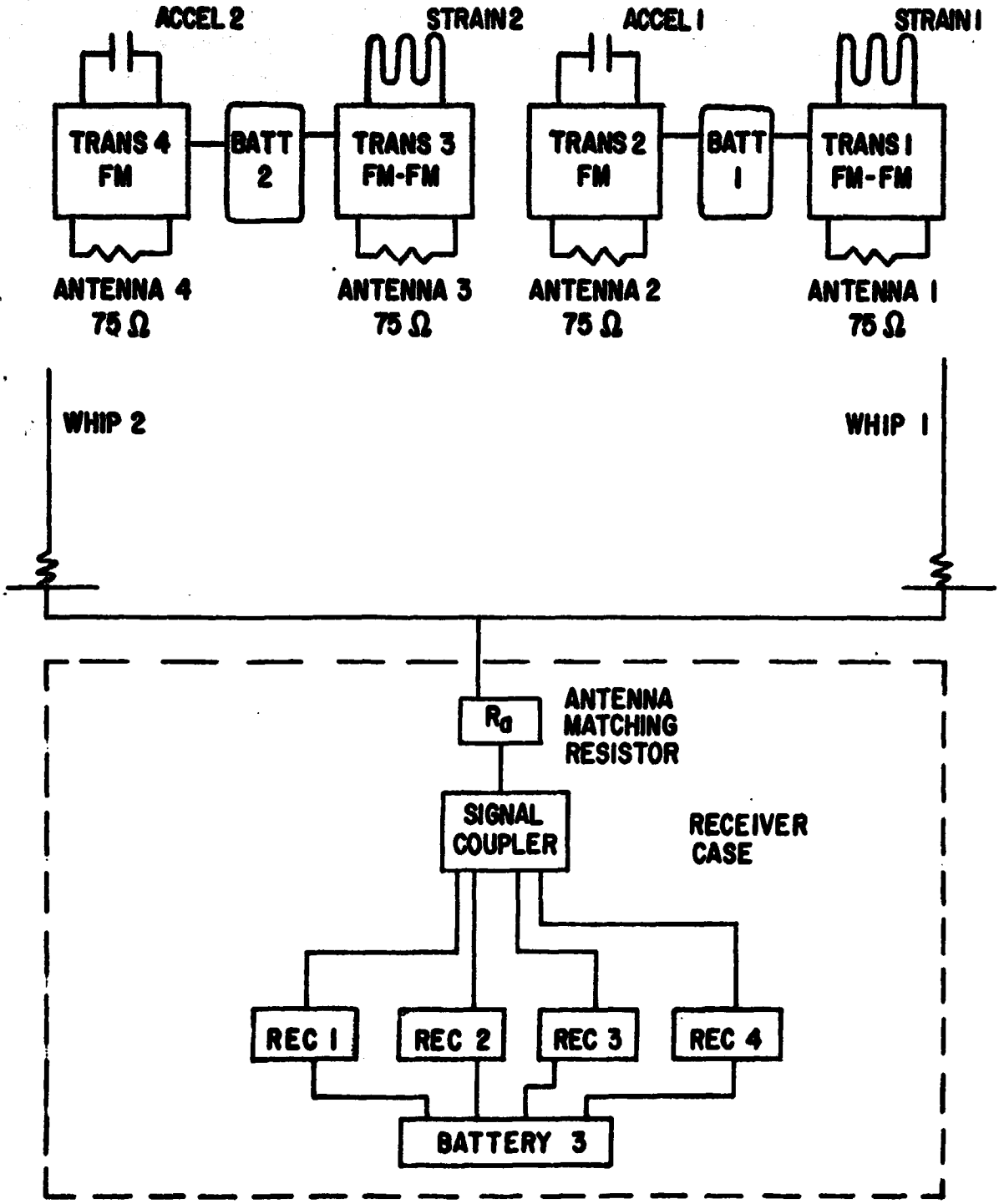

Figure 38. Data transmission system sensitized pick detector.

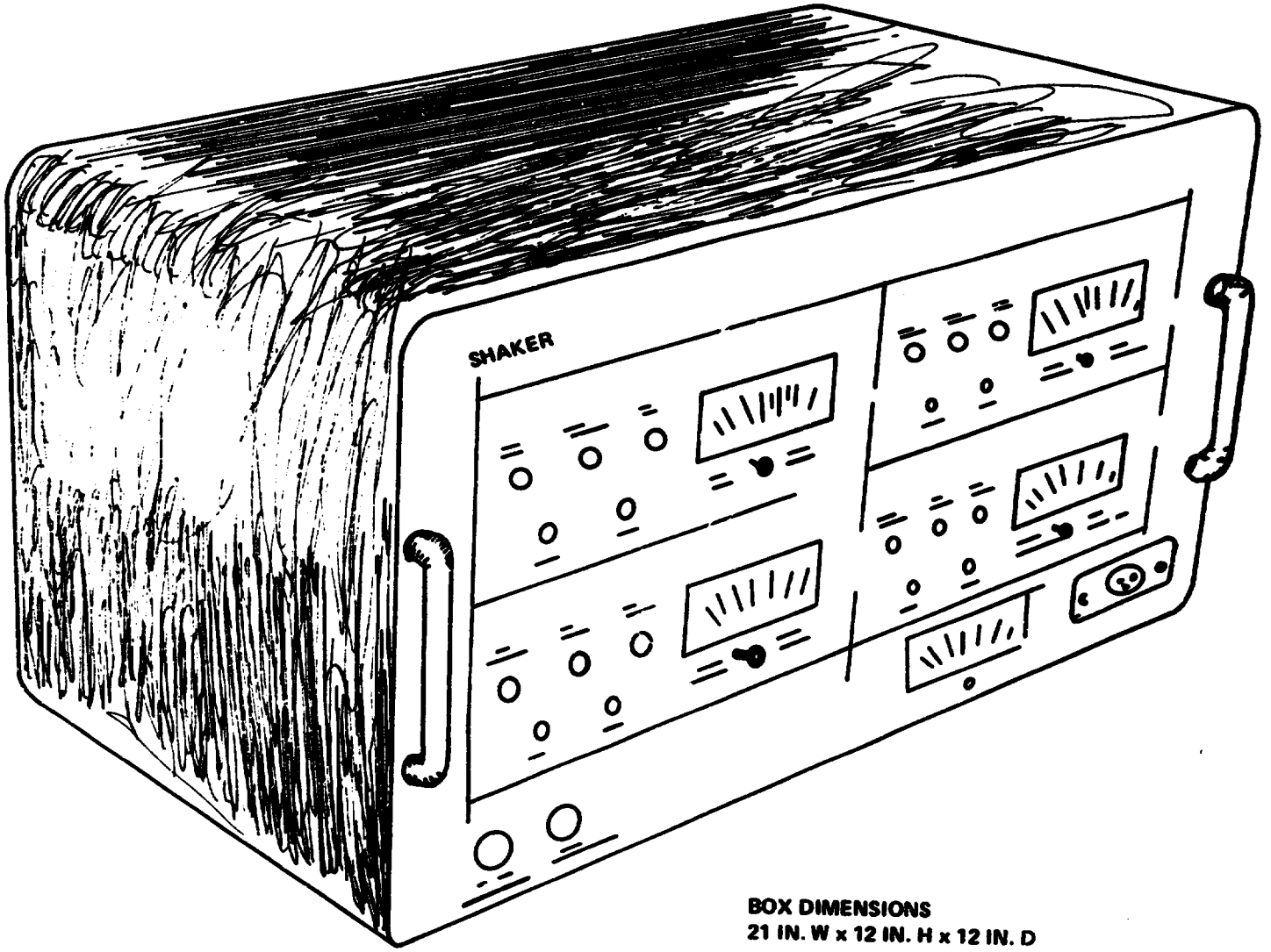

Figure 39. Shaker research 4 channel telemetry system.

4.1.2.2 Alternative Concepts. Several questions concerning the optimum application of the sensitized pick CID cannot be answered until some additional testing has been accomplished. The basic concern is for detection of differences in output for coal cutting versus rock or clay cutting at the very top drum position (0°) or very bottom drum position (180°) when the depth of cut is only a fraction of an inch as shown by Figure 35. Maximum sensitivity is desired at these probable foreign material locations; however, in another 90° of rotation, the transducer system must withstand a full depth of coal cut which may be 1 1/2 to 2 in. thick. Several schemes have been devised to minimize this problem:

(a) Provide a mechanical stop so that high sensitivity is available for light cuts but a substantial limit is reached before the tool begins to absorb the full depth cut stress.

(b) Provide a broad dynamic range transducer system so that very fine resolution can be attained over light and heavy cuts.

(c) Mount the instrumented cutting bit immediately behind another bit (in its shadow) so that the depth of cut is less than the 1 1/2 to 2 1/2 in. normally experienced, and is in fact almost a constant depth cut from ceiling to floor.

The first technique has a real advantage in sensitivity because a mechanical stop can take the extremes of operating loads experienced from sulfur ball inclusion encounters or unavoidable operation with dull bits. However, the design of a linear system with stops may require machining precision and cutting cycle definition which will not be available until significant study has been done. (Another disadvantage of this system is that linear measurement of forces during maximum thickness cutting of coal is probably the best way of judging the sharpness of the cutting bits. Normalization of bit load data for different cutting edge conditions will almost certainly be required for any long term operating control system.)

The second technique has the primary advantage of complete compatibility with normal drum lacing techniques. The instrumented pick experiences absolutely typical loads and shocks, and the data output would be most useful to machine operators and cutting bit suppliers for improving overall machine performance. However, the application of these data to a machine control logic system will be quite difficult and may require much more sophisticated pattern recognition capability to produce drum control ranging signals. Most definitely these measurements should be made to advance understanding of the drum shearing process.

The third pick arrangement has several attractive features which suggest that a variant of it will be used in any production version of this transducer system. Figure 40 shows to possible examples of shadow pick mounting: one directly behind the next pick (single spaced), and the second two picks back (double spaced). For the Joy machine purchased by the Bureau of Mines, the single-spaced pick is 15° behind its lead pick, and the double-spaced pick is 30° behind.

To evaluate various combinations of shadow pick cutting depths, a simple program has been assembled in the computer Basic language which can accommodate variations in drum diameter and speeds, traverse velocity, angular offset, and pick extension. The base-line case shown in Figure 41 was for a standard drum with two bits 180° apart in each cutting plane. Zero degree is the ceiling and 180° is the floor with the maximum depth of cut equal to 1.5 in. when the cutting bit is at 90°.

For a shadow pick located 15° behind the next pick, the cutting depths are shown on Figure 41 for a standard length bit and for one extended 0.15 in., 0.25 in., and 0.50 in. beyond the nominal bit radius. The base-line case is also shown in Figure 41. Note that the depth of cut for any of the extended bits becomes almost a constant throughout the 180° arc; therefore, evaluation of the hardness of the material at ceiling and floor is greatly simplified because it can be compared directly with the average cutting force for the main seam cut. Variations in machine traverse velocity or bit sharpness are taken care of automatically, reducing significantly the "intelligence" required in circuitry to digest cutting bit outputs. Figure 42 shows the same bit extensions for a pick 30° behind its leader. The conclusions are the same as for the 15° pick except that the greater lag causes increased difference in cutting depth from initiation of cut through maximum depth.

It would seem from these plots that a 1/2 in. extended sensitized pick placed approximately 15° behind a normally located bit would provide good cutting characterization with moderate wear, and that a maximum amount of coal could be recovered with minimal rock cut. To define the presence of very soft material, it may be desirable to include a drum angular position indicator so that ceiling and floor locations are readily recognized for the initial evaluations; at least an angular position sensor should be recorded together with pick output data and a voice commentary of operating conditions.

After completion of the initial design of the telemetry transmitter assembly, a review was held with the operators of the Jane Mine at Indiana, Pennsylvania, to obtain some general reactions to the proposed installation.

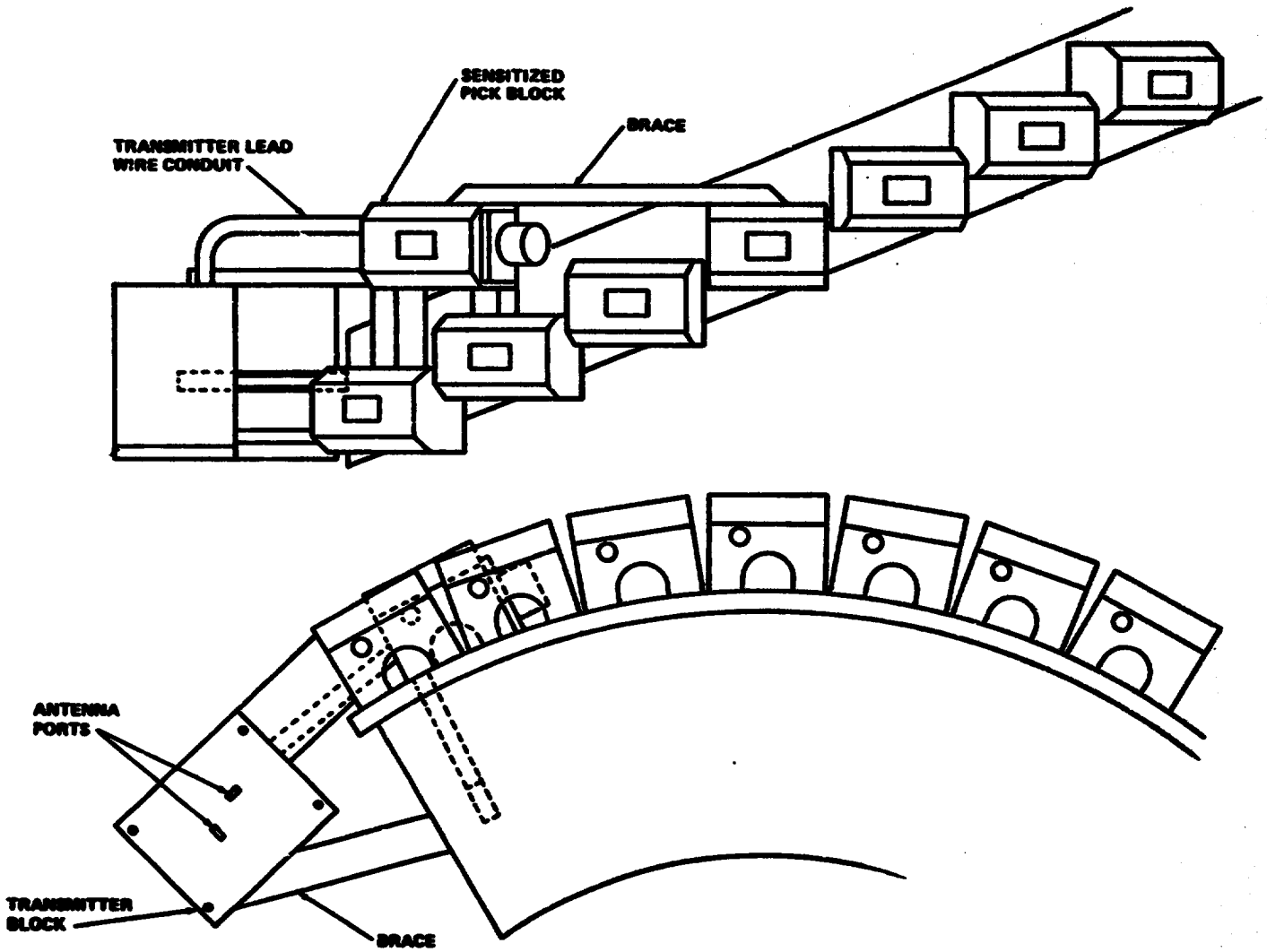

Figure 40. Pick mounting on drum.

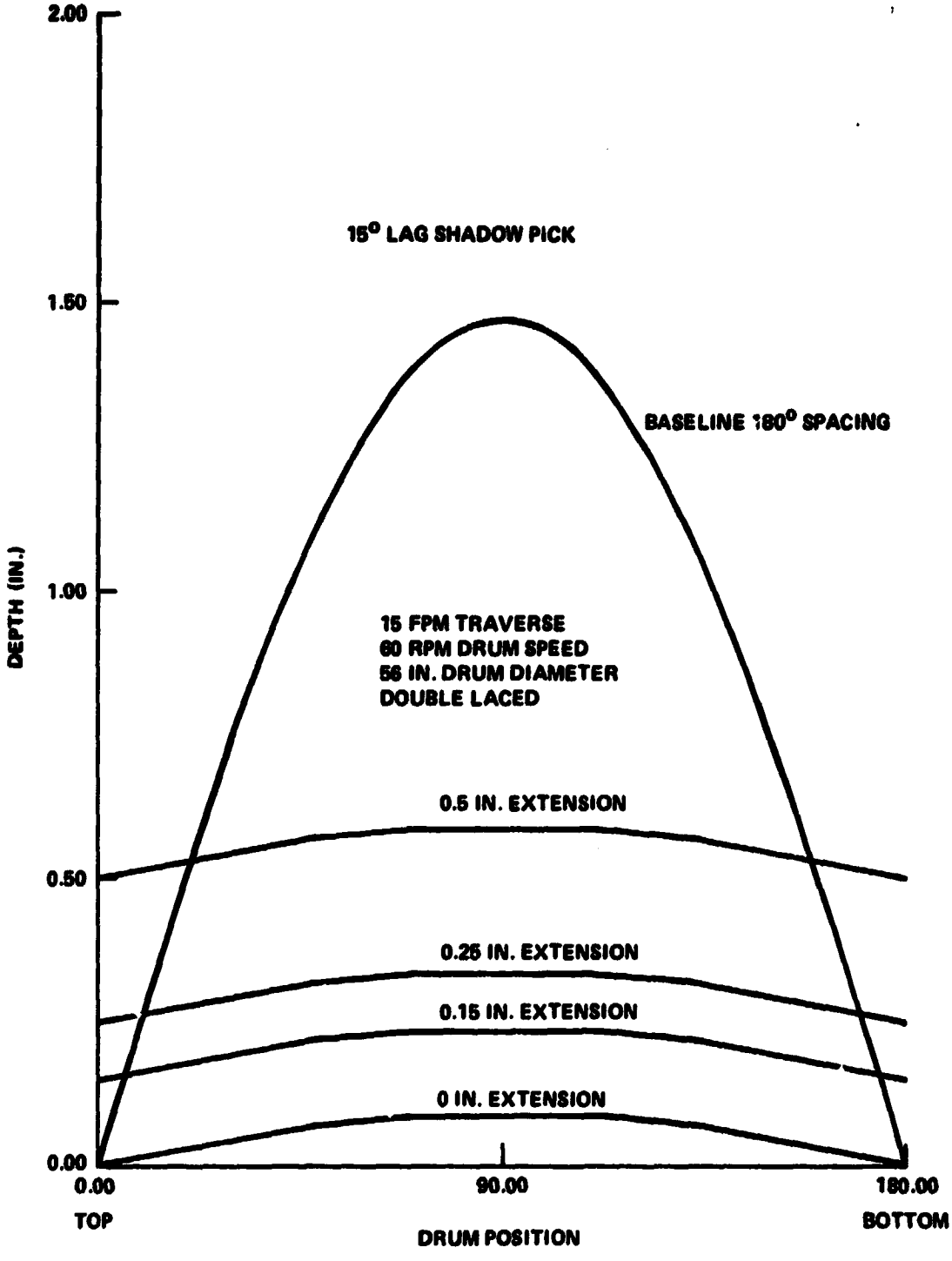

Figure 41. Cutting depth versus drum position (15° lag shadow pick).

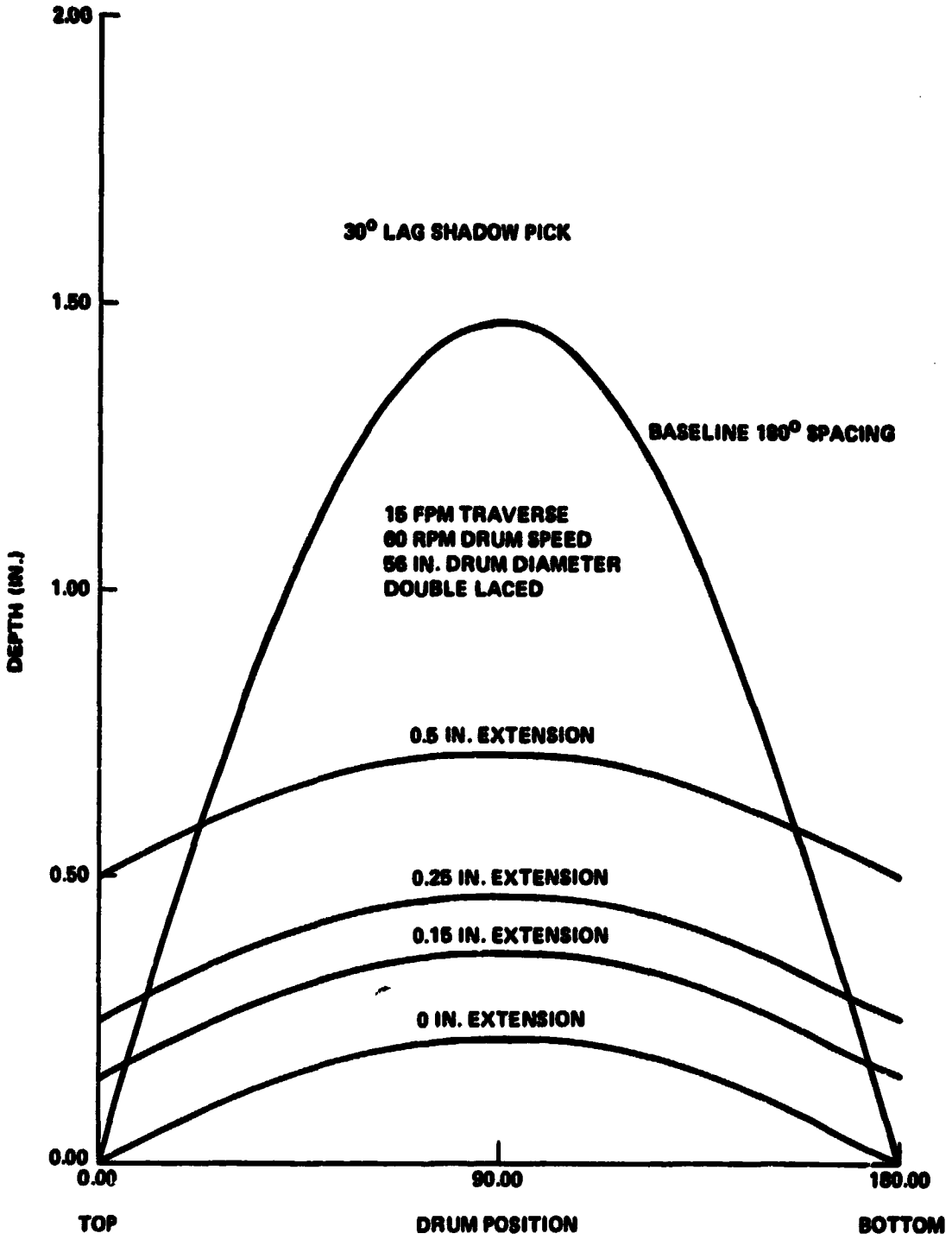

Figure 42. Cutting depth versus drum position (30° lag shadow pick).

The reception of the concept was generally good; however, it was suggested that a surface mounting for the transmitter block would be more easily attached and would require less modification to the drum. With that in mind, an alternate mounting (Fig. 43) was designed which should minimize attachment concerns. Overall dimensions are 4 1/2 by 5 by 2 in. Figure 44 shows the installation of the surface mount transmitter assembly with an additional bolt-on guard to protect the instrument lead tube from mechanical damage.

4.1.2.3 Computer Program for Drum Depth-of-Cut Analysis. This section contains a brief description of the technique used in estimating the depth of cut of a lagging drum pick.

Figure 45 is a vector diagram of two cutting picks mounted on a drum which moves at a constant velocity (v). By inspection of the diagram it is noted that the cutting depth at the drum position angle (α) for small offset angles (θ) can be approximated by the sum of two components; i.e.,

$$\text{Cutting Depth} = \Delta R + R_x \quad ,$$

where $\Delta R = R_2 - R_1$ and R_x = the projection of $(v \cdot t_\theta)$ along R_1.

Since the drum is rotating and translating at a constant rate, the displacement projection of $(v \cdot t_\theta)$ in the direction of R_1 can be estimated by

$$R_x \simeq v \cdot \sin\alpha \; t_\theta$$

where t_θ is the time in seconds it takes the drum to rotate through the angle θ and is given by

$$\frac{60.0}{2\pi N(57.295)} \quad ,$$

where θ = offset angle in degrees and N = drum rotation rate in rpm. The depth of cut of the lagging pick is then

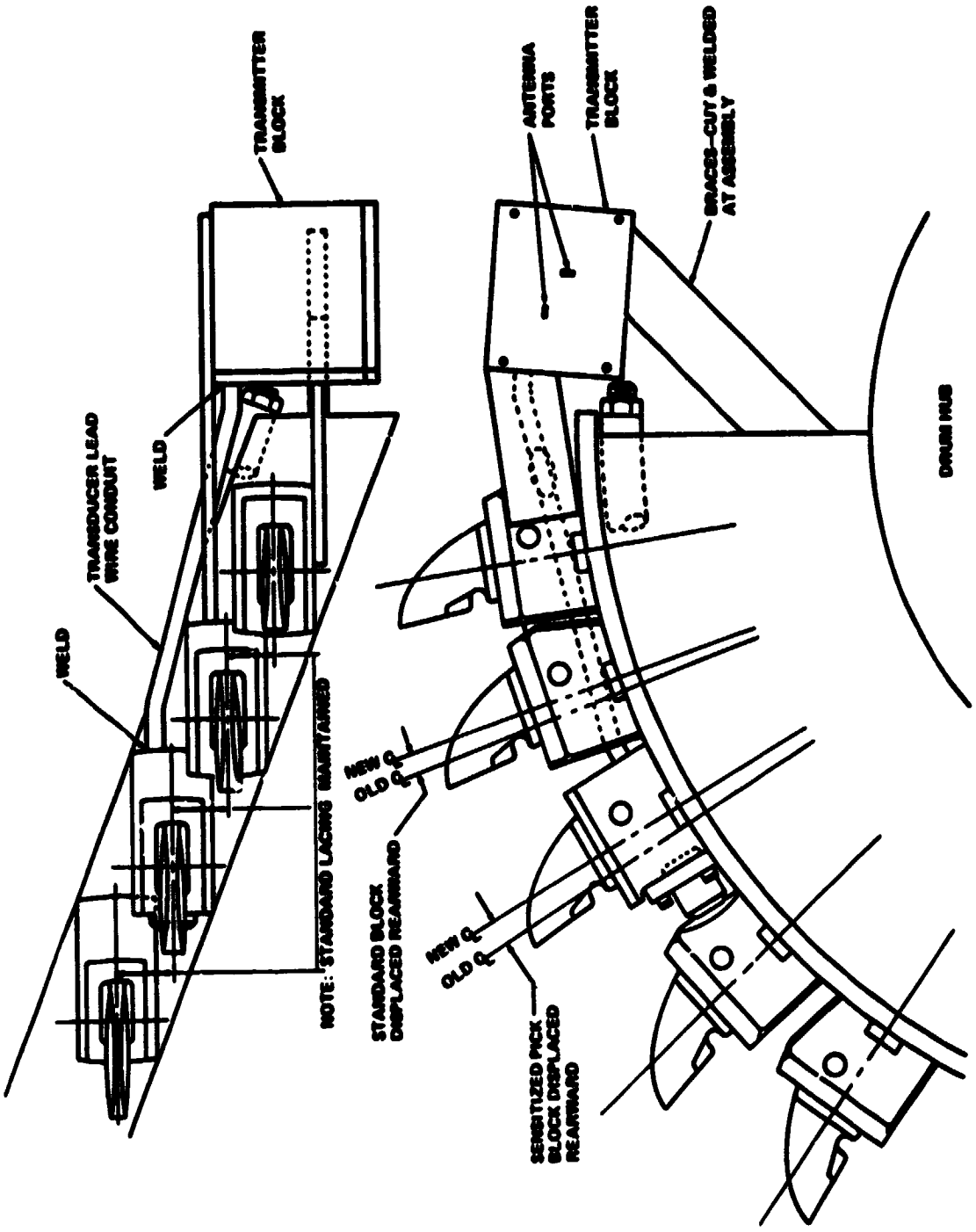

Figure 43. Cutting picks mounted on drums.

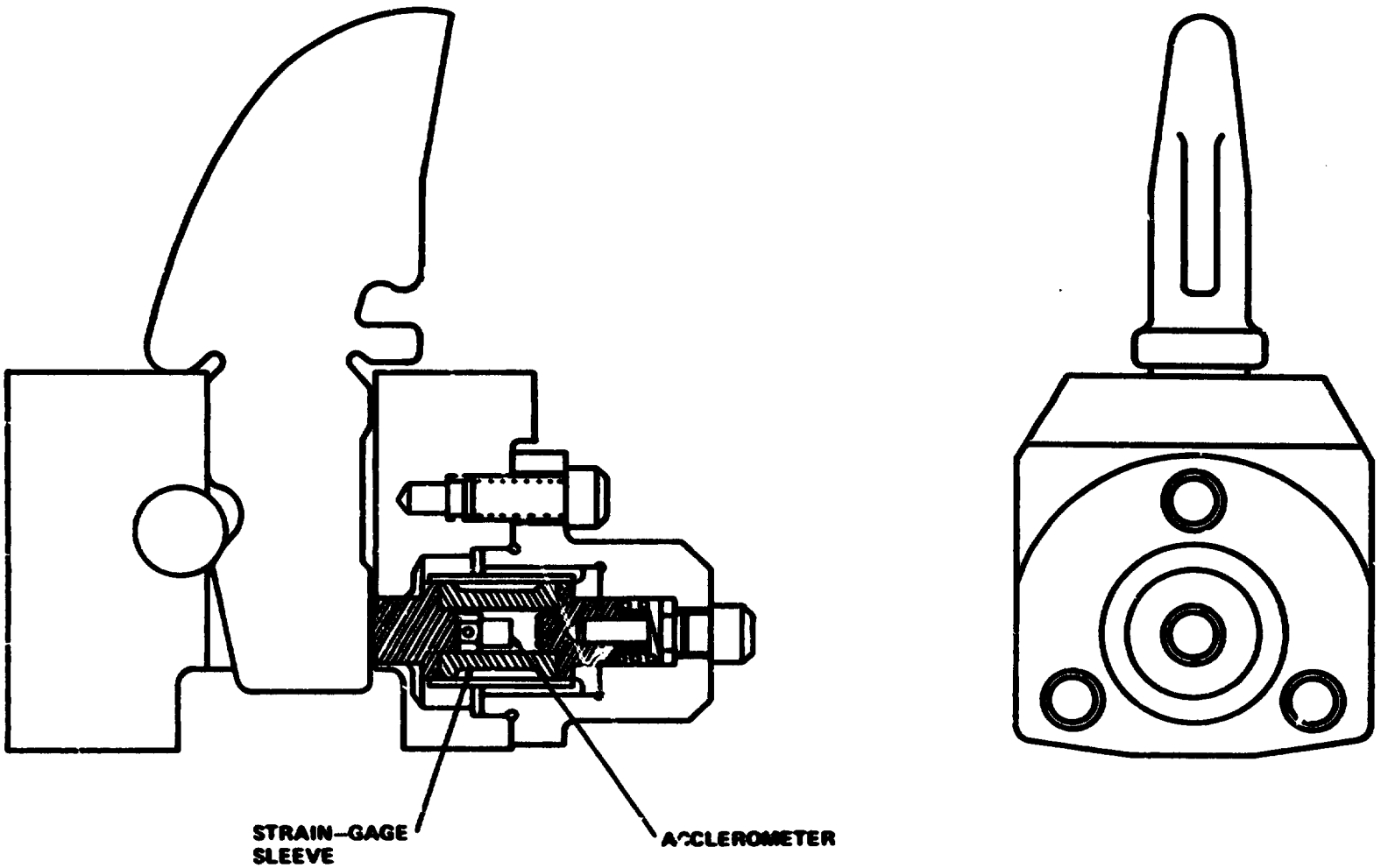

Figure 44. Pick block assembly.

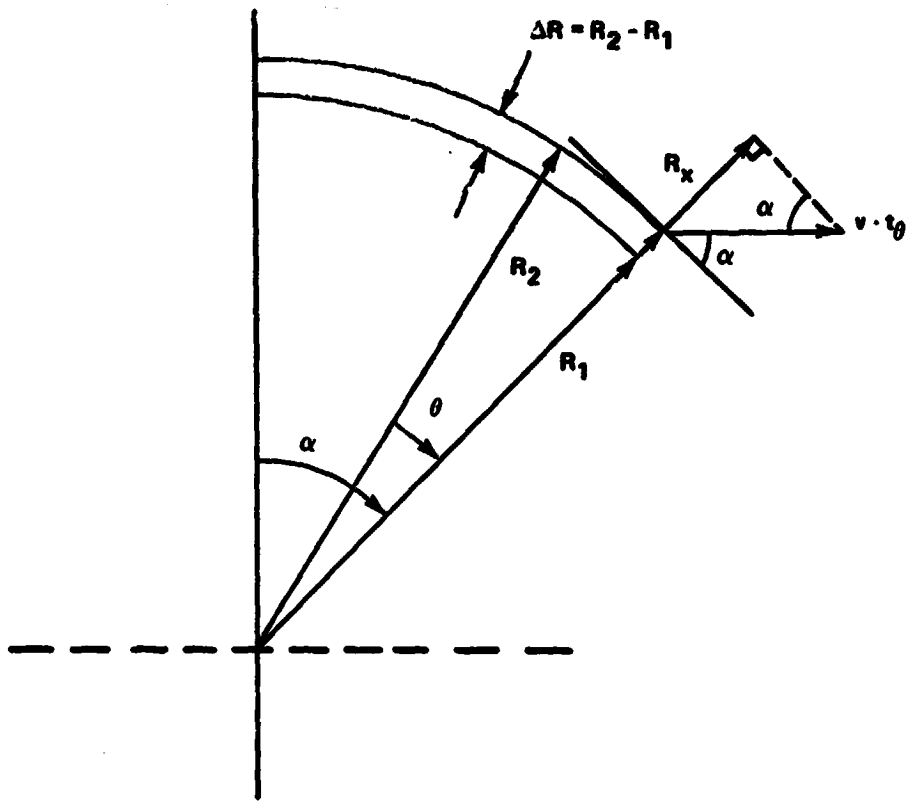

R_1 = LEADING PICK RADIUS
R_2 = LAGGING PICK RADIUS
$\Delta R = R_2 - R_1$
θ = PICK OFFSET ANGLE
α = DRUM POSITION ANGLE
v = DRUM HORIZONTAL VELOCITY VECTOR
t_θ = TIME TO ROTATE DRUM THROUGH ANGLE θ

Figure 45. Vector diagram for use in estimating depth of cut by pick (R_2).

$$\text{Depth} = \Delta R + 60.\theta.v.\sin\alpha/2/\pi/N/57.295$$

$$= R_2 - R_1 + 60.\theta.v.\sin/2/\pi/N/57.295 \quad .$$

C-2

The computer code used calculates the depth of cut at 3° intervals over the forward moving semicircle and plots these results. For a standard double-laced drum, the offset angle is 180° and $R_1 = R_2$. Computational results of the base-line case are shown on Figure 41.

4.1.2.4 Test and Evaluation Plans. Field tests of the sensitized pick CID data transmission system are planned in one or more mines to obtain detailed magnetic tape data for definition of signal processing techniques and control logic analysis. These test data are not presently available in any suitable form and are a necessary step in the application of this CID to automated machine control.

Application of the telemetry system was carried out in three parts. The initial phase included the finalizing of the receiver package design, procurement of components, assembly, and laboratory checkout. Following this the necessary MESA and State of Pennsylvania permits and approvals are to be obtained to satisfy intrinsic safety requirements for use in gaseous coal mines.

In the second phase, it is planned that the telemetry system be taken to the Bruceton Surface Test Facility and attached to the Joy mining machine for evaluation of telemetry output characteristics and as a check for interference with the remote control instrumentation system used with that machine. The influence of RF fields around electrical components can also be evaluated, and an initial evaluation of telemetry antenna location can be accomplished. Checkout with this machine would insure minimum difficulties in the underground test phase.

In the third phase, mine testing is planned to provide examples of normal pick dynamic load conditions with a number of variations which can direct the selection of an optimum measurement system. For control, it is planned that one standard bit location be instrumented with strain and acceleration transducers and monitored throughout the test. At a location 180° around the drum, a shadow pick arrangement will be installed which follows as closely behind its lead pick as possible. The output of the shadow pick with a standard bit, one 0.25 in. longer than normal and one 0.50 in. longer than normal installed, will be recorded while operating in a variety of materials (coal, rock, and clay) together with the output of the control pick. In addition, a phase indicator which produces a voltage pulse at a known angular drum position should be recorded concurrently with strain and acceleration measurements, as well as a voice commentary describing the operating conditions.

If practical a measure of machine traverse velocity will be made simultaneously; one possible scheme is to count links as the haulage chain is pulled through. The seventh channel of the analog tape recorder can be used to record machine background sound level or acceleration to further characterize the operating environment.

Installation of the sensitized pick CID data transmission system appears to be possible at the Jane Mine of Rochester and Pittsburgh Coal Company. A detailed explanation of installation and operational requirements for this system was presented to the operations management of that mine, and assurance was given that they would aid in obtaining the required test information.

4.1.3 Surface Recognition CID. Both the impact penetrometer and reflectometer CID's have undergone two sets of tests at the Safety Research Mine at Bruceton, Pennsylvania; the first in April of 1976 and the second in August of 1976. The reflectometer operation is based on the assumption that the reflecting properties of coal and shale are different. This was demonstrated to be a reasonable assumption and gave positive results during both tests. The impact penetrometer, however, is based on the assumption that coal is more compliant than shale. This was the case for the first series of tests performed in April; however, one-site observation and analysis of the test data showed that the conditions at the test sight in August were considerably different from those in April. In April, the shale was hard and less compliant than the coal, but in August-September the coal was harder than the shale. As a result of this change in physical properties, the impact penetrometer tests performed in September were not able to correctly differentiate the coal surface from that of the shale. It is still unknown whether this change in physical properties of the materials is a normal seasonal change, or if it was due to other causes.

Following these tests it was decided to combine the reflectometer and impact penetrometer CID's into one surface recognition CID. This CID would use an electronic majority voting circuit to identify the surface. This new CID was designed to include two reflectometers and one impact penetrometer.

The instrument design (Fig. 46) is currently being fabricated by Pedigo Welding and Fabricating Co., Lacey's Spring, Alabama, and is now scheduled for delivery in November 1977.

4.1.4 Radar CID. A series of field tests were performed in the Bureau's experimental coal mine at Bruceton, Pennsylvania. Tests were conducted during the week of November 15, 1976. The test area consisted of a series of steps cut approximately 4, 6, and 10 in. thick as measured from the surface of the coal

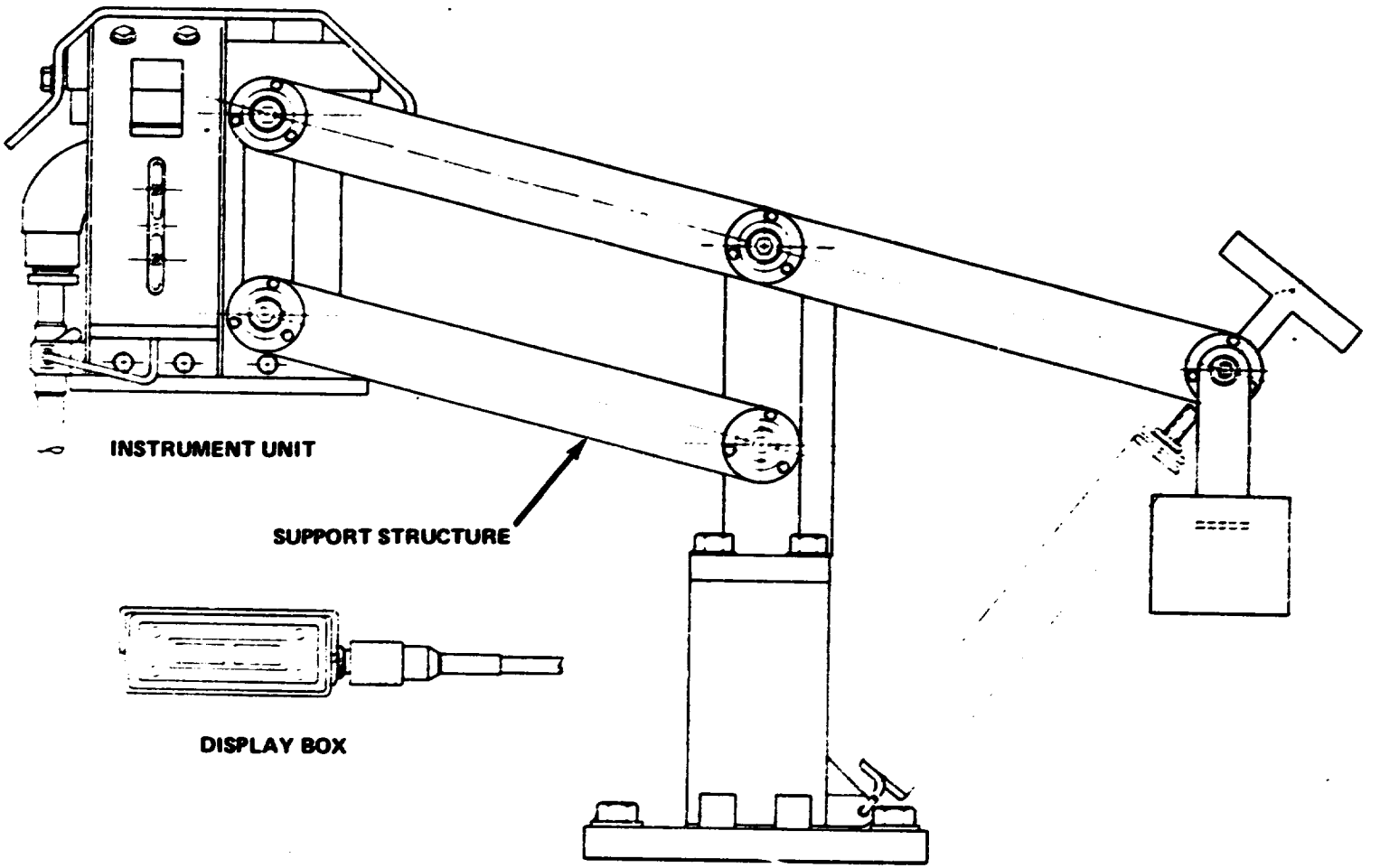

Figure 46. Impact penetrometer reflectrometer CID.

to shale roof interface. Steps were also cut for floor coal thickness tests. A metal track was installed under the test section to allow easy movement of radar (mounted on a wheeled cart) under coal steps.

Four FM/CW radar configurations, operating over swept RF frequency range of 1.7 to 4.3 GHz, were used in this series of tests:

(a) A two antenna, linearly polarized radar (identical to the one used in the March 1976 field test at Bruceton).

(b) A single horn antenna radar, linearly polarized, using a hybrid coupler to accomplish the transmit-receiver diplexing function.

(c) A circularly polarized, low gain (6 to 8 dB) horn antenna radar, similar to that in (b).

(d) A circularly polarized, high gain (20 dB) horn antenna radar, also similar to that in (b) except for antenna.

Configurations (c) and (d) used polarization diversity to accomplish the transmit/receive function.

The interface return signals were quite weak when compared to measurements made in March 1976. The shale interface was detected at a range of 5 to 6 in. thickness but was of insufficient amplitude for the reliable signal processing required for automated control. (Test results, documented as test No. T7-1 to T7-11, dated 11-18-76, not included in report.) Overall, radar configurations (a), (b), and (c) did not have any particular performance advantage over one another. Laboratory tests indicated two antenna radars had a slight sensitivity improvement (3 to 5 dB) because of better transmitter to receiver isolation. Single antenna radars have better accuracy at short coal surface to antenna spacings (<30 cm) because of geometric errors. Configuration (d) showed a slight advantage at larger depths of coal because of higher antenna gain; however, because of its large physical size this antenna was not practicable for most machine installations.

It is believed that the most probable cause of the relatively poor performance in this test series is the difference in moisture content. Moisture content was reported in March 1976 as 1.4 percent; however, by November it had increased 78 percent to 2.54 percent which increased coal attenuation from 2.2 to 2.9 dB/in. at 3 GHz (Fig. 47). Therefore the interface return signal was attenuated to the point that it could not overcome the masking effect of the front (coal) face reflection.

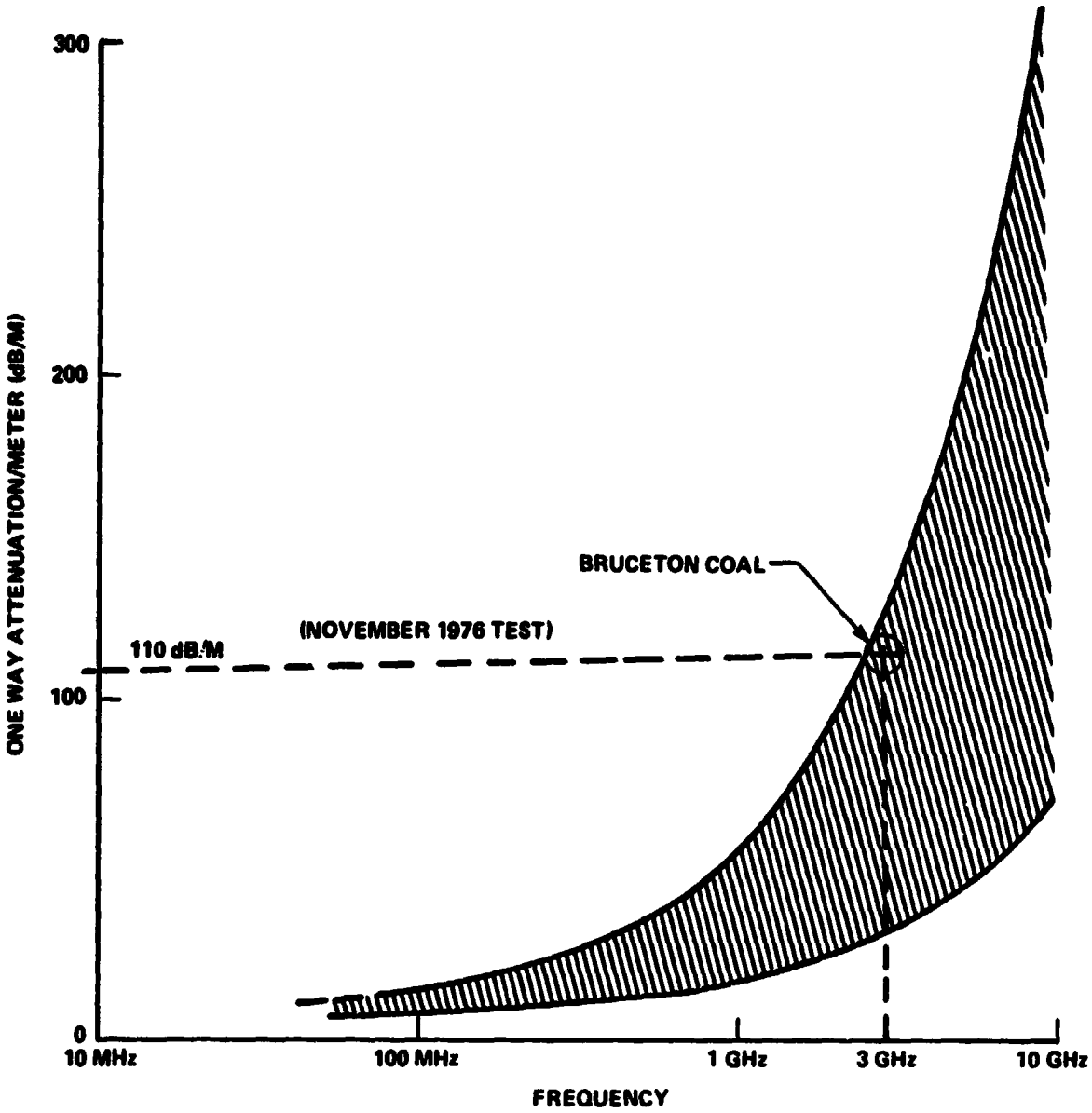

Figure 47. RF attenuation for coal.

4.1.4.1 RF Properties of Coal. To better understand the effect of coal RF property variations, such as attenuation, several field tests were made. Prior to this, available data had been extrapolated from low frequency measurements of other investigators [7]. This information together with a few discrete dielectric constant and dissipation measurements made at MSFC by P. Swindall [8] resulted in a projection of an envelope of attenuation as a function frequency (Fig. 48). Actual attenuation measurement at Bruceton, Pennsylvania, are superimposed on Figure 48.

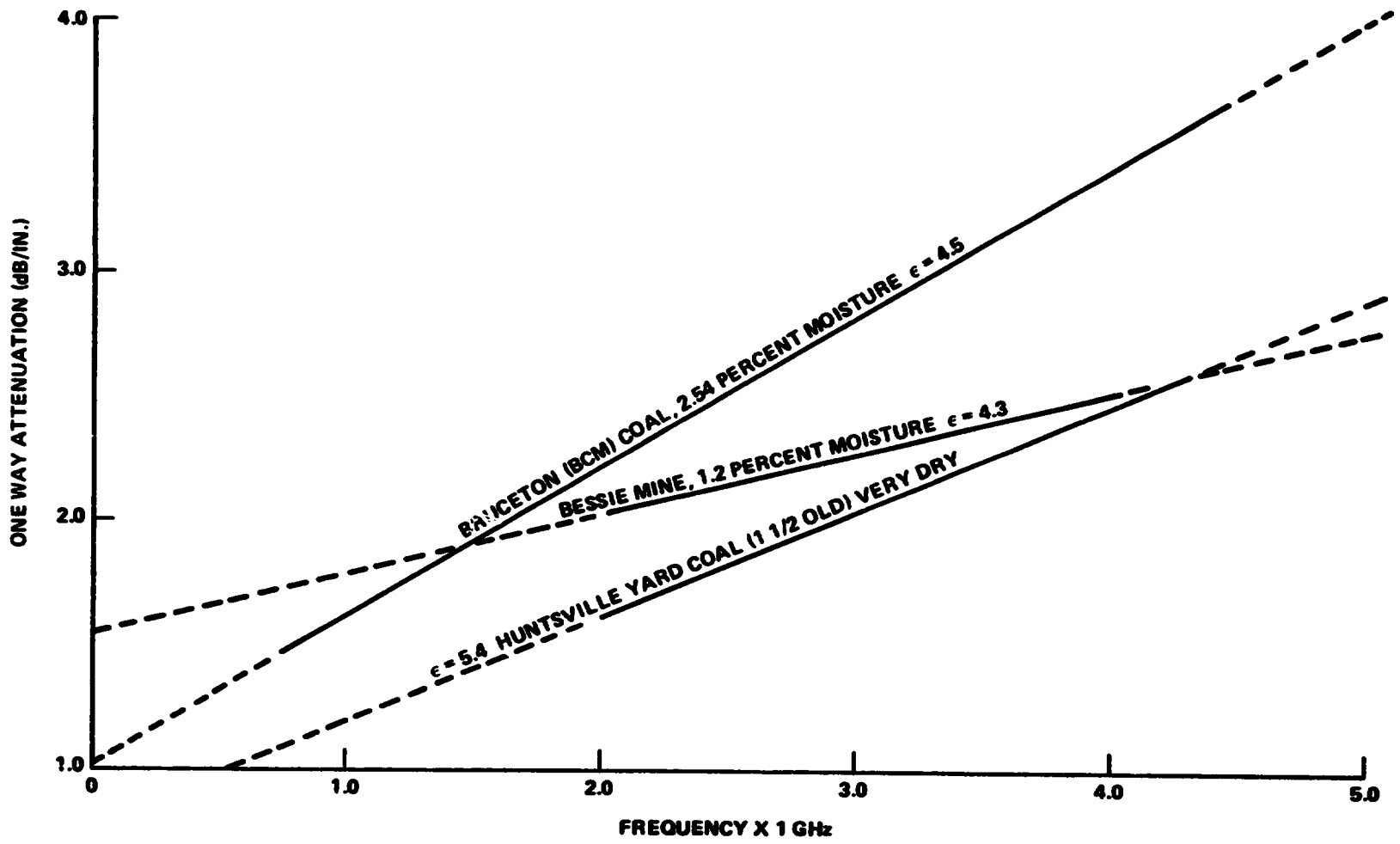

Figure 48. Coal attenuation.

J. R. Lundien [9] and A. Von Hippel [10] have performed experiments relating moisture content to RF loss of a plane wave passing through a dielectric. The RF attenuation tests made on several coal samples show a close relationship to moisture content (Fig. 48).

An accurate measurement of RF attenuation of the Bruceton coal was made September 1976. A large unbroken sample of coal (27 by 27 by 18 in.) was obtained during face preparation for radar tests. This sample was measured in the mine over the frequency range of 2.2 to 4.3 GHz. At 2.3 GHz, attenuation was 2.2 dB/in. and increased to 3.6 dB/in. at 4.3 GHz. Average attenuation at radar center frequency was 2.9 dB/in. at 3 GHz. Total round trip loss for 10 in. of coal (assuming 100 percent reflection at shale interface) is 58 dB.

A second large coal sample was obtained and measured in the Jim Walters Resources Bessie Mine, Graysville, Alabama. The sample was approximately 38 by 37 by 19 in., and tests were made in the repair area within the mine. The sample was approximately 48 hr old at time of measurement. Measurements were made by placing coal between the transmitter and receiver and recording the power level during the sweep period of transmitter. The frequency range of measurement covered was 2 to 4 GHz. A dielectric constant of $\epsilon = 5.4$ was determined by measuring radar thickness of coal and comparing with the equivalent open air spacing.

The third sample, of unknown origin, was a random sample obtained from The City Coal Company, Huntsville, Alabama. The sample was extremely dry, having been in the MSFC laboratory for over one and one-half (1 1/2) years.

Comparison of tests is shown in Figure 48. The number of tests conducted, measuring attenuation, and its relation to moisture contents are not sufficient for good statistical data, but show a trend relating moisture level to attenuation.

4.1.4.2 Target Masking. An inspection of the RF attenuation chart for the Bruceton grade coal shows approximately 2.9 dB attenuation per inch at 3 GHz. A 10 in. coal thickness would have 29 dB loss for each direction plus scattering loss at shale interfaces for a total of approximately 58 dB. This loss sets the minimum radar performance for a 10 in. coal section. A section with a smaller thickness would have less loss or a stronger reflected signal from the coal/shale interface.

The mixer output signal of a FM/CW radar range is a frequency function. A target is indicated by a peak in amplitude at a specific frequency which is

related to coal thickness. It is, however, not a discrete frequency but an envelope of components every 100 Hz reaching a maximum at target range. The components diminish in amplitude at higher and lower frequencies but do not reach a zero value. These components (resulting from the RF modulation) form, in effect, an envelope that extends above and below the actual target. The envelope resulting from the front coal target surface masks the second or coal shale interface target. The masking obscures the interface unless the coal is thin (less than 5.5 in.). Figure 49 presents a graphic illustration of the masking effect and also shows the range at which coal/shale target signal is larger than masking envelope. It should be noted that Figure 49 relates only to performance of radar operating over an RF range of 1.7 to 4.3 GHz, with a 100 Hz triangular frequency sweep. Other values will change the picture dramatically, but with tradeoff in size and complexity. For example, lowering the RF range to 0.7 to 2.7 GHz would increase the level of interface signal because the coal attenuation is approximately one half the 1.7 to 4.3 GHz values which was used in most testing to date. The improvement would make the antenna significantly larger, but should be considered for system improvement. These tradeoffs are being considered as one of several ways to overcome the masking problem. Generally, at least 10 dB signal above noise is required for accurate target identification, regardless of the signal processing system. It is suspected, but not analytically proven, that a monocycle radar suffers from the same masking effects.

4.1.4.3 Radar Design/Improvements. The existing FM-CW radar operating over a frequency range of 1.7 to 4.3 GHz is limited in effective coal thickness range from a 2 in. minimum to approximately 5.5 in. maximum. This design is considered satisfactory to support guidance and control testing planned in 1978 at the Bruceton Surface Test Facility. It is not recommended for in-mine longwall applications. As explained previously the range limits are set by coal RF attenuation and front target masking effect. Figure 50 shows the approximate coal thickness or resolution (minimum distance between two targets) as a function of the RF transmitter deviation and includes a 10 dB signal to noise allowance.

New designs are proposed that will improve resolution as well as extend maximum depth measuring range. The range improvement will come from extending the frequency deviation range of the transmitter from 0.7 GHz at the low end of 4.3 GHz at the high end on the first design and from 0.7 GHz to 8 GHz on the second design. At large ranges the higher frequencies will not be able to penetrate the coal; however, this only affects accuracy for thick coal sections. Thin coal sections will not attenuate the higher RF allowing use of the full FM sweep capability at the radar.

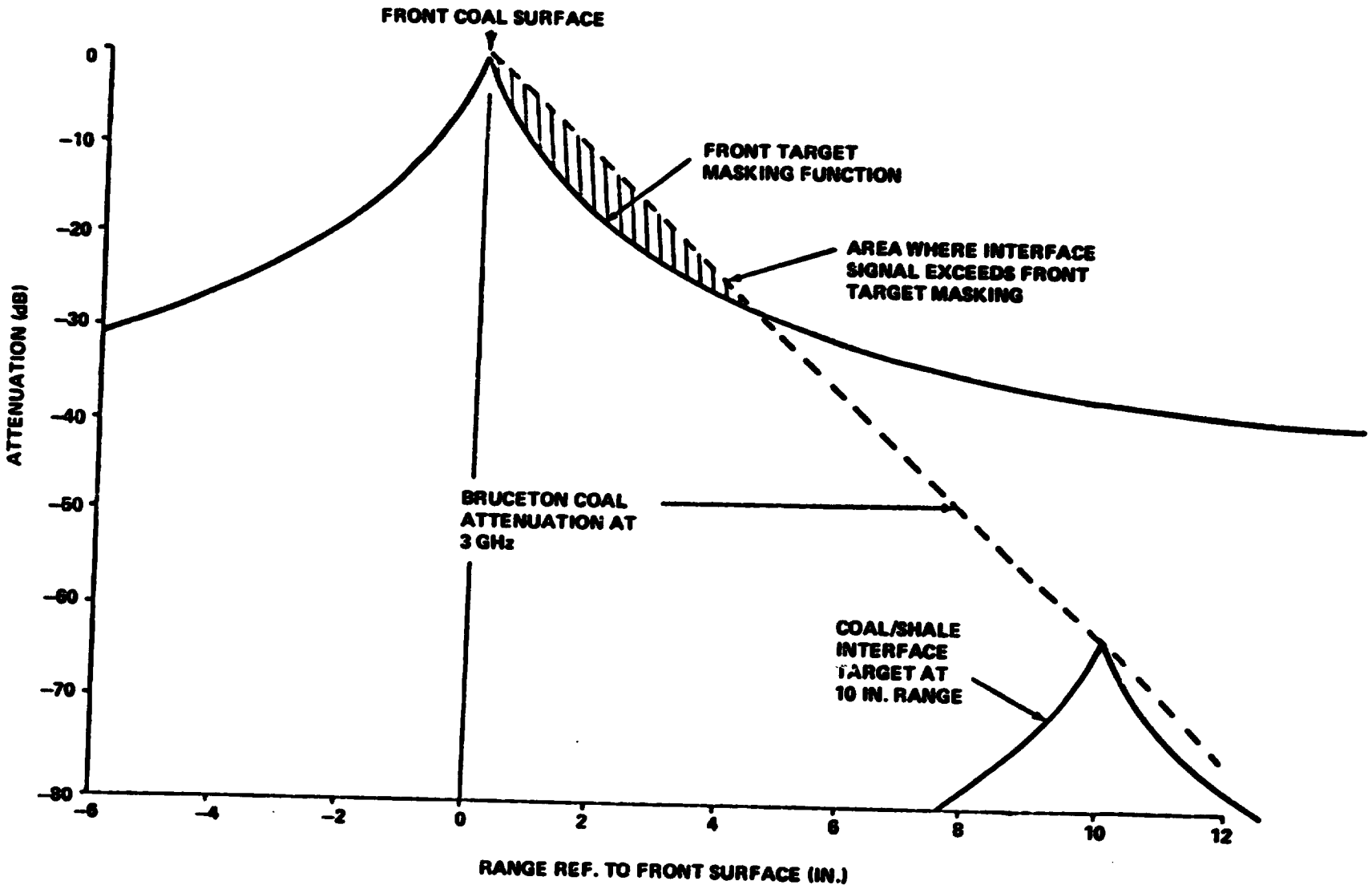

Figure 49. Front target masking.

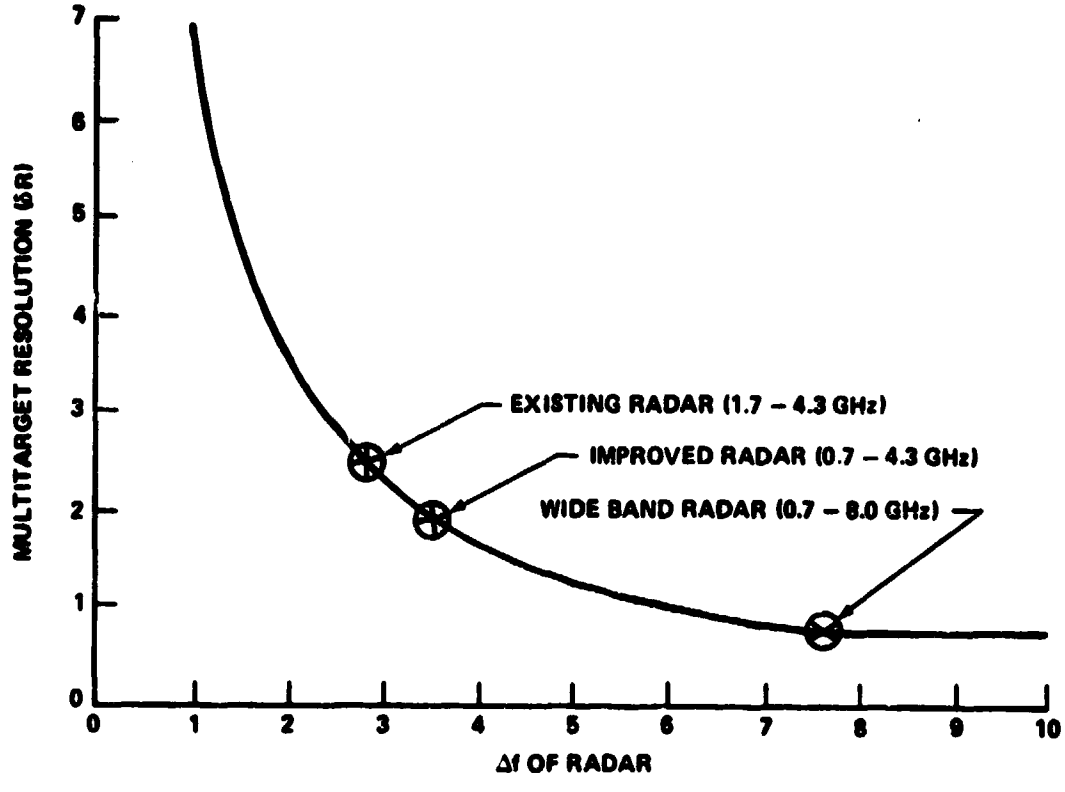

Figure 50. Multiple target resolution.

This design demands antenna, oscillators, and related RF components to cover extremely wide RF bandwidths. In the case of the 0.7 to 8.0 GHz design, covering four octaves with the sweep is not possible with available components. One solution is to segment the frequency bands in four, one octave segments. The RF sweep will also be segmented and switched between various amplifiers and antennas to give the effect of a wide bandwidth sweep. Further refinements will include continuous power leveling and the use of gated and switched baseband preamplifiers. The overall objective is to supply the signal processor with a best signal that is continuous during the complete RF sweep from 0.5 go 8 GHz. The disadvantages to this approach is that the number and

cost of YIG oscillators, amplifiers, etc., are high, also antennas are limited to one octave sgement and are very large in size at the lower frequencies. For example, a 0.5 to 1.0 GHz antenna will be approxi mately 60 in. long with front opening of 14 by 14 in. Size could possibly be reduced, but with performance reduction. Signal processing of data will be identical to that used with existing FM-CW coal thickness radars. Component specifications are complete. Early experiments are planned during FY78.

4.1.4.4 Signal Processing. The detector output of a FM-CW radar is a complex waveform containing frequency components of the true target range, frequency components of false targets, and noise. The usual procedure used to display radar range data is to use a spectrum analyzer which will display all frequency components of the radar. The spectrum analyzer's horizontal axis is a display of radar range; amplitude is related to target signal strength. Typical frequency values of the target run from 0 to 18 kHz. A second means of range readout is the Fourier transform which is a quicker and a more accurate procedure than is using analog spectrum analyzers. Since the transform is done within a digital computer, data are then transferred to computer storage and are available for other algorithms necessary to pin point target location.

Figure 51 shows a typical plot of a FM-CW radar signal returned from coal. The figure shows the many false targets common to this type of radar. An unexpected finding, as a result of dynamic testing of the radar moving over a coal bed (simulating a long wall machine), was the 6 to 8 dB glint (the random amplitude or angle fluctuations of a radar target) level of the interface return. The target glint simplifies identification because it is continually changing in amplitude, whereas most other targets are constant in amplitude. The following are some of the more conventional techniques used to process radar signals:

(a) Background subtraction for removal of systematic noise and false, non-moving targets associated with the radar.

(b) Low frequency filtering to suppress the DC component, and removal of 60, 120 Hz noise common to power lines. Low cutoff is usually set just below the front target return.

(c) Radar antenna target — Over the extreme frequency bandwidth of this type of radar, it is difficult to match the antenna impedance to the rest of the coaxial network.[4] The antenna will also show up as a false target and is easily identifiable because it appears just prior to front surface target. However, it also will have a multiple internal reflection within the coaxial network and will

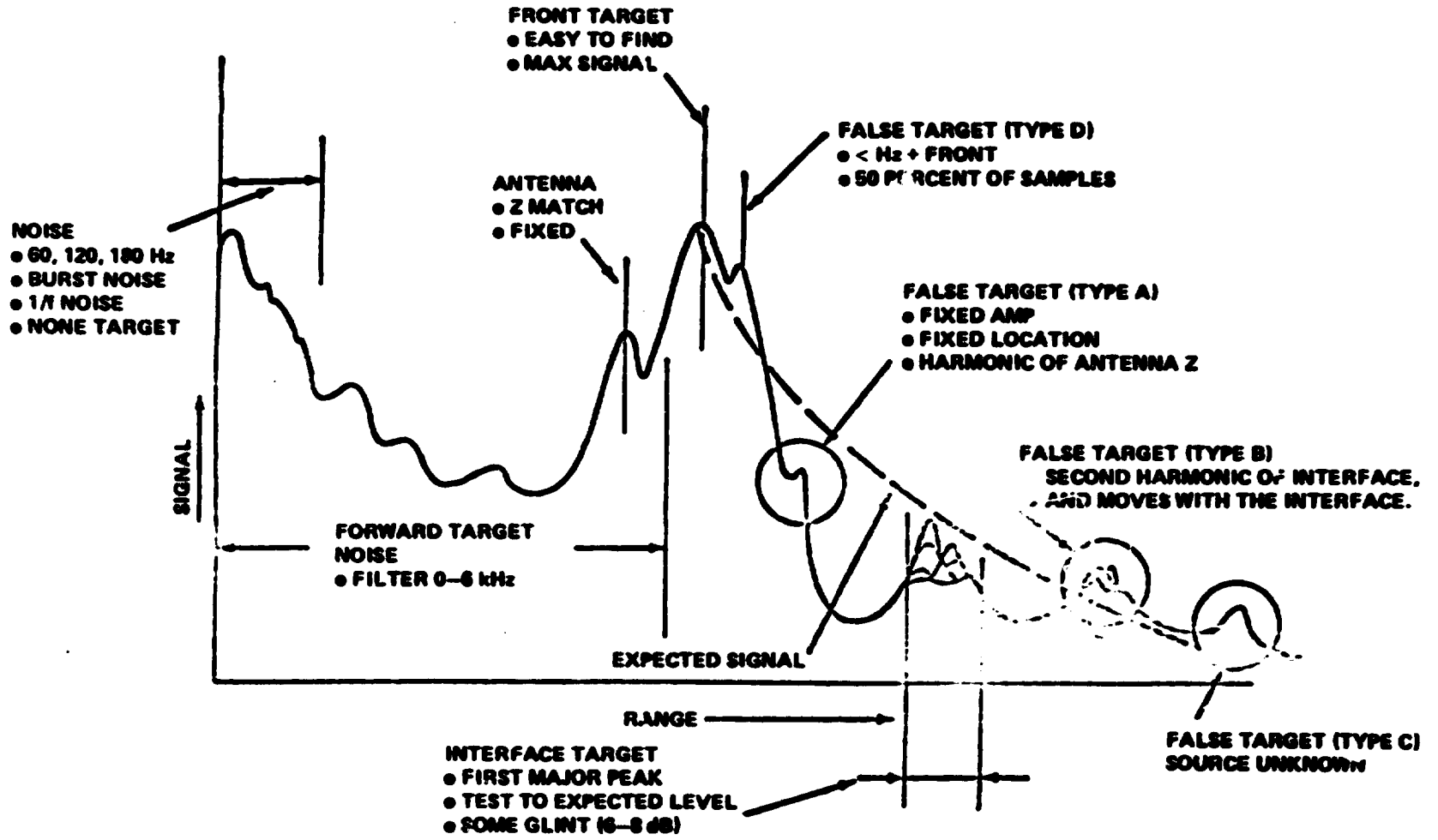

Figure 51. Typical spectrum of return FM-CW coal radar.

return to the antenna, resulting in a second echo for which the apparent range is greater than the front surface echo and is easily mistaken as the interface target. Antenna-originated false targets are predictable and therefore can be removed by the signal processor.

(d) Another false target results from the second round trip of the signal returned from the radar antenna and is also predictable in location (computed from radar to front coal distance). Careful radar positioning can usually distinguish this target from the true interface.

Signal processing will almost always involve one or more of the following operations:

(a) Storage

(b) Filtering

(c) Correlation

(d) Fourier Transformation

(e) Averaging.

The sequence of these operations varies for each algorithm and therefore a digital, programmable signal processor is the most desirable form. Digital processing does have the potential problem of encoding noise and limited resolution of input analog to digital converter. Minimum input A/D must have a dynamic range exceeding maximum to minimum target ratios of 70 dB or 12 bits.

Most signal processing experiments have been conducted on a Hewlett Packard 5481B Fourier analyzer. Its larger size limits in-mine use and therefore a miniaturized version is planned for later use in the program.

Several techniques have been tried in recent weeks to reduce the magnitude of the front surface target. The objective is to make visible the interface that may be attenuated as much as 60 dB by the coal.

Several techniques have been tried:

(a) Direct RF subtraction

(b) Glint averaging

(c) Feedforward filtering[5]

(d) Zero Hertz dynamic filter[5]

(e) Linear deconvolution.[6]

Direct RF subtraction works very well under stationary conditions and where some means are available to modify the rear target (enhance reflection). This requires very accurate successive data sampling. The process consists of simply recording the target signal, enhancing the rear target and subtracting the two. To modify the rear target a second sample of coal can be used but it requires an almost identical surface quality and careful duplication of the distance to the front surface. This is not a very practicable method; however, dramatic results are obtained when the front surface is nulled out.

Glint averaging is the same technique but takes advantage of the varying amplitude of the interface. The procedure is to subtract two successive samples, which requires moving the radar parallel to the coal surface. The first sample is then subtracted from the second sample. The results are encouraging but not dramatic because front surface return also glints. Fortunately, the surface glint of the front face seems to be less than the glint from the rear surface, thereby allowing subtraction to reduce the magnitude of the front face reflection more than the magnitude of the rear surface (the interface) reflection.

The feedforward filtering and Zero Hertz Dynamic Filter make use of the limiting of the FM radar signal to enhance the stronger (front face) signal. Once the strong front face signal is isolated, it can be subtracted from the raw radar signal (signal containing both front surface and interface), leaving only the interface target. The zero hertz dynamic technique works in a similar manner; however, the final step is to multiply the two signals together. This causes the rear target to show up as a DC component that can be blocked out with a simple filter. Both techniques are in early test and have encouraging results.

Figures 52, 53, and 54 illustrate the convenience of the zero hertz dynamic signal processing method in determining target range (thickness). In (a) of Figures 52, 53, and 54, the front and interface targets lay with a range of 6 to 7.5 kHz. This signal was amplitude leveled, bandpass filtered (Fig. 55). A front target was synthesized by amplitude limiting and filtering. This signal

5. Technique suggested by Dr. Ely Baghdaddy, Info Systems Inc., under contract Coal Radar Studies, NAS8-32655.

6. Technique suggested by Dr. Larry Kennedy. National Research Post Doctoriate Fellow, assigned to MSFC.

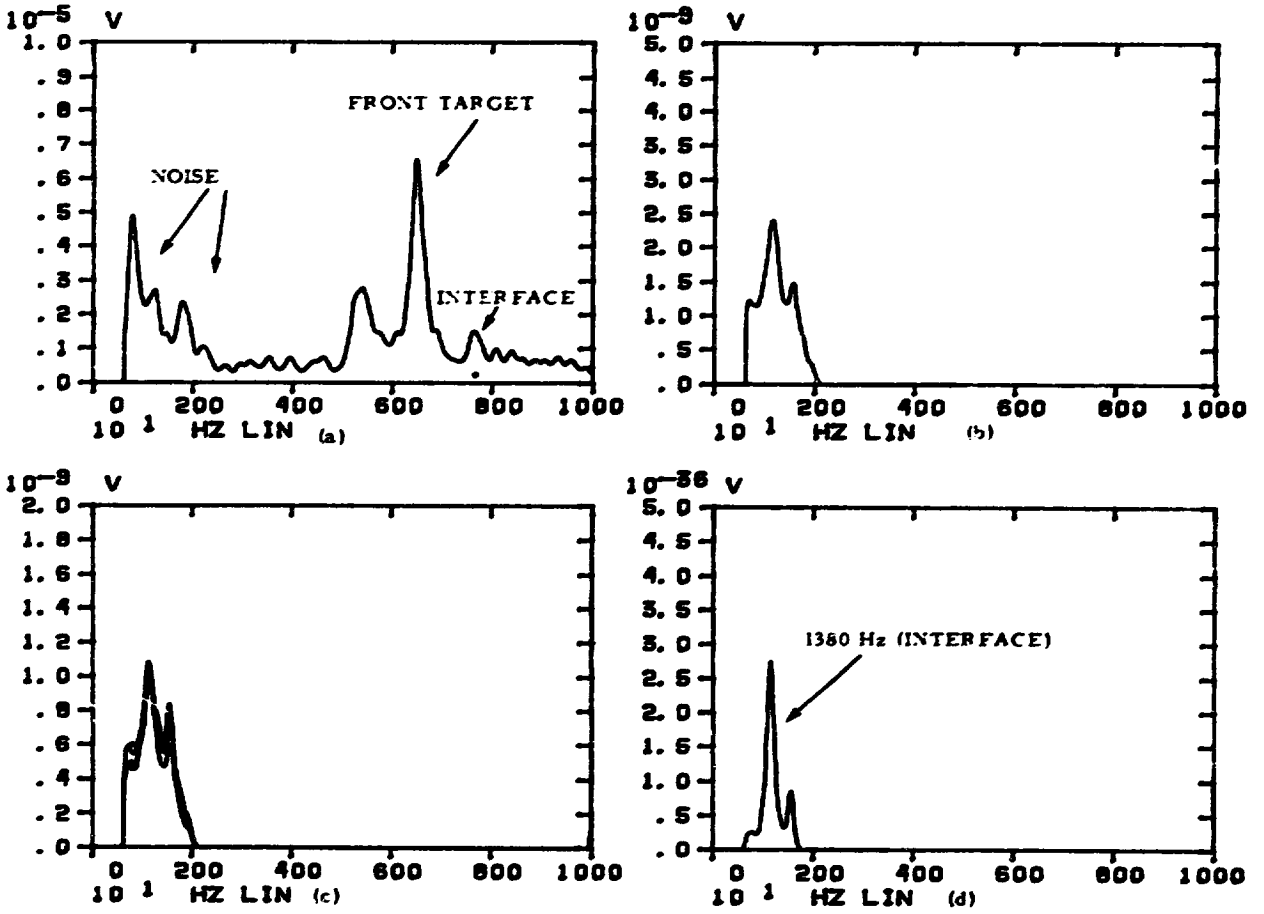

(a) Raw radar signal.
(b) Single sample, after limiter and filter.
(c) Four samples superimposed.
(d) Results of four samples multiplied together in frequency domain. Eight in. thick coal is represented by 1380 Hz peak in (d).

Figure 52. Signal processing example for 8 in. thick coal.

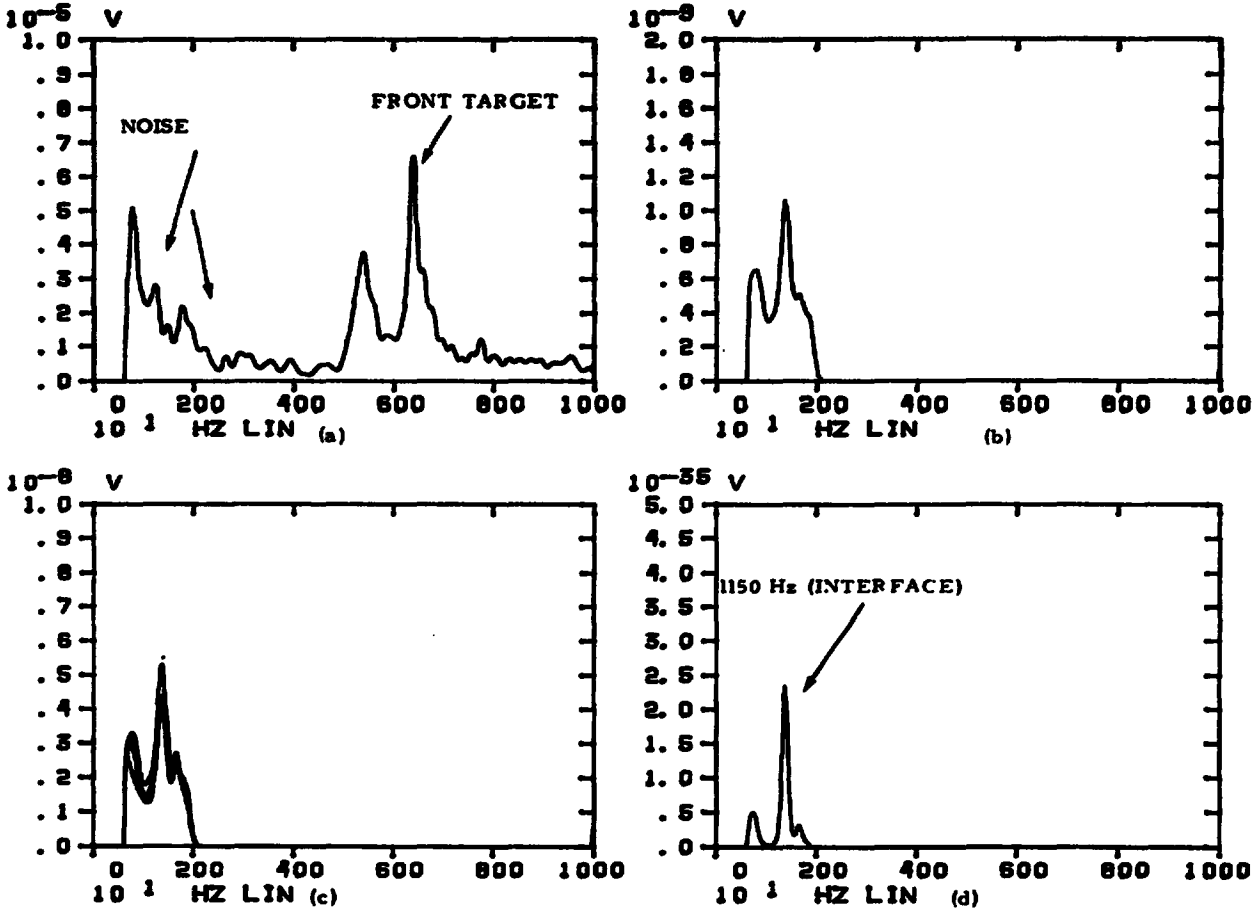

(a) Raw radar signal.
(b) Single sample after limiter and filter.
(c) Four samples superimposed.
(d) Results of four samples multiplied together in frequency domain. Six in. coal is represented by 1150 peak in (d).

Figure 53. Signal processing example for 6 in. thick coal.

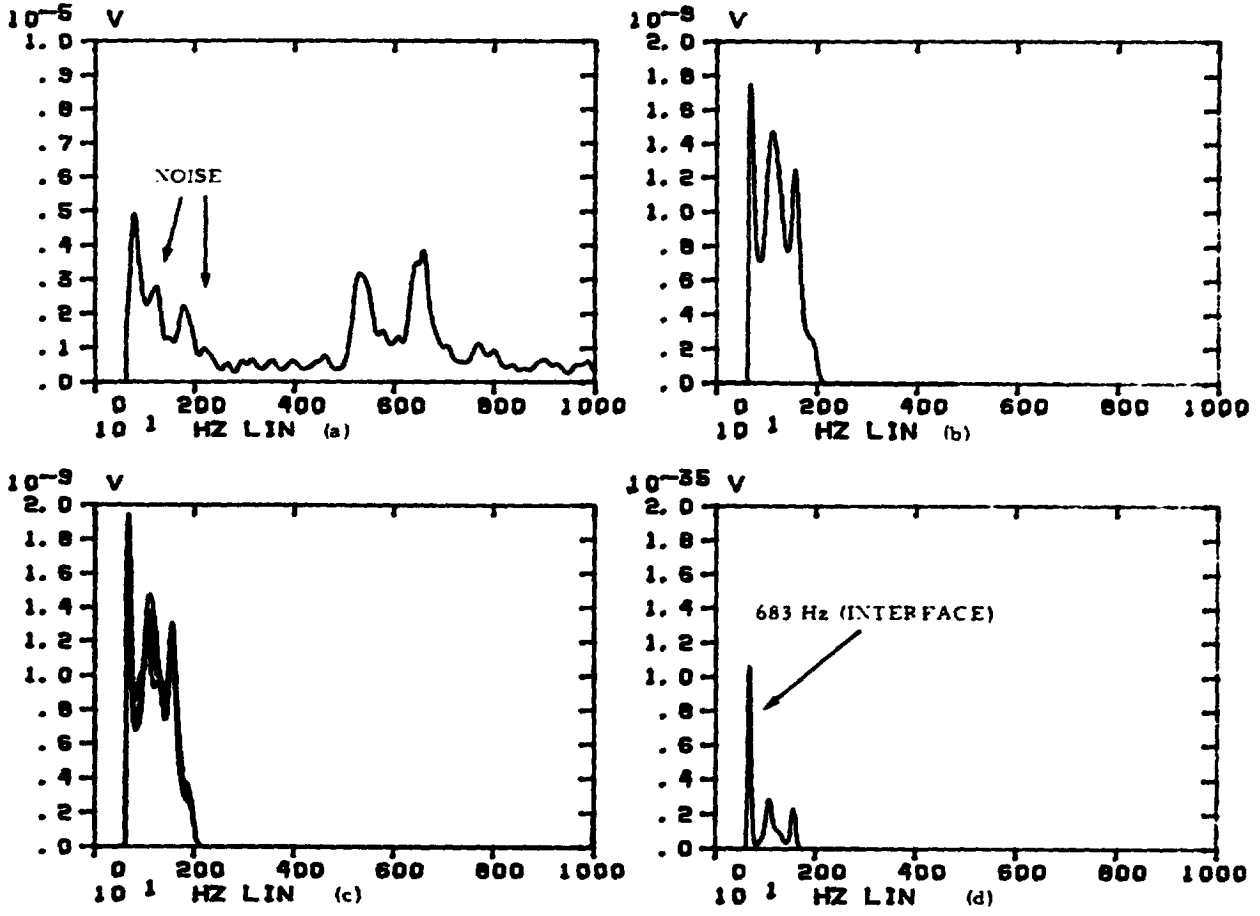

(a) Raw radar signal.
(b) Single target sample after limiter and filter.
(c) Four samples superimposed.
(d) Results of four samples multiplied together in frequency domain. Four in. coal is 683 Hz in (d).

Figure 54. Signal processing example for 4 in. thick coal.

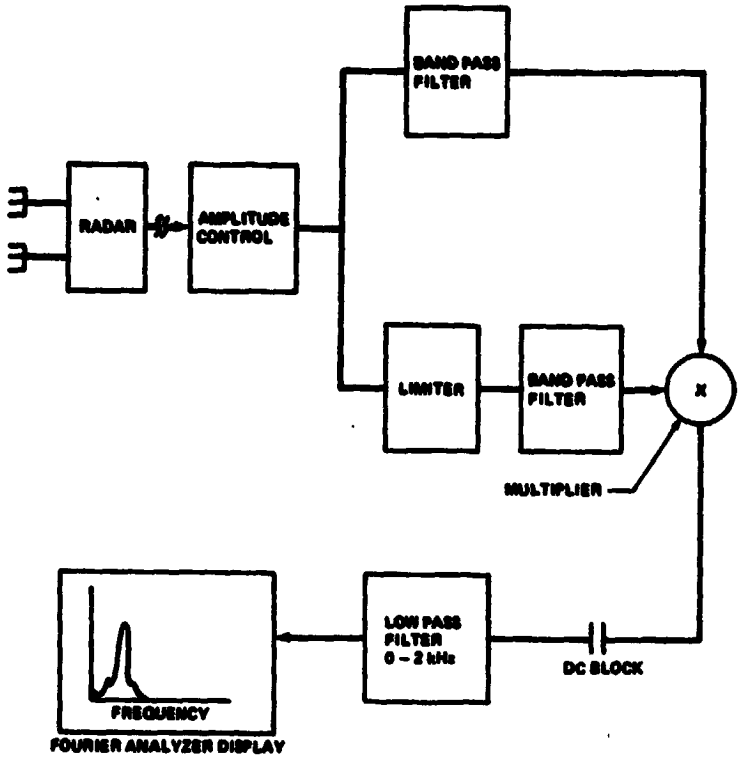

Figure 55. Elemental steps for signal processing longwall simulator test.

was then mixed with the complex (front and rear) targets. Result (b) of these figures was to translate the front target to a DC value which was then eliminated by a blocking capacitor. The difference frequency (front minus the interface) is then proportional to coal thickness. Four data samples (c) were multiplied together to suppress the background, resulting in a strong target identification (d).

The data are from actual tests performed on the longwall simulator and processed on a digital computer. The radar was mounted over a coal bed arranged in 2, 4, 6, and 8 in. thick steps. The radar was slowly moved over each step and signal recorded for later processing. The 2 in. coal step was just below minimum range capability of the radar. The coal used was very dry and had approximately 35 percent less attenuation than normal mine fresh coal.

Data points for the tests are shown in Figure 56. The radar operated over an RF band of 1.7 to 4.2 GHz with a sweep rate of 100 Hz. Two circular polarized antennas were used.

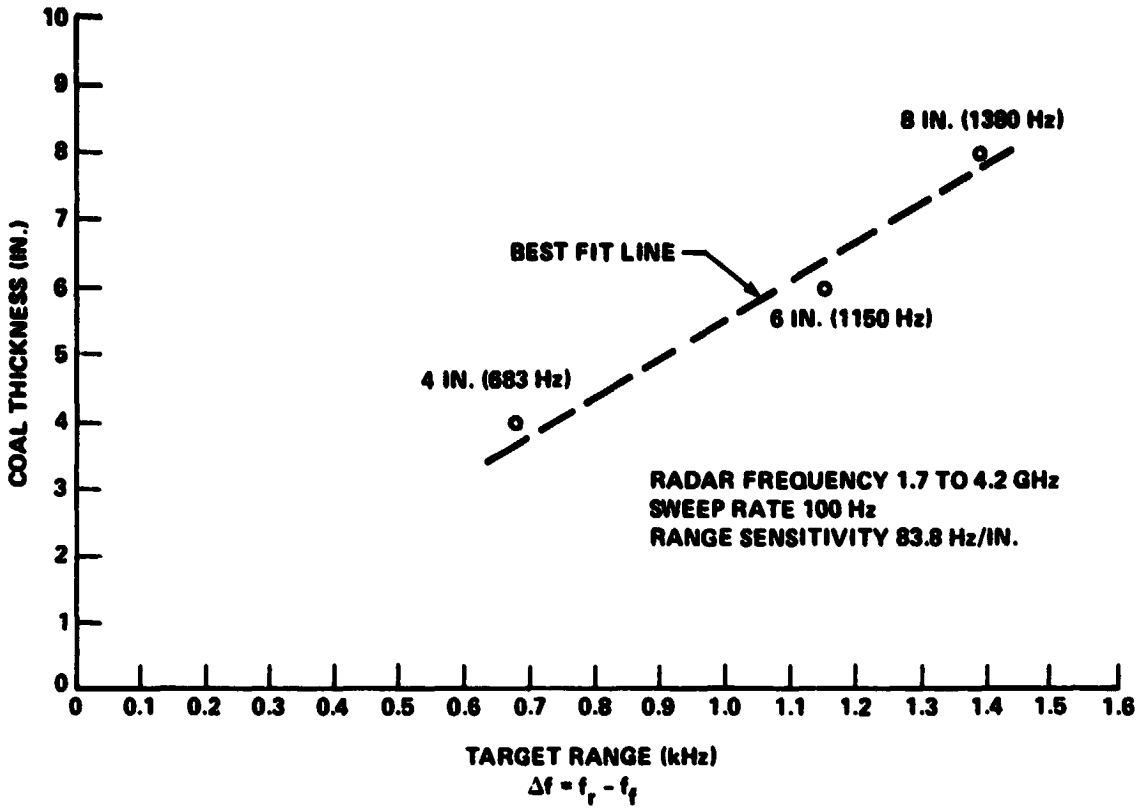

Figure 56. CID radar longwall simulator test.

4.1.4.5 Conclusions. Very high attenuation of the radar signal passing through coal combined with front target, masking the weak interface signal and comprising the primary obstacle to developing a successful coal thickness radar. These factors have, thus far, restricted performance to a limited range of coal thicknesses (2 to 5.5 in). Several signal processing procedures are complete that output coal thickness reading every 5 sec using conventional moderate speed digital computers. Development of a miniaturized signal processor has been temporarily halted, awaiting industry development of second generation Fourier transform circuits that meet the "time of computation" requirements necessary for shearer drum control.

Continuing activity in radar development will be directed toward increasing range thickness capability by a substantial increase in RF bandwidth, reduction in transmitter FM noise, and increase in dynamic range of signal processor input analog circuits. Problems in reducing FM noise in YIG oscillators have renewed interest in two frequency radars and analytical studies are continuing.

4.1.5 Artificial Coal and Rock Material Test. Samples of the artificial coal and rock materials which are planned for use in the mock Longwall test facilities at Bruceton have been tested for experimental CID's operations and physical properties. The five samples are identified in Table 9.

TABLE 9. ARTIFICIAL COAL/ROCK SAMPLES

Sample	Size	Composition
No. 1 Artificial Coal	24 × 24 × 24 in.	See note
No. 2 Artificial Coal	36 × 36 × 3 in.	See note
No. 3 Artificial Rock	36 × 36 × 3 in.	8:1 (fly ash: cement)
No. 4 Artificial Rock	18 × 18 × 10 in.	8:1 (fly ash: cement)
No. 5 Artificial Coal	3 × 3 × 3 in.	See note

Note: Coal: 10, Fly Ash: 8, Cement: 1, Water: 1 1/2

4.1.5.1 Experimental CID Tests. The operational tests performed on artificial coal sample No. 1 were limited to the surface recognition CID's, i.e., reflectometer and impact penetrometer, because the test specimens depth (24 in.) exceeded the depth measuring capabilities of the radar and nucleonic CID's. The reflectometer and impact penetrometer identified the surface of the test specimen as shale because of the predominance of the binding material on the surface of the test specimens. Its light color and nonresilient nature are discriminating factors for shale.

A second group of samples was provided in March 1977. These samples were poured in thinner sections to specifically accommodate testing the radar and nucleonic CID's. The test specimen was arranged with the artificial coal specimen No. 2 placed on top of the artificial rock specimen No. 3 (Fig. 57).

Attempts to measure the thickness of artificial coal in this configuration with the FM/CW radar were unsuccessful. Reflected electromagnetic waves occur when there is a distinct change in the dielectric constant of the media through which the radar signal is being transmitted. The dielectric constants of the artificial coal and rock were too similar to generate the reflected wave and thus the radar was unable to measure the artificial coal thickness. A second test was performed after placing a sheet of aluminum foil at the artificial coal/rock interface. Under these conditions, the radar was able to measure the depth of the artificial coal.

The backscatter gamma ray nucleonic CID was also tested on the artificial test specimen per Figure 57A. The nucleonic CID was configured with a 20 in. separation distance between the 30 millicurrie cesium source and the detector. Measurements of the artificial coal depth with this CID were also unsuccessful because of the similarity in densities of the two substitute materials: artificial coal 1.6 gm/cc and artificial rock 1.66 gm/cc. However, a second test (Fig. 57B) was performed with the artificial coal sample No. 2 placed on top of solid cement blocks, density 2.4 gm/cc. With this configuration of artificial materials, the nucleonic CID was able to measure the depth of the artificial coal.

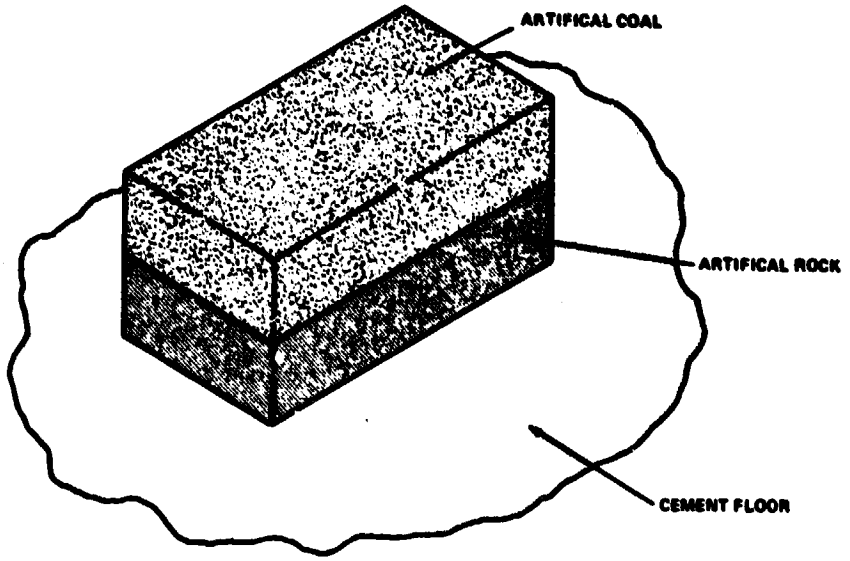

(A)

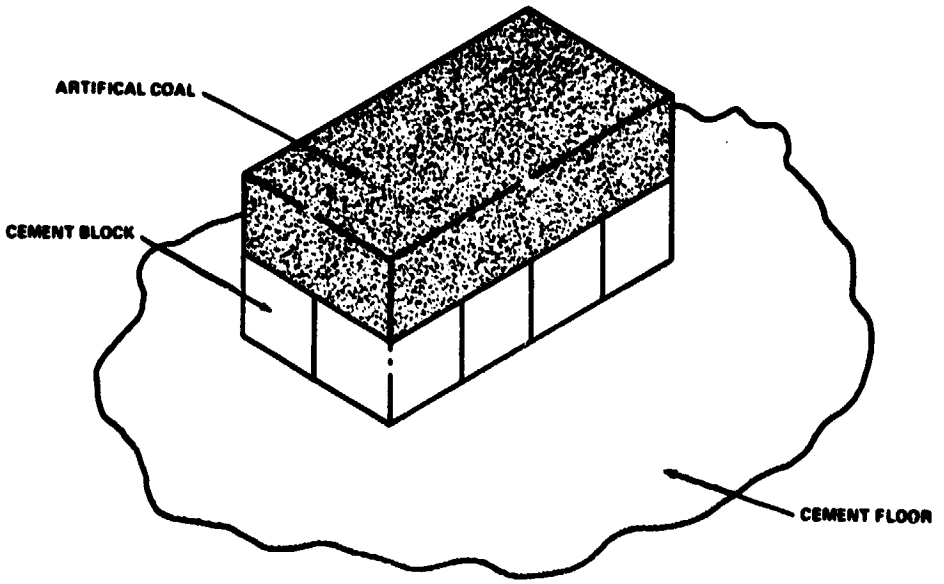

(B)

Figure 57. Test specimen arrangements.

Surface recognition tests were also performed on test specimens No. 2, No. 3, and No. 4. Again, the reflectometer and impact penetrometer CID's could not correctly identify the artificial test specimens. This was again due to the predominance of the light color and hard binding material on the surface of the test specimens.

4.1.5.2 Physical Property Tests. In addition to the operational CID tests, the test specimens were also tested for determination of those physical properties which directly affect the operations of the CID's. These properties include shore D hardness, moisture content, density, compressive strength, dielectric constant, and loss tangent. The values listed as the physical properties in Table 10 can only be regarded as mean values because of the extremely nonhomogeneous nature of these test specimens.

TABLE 10. PHYSICAL PROPERTIES OF ARTIFICIAL COAL AND SHALE

Specimens	Shore D Hardness	Moisture (%)	Density (g/cc)	Compressive Strength (psi)	Dielectric Constant	Loss Tangent (dB/in.)
Artificial Coal (Specimen No. 1)	50-63	3	1.6	500	12.1	2.0
Natural Coal	65-82	1.4-0.28	1.5	—	4.5	3.0
Artificial Rock (Specimen No. 3)	40-65	3.5	1.6	—	15.7	—
Shale (Natural)	87	—	2.5	—	—	—

4.1.5.3 Recommendations. The following recommendations are made to enable testing/operation of the experimental CID's with the artificial coal and rock materials. It is not known whether these changes will adversely affect the cutting characteristics of these materials.

4.1.5.3.1 Radar. The addition of aluminum foil strips, steel needles, or some similar arrangement at the artificial coal/rock interface will enable the FM/CW radar to measure the depth of the artificial coal.

4.1.5.3.2 Nucleonic. The nucleonic CID will function correctly by either increasing the density of the artificial rock mixture by 60 to 80 percent or by substituting solid cement block for artificial rock material.

4.1.5.3.3 Impact Penetrometer. The concentration of coal lumps (2 in. diameter or greater) in the artificial coal mixture must be increased to the extent that the probability that the striking head will hit coal rather than binder material is 4:1 or greater.

4.1.5.3.4 Reflectometer. The color of the artificial coal must approximate that of real coal, which can be accomplished by the addition of powdered coal to the artificial coal mixture.

4.2 Vertical Control System (VCS)

4.2.1 Current Concept. Since the last annual report, changes have taken place in the Longwall miner design which affect the performance of the VCS. These changes have been implemented in the Longwall miner simulation and their effects are included in this report.

One important design change is the replacement of the gob side trapping shoes with a single skid located in the center of the chassis. The trapping shoes (located 115 in. apart) were previously considered to be the chassis/track points of contact for purposes of simulation. The face skids (located 81 in. apart) now control the pitching motion of the chassis as it traverses the track. The closer contact points result in more severe chassis undulations for given track variations.

One of the original ground rules for VCS design is that the miner will be automated with the machine configuration as specified by the manufacturer. If changes are to be made (such as this one), it may be possible to make some performance improvement suggestions as to the implementation of these changes.

Performance studies indicate that drum height variations due to track undulations are diminished if the chassis/track contact points are moved as far apart as possible and the boom pivot points are moved as close as possible. Ideally, the skid separation would be greater than the distance between the boom pivot points. This would improve performance for the operator controlled as well as the automated Longwall miner.

Other dimensional changes affecting performance are:

(a) Boom length — changed from 44.25 in. to 74.5 in.

(b) Distance of boom pivot above skid plane — changed from 32.5 in. to 35.25 in.

4.2.1.1 Hydraulics (Drum/Actuator Linkage). The actuation system has been changed from a maximum flow of 7 gal/min to 8 gal/min. The comparison (Table 11) of the effects of this change are theoretical and do not reflect actual tests.

TABLE 11. THEORETICAL COMPARISON OF CHANGE IN FLOWRATES

Single Boom Operation		
Flow (gal/min)	Actuator Extension Rate (in./sec)	Actuator Retraction Rate (in./sec)
7	0.653	0.788
8	0.746	0.900
Dual Boom Operation (Flowsplit)		
3.5	0.326	0.394
4.0	0.373	0.450

This change becomes more significant when coupled with the revised shearing boom geometry shown in Figure 58. Drum height (above the skid plane) is shown as a function of actuation position and boom angle in Figure 59.

The flowrate and boom length increases combine to produce the changes in the maximum drum rise and fall rates as shown in Table 12.

Longwall miner data taken from actual test of the actuation system under the boom load are available. These data have been modeled and programmed and are currently in the debugging stage. The models will be implemented in the simulation as soon as the checkout phase is complete.

4.2.2 VCS Simulation Modifications. This section contains a brief discussion of the most important modifications made to the simulation during the past year.

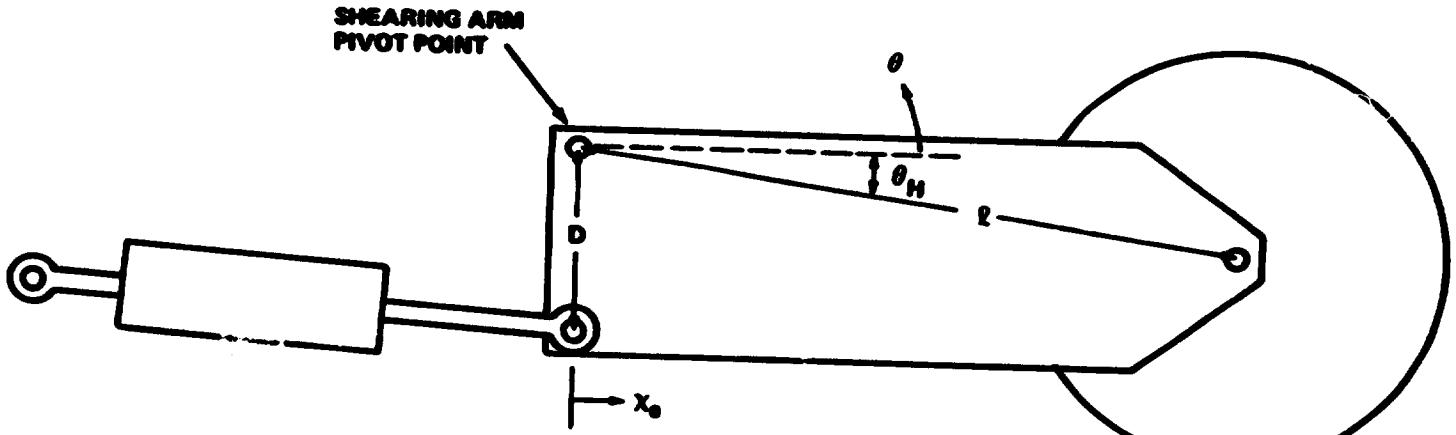

$\theta_H = 4.84°$ $\quad \ell = 74.5$ IN. $\quad D = 16.5$ IN.

$$\theta = \cos^{-1}\left[\frac{912.498 - (23.25 + X_a)^2}{594.804}\right] - 72.911°$$

r = RADIUS OF SHEARING DRUM = 27 IN. AT PICK TIP

b = DISTANCE OF PIVOT POINT ABOVE SKID PLANE = 35.25 IN.

Figure 58. Boom and actuator geometry (horizontal position parallel to chassis).

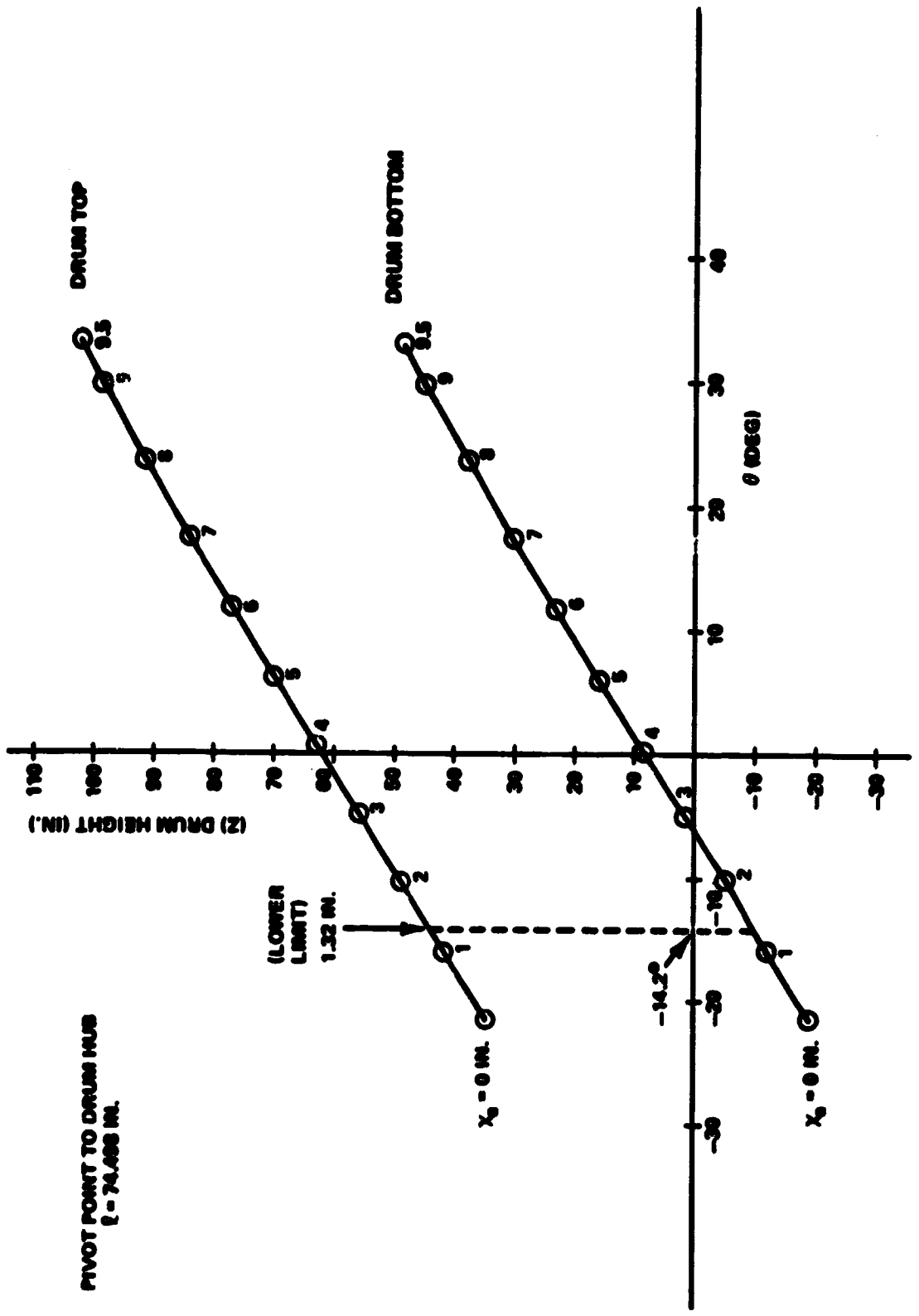

Figure 59. Boom angle versus drum height.

TABLE 12. CHANGES IN MAXIMUM DRUM RISE AND FALL RATES

Flow (gal/min)	Boom Length (in.)	Rise Rate (in./sec)	Fall Rate (in./sec)	Single or Dual Actuator Operation
7	44.25	2.81	3.39	Single
8	74.5	5.32	6.41	Single
3.5	44.25	1.41	1.70	Dual
4	74.5	2.66	3.21	Dual

4.2.2.1 CID Models Utilizing Statistical Errors. One of two statistical models can be chosen. Each model begins with the output (ϵ) of a perfect coal depth sensor. The output is in inches and is defined as the average coal depth taken over the sensor output period.

4.2.2.1.1 Model A. The output (ϵ) is assumed to be the sum of the average coal depth (d_c) and the average air gap (d_{AG}) between the sensor and coal surface, i.e.,

$$\epsilon = d_c + d_{AG} \quad .$$

A random number generator is then used to select an air gap from a histogram constructed from actual mine data and this equation is used to calculate the depth of coal, d_c.

A series of curves which represent the sensor output in counts as a function of coal depth and air gap have been permanently loaded into the simulation. Since the coal depth and air gap have been calculated and statistically selected, these curves may be entered and the corresponding count read.

This count number must now be interpreted as a depth of coal to be passed on to the VCS. This is accomplished by means of the sensor calibration curve which is a single curve of counts versus coal depth. The coal depth as read from the calibration curve is then passed to the VCS, and the shearing drum is positioned accordingly.

4.2.2.1.2 Model B. This model allows the selection of a 3σ error band which is then applied to the perfect sensor output. The distribution about the

perfect sensor value is assumed to be normal and the statistically selected error is added to the actual coal depth and then passed to the VCS. If the selected coal depth is less than zero, the depth is assumed to be zero. For this reason the distribution becomes skewed toward the positive values as the perfect sensor output becomes small.

This model is used in the generation of the data presented in the simulation results section.

4.2.2.2 More Accurate Determination of Actuator Command. The exact solution for the conversion of the drum height command to the actuator position command has been included in the simulation. In the past a straight line approximation to this solution was used. The approximation introduced errors which have now been eliminated. The revised VCS diagram is shown in Figure 60.

4.2.2.3 Drum Filtering. This subject was discussed in the first yearly report and has now been implemented in the simulation. This feature simulates the movement of the drum circumference through the coal and has a smoothing effect on the remaining coal surface. Previously, the shearing drum cut was considered to be the trajectory of a point at the top or bottom of the drum on a line drawn vertically through the hub.

4.2.2.4 CID to Drum Top/Bottom Distance Indicators. In the baseline VCS, the coal depth sensor is mounted on an arm which trails the shearing drum (Fig. 61). The current design calls for the mounting arm to maintain the same height (relative to the skid plane) as the drum hub. The arm is connected in a parallelogram fashion to the chassis and will therefore lie in a plane parallel to the chassis and through the drum hub. This tilting of the mounting arm according to chassis undulations produces inherent errors in the distance indicators. This effect has been included in the simulation during the past year and tends to lessen the VCS performance for coal seams with undulating floors.

4.2.2.5 Turnaround. One of the problems involved in making multiple pass studies is simulating the Longwall miner turnaround at each end of the coal face. For simulation purposes the miner is assumed to traverse the entire coal face in one direction (no sumping) before the turnaround. One multiple pass study is presented in the simulation results (Section 4.2.2.6) of this report.

4.2.2.6 Simulation Results. The coal interface profile used to obtain the simulation results in this section is shown in Figure 62. It is assumed that the coal/rock interface variations remain constant as the miner is advanced into the coal face. To insure that the chassis will undulate, a last cut remainder has

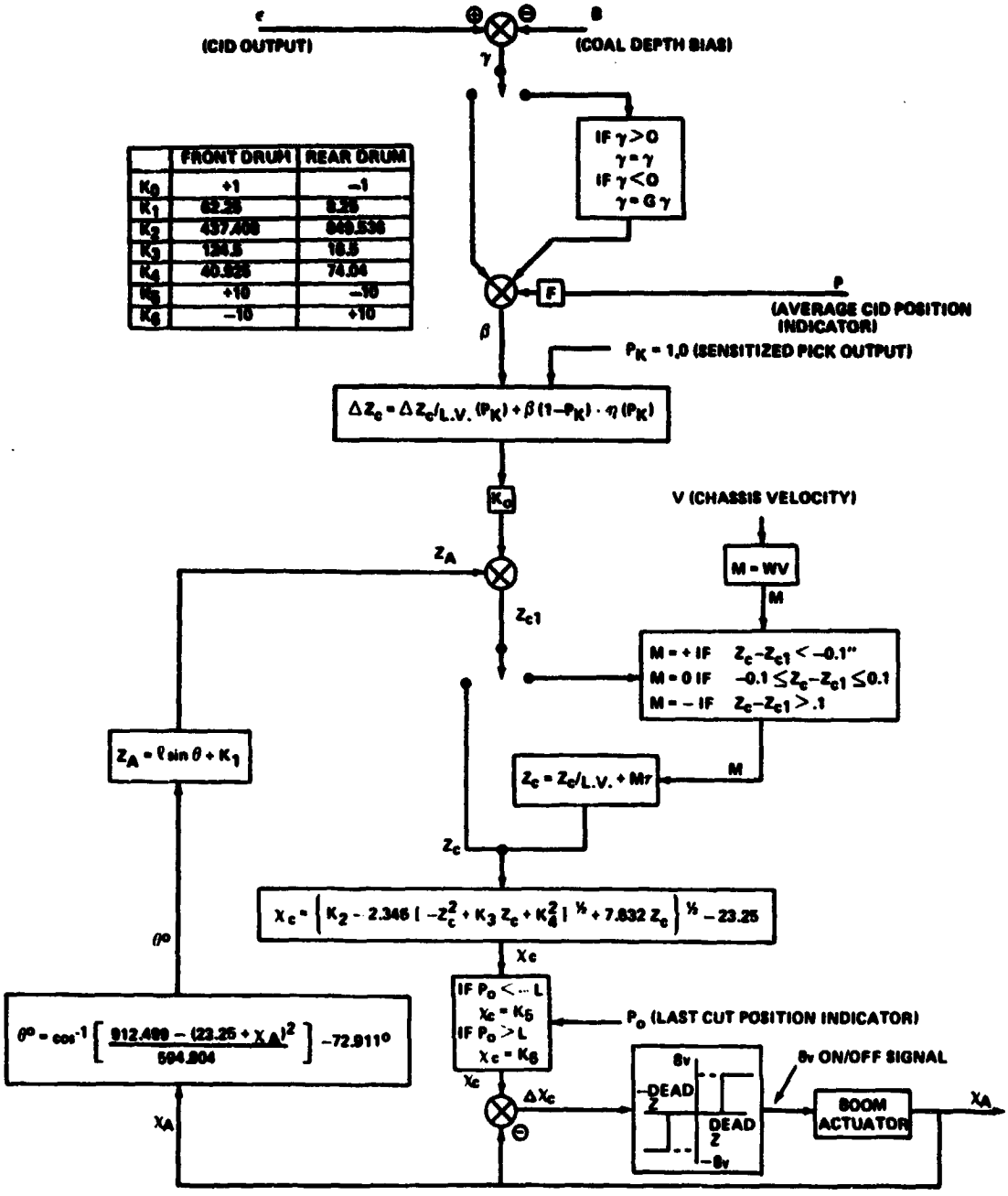

Figure 60. Vertical control system description.

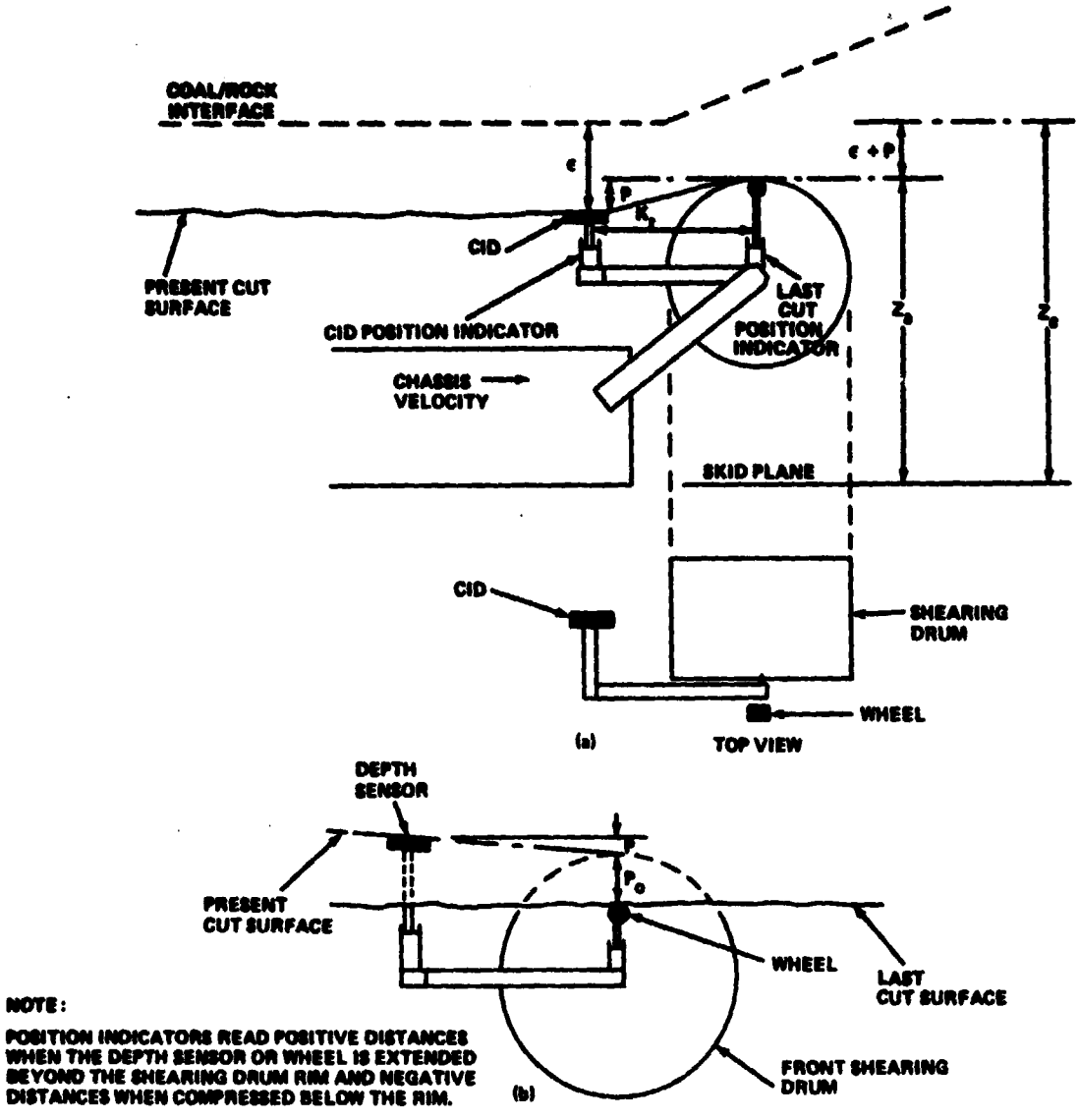

Figure 61. Vertical control system (pictorial representation).

been specified (Fig. 62). This remainder is assumed to be the coal thickness remaining (positive remainder) and the depth of rock taken (negative remainder) as the coal face was being prepared for the first pass of the Longwall miner. This remainder, when superimposed on the floor profile, specifies the lay of the track for the first pass. When superimposed on the ceiling profile, it specifies the trajectory that the front drum last-cut follower will trace on the first pass. On the second and succeeding passes, these paths are determined by the cut of the preceding pass.

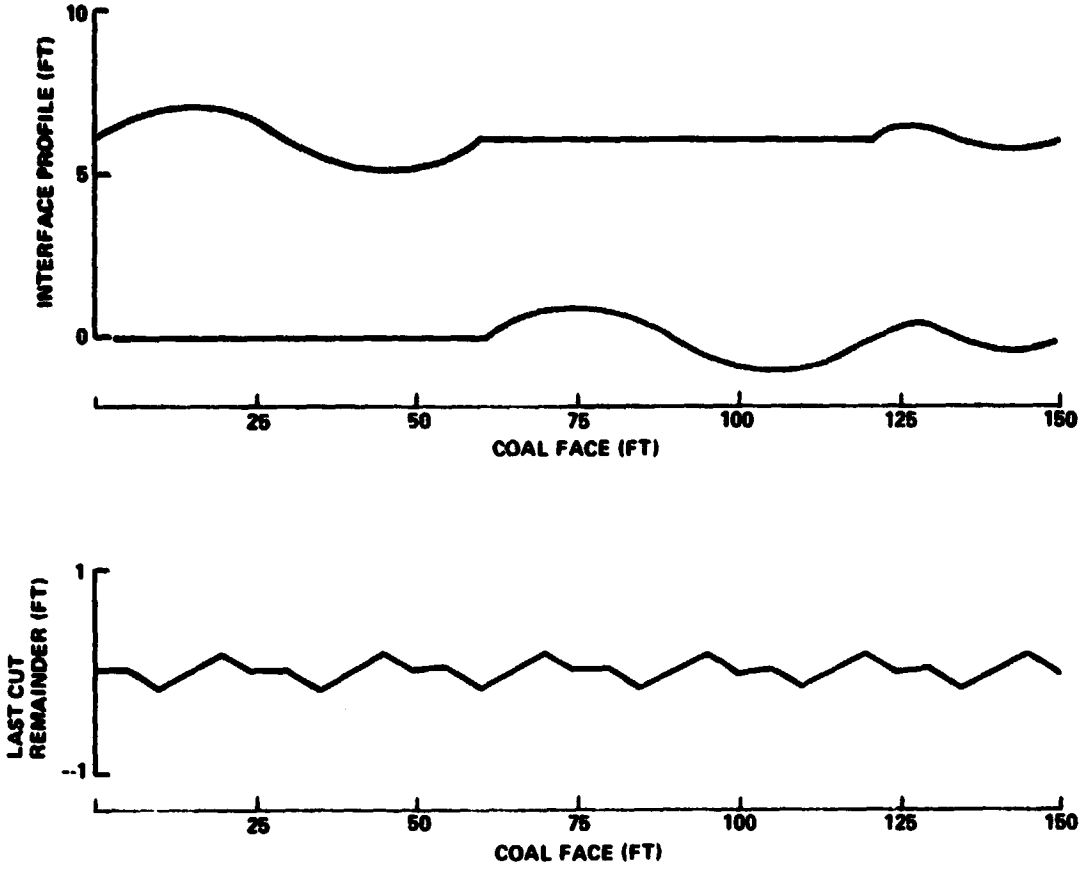

Figure 62. Profile and last cut remainder.

Data have been generated which show performance trends as a function of depth sensor accuracy, depth sensor output period, and the use of sensitized picks as opposed to a rock avoidance scheme.

Typical runs are shown in Figure 63 with the conditions of each run shown on the plot. The performance indicator was taken to be the volumetric sum of the coal left and the rock taken. The VCS has been biased to 1 in.; therefore, a perfect cut would leave 1 in. of coal on the floor and ceiling and take no rock. The last-cut following devices are not active for this series of runs. Performance trends are more evident when the VCS is free to position the drum, unaffected by limited excursions, relative to the last cut. The data for this study are summarized and presented graphically in Figure 64.

The plotted points in Figure 64, where sensitized picks are used, are very close together. This indicates that for this range of σ values, the effect on performance is small. The lengthening of the CID output period shows a

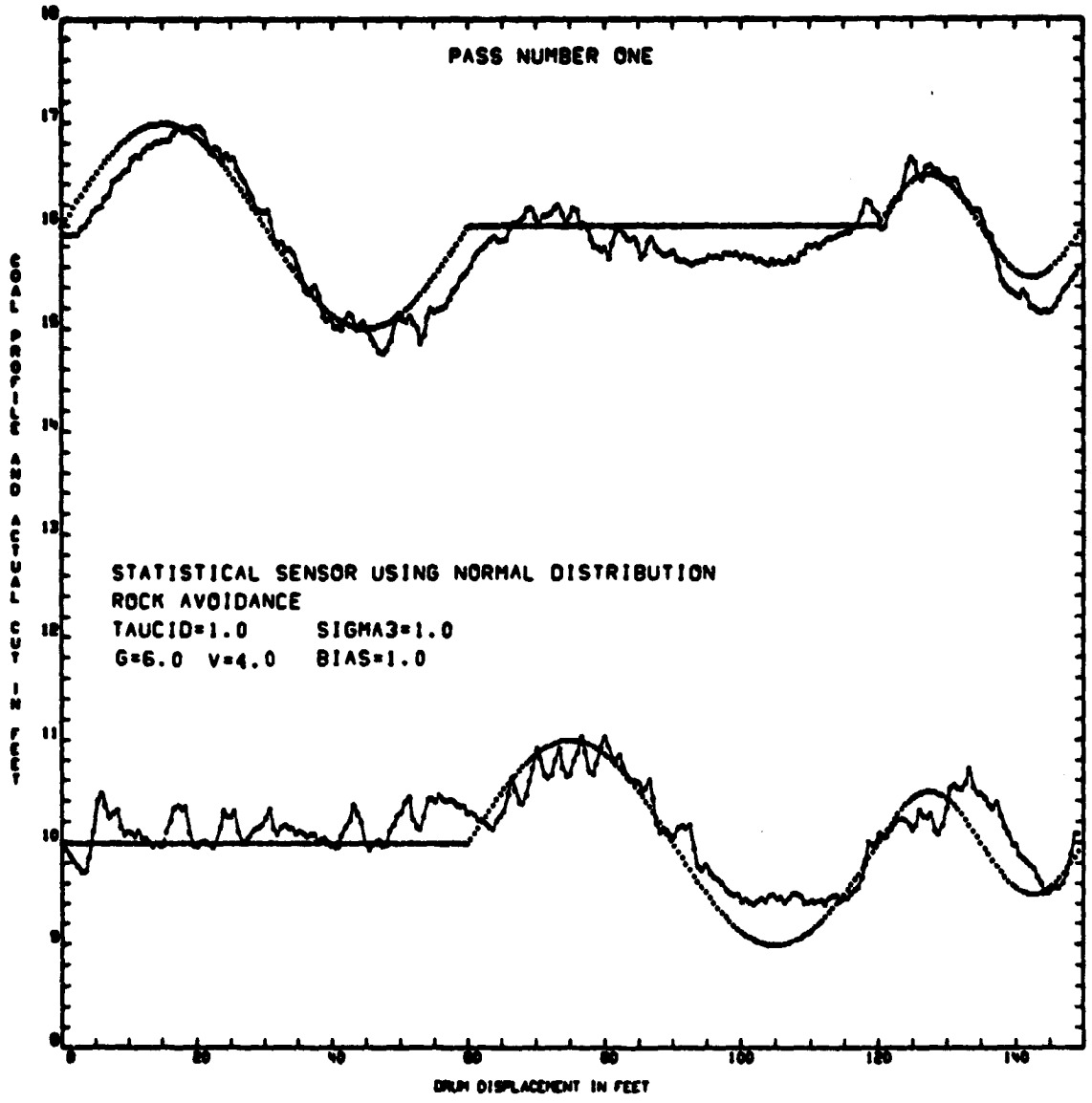

Figure 63. Typical runs.

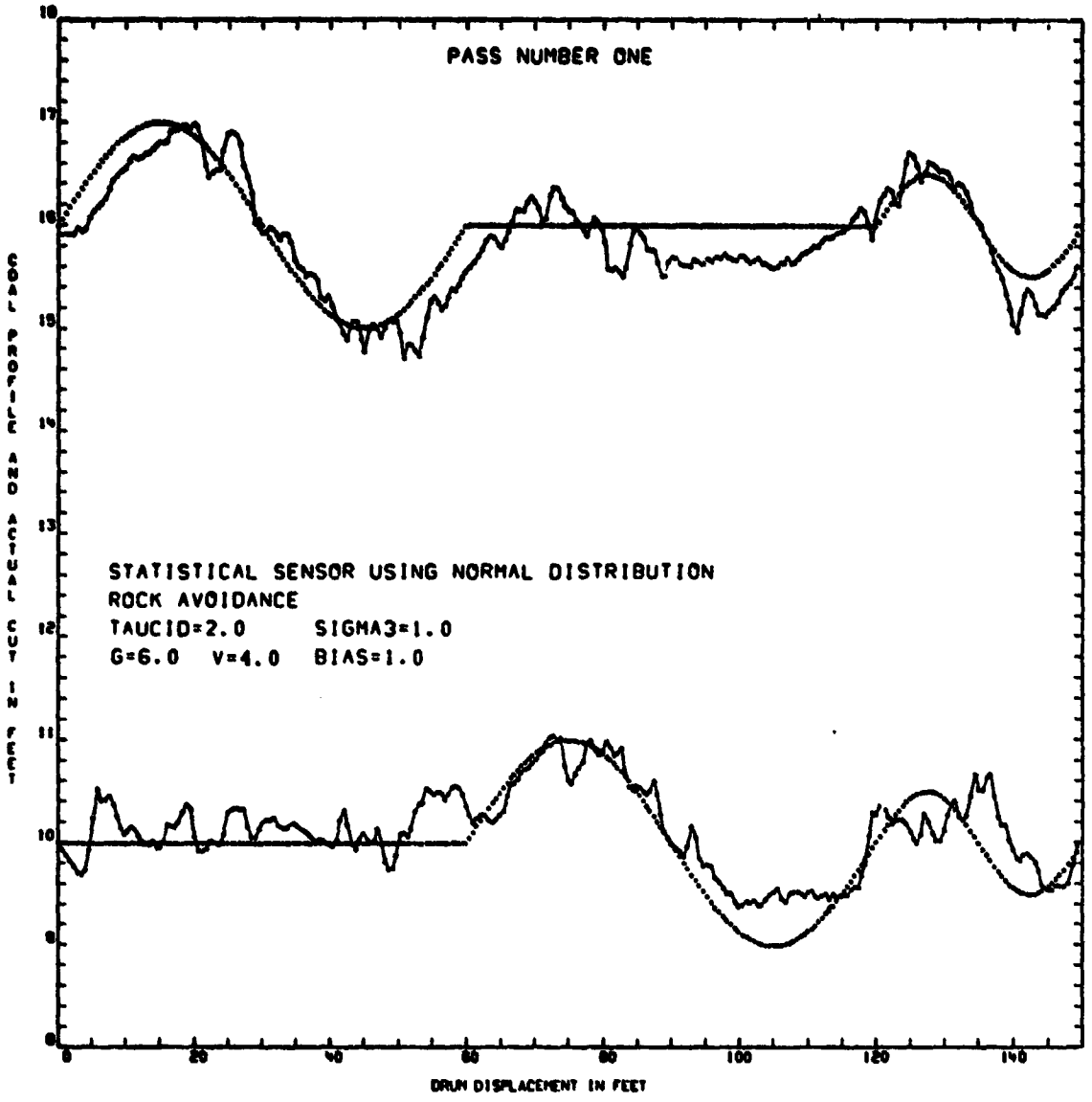

Figure 63. (Continued).

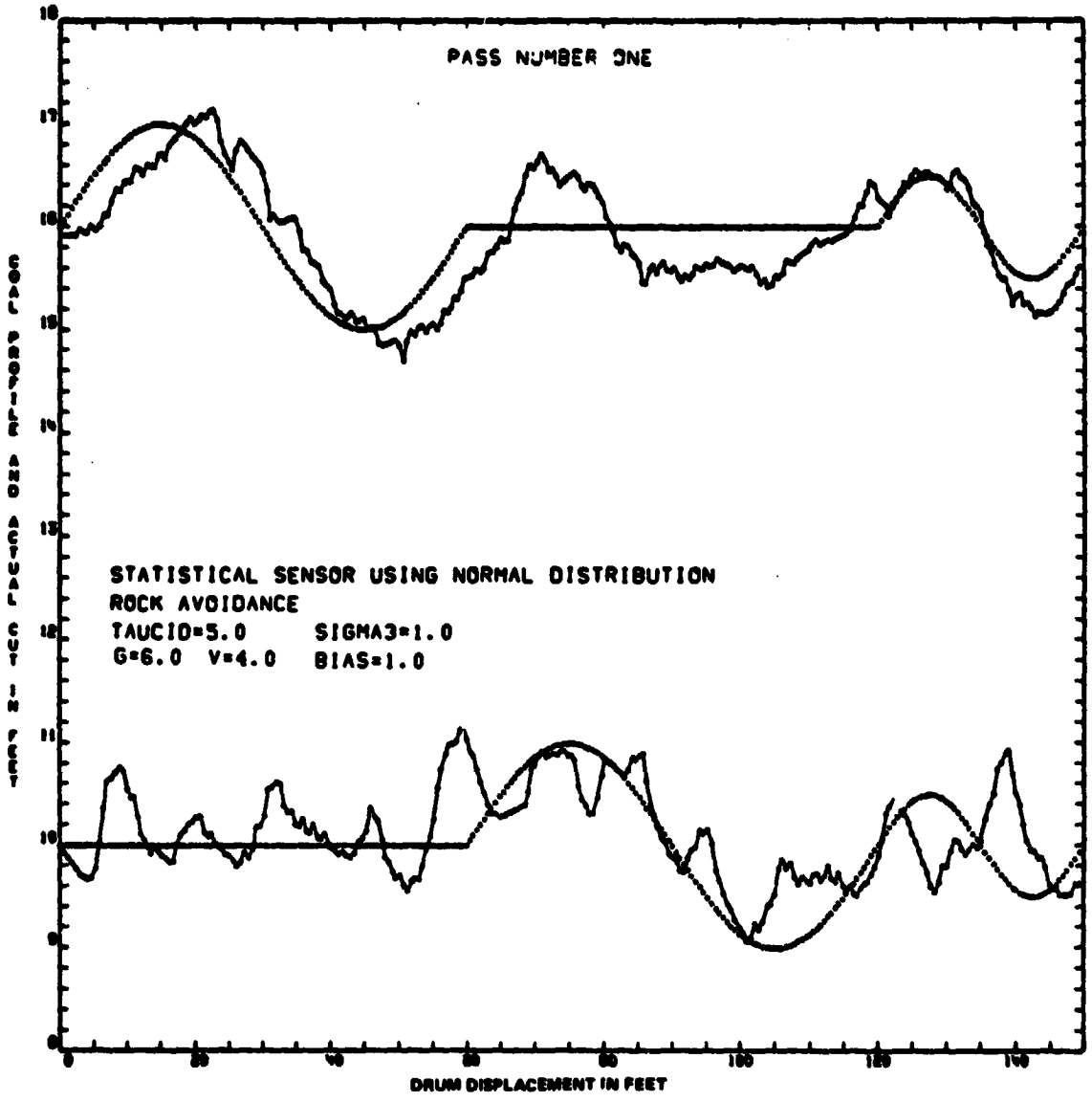

Figure 63. (Continued).

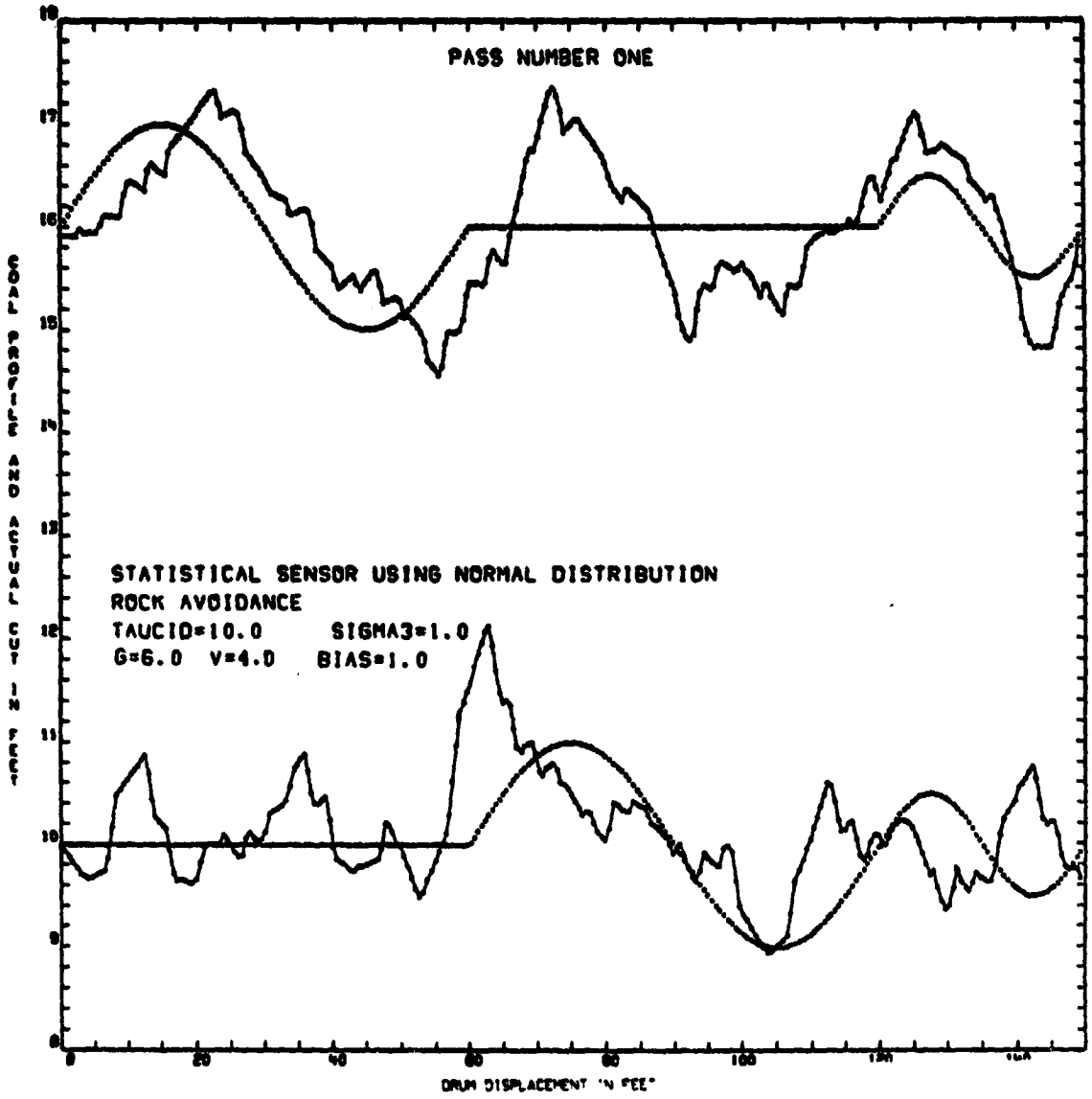

Figure 63. (Continued).

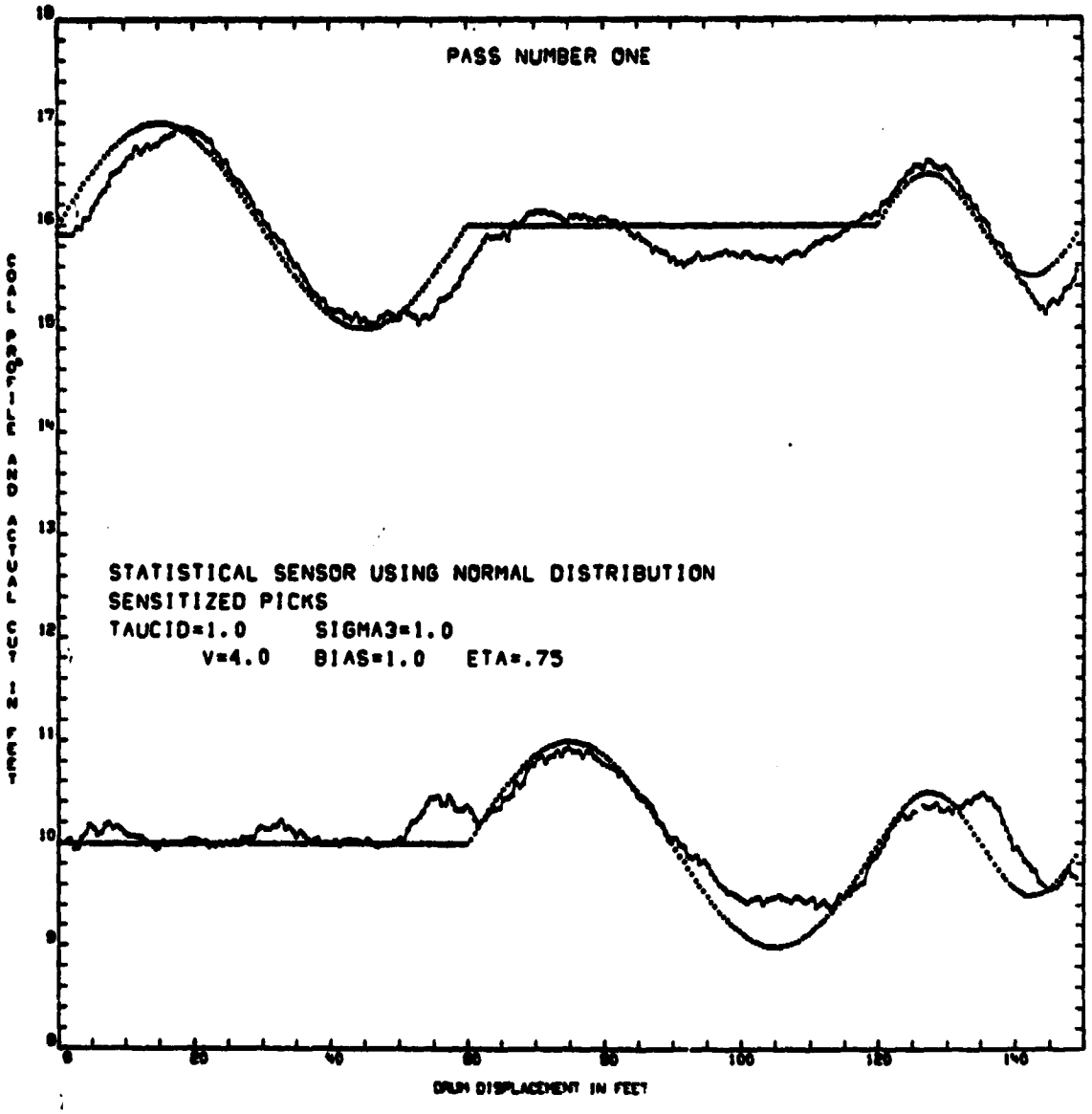

Figure 63. (Continued).

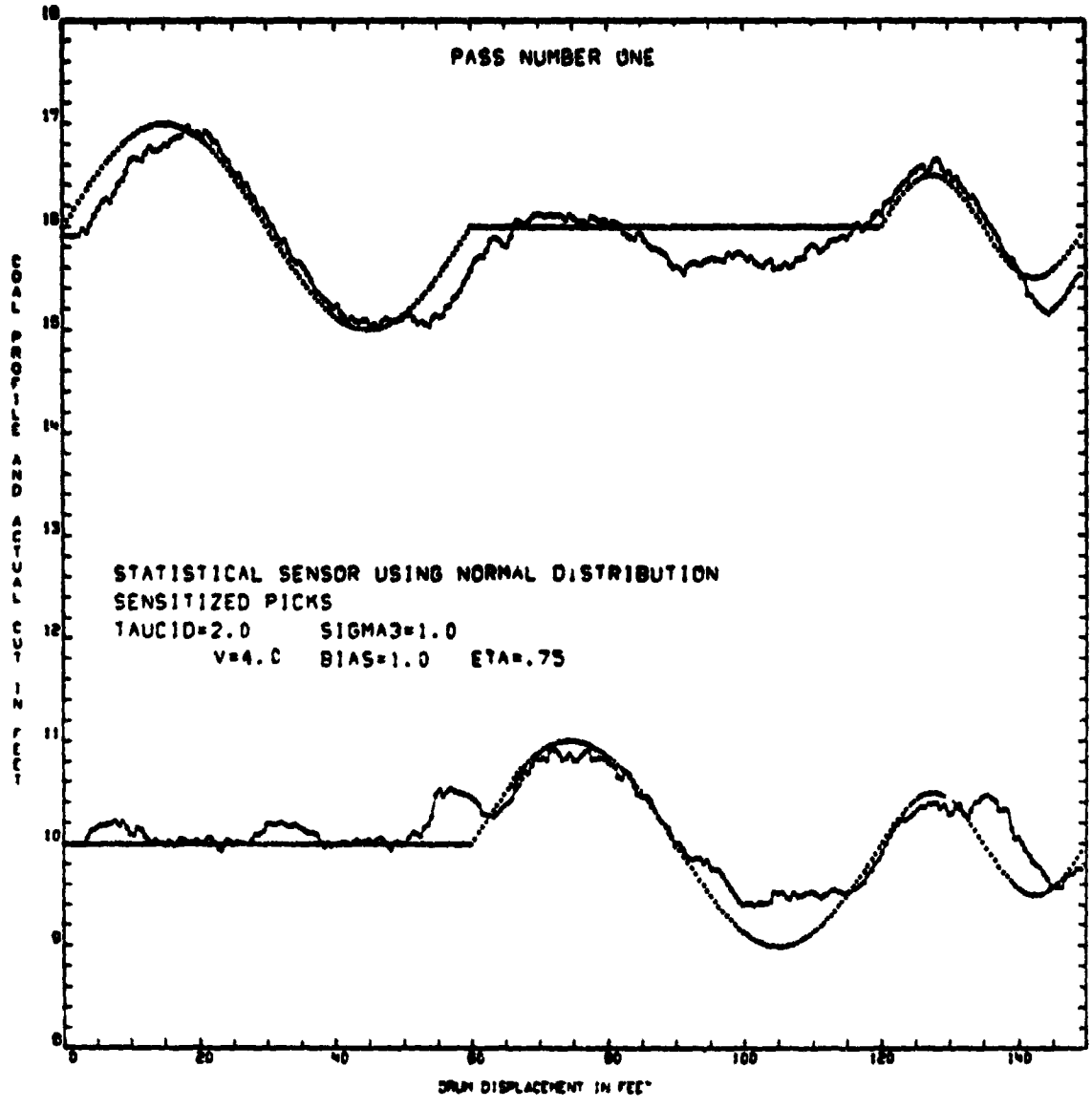

Figure 63. (Continued).

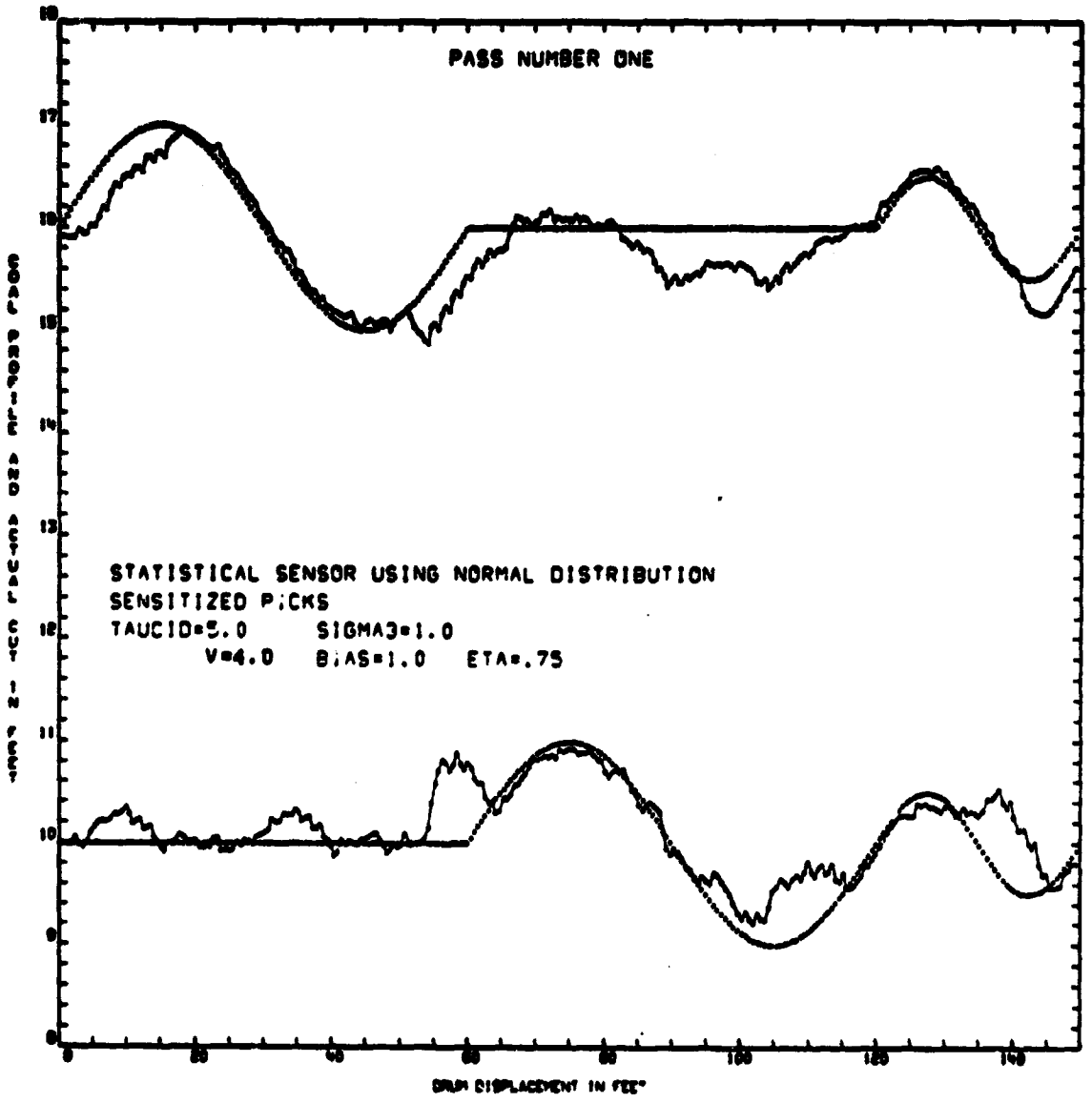

Figure 63. (Continued).

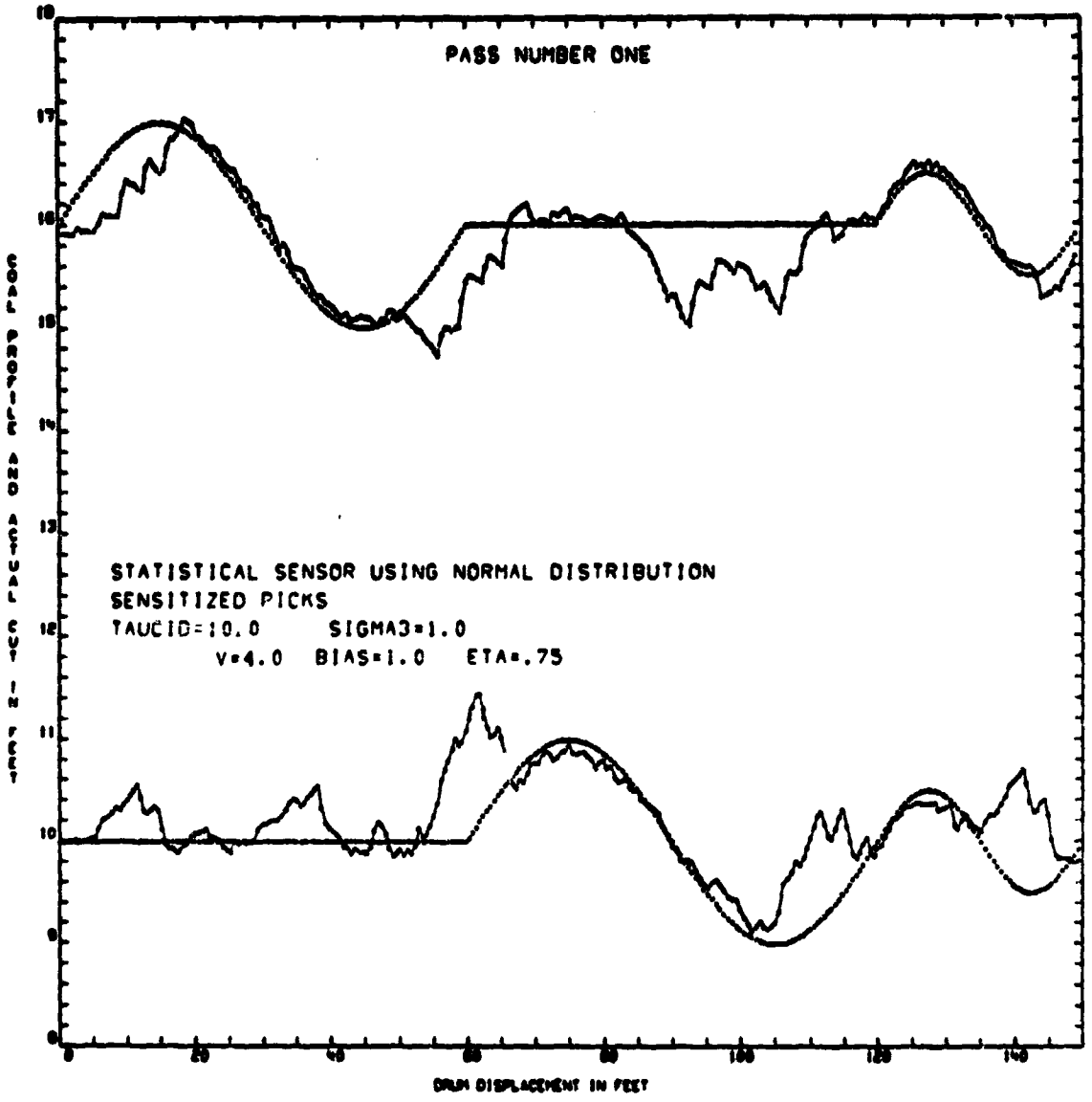

Figure 63. (Concluded).

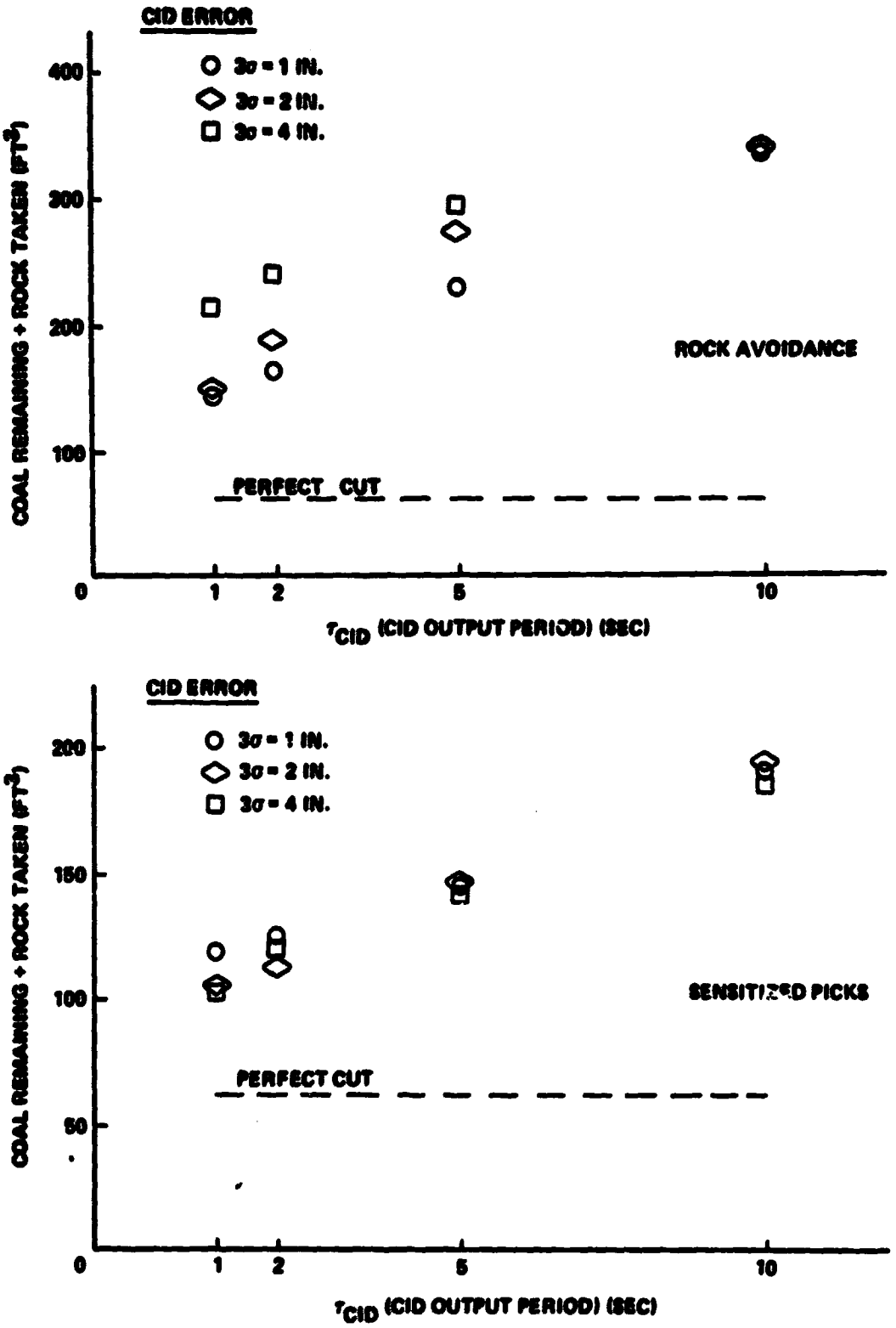

Figure 64. Performance data.

pronounced reduction in performance (for rock avoidance and sensitized picks) as it has in past studies. Sensitized picks are definitely preferable to rock avoidance schemes as shown by comparison in Figure 64.

Figure 65 shows the effect of chassis speed on performance. The point at 50 ft/min represents the maximum speed at which the VCS is capable of removing 95 percent of the available coal. The volume of rock taken also increases with chassis speed.

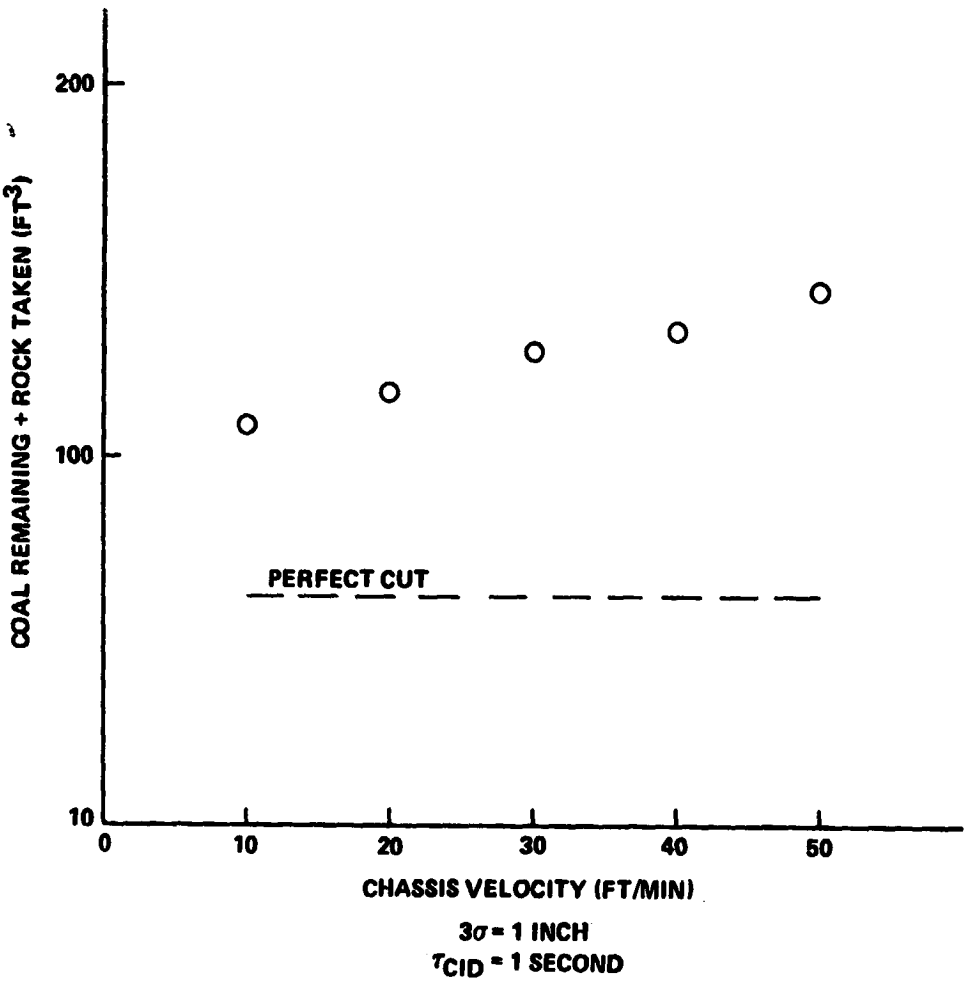

Figure 65. Effect of velocity on performance.

The results from a multiple pass study with the last-cut follower active are shown in Figure 66. This sensor insures that the present cut is within 2 in. of the last cut. Passes No. 1 and No. 10 from this study are shown in Figures 67 and 68, respectively. The miner travels from left to right in Figure 67 and right to left in pass No. 10 and all even numbered passes. Figure 66 presents the performance of the front and rear drums separately. An undulating track has a greater effect on rear drum control than on the front drum because of the greater lever arm of the drum and the CID to drum bottom distance indicator.

Figure 66 indicates that total performance has reached a near steady state level by pass No. 6 and the total mining operation is stable through pass No. 10. There is no indication that this situation would change in succeeding passes.

4.2.3 Summary. A more detailed view of the Longwall shearing machine together with the various sensors and deployment devices is shown in Figure 69. The floor position sensor serves the same purpose for the rear drum as the last-cut follower does for the front drum. This miner configuration with the last cut sensors inactive and a chassis speed of 20 ft/min was used to generate the performance data presented in Figure 64. Figure 64 shows the performance trends in terms of the volumetric sum of the coal remaining and the rock taken. It should be noted that a perfect cut removes no rock; therefore, the line showing the perfect cut volume represents only the amount of coal remaining — 1 in. on the floor and ceiling for this case. To say that a certain percentage of the available coal was removed on any particular pass is to present an incomplete picture of machine performance. For this reason, Table 13 has been compiled for the case where sensitized picks are used and the depth sensor has an output period of one second. This equivalent depth represents the volume of coal remaining and rock taken when distributed over the entire length of the coal face.

TABLE 13. PERFORMANCE SUMMARY FOR STATISTICAL SENSOR

Coal Depth Sensor Uncertainty σ (in.)	Percent of Available Coal Removed	Equivalent Coal Depth On Floor and Ceiling (in.)	Rock Percentage Of Total Material Removed	Equivalent Depth of Rock Taken On Floor and Ceiling (in.)
1	95.72	1.50	1.10	0.38
2	96.20	1.33	1.24	0.44
4	96.68	1.16	1.35	0.48
Ideal case	100.00	1.0	0	0

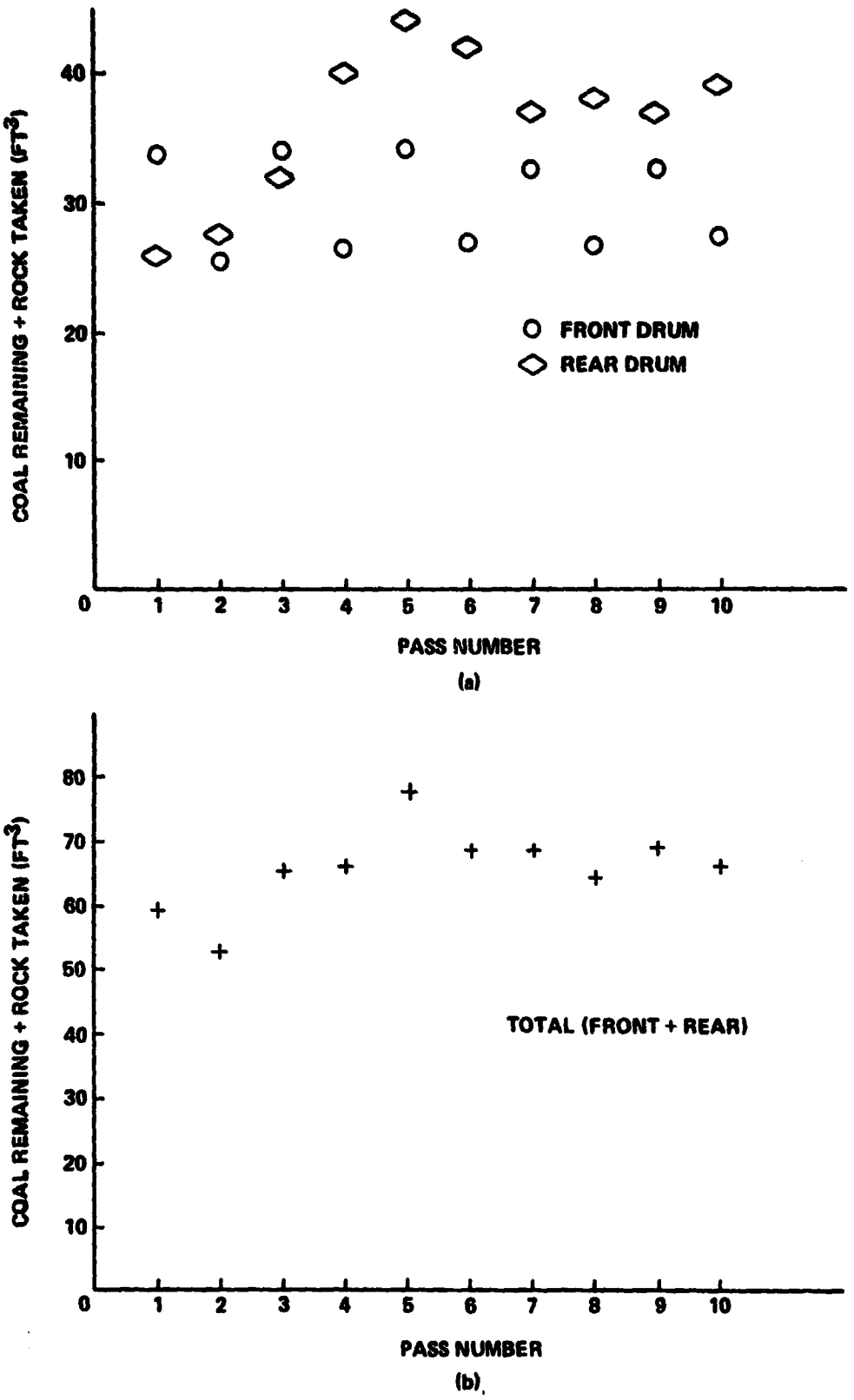

Figure 66. Multiple pass performance.

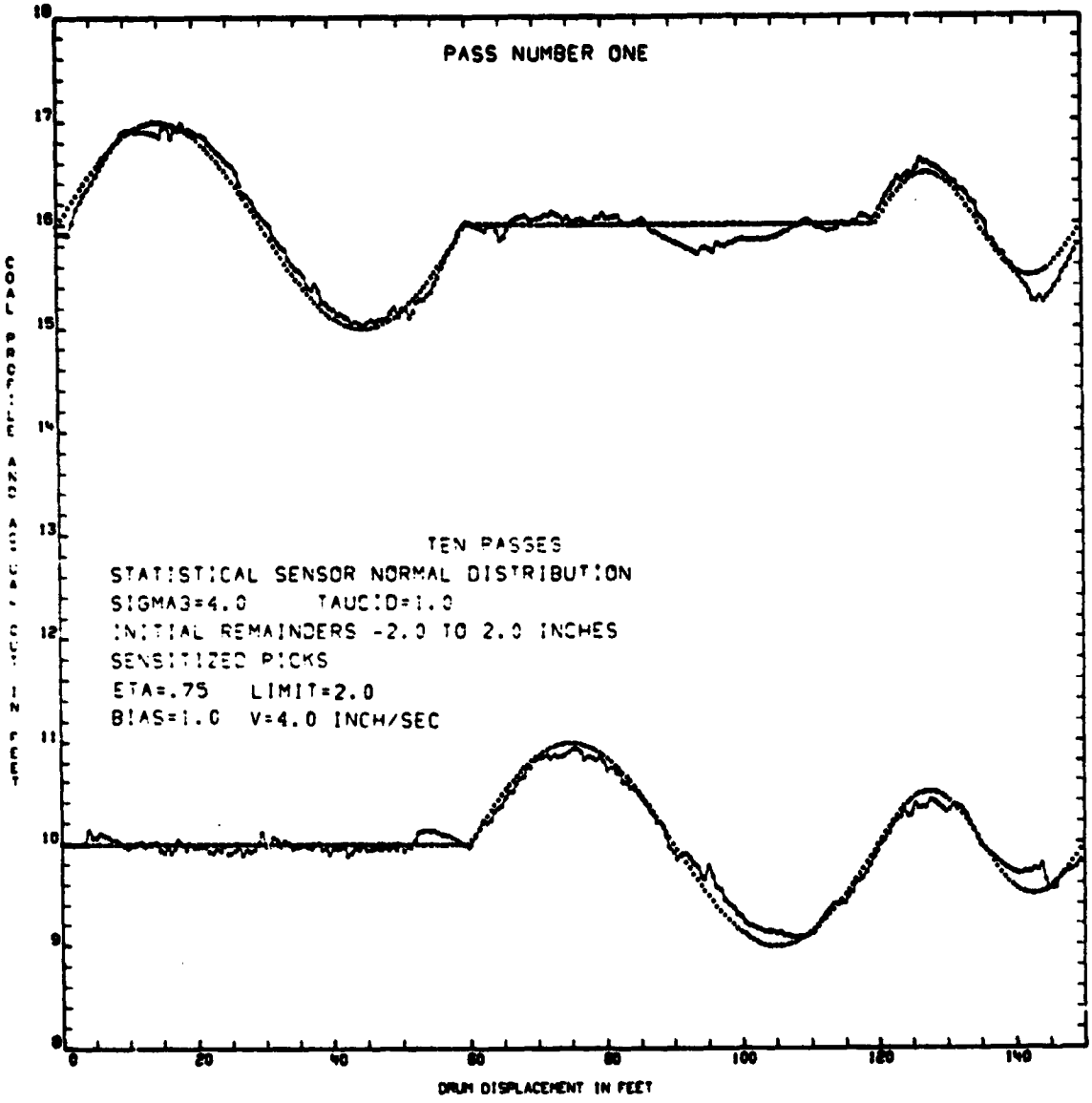

Figure 67. Pass No. 1.

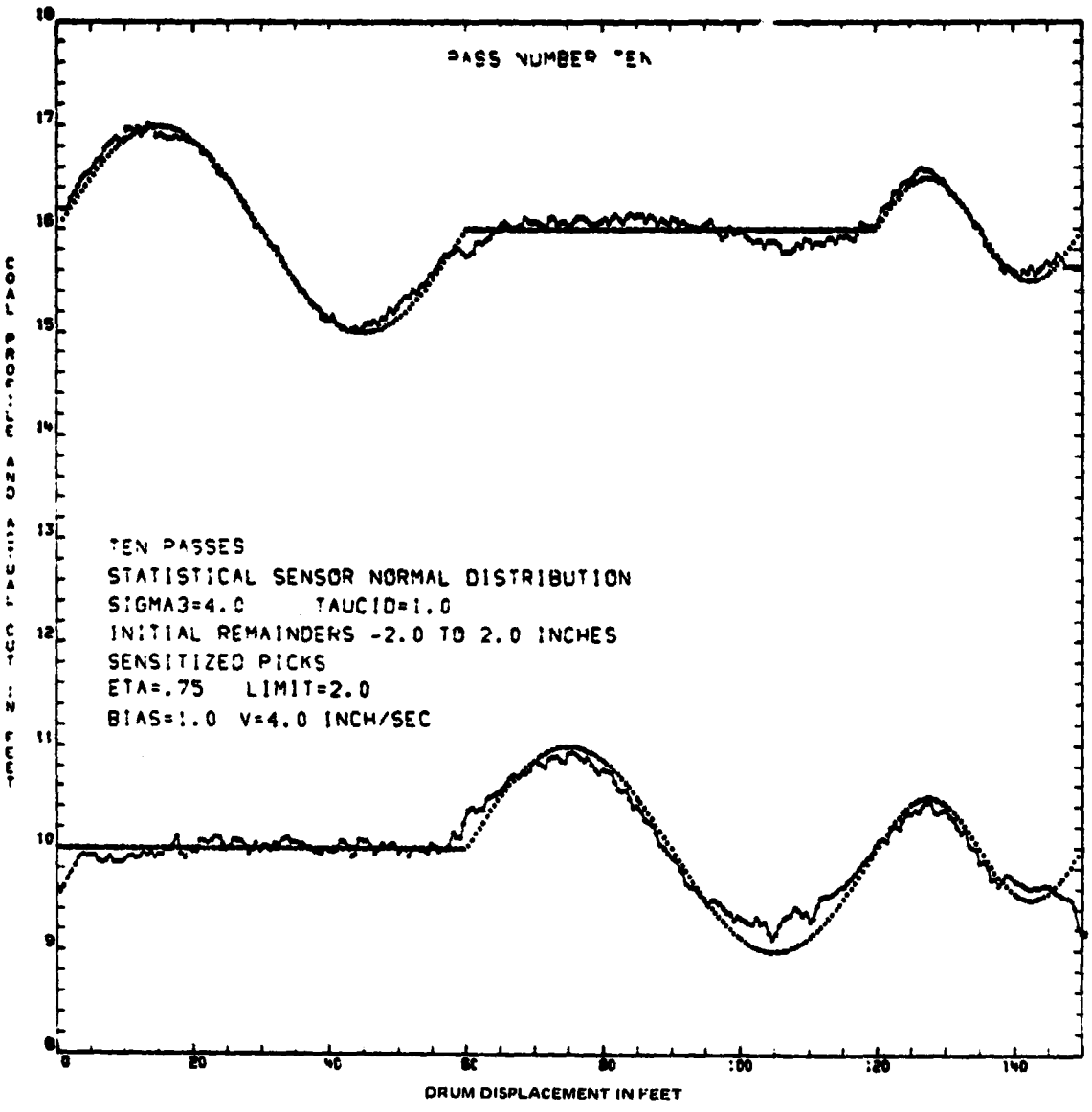

Figure 68. Pass No. 10.

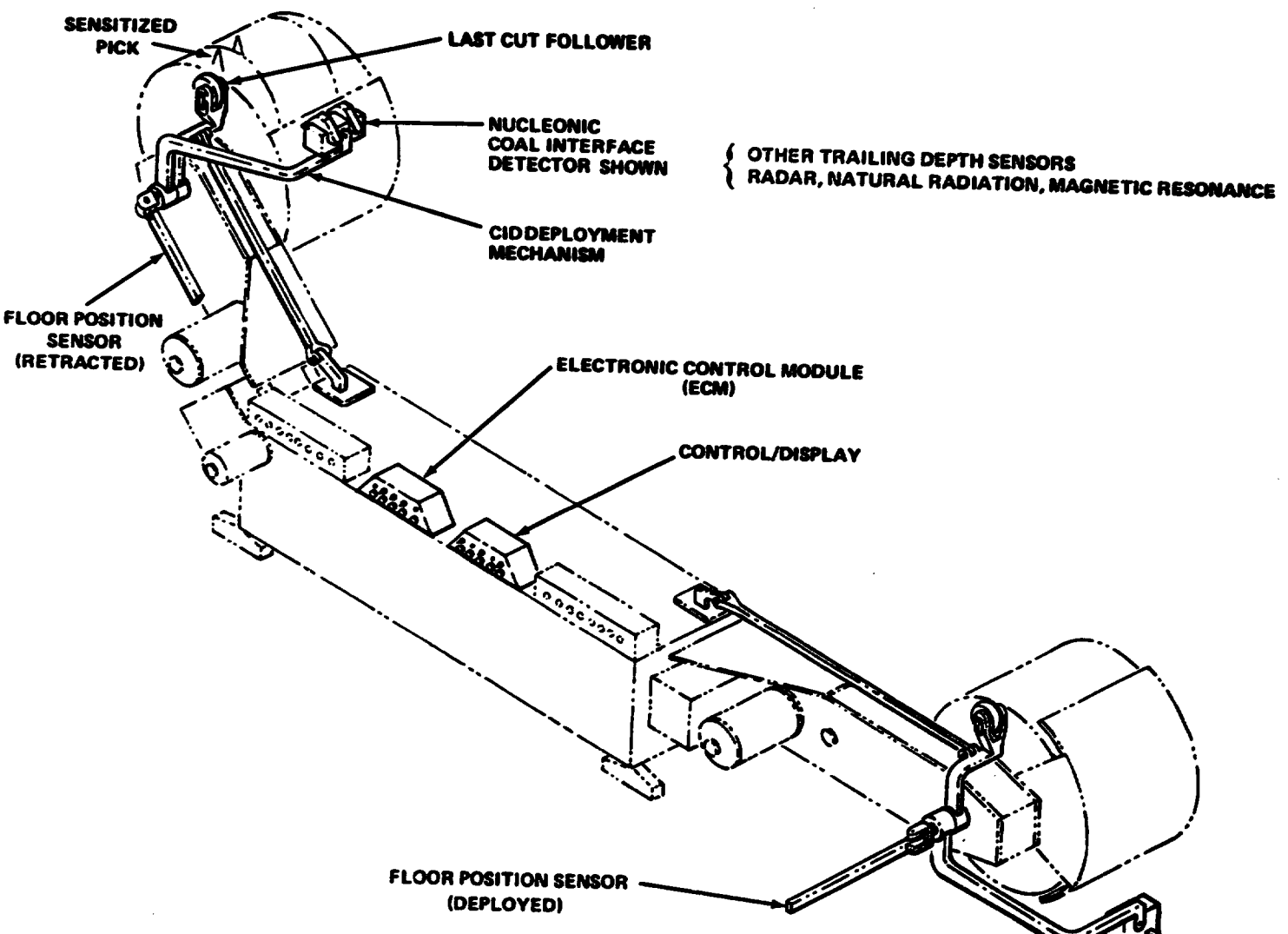

Figure 69. Automated longwall shearer concept.

4.2.3.1 VCS Symbol Definition.

B	Coal Depth Bias (in.)
DEAD Z	Dead Zone for Actuator On/Off Signal (in.)
F	CID to Drum Top/Bottom Gain (unitless)
G	Rock Withdrawal Gain (unitless)
K_R	CID Trailing Distance (in.)
L	Last Cut Step Limit (in.)
M	Slope of Command Ramp (in./sec)
P	Output of CID to Drum Top/Bottom Indicator Averaged Over τ_{CID} Seconds (in.)
P_K	Sensitized Pick Signal (1 if rock; 0 if coal) (unitless)
P_O	Instantaneous Output of Last Cut Position Indicator (in.)
V	Chassis Velocity (in./sec)
W	Control Ramp Gain (in./in.)
X_A	Boom Actuator Displacement (in.)
X_C	Commanded Boom Actuator Displacement (in.)
Z_A	Instantaneous Drum Height Relative to Skid Plane (in.)
Z_C	Commanded Drum Height Relative to Skid Plane (in.)
ΔX_C	Commanded Change in Boom Actuator Displacement (in.)
ΔZ_C	Commanded Change in Drum Height Relative to Skid Plane (in.)
ΔZ_V/L.V.	Last Value of ΔZ_C (in.)
ϵ	Coal Interface Detector Output (in.)

η Rock Withdrawal Increment (in.)

τ Ramp Change Time Increment (sec)

τ_{CID} Coal Interface Detector Output Period (sec)

4.2.4 Alternative VCS Control Laws Study. This section summarizes the results of alternative ways to combine various CID measurements in an attempt to produce a single-drum cut exactly as desired. The baseline scheme uses a single drum and a trailing CID. The baseline CID effectively produces one data point at each sample with no memory. The alternative schemes use CID error data, not only real time but also as stored in a memory from the present point back through as many as three complete cuts.

This study used a desk top calculator (HP-9830) which is relatively easy to work with and allows many different things to be tried in a fairly short time. The 1108 detailed simulation is much more difficult to change. The idea was to compare all these different schemes under the same conditions, and if one or more looked better than the baseline scheme they would be incorporated into the large simulation for further study.

One scheme was tried that required an additional simultaneous measurement behind the CID with the one at the CID. These two measurements are not of the coal interface but rather just the coal surface. Knowing the distance between these two points allows the slope of the cut coal surface to be determined. It was hoped that this information could be used to predict the drum position. It worked very well for zero CID measurement error, but at expected CID error levels it was unusable.

4.2.4.1 Control Law. The control law is basically given by

$$C_{i+1} = C_i + B\, f(\epsilon_i) \quad ,$$

where C_i is the coal cut surface either behind or beside the drum to be updated, C_{i+1} is the new drum cut, B is a weighting coefficient, and $f(\epsilon_i)$ is the error function for the scheme under consideration.

ϵ is given generally by

$$\epsilon_i = P_i - (C_i + K + D_i) \quad ,$$

where P_i is the coal-rock interface (profile) height, K is the desired amount of coal to be left, and D_i is the CID error in the ith measurement. A positive ϵ_i means the cut was too low.

Although the profile was referenced to the floor throughout this study, it was done only to have a mental reference frame. The equations can be changed slightly so that the floor is not needed. One needs only to keep up with the profile change at each sample position.

4.2.4.2 Simulation Model. The simulation model is shown in Figure 70. The CID is located 2.5 ft behind the drum in the present cut. The CID takes a measurement at 0.5 ft intervals, and each of the errors is stored in a memory matrix. The last cut is 2.5 ft (drum width) away from the present cut and those errors have also been stored. The last-cut sensor is in the last cut directly beside the drum. At least three previous cuts are similarly remembered. The cuts are sometimes referred to here as rows, and the same location in previous cuts form what is called here a column (Fig. 70).

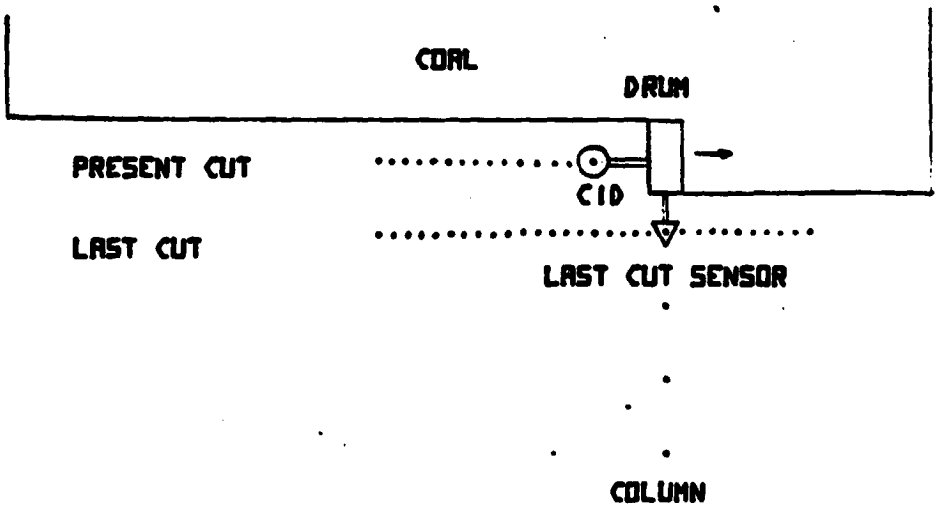

Figure 70. Simulation model (top view).

In this simulation, when the drum height is determined the drum changes to that new height without delay. This gives a physical basis to the model. Calculations and plots are made on a point-to-point basis however. The procedure is the same throughout so that valid comparisons can be made.

This simulation is just a mechanization of the control law as previously shown. Cuts are spaced a drum's width apart, although this only matters for a profile varying into the face. Samples are taken each 0.5 ft by the CID. Various combinations and weighting factors for all the data can be used.

An important feature of this simulation is the ability to use various values of CID measurement error. This error is assumed to be normally distributed with a mean of zero. This is a reasonable approximation for the radar CID and also the nucleonic CID when trying to leave 4 in. of coal. The actual distribution used in the simulation was triangular which is a fair approximation to the normal distribution. The computation speed is much faster for the triangular than for the normal. A triangular distribution with 1 σ of 1 in. is equivalent to a normal distribution with a 1 σ of 1.2 in.

The profile was varied across the face and into it. The profile shape was sawtooth with a slope of 1 in 30 and a period of 24 ft. The profile varying into the face at 1 in 30 is equivalent to shifting each successive profile to the left by 2.5 ft, which was done in simulation.

The simulation flow chart is shown in Figure 71. Parameter definitions and a listing (in BASIC) are given in Paragraphs 4.2.4.7 and 4.2.4.8, respectively.

4.2.4.3 Alternative Error Functions. The simplest error function is just the error itself at either the CID or last-cut follower. This gives a simple proportional control law.

An intuitively better error function is the average of several error measurements near the CID or last-cut follower. For the CID, several points behind it can be averaged to help reduce the effect of sensor error although the effect of the varying profile introduces a new error. For the last-cut follower, points both ahead and behind it in the same cut can be averaged. Points can also be averaged in successive cuts (columns) away from the last-cut follower. Profile variation affects these previous-cut averages also.

A further step is to use various combinations of CID (present-cut), last-cut (row) and other previous-cut (column) data. The relative importance of each term can be controlled as desired.

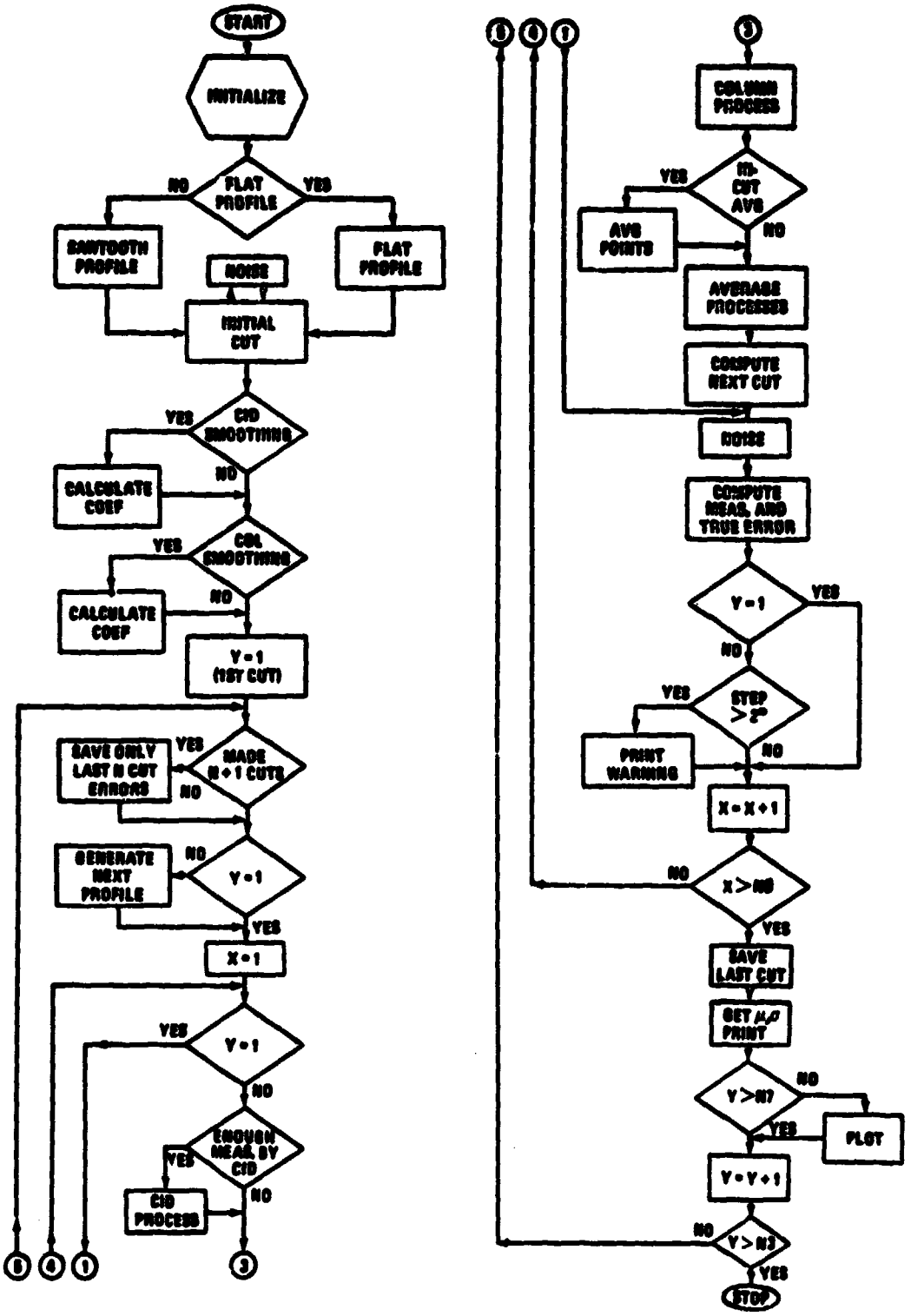

Figure 71. Simulation flowchart.

There are many other error functions that could be tried. One that was originally tried was the exponential smoothing function. This function effectively gives the most recent (nearest) point the largest weight and decreasingly weights the rest of the points in an exponential manner. It was determined that this function gave results between those obtained with the single point and the average, so (for now) it was not considered further.

Another untried function is one containing derivatives of the errors. Least squares curve fits rather than averages were tried with inconclusive results. There are also many more ways to combine the previous-cut data. Various prediction schemes could be used, considering the entire matrix of data rather than just a row and column. The list of functions that could be tried is almost endless. Time allowed only the single point and average to be checked in any detail.

4.2.4.4 Comparison Criteria. The basis for comparing one trial against another is a mean and standard deviation. The mean is with respect to the desired coal depth (e.g., 4 in. from the coal-rock interface) and is for one complete cut. The standard deviation is about this mean and is also for one cut. All trials in this study showed that the mean tended toward zero if an initial step was given and remained near zero if no step was given. This was true even when the standard deviation was unstable. There were some differences in settling time for the mean, but these differences were overshadowed by the standard deviation performance. Sensor noise is a major parameter in this study, and the standard deviation shows the effect of sensor noise after it passes through the system. The tabulated results show the 1σ values, and these can be compared directly with the simulated 1σ sensor noise for any error function used. They can also be compared with each other to determine which data combination produces the best cut (lowest value).

4.2.4.5 Results and Conclusions. The first simulation tried used only the data point in the last cut beside the drum and it gave good results. It was expected that averaging several points in front of and behind this same point in the last cut would improve the results even more; however, that was not the case. In fact, averaging more than two points produced an unstable system. Instability here means that each cut generally has a larger standard deviation (i.e., a rougher cut) than the one before. Even two points produced a rougher cut than just the one point although this case was stable.

A satisfactory theoretical explanation for this instability has not been seen. Picking the simple case of a three-point average, one point to each side of the last-cut follower, does show what happens to produce the instability. As previously stated, the mean remains near zero. Eventually the random points

fall into the pattern where the end points are of the same sign and opposite the sign of the center point. In this situation the sign of the average will usually be opposite that needed to improve the error at the center point; hence, the updated error is worse instead of better. This pattern eventually develops completely across the cut, and the system goes unstable.

Many combinations of points were tried in an effort to determine if the instability could be broken. For example, least squares were tried instead of the average, but the result was no better.

Next the column average alone was simulated. These results were always stable although many cuts were required before the standard deviation (and mean) settled down to a steady-state value.

Combinations of row and column data were tried, and the previously unstable row average became stable when used in combination with the column data. The results were not noticably different from those when using only column data. Row alone was better than column alone, but using both produced a little smoother cut when it finally settled out. All the runs made up to this point did not vary the profile on successive cuts (into the face).

The CID present-cut data were simulated and then combined with the row and column data, and the profile was varied into the face. A typical simulation output is shown in Figure 72. Sequential cuts go from bottom to top of the plot, and each cut contains 100 samples spaced at 0.5 ft. The first cut was generated from random CID measurements relative to the desired profile. Later cuts were determined by the error function being tested. Figure 72 shows the profile changing into the face and how the error function of the one CID point and one last-cut point performs with a CID error of 1.2 in.

The result-summary matrix is shown in Figure 73. The control law B = 1, and when both previous-cut and present-cut data are used, each is given equal weight. When row and column data are used together, each is given equal weight. Any combination of parameters can be evaluated by studying this matrix.

Several conclusions can be drawn from Figure 73. The relatively large result with no sensor noise at all is due to having at least 2.5 ft of sensor lag with any combination. This lag will not allow the variable profile to be followed exactly (Fig. 74).

The column average generally degrades performance because the data are so far away from the drum and no data are assumed to be available between cuts. Results using column averages were not only larger but also took longer to settle out as shown in Figure 75.

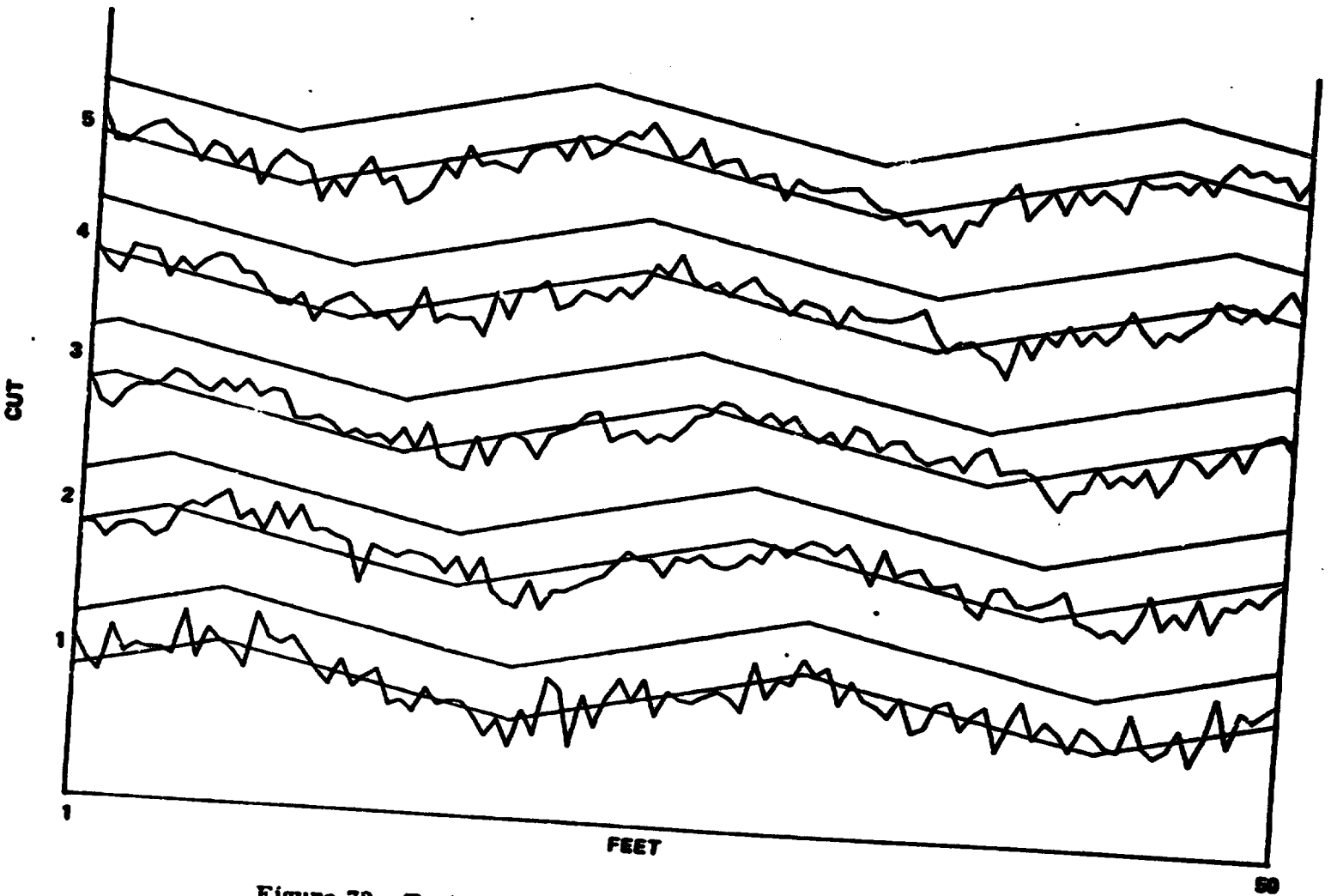

Figure 72. Typical cut sequence using CID and last-cut sensor.

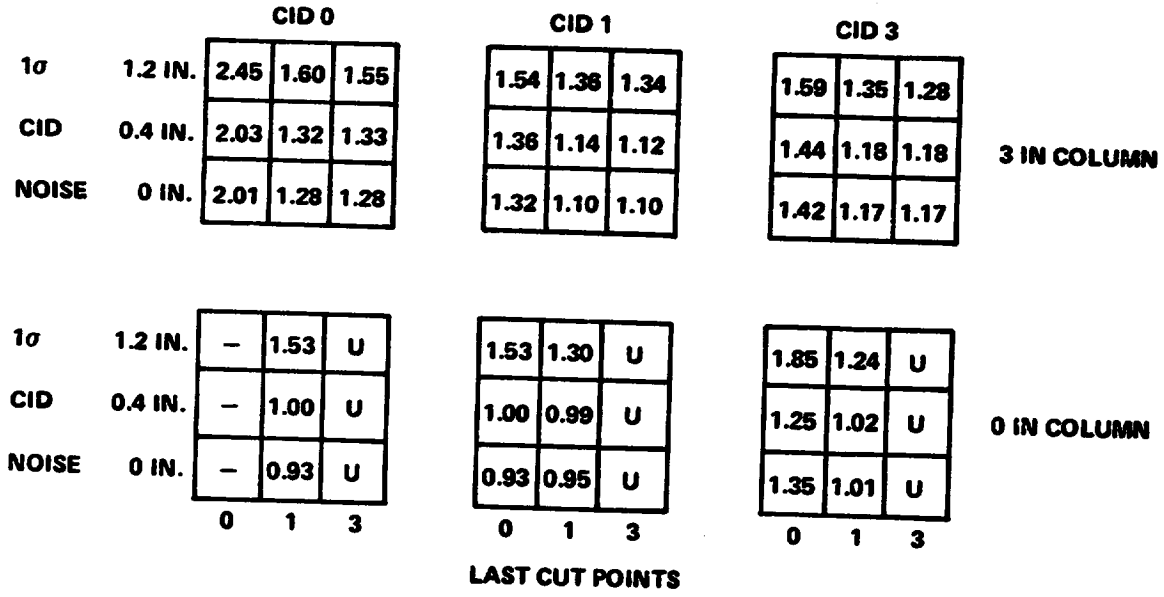

NOTES:
1. CID MAKES ALL MEASUREMENTS
2. DATA ARE 1σ VARIATIONS W.R.T. DESIRED PROFILE
3. PROFILE CHANGING BOTH WAYS AT 1 IN 30
4. CID LAGS 2.5 FT BEHIND DRUM
5. U = UNSTABLE

Figure 73. Result summary.

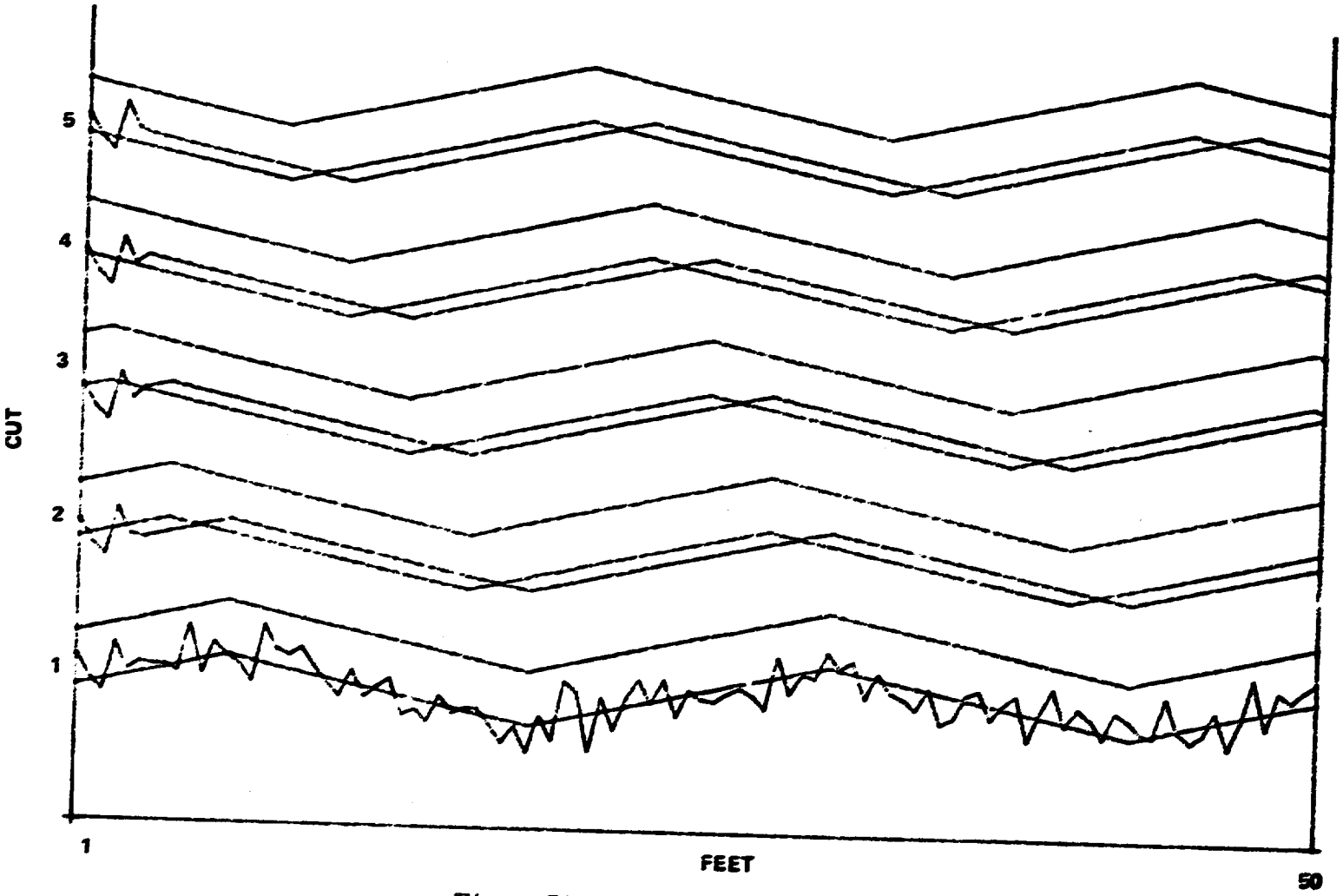

Figure 74. CID 1 only, no noise.

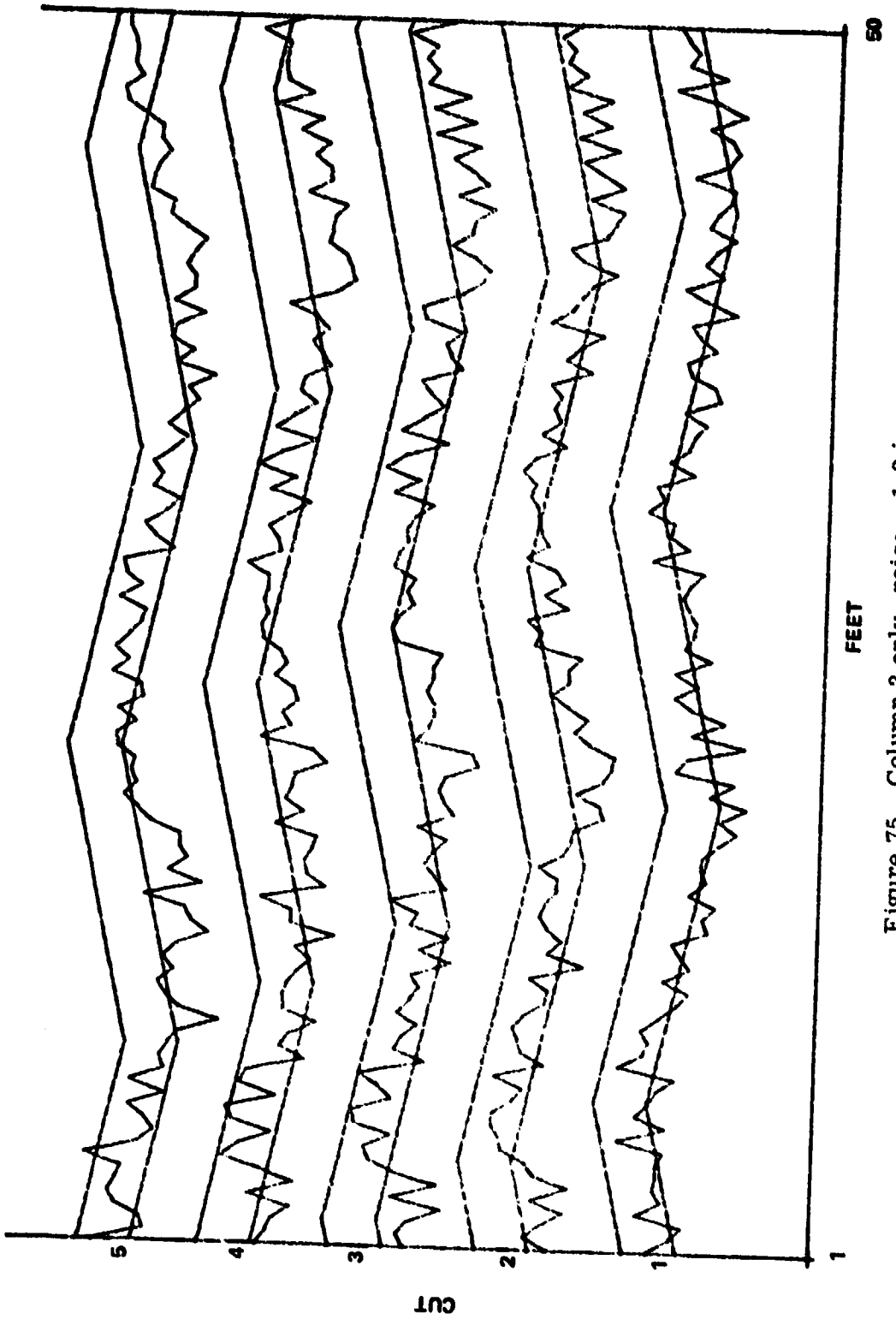

Figure 75. Column 3 only, noise = 1.2 in.

Using a CID average with previous-cut data generally improves the results at higher noise levels. Compare Figure 72 with Figure 76. When used alone it tends to drop in and out of a limit-cycle oscillation and gives erratic results, as shown in Figure 73 and Figure 77, for CID σ along. The CID-average algorithm averages the two errors behind the CID with the error just found at the CID and modifies the cut height measured at the CID. This modified cut height becomes the actual drum height command.

The last-cut average is unstable when used alone (Fig. 78) or with present-cut data. It is stabilized, however, by using the column average with it as shown in Figure 79. The data point at the last-cut sensor is used in both averages in this case. This puts enough weight on that point which is nearest the drum to make the system stable. Another scheme which stabilized the three-point average was to take the absolute value of the average and give it the sign of the point beside the drum. Neither scheme was as good as the one point alone, however.

One requirement of the control system is to limit the cut-to-cut step to less than 2 in. at any point. At the simulated noise level of 1.2 in. the step was greater than 2 in. approximately one-third of the time. A last-cut sensor must be used to measure the cut-to-cut difference so it can be controlled.

The best control-law algorithm in this study was the one last-cut data point used with one CID data point for low noise in Figure 80 and one last-cut data point used with the CID average for high noise in Figures 76 and 81. The high simulated noise level is close to that actually obtained from the nucleonic CID (approximately 1.4 in. versus 1 in.). The last-cut sensor does not improve results significantly for a noise level of 0.5 in.

The baseline scheme was set up on both simulations so that simulated conditions were as much alike as possible. Two runs were made with each program: one was with no CID error and the other was with the actual nucleonic CID error. The simple simulation gave 0.93 in. with no sensor error and 1.60 in. with it. The complex simulation gave 1.30 in. without and 1.96 in. with error. The effects of detailed modeling cause the no-error difference, and the error-to-no-error ratio is within 15 percent for the two simulations. This is very close agreement for two independently developed simulations.

The previously mentioned scheme which measured the cut-coal surface was originally proposed assuming that the distance between the coal surface measurements was one sample period. Without sensor noise this worked well, as shown in Figure 82, but even a small amount of sensor error produced very poor results as shown in Figure 83. The distance between coal surface

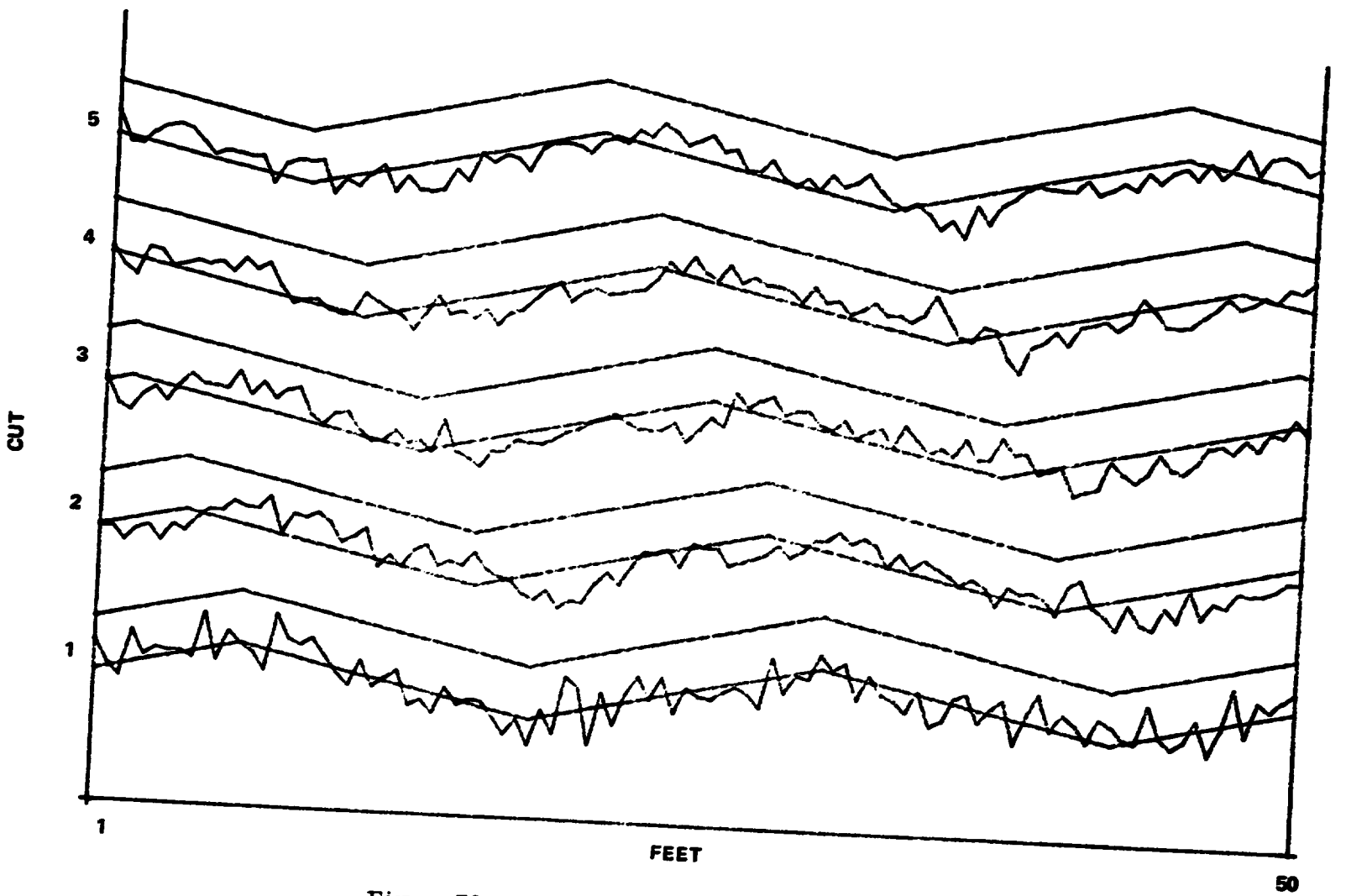

Figure 76. CID 3, last-cut 1, noise = 1.2 in.

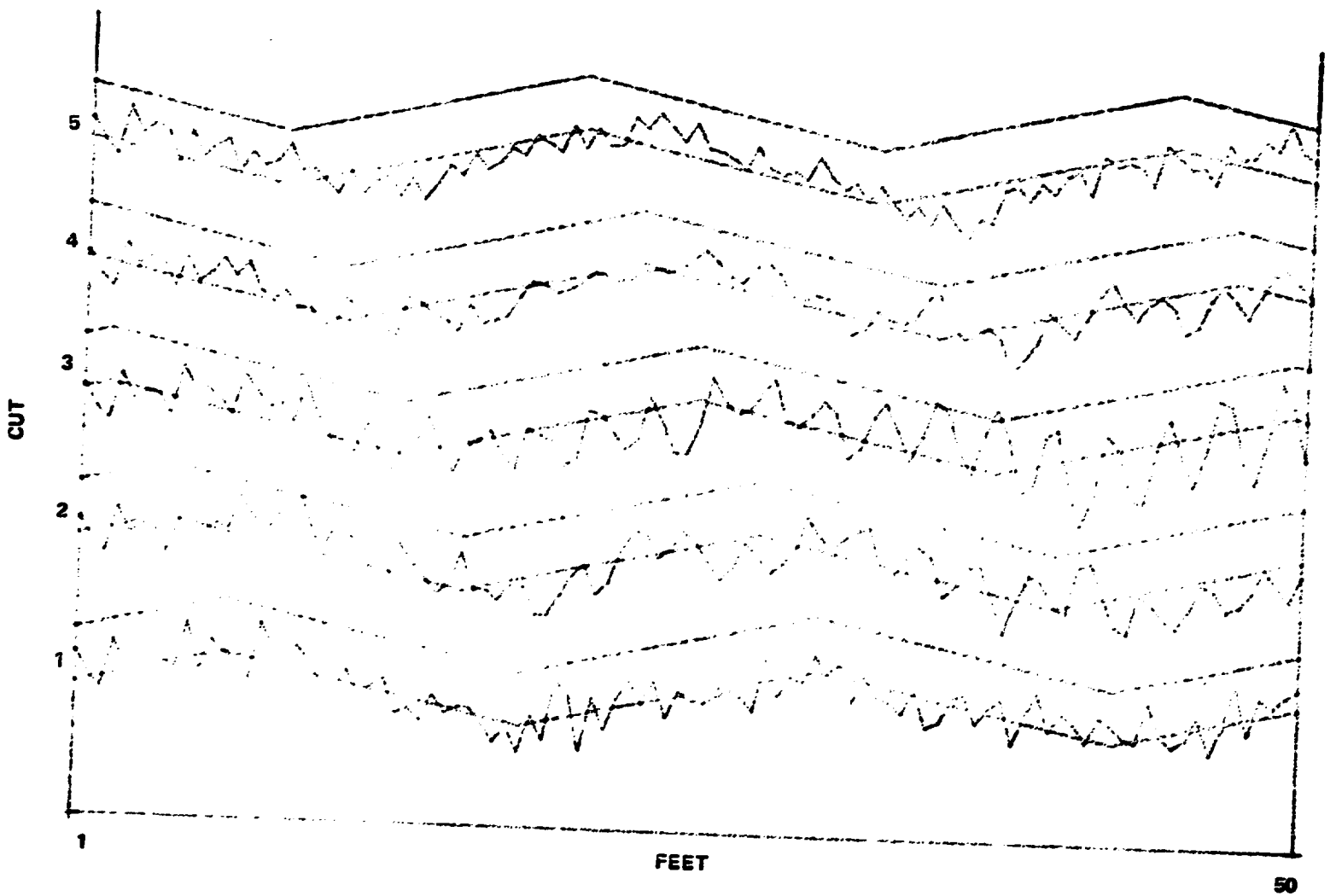

Figure 77. CID 3 only, noise = 1.2 in.

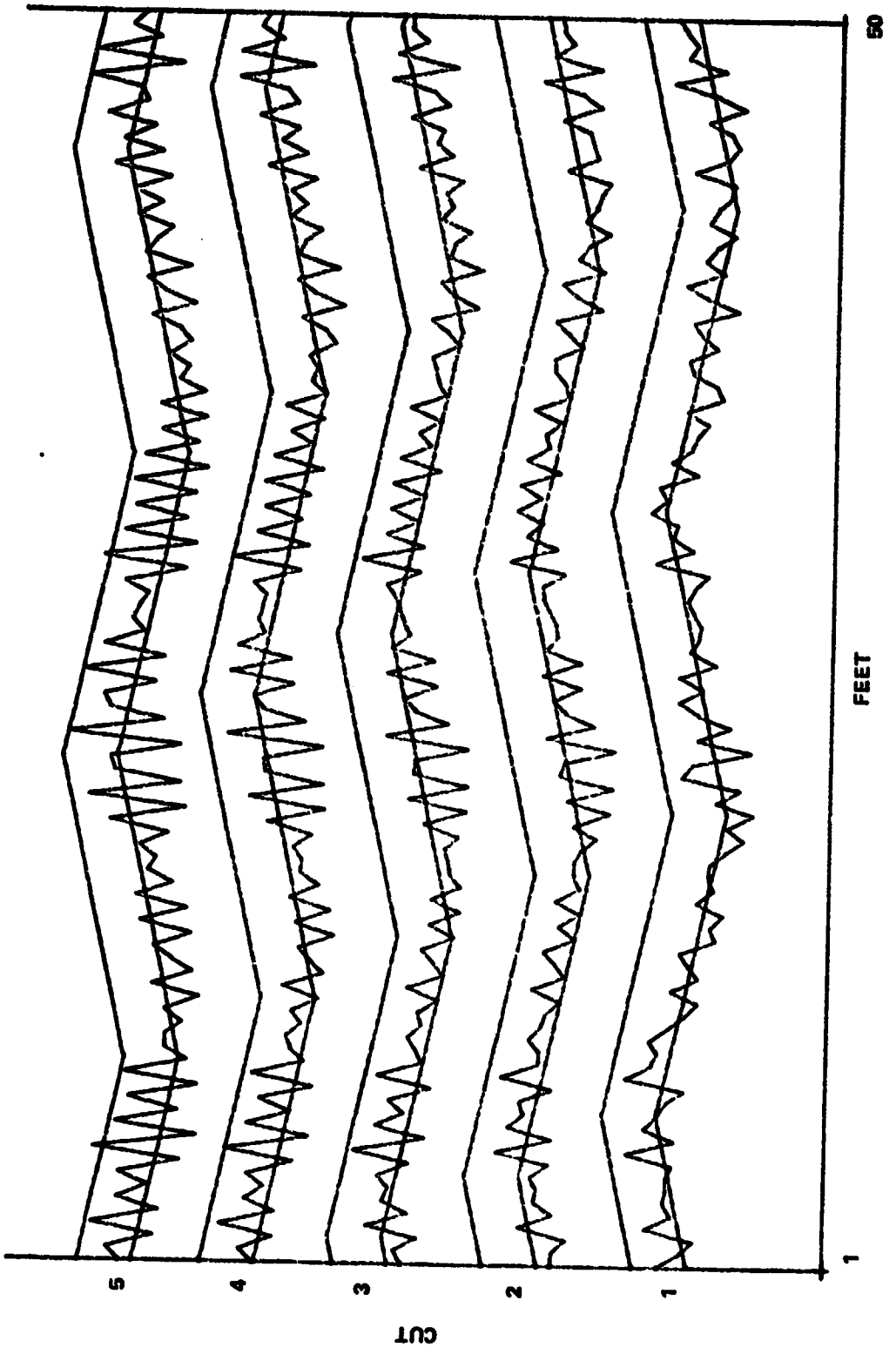

Figure 78. Last-cut 3 only, no noise.

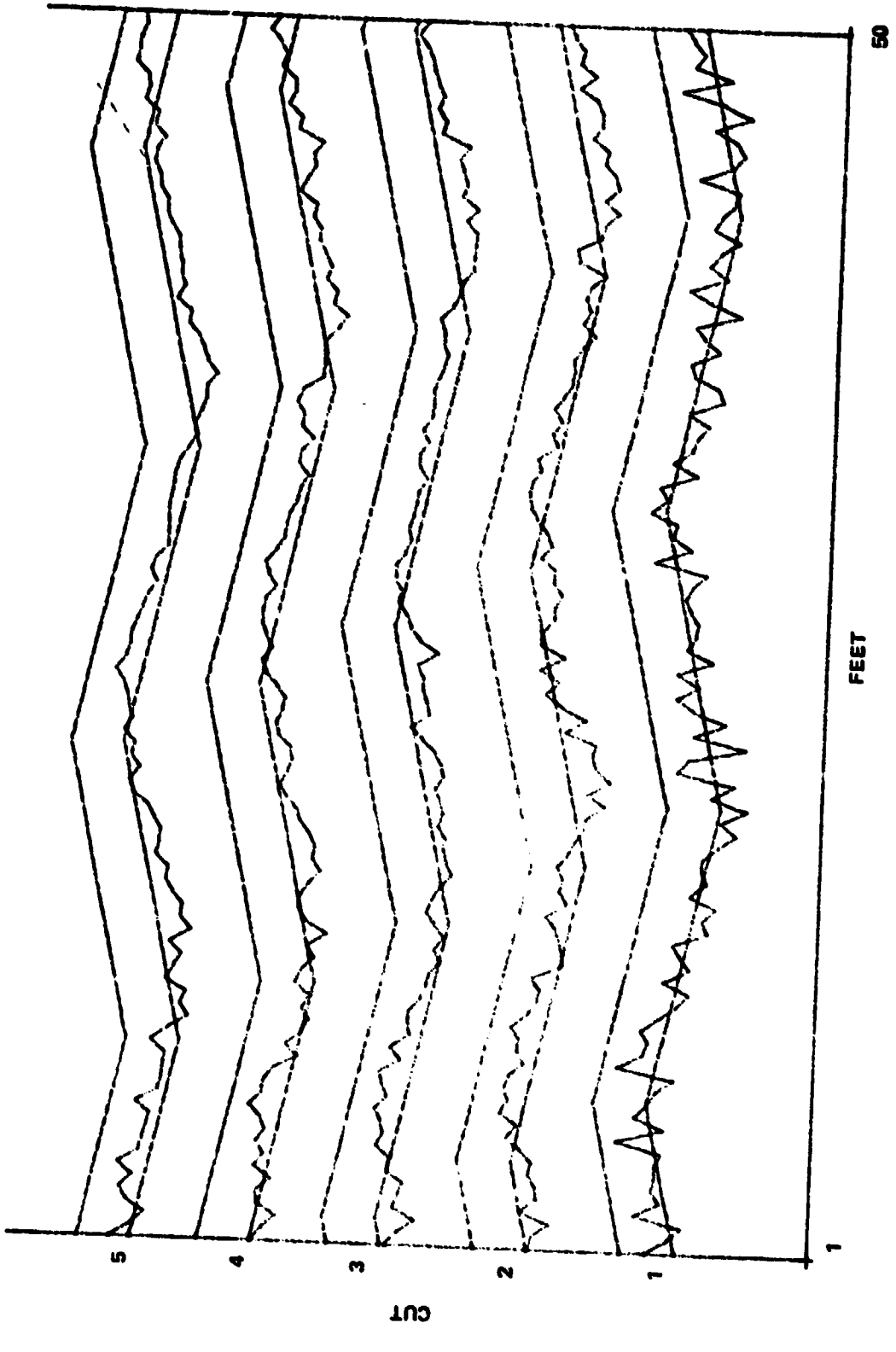

Figure 79. CID 3, column 3, last-cut 3, noise = 1.2 in.

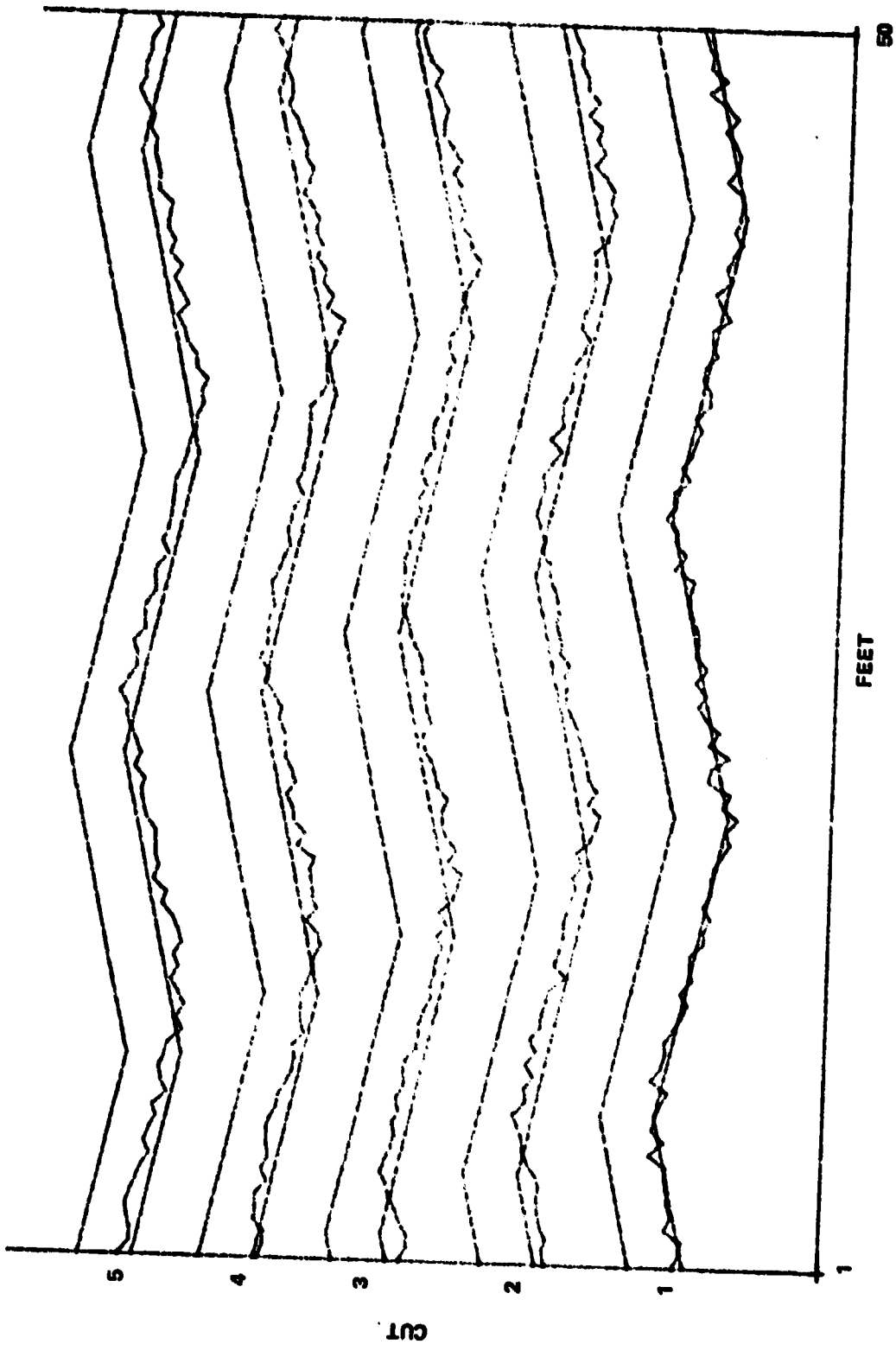

Figure 80. CID 1, last-cut 1, noise = 0.4 in.

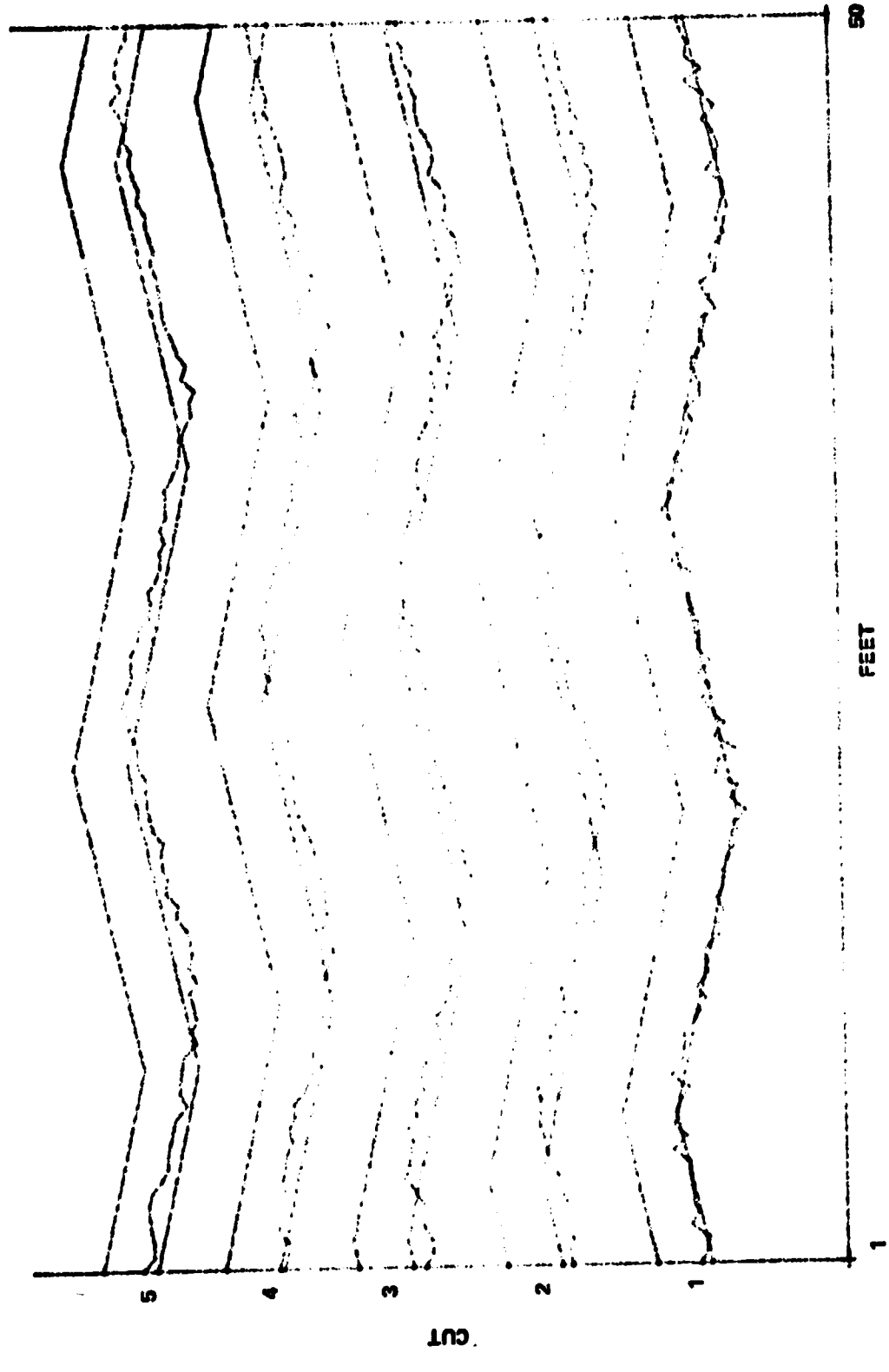

Figure 81. CID 3, last-cut 1, noise = 0.4 in.

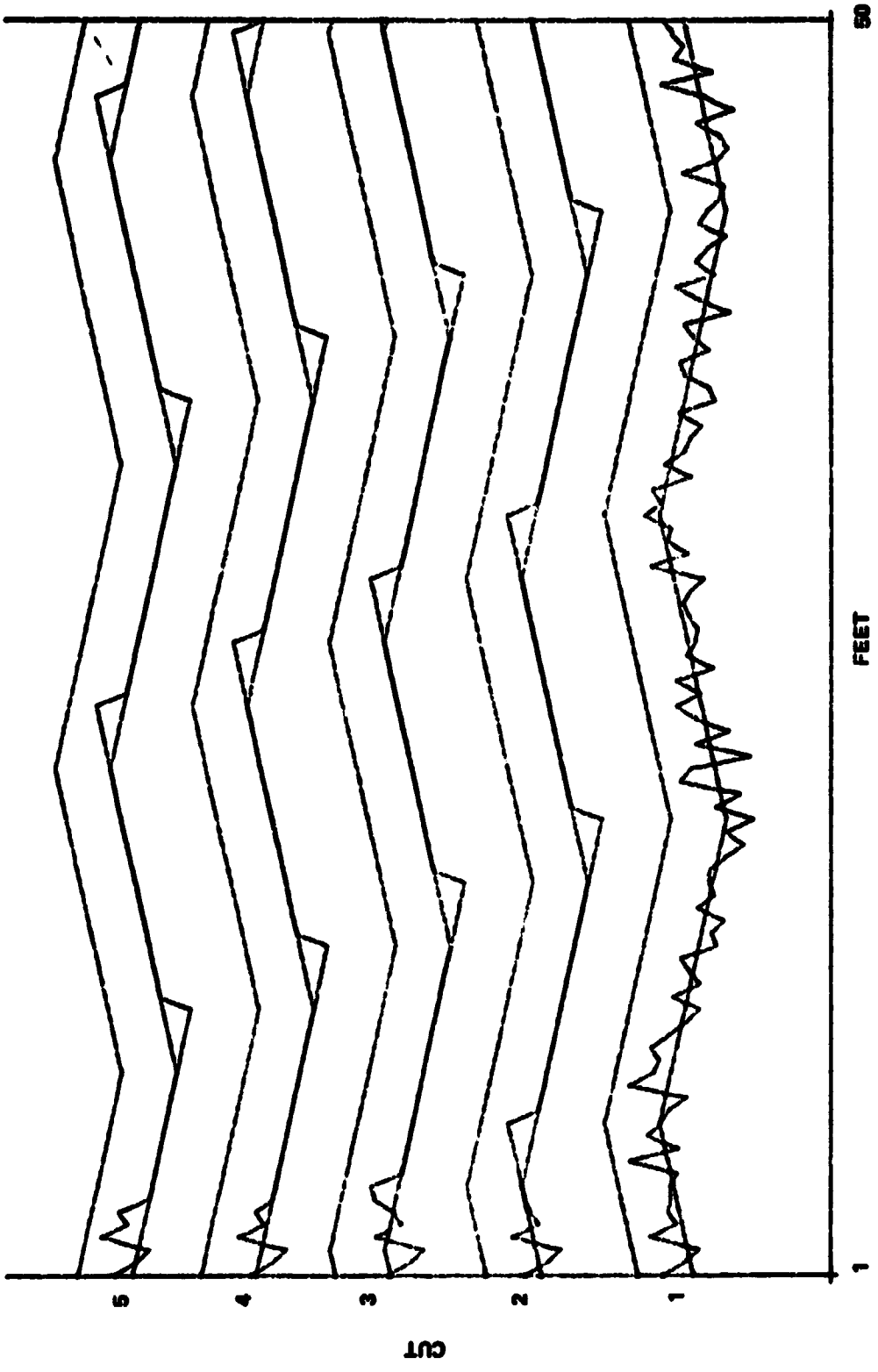

Figure 82. Coal slope scheme, noise = 0.

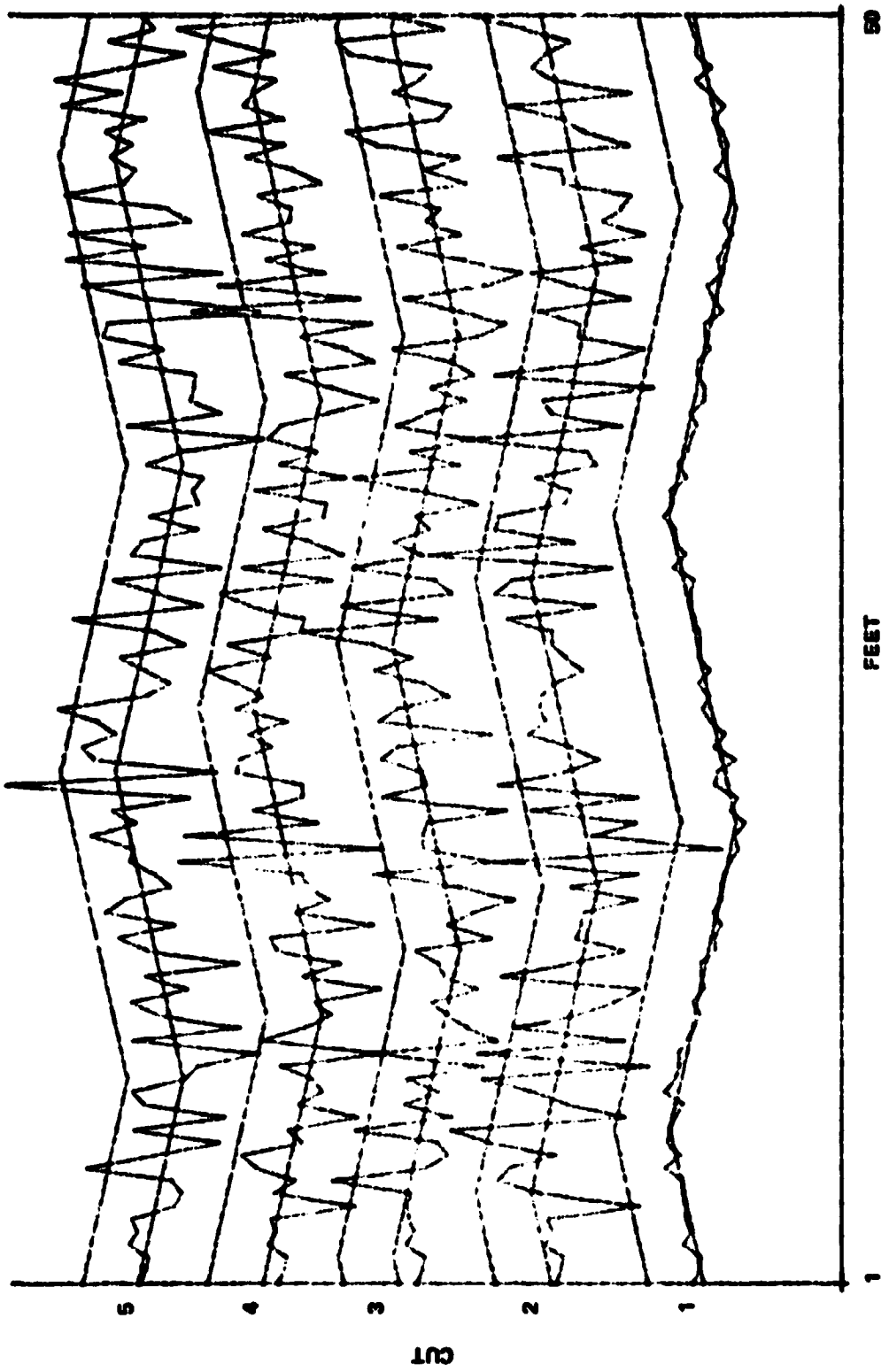

Figure 83. Coal slope scheme, noise = 0.4 in.

measurements was then increased in steps until it was equal to the CID distance behind the drum. Results improved as this distance increased because the predicted slope became less and less for a given difference between sensor outputs. However, the results were still very poor.

4.2.4.6 Future Work. Several areas come to mind for continued work. One is to map the interface profile using many stored previous cuts so that some kind of prediction can be made concerning the interface. The system could even allow on-the-spot measurements (known profile) to be included in the prediction scheme. One problem will be knowing exactly where the points are located as mining progresses from cut to cut.

There are many more combinations of data that could be tried with the variables used in this study. The weighting factors B are actually functions of the sensor noise and profiles and need to be determined. There are many other realistic profiles that could be used including some with discontinuities. Profiles varying into the face may also make it necessary to consider cut performance across the drum surface.

Considerable analytic work should be done to determine reasons for instability and get functional relationships between all the variables. This work could include stochastic variables as well. The CID accuracy requirements would then be a straightforward calculation.

4.2.4.7 VCS Alternate Control Laws Simulation.

```
10 DIM ES[100,10],CS[100],PS[100],DS[10],RS[10],AS[100]
20 I1=2
30 I2=4
40 I4=0
50 I5=4
60 I6=0
70 B=1
80 B0=1
90 B1=0.5
100 A=0.4
110 A1=0.4
120 K=4
130 N7=5
140 M=3
150 S1=0
160 N4=0
170 N2=0
```

```
180 N8=5
190 N9=3
200 N=3
210 N0=100
220 N3=10
230 N9=N9*(I2#1 AND I2#5)+(I2=1)+2*(I2=5)
240 N=(I1=1 OR I1=4)+N*(I1#1)*(I1#4)
250 B1=B1*(I2#4)*(I1#4 OR I4#0)+(I2#4)*(I1=4 AND I4=0)
260 B0=B0*(I2#5)+(I2=5)
270 N1=E1=E=E3=0
280 PRINT "COLUMN SCHEME "I1;" BETA"B
290 PRINT "ALPHA "A;"      COAL BIAS "K
300 PRINT "SENSOR 3 SIGMA "M;" CUTS TO PROCESS "N*(I1#4 OR I4#0)
310 PRINT "NUMBER SAMPLES "N0;" TOTAL CUTS "N3
320 PRINT "AVERAGE" (N2+N4+1)*(I4=1)"COLUMNS"N2"BEHIND"N4"AHEAD
330 PRINT "STEP="S1"   CID SCHEME"I2
340 PRINT "CID BEHIND"N8"  PROCESS"N9*(I2#4)*(I2#1)+(I2=1)"CID POINTS"
350 PRINT "PROFILES"I5"   NOISE USED"I6
360 PRINT "CID BETA"B0;"   CID PROPORTION"B1
370 I3=I7=1/5
380 E6=24
381 PRINT "FEET/SAMPLE"2.5*I3;"  SAMPLES/CYCLE"2*E6
390 E7=60
400 P[1]=E7
410 REDIM A[N0],C[N0]
420 GOSUB I5 OF 1150,1090,1150,1090
430 N5=N2+N4+1
440 N6=N8+N9-1
450 E4=(I1#4)+(I4=1)
460 GOSUB 1190
470 M=M*I6
480 IF I2#3 THEN 500
490 GOSUB 1860
500 IF I1#3 THEN 520
510 GOSUB 1370
520 SCALE 1,110,-5,10*N7+5
530 PRINT
540 PRINT "CUT MEAN SIGMA STEPS"
550 FOR Y=1 TO N3
560 E0=E2=I8=I9=E8=0
570 OFFSET 0,-51+(Y-1)*10
580 N1=N1+1
590 IF N1 <= N+1 THEN 610
```

```
600 GOSUB 1300
610 IF Y=1 THEN 630
620 GOSUB 1900
630 FOR X=1 TO N0
640 IF Y=1 THEN 880
650 IF X <= N6 THEN 670
660 GOSUB 1680
670 GOTO I1 OF 790,680,740,800
680 E=0
690 FOR L=1 TO N1-1
700 E=E+E[X,L]
710 NEXT !
720 E=E/(N1-1)
730 GOTO 800
740 E=0
750 FOR L=N1-1 TO 1 STEP -1
760 E=E+D[L] *E[X,L]
770 NEXT L
780 GOTO 800
790 E=E[X,N1-1]
800 IF I4=0 THEN 820
810 GOSUB 1410
820 IF I2=4 OR X <= N6 THEN 840
830 I8=C[X-N8]+B0*E3
840 IF I4=0 AND I1=4 THEN 860
850 I9=A[X]+B*(E+E1)/E4
860 I8=I8*(X>N6)+A[X]*(X <= N6)
870 C[X]=B1*I8+(1-B1)*I9
880 GOSUB 1240
890 E[X,N1]=P[X]-(C[X]+K+D)
900 E0=E0+(E[X,N1]+D)*(E[X,N1]+D)
910 E2=E2+E[X,N1]+D
950 NEXT X
951 IF Y=1 THEN 960
952 FOR X=1 TO N0
953 IF ABS(C[X]-A[X]) <= 2 THEN 955
954 E8=E8+1
955 NEXT X
960 MAT A=C
970 E2=E2/N0
980 E0=SQR(E0/N0-E2*E2)
990 PRINT Y;
```

```
1000 FIXED 2
1010 PRINT E2;E0;
1020 STANDARD
1021 PRINT E8
1030 IF Y>N7 THEN 1050
1040 GOSUB 1500
1050 NEXT Y
1060 PRINT
1070 PRINT
1080 END
1090 FOR I=1 TO N0-1
1100 P[I+1]=P[I]+I3
1110 IF I#(INT(I/E6)+0.5)*E6 THEN 1130
1120 I3=-I3
1130 NEXT I
1140 RETURN
1150 FOR I=1 TO N0
1160 P[I]=E7
1170 NEXT I
1180 RETURN
1190 FOR I=1 TO N0
1200 GOSUB 1240
1210 C[I]=P[I]-(K+D+S1)
1220 NEXT I
1230 RETURN
1240 R=RND1
1250 IF R>0.5 THEN 1280
1260 D=(1.414*SQR(R)-1)*M
1270 RETURN
1280 D=(1-1.414*SQR(1-R))*M
1290 RETURN
1300 FOR I=1 TO N0
1310 FOR J=2 TO N+1
1320 E[I,J-1]=E[I,J]
1330 NEXT J
1340 NEXT I
1350 N1=N1-1
1360 RETURN
1370 FOR I=0 TO N-1
1380 D[N-I]=A*(1-A)↑I
1390 NEXT I
1400 RETURN
```

```
1410 E1=0
1420 IF X>N2 AND X <= N0-N4 THEN 1450
1430 E1=E[X,N1-1]
1440 GOTO 1490
1450 FOR I=X-N2 TO X+N4
1460 E1=E1+E[I,N1-1]
1470 NEXT I
1480 E1=E1/N5
1490 RETURN
1500 FOR X=1 TO N0
1510 PLOT X,P[X]-K
1520 NEXT X
1430 PEN
1540 FOR X=1 TO N0
1550 PLOT X,C[X]
1560 NEXT X
1570 PEN
1580 FOR X=1 TO N0
1590 PLOT X,P[X]
1600 NEXT X
1610 PEN
1620 IF Y#N7 THEN 1670
1630 OFFSET 0,0
1640 YAXIS 1
1650 XAXIS -5
1660 YAXIS N0
1670 RETURN
1680 GOTO I2 OF 1840,1780,1710,1850,1690
1690 E3=E[X-N8,N1]+N8*(E[X-N8,N1]-E[X-N8-1,N1]+C[X-N8]-C[X-N8-1])
1700 GOTO 1850
1710 E3=0
1720 I0=N9
1730 FOR I=X-N8 TO X-N6 STEP -1
1740 E3=E3+R[I0]*E[I,N1]
1750 I0=I0-1
1760 NEXT I
1770 GOTO 1850
1780 E3=0
1790 FOR I=X-N6 TO X-N8
1800 E3=E3+E[I,N1]
1810 NEXT I
1820 E3=E3/N9
1830 GOTO 1850
```

```
1840 E3=E[X-N8,N1]
1850 RETURN
1860 FOR I=0 TO N9-1
1870 R[N9-I]=A1*(1-A1)↑I
1880 NEXT I
1890 RETURN
1900 IF I5=1 OR I5=2 THEN 2040
1910 IF I5=4 THEN 1980
1920 FOR I=1 TO N0
1930 P[I]=P[I]+N8*I7
1940 NEXT I
1950 IF (Y-1)#(INT((Y-1)*0.25)+0.5)*4 THEN 2040
1960 I7=-I7
1970 GOTO 2040
1980 FOR I=N8+1 TO N0
1990 P[I-N8]=P[I]
2000 NEXT I
2010 FOR I=N0-N8+1 TO N0
2020 P[I]=2*E7-P[I-E6]
2030 NEXT I
2040 RETURN
```

THE FOLLOWING SUBROUTINE USES DRUM CURVATURE TO MODIFY THE CUT. IT WAS NOT USED VERY MUCH AND NEEDS FURTHER CHECKOUT.

THE FOLLOWING STATEMENTS ARE NEEDED TO USE THIS SUBROUTINE.

```
869 B5=C(X)
871 GOSUB 2050

2050 IF X <=4 OR X>N0-5 THEN 2200
2060 B6=C[X]-0.606
2070 B2=C[X]-2.504
2080 B3=C[X]-6
2090 B4=C[X]-12
2100 C[X+5]=C[X]-30
2110 C[X]=C[X]*(C[X] >= B5)+B5*(C[X]<B5)
2120 C[X+1]=C[X+1]*(C[X+1] >= B6)+B6*(C[X+1]<B6)
2130 C[X-1]=C[X-1]*(C[X-1] >= B6)+B6*(C[X-1]<B6)
2140 C[X+2]=C[X+2]*(C[X+2] >= B2)+B2*(C[X+2]<B2)
2150 C[X-2]=C[X-2]*(C[X-2] >= B2)+B2*(C[X-2]<B2)
2160 C[X+3]=C[X+3]*(C[X+3] >= B3)+B3*(C[X+3]<B3)
2170 C[X-3]=C[X-3]*(C[X-3] >= B3)+B3*(C[X-3]<B3)
2180 C[X+4]=C[X+4]*(C[X+4] >= B4)+B4*(C[X+4]<B4)
2190 C[X-4]=C[X-4]*(C[X-4] >= B4)+B4*(C[X-4]<B4)
2200 RETURN
```

4.2.4.8 Parameter Definitions.

I1	Column Scheme: 1 = Single Point, 2 = Avg. of N Rows, 3 = Exp. Smoothing of N Rows, 4 = None
I2	CID Scheme: 1 = Single Point, 2 = Avg. of N Cols., 3 = Exp. Smoothing of N Cols., 4 = None, 5 = Surface Measurements
I4	Use in-cut avg. ? 0 = No, 1 = Yes
I5	Profiles: 1 = Both flat, 2 = sawtooth cut, slope I7 and E6 samples per half cycle, 3 = Flat cut, sawtooth into face, 4 = sawtooth both ways
B	Control law error coefficient
A	Exponential coefficient for column
A1	Exponential coefficient for CID data
K	Coal to be left (Bias), inches
N7	No. cuts/plot
M	CID 3 sigma (triangular) error, inches
SI	Initial step added to first cut profile
N4	No. Columns ahead of present position to average
N2	No. Columns behind present position to average
N8	No. Columns CID trails present position of drum
N9	No. Columns (CID measurements) to average or smooth
N	No. last cuts to use
No	No. samples in one cut
N3	Max. no. cuts per run
I3 (=I7)	Profile step (inches/foot)

I6 Noise after initial cut? 0 = No, 1 = Yes

B0 CID B

B1 Proportion of Control Signal from CID

Drum assumed to Be 2.5 ft wide

Plots N7 cuts/page then just computes, rest up thru N3

Prints: Cut, mean, 1 σ, No. steps > 2 in.
mean is average of (profile-cut) across face = average error
1 σ is RMS deviation of cut from mean

4.2.5 Joy Boom Actuation Transfer Function. A series of operational tests were performed on the Joy longwall shearer located at the Bureau of Mines in Bruceton, Pennsylvania. The purpose of these tests was to determine the transfer function and operational characteristics of the system. These characteristics were used to generate a simulation model of the longwall shearer to be used in the development of closed-loop VCS.

The data obtained were for an unloaded condition since the drum was not cutting coal or driven into the coal seam by the linear drive along the track. The magnitude of the observed coupling between the booms is expected to change in the operational mode when the cutting drums and boom are under load. The loads on the system will result in higher system temperature and hydraulic pressures than have been obtained in these tests.

Commands to the system were used to drive the boom cylinder control valves. A sinusoidal and a pulsed command were inputs. The outputs of the system will be the boom position, rate, and acceleration. Other selected internal system parameters were monitored such as hydraulic pressures, temperature of the hydraulic fluid, and boom cylinder position. During the system, data were tape recorded for later processing.

The pressure sensors, temperature probe, accelerometers, rate gyros, and linear potentiometers were obtained as off-the-shelf, hardware items that had been used to support previous projects. The mounting fixture for the potentiometers, and the rate gyros and accelerometers was designed and fabricated. Two 11-channel tape recorders were used to record data. A multi-channel strip chart recorder was obtained to provide onsite monitoring of selected system parameters during tests.

Signal conditioners were obtained and calibrated for the accelerometers, pressure transducers, and the temperature probe. The temperature probe was calibrated to 250°F, and a calibration fixture was built and used to calibrate the pressure transducers to 2500 psi. The tangential accelerometer was selected at 5 g's and the radial accelerometer at 1 g.

Inhouse design and development of supporting electronics included two demodulator outputs for the rate gyro packages for each boom, the pulse command generator, a linear isolation amplifier for the simusoidal input, and a power supply and output signal distributor box which contained the signal conditioners. A left boom potentiometer (Y_L) support fixture was built to support the pot at a low and high boom position.

An increase in the threshold for pulsed inputs was observed and was reflected in the simulation model together with the other significant characteristics determined by this study.

No external loads were applied to the cutting drums or booms. Before the tests, the tilt cylinders (roll) were positioned so the chassis was horizontal and the cowl was rotated vertically to permit the boom to be lowered to a horizontal position. This differs from the operational mode in that the cowl mass adds to the boom mass and inertia during these tests.

Input commands to the system (8 V) were selected from a pulse generator (which provided for a selection of various pulse durations and frequencies) or from a sine wave generator (for a range of frequencies and amplitudes). These inputs were used to drive the right and left booms individually or simultaneously. The input command to the left boom and right boom was interfaced through an oceanic connector to the control valves and recorded on tape with the other system parameters.

The system pressures were monitored with pressure transducers calibrated from 0 to 2500 psi. The supply pressure regulator was set at 2200 psi, but due to limited access the pressure sensor was located between the pump and the regulator. During several tests, pressures exceeding 2500 psi within the system saturated the pressure sensors. Hydraulic temperature (T) was monitored in the return line. The hydraulic temperatures were found to be excessive, and a heat exchanger was installed.

The position of the boom cylinders was obtained by mounting linear potentiometers to the boom cylinder body and the slider to the boom cylinder rod. The boom cylinder stroke is 9.5 in. The resultant boom angle is 36°. A boom angle of zero occurs when the boom is collinear with the chassis or when the boom cylinder stroke is 3.25 in.

The boom height potentiometer was monitored on the left boom to detect boom position relative to the ground reference. A potentiometer stand for low boom angles and a stand extension were used for larger boom angles to support the potentiometer.

Angular boom rates were detected by the rate gyro package. The operational range of this sensor is ±20°/sec with a natural frequency of 23 Hz.

The sensor disc which contains the rate gyro and the tangential and normal accelerometers was aligned such that the tangential accelerometers were perpendicular to the centerline of the boom.

The outputs from the sensors were routed to the signal conditioner and distribution box and then to the two Ampex 1300 tape recorders. Selected parameters were monitored and recorded on an eight channel Brush recorder. The Ampex recorder speed provided a 20 kHz frequency response but data acquired on the Brush recorder are flat to 55 kHz. Eleven channels of data were recorded on each tape recorder.

4.2.5.1 Discussion. The closed-loop VCS will be used to detect the difference between a desired cutting depth of coal and the actual cutting depth that occurs, and to maintain that difference within prescribed limits. Commands from the controller to the longwall shearer control valve will be constant in magnitude but of variable duration. Since the present longwall shearer control valve is a proportional valve, a series of system tests were performed to investigate the linear and nonlinear system characteristics. These tests resulted in the identification of characteristics needed to develop an improved simulation model of the longwall shearer.

As a result of these tests, it has been determined that the needle-check valve is a significant component in the dynamic response characteristics of the system. The needle valve can be opened such that the rates to lower the boom exceed those to raise it. A decrease in boom rates occurred when the booms were raised simultaneously, but this did not occur when they were lowered simultaneously. The complete closing of the needle valve restricts the flow so that the boom can only be raised. The needle valve position determines the down pulse duration for sustained oscillation, the rate the boom can be lowered, the frequency response curve, and the chatter level for a proportional input command.

The primary control components of the Joy longwall shearer are shown in Figure 84 for a single boom. A ±8 V step command is provided as an electrical input to the control valve. The output is hydraulic flow through the dual

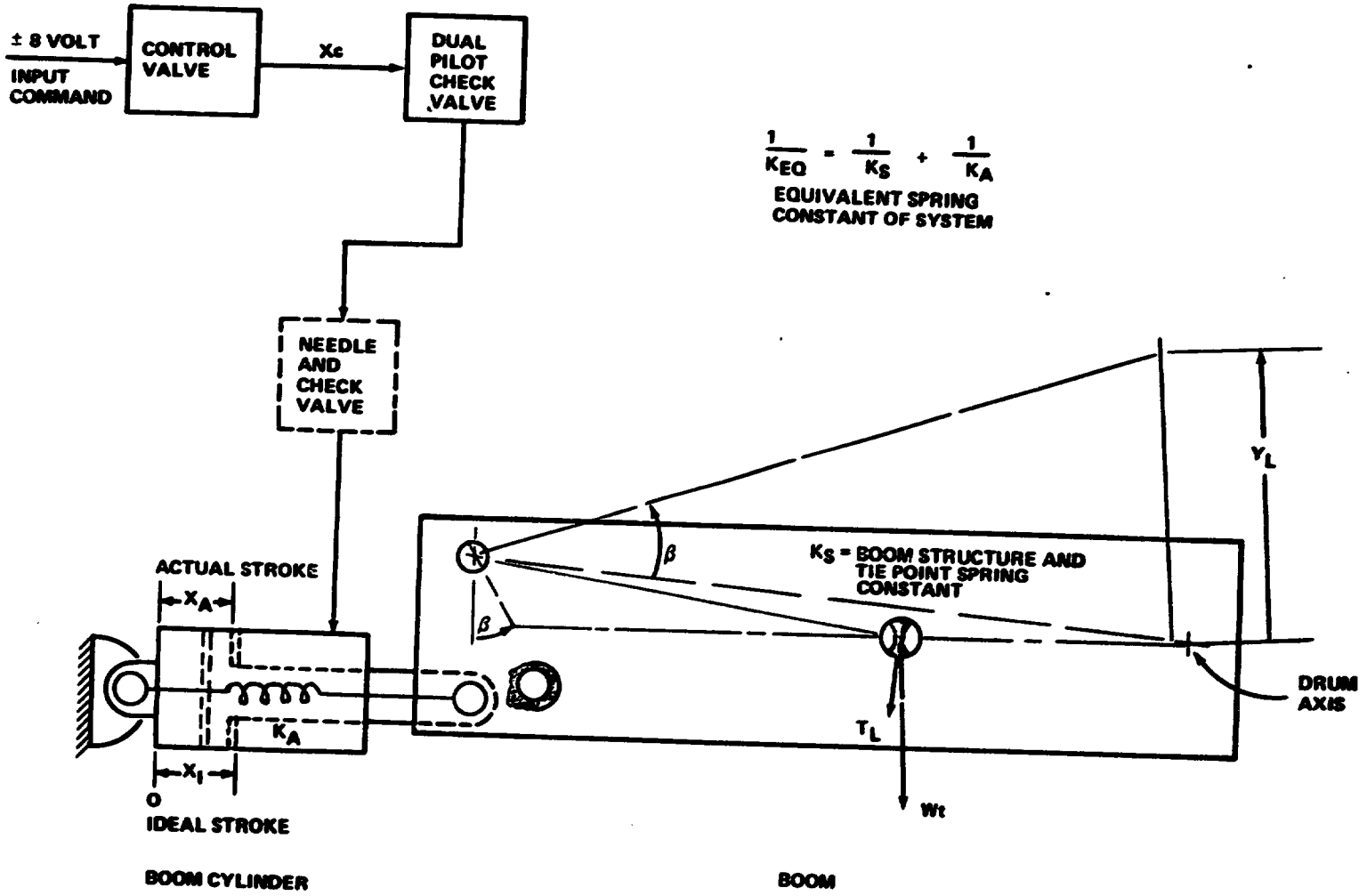

Figure 84. Primary control components of the Joy longwall shearer.

pilot check valve to the needle check valve and to the boom cylinder. When the boom is lowered the flow is restricted in the return line by the needle and check valve. This determines the rate the boom may be lowered. The flow through this valve should be adjusted (by the needle valve) such that the lowering and raising rate of the boom is the same. Since an equal rate can be preset, the simulation model (at this level of definition) does not include the effects of the needle and check valve shown in Figure 84.

When the actuator stroke (X_I) is changed, the boom angle (B) changes and the drum is raised or lowered (Y_L). If the mass of the boom, drum, cowl, and motors is represented by a weight vector at the composite center of gravity of the boom then a load torque (T_L) is produced about the pivot point. The load torque applies a compressive force on the boom cylinder such that the actual piston position (X_A) is less than (X_I). This compressive load is isolated from the control valve by the dual pilot check valve. The difference between X_A and X_I is determined by the system stiffness represented by an equivalent spring constant K_{EQ}. The equivalent spring constant is determined by the structural stiffness K_S and actuator stiffness K_A. The values of each of these will be determined by the bulk modules of the oil, the boom cylinder structure, length and size of hydraulic lines, tie points, and pivot pin stiffness. Each of these parameters could be determined with further analysis and tests. The simulation model developed from the system tests is an end-to-end model which incorporates the component characteristics but does not include a model of the components.

The control valve was modeled for a 6 Hz frequency with a damping factor of 0.9. The velocity was limited such that a 100 percent step input provides a 100 percent output in 0.25 sec with a 30 percent activation threshold. Maximum flow occurs before the valve is fully open because it is rated at 10 gal/min and the pump supplies 8 gal/min for single boom operation (Fig. 84).

The dual pilot check valve isolates the flow until a force is applied to exceed the pilot centering spring. The return line is opened before this primary flow occurs. This provides an impulse to the system when the valve is initially opened and is due to the weight of the boom. This is shown as Q_T in Figure 85 and is the result of the torque load T_L being applied for t + 250 msec when the flow is negative. The switch closes when $Q_P = 5.6$ for single boom operation and $Q_P = 2.8$ for dual boom operation. The resulting flow, when multiplied by

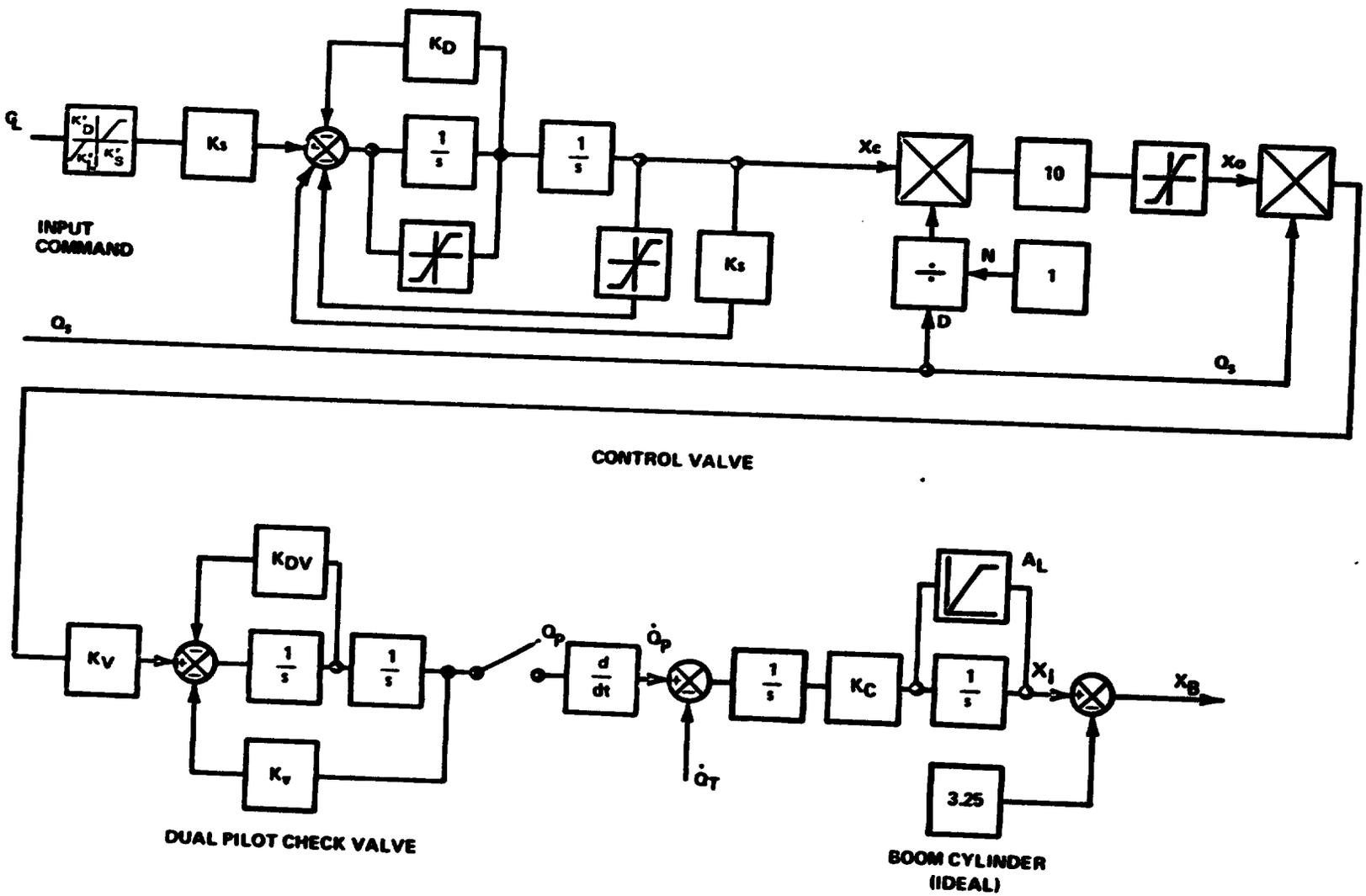

Figure 85. Boom dynamics.

K_C and integrated, represents the boom cylinder stroke which ranges from 0 to 9.5 in. A 3.25 in. bias is included, which represents the stroke when the boom is horizontal and B = 0.

The linear equivalent spring constant is shown in Figure 86. The spring compression due to the actuator stroke produces a boom torque about the pivot and an angular acceleration B. The boom angle (B) when multiplied by the constant K_B and summed with the 3.75 in. bias provides the actual actuator stroke X_A.

The weight of the boom produces the torque T_L. This torque is applied to the boom dynamic in the form of a change in flow rate Q_T for a duration of T_T. The torque when multiplied by the gain factor K_T and for Δ_T seconds results in a peak amplitude even when the boom is lowered.

An additional frequency component was observed from the rate gyro output during the test that was not seen at the boom cylinder. This frequency has been included in the K_F loop and combined in rates and integrated to provide a change in drum position Y_L.

An example of the data obtained from the tests is provided in Figure 87. The left boom was commanded to raise and then lower by inputs C_L. The resulting outputs of acceleration, rate, actual boom cylinder position, and supplied system pressure are given in Figure 87.

System parameters and constants which were determined from analysis of the test data results and used to develop the simulation model are presented in Paragraph 4.2.5.2.

4.2.5.2 Symbol Definitions.

Symbol	Units	Definition
A_{SL}	g	Linear acceleration normal to boom and at drum axis
C_L	V	Step command to control servo valve, ±8 V
J	lb-ft-sec^2	Moment of inertia of boom, drum, cowl and components, 8886.6

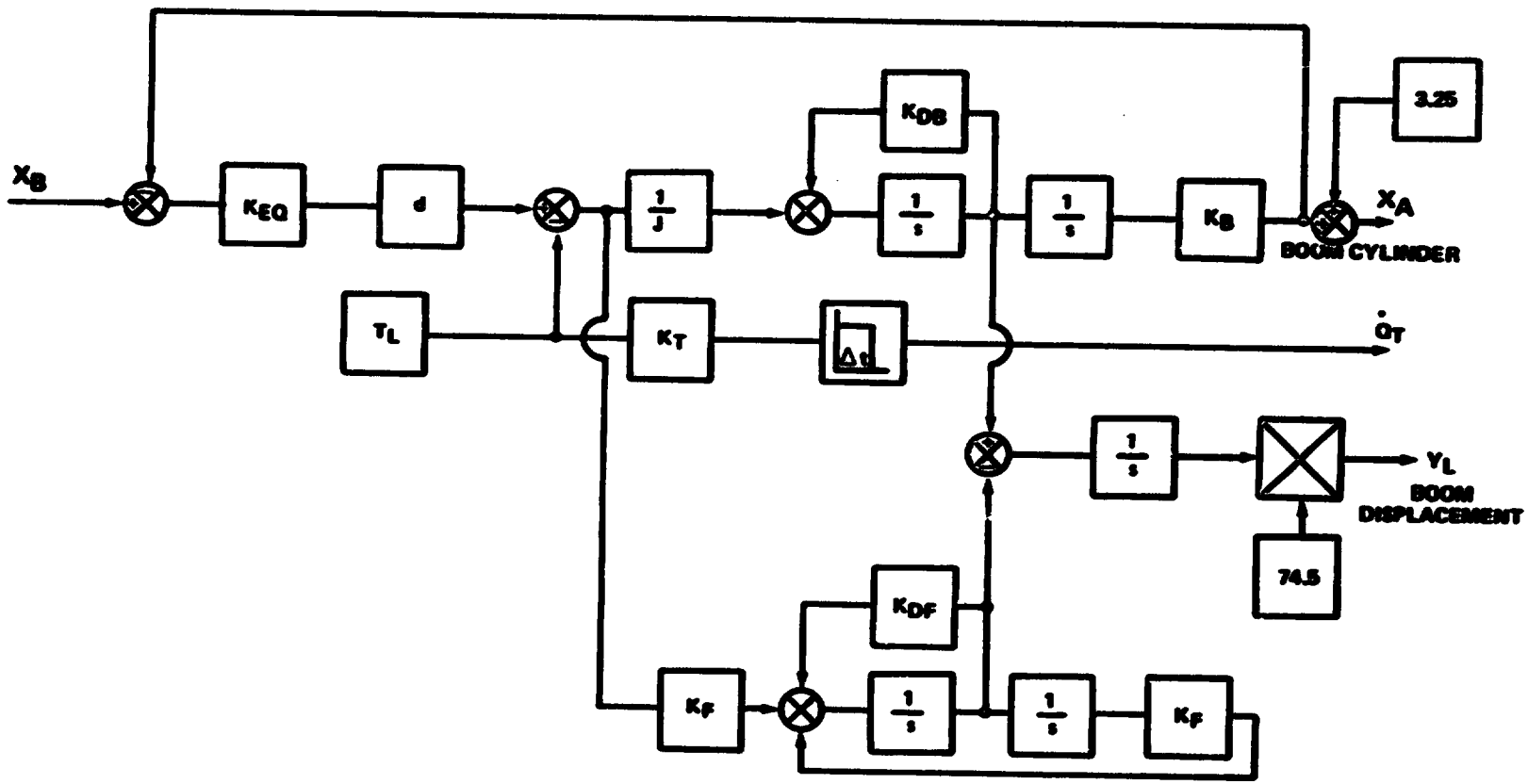

Figure 86. Linear equivalent spring constant.

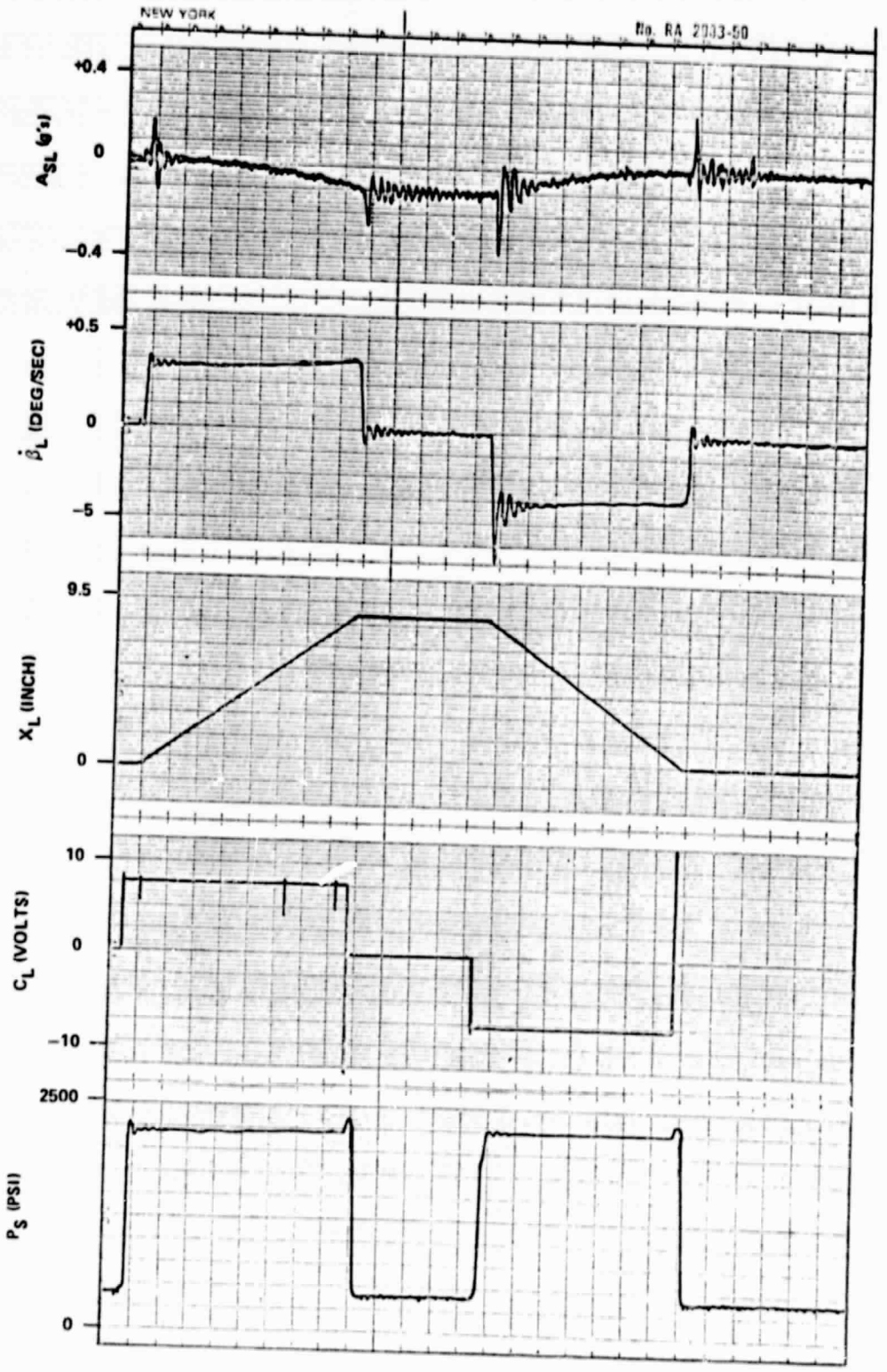

Figure 87. Test data example.

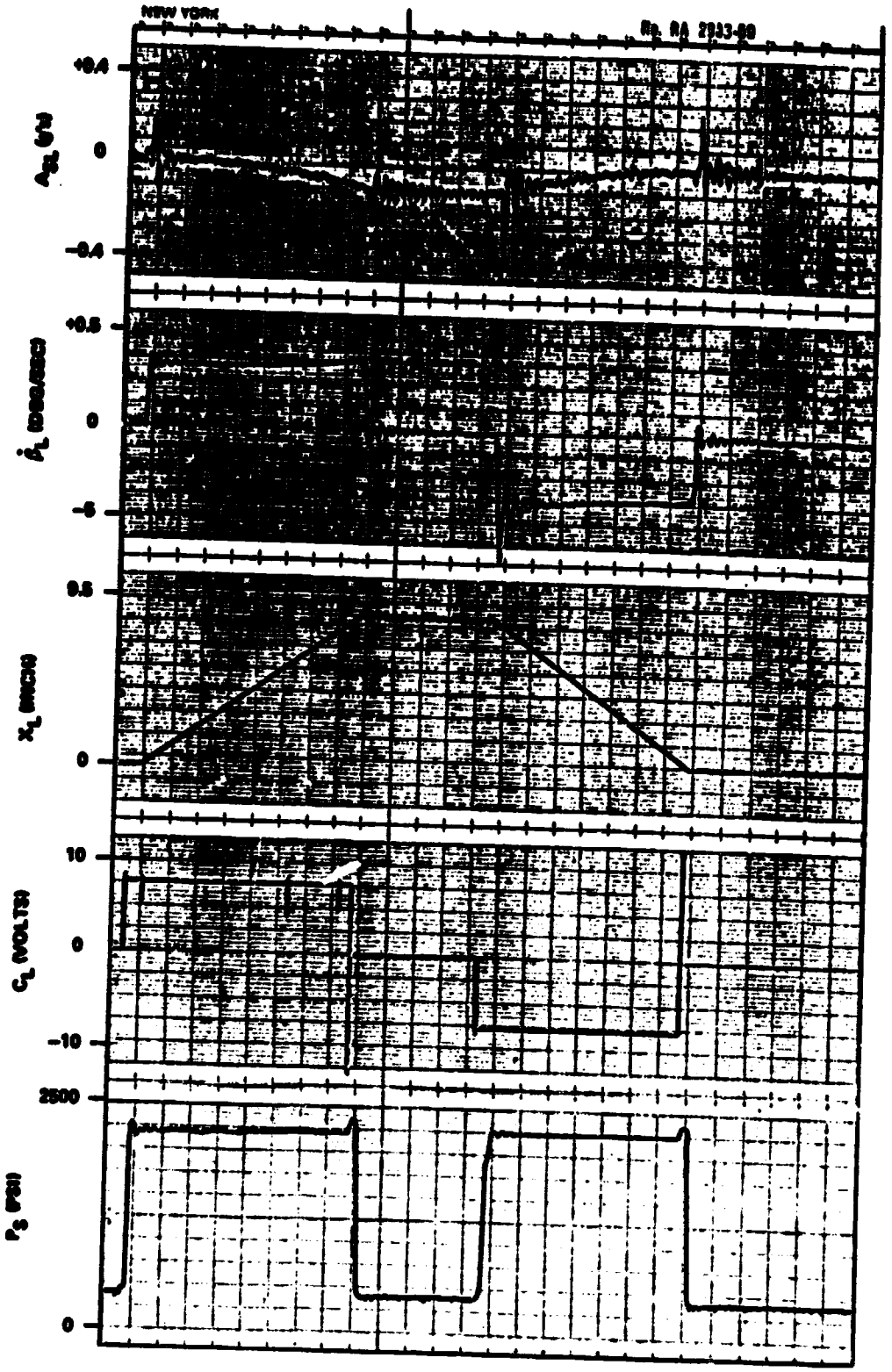

Figure 87. Test data example.

Symbol	Units	Definition
K_A	lb/in.	Spring constant of the boom cylinder
K_B	in./rad	Actuator displacement per radian boom rotation, 10.5
K_C	in.-min/sec-gal	Actuator velocity gain factor, 0.933
K_D	1/sec	Inner loop damping gain factor of control valve, 67.9
K_D	V	Control valve dead band, 2.4
K_{DB}	1/sec	Inner loop damping gain factor, 5.8
K_{DF}	1/sec	Inner loop damping gain factor, 2.95
K_{DV}	1/sec	Inner loop damping gain factor of dual pilot check valve, 7.04
K_{EQ}	lb/in.	Equivalent system linear spring constant, 610, 967
d	ft	Moment arm from pivot to boom cylinder tie point, 0.875
K_F	$1/sec^2$	Outer loop gain of a boom frequency component, 872
K_s	$1/sec^2$	Control valve input gain, 0.179
K_s	$1/sec^2$	Control valve outer loop gain, 1421
K_S	lb/in.	Spring constant of boom structure and pivot and actuator tie points
K_L	V	Input voltage limit, 8
K_T	(gal sec/min)/ft-lb	Torque to flow rate conversion factor, 13

Symbol	Units	Definition
K_V	$1/sec^2$	Outer loop gain factor of dual pilot check valve, 25.27
P_S	psi	System supply pressure
Q_S	gal/min	Hydraulic flow supplied to boom control valve, 8 or 4
T_L	ft-lb	Torque on boom cylinder due to weight of boom, 54×10^3
Δt	msec	Simulated response time of the dual pilot check valve, 250
W_t	lb	Weight of boom, drum, cowl and motors, 12 185
X_A	in.	$(X_A = X_L)$ Actual position of the boom cylinder when T_L is applied
X_I	in.	Ideal position of boom cylinder, X = 3.25 in. when B = 0
Y_L	in.	Linear change of boom height at drum center line
B	rad	Position angle of boom from a horizontal position
$\dot{B}$	rad/sec	Angular rate of boom
$\ddot{B}$	rad/sec^2	Angular acceleration of boom

4.2.6 Joy Shearer Vibration Measurements. The t[ask] of obtaining in-mine vibration data from an operational Longwall shearing m[achine] was completed this year. This work was performed by the Shaker Corporation and consisted of design, manufacture, and mine-permissible testing of instrumentation and recording equipment and the in-mine acquisition of the data. Table 14 and Figure 88 identify the test sensor and their locations on the Joy shearer.

TABLE 14. MINE TEST SENSORS — JOY LONGWALL SHEARER (KOPPERSTON NO. 2 MINE — KOPPERSTON, WEST VIRGINIA)

Tape No. 169 Lockheed Electronics Recorder 15 ips tape speed

Tape No. 170

Location	Sensor Description
1	Vertical Main Frame Accelerometer — PCB 308A03, Left-Hand Upper Frame, Encore 501-1, Meg Input, Gob Side, and FM Record Channel 1
2	Axial Ranging Arm Accelerometer — B& K 4344, Left-Hand Drum (Prime), Encore 501-2, 100K Input, and Direct Record Channel 2
3	45° Drive Sproket Accelerometer — PCB 308A03, Encore 501-3 Amp, Meg Input, Gob Side, and FM Record Channel 3
4	Axial Ranging Arm Accelerometer — B& K 4344, Right-Hand Drum (Clean-Up Drum), Encore 501-4, 100K Input, and Direct Record Channel 4
5	Vertical Shoe Accelerometer — PCB 308A03, Right-Hand Side Lower Frame, Encore 501-5, Meg Input, Gob Side, and FM Record Channel 5
6	Left-Hand Drum Sound — B& K 1/2 in. Microphone with 2203 SLM Microphone at Left-Hand Edge of Main Frame, Horizontal, Aimed Toward Left-Hand Entry, and Direct Record Channel 6
7	Face Side Main Frame Accelerometer — Vertical PCB 308A03, Center of Machine (nominal) Beside Venturi, Encore 501-6 Amp, Meg Input, and FM Record Channel 7
V.T.	Voice Commentary of Test Conditions

Notes: 100K Encore Input AC 16 Hz to 100 kHz
Meg Encore Input AC 1.6 Hz to 30 kHz
Accelerometers Stud Mounted on Cemented Blocks Using Eastman 910 Cement.

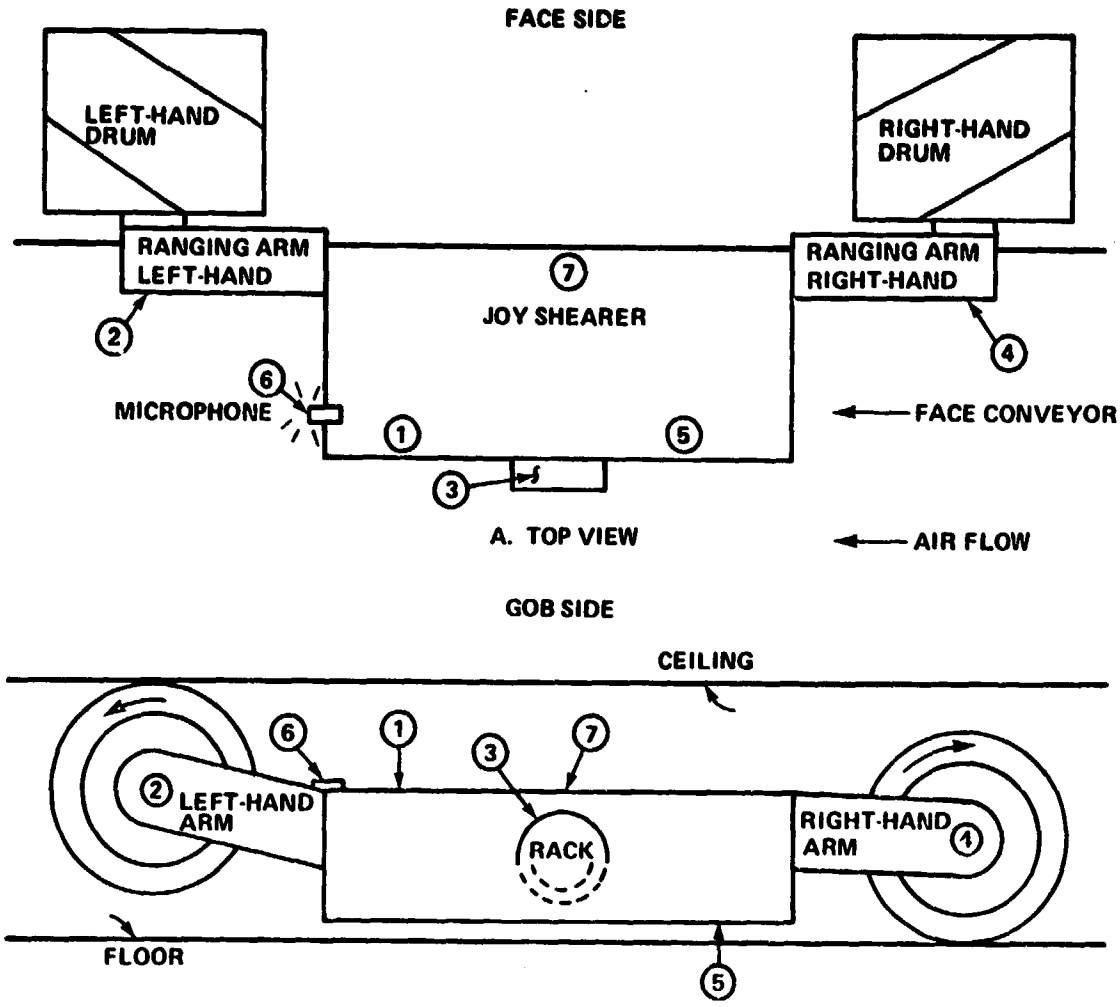

NOTE: ACCELEROMETERS ARE STUD MOUNTED TO TAPPED PADS ATTACHED BY EASTMAN 910 CEMENT TO SHEARER STRUCTURE.

Figure 88. Sensor locations — Joy shearer.

4.2.6.1 Review of Recorded Data. Review of these test data provides some insight into the type of responses that chassis-mounted transducers and electronics will experience during normal coal mining activities. Several observations can be made which will assist in making use of this information.

Accelerations recorded from the ranging arm accelerometers (B&K 4344 units) are quite moderate with peak responses occurring during what

seemed to be difficult cutting; a maximum level of 4.3 g peak was recorded for the left-hand drum. The trailing drum generally has response levels one-fourth to one-tenth as great as the leading drum which is proportional to the work being done by each.

Maximum recorded mining machine chassis vibration occurs at about the center of the gob side frame, our location 3. A review of the acceleration peak hold spectrum analysis plot, Figure 89, shows a major frequency response at 8 Hz of 0.26 g peak which, when converted to displacement, is equal to 80 mils peak-to-peak. The time averaged spectrum analysis level for the same operating region shows levels of 0.05 g, equivalent to 15 mils peak-to-peak displacement at 8 Hz.

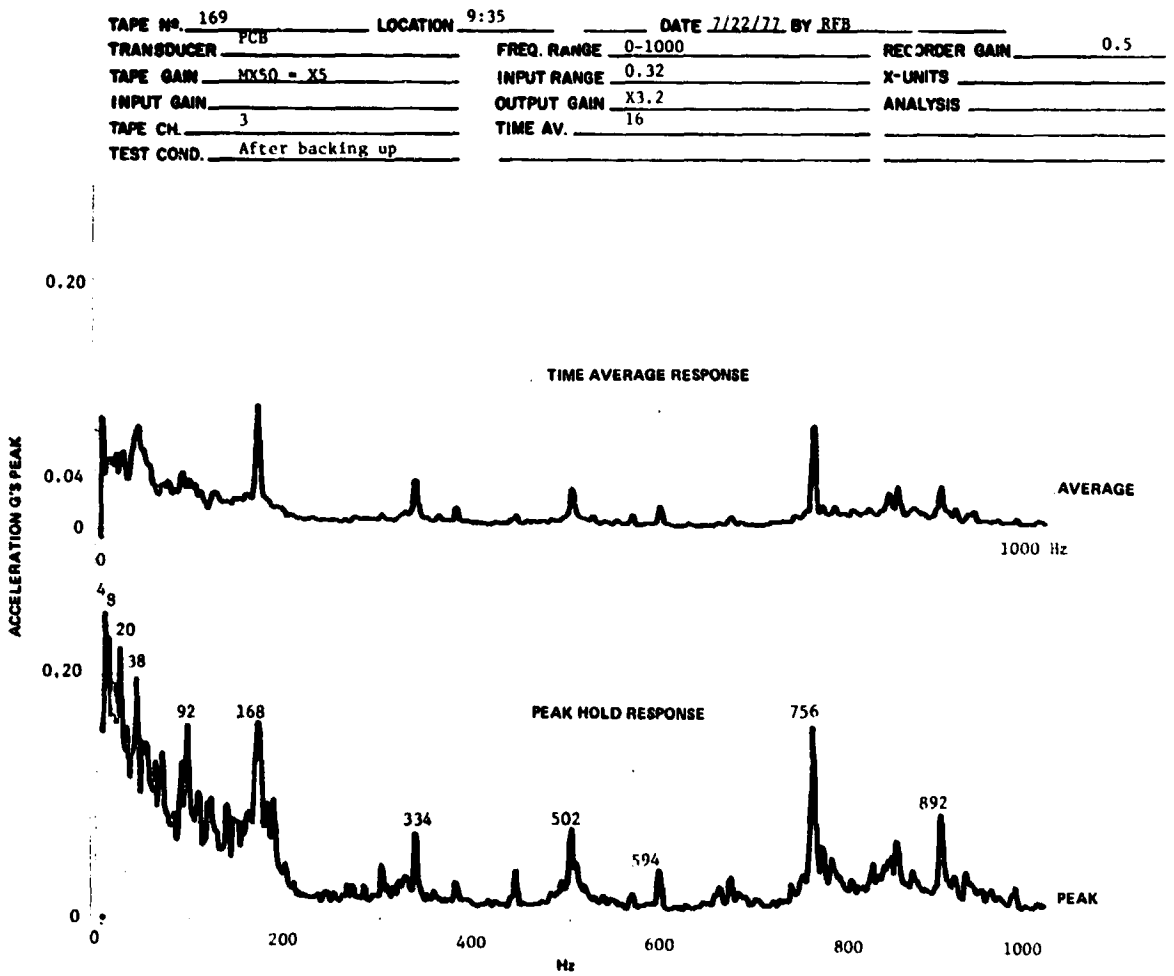

Figure 89. Tape channel 3 accelerometer output spectrum analysis, normal cut moving left.

The face side chassis accelerometer, location 6, seems relatively lower in amplitude response with little of the low frequency vibration. It is assumed that the face side guide shoes stay in contact with the face conveyor rails with that as the pivot point for drum input force variations; a down force on the lead drum causes the gob side of the chassis to rise. Higher frequency components, however, are up somewhat in level with response at 760 Hz of a character which might cause loosening of bolts. Its source is unknown.

The gob side chassis sensor, location 5, was assumed to be near a guide shoe when it was selected; however, because of machine modifications face conveyor contact was not in that region, and only one shoe remained on that side right under the rack drive sprocket. The reduced amplitude low frequency response (below 10 Hz), as compared to sensor location 3, indicates that the major responses are forced by the harder working drum and that chassis flexibility reduces responses away from the point of major load application. If this installation was cutting both directions, the sensor would have had increased response.

One possible use of these test data would be the definition of platform vibration characteristics for qualification of mining machine transducers and conditioning equipment which are being developed for coal interface detection. It is expected that this is as typical of normal mining as can be obtained, at least in the full-cut conditions while moving left. Tramming speeds are fairly low at 10 ft/min. A recommended typical test level for equipment qualification would be as follows, assuming a sinusoidal sweep to a shaker system:

3 to 10 Hz = 0.100 in. peak-peak amplitude

10 to 30 Hz = 0.020 in. peak-peak amplitude

30 to 500 Hz = 1 g peak acceleration

500 to 3000 Hz = 3 g peak acceleration.

A resonant search of the tested device should be conducted with a minimum of 10 min spent at each identified natural frequency. Natural frequencies of the Joy machine structure occur at 8, 20, 38, 90, 168, 334, 502, 756, and 892 Hz; therefore, components to be mounted on this machine should not have resonances present within 5 percent of these frequencies.

4.3 Yaw Measurement Instrument

4.3.1 General. The concept for the yaw angle measurement has been tested and verified feasible. This concept involves knowing the end location of the conveyor sections and the angles between successive sections. Using only the angle information and knowing the length of each section, the curve of the conveyor between end points can be calculated.

During the past year, the original yaw angle cart was modified into the configuration shown in Figure 90. This cart was able to measure its own bias angle error so that initial alignment of the first section was no longer necessary. The yaw angle cart measured only the bias angles and the angles between sections. These data were recorded by hand as the cart moved down the actual track. Conveyor trajectory was calculated by putting the data into a desk-top calculator and solving some equations. These calculated curves (Fig. 91) agree well with the measured or true curve.

A request for proposal (RFP) has been written for the design and fabrication of one yaw angle measuring device, to be mounted on the Joy longwall mining machine located at the Bureau of Mines in Bruceton. The concept for attaching the mechanical hardware to the Joy machine is shown in Figures 92, 93, and 94. The RFP also includes the design and construction of one electronics box to be mounted on the Joy machine and one processor and display panel control package to be located 150 ft from the machine. The electronics will process the data and transmit it to the processor by cable. The processor will accumulate all data until a measurement is complete, then it will solve several algorithms to determine the yaw displacement along the coal face. This information is transferred to the control package that will drive the display panel.

The face measuring instrument, whose concept was embodied in the "angle cart" breadboard design has been investigated to find a suitable solution for its functional integration into the longwall shearer. One possible method for design integration is shown in Figure 94. Figure 95 shows the breadboard of the control electronics for the display panel. This breadboard functions as it should and is ready to be packaged.

The angle measurements are made while the machine is operating and the alignment of the face is displayed at the end of the cut. The only inputs to the yaw measurement system after initial setup are the end-point locations of the conveyor sections. These data need to be updated every 8 to 10 cuts. With this information, the display panel will show the misalignment of each conveyor section. The data are ready for either manual face alignment control or an automated face alignment control.

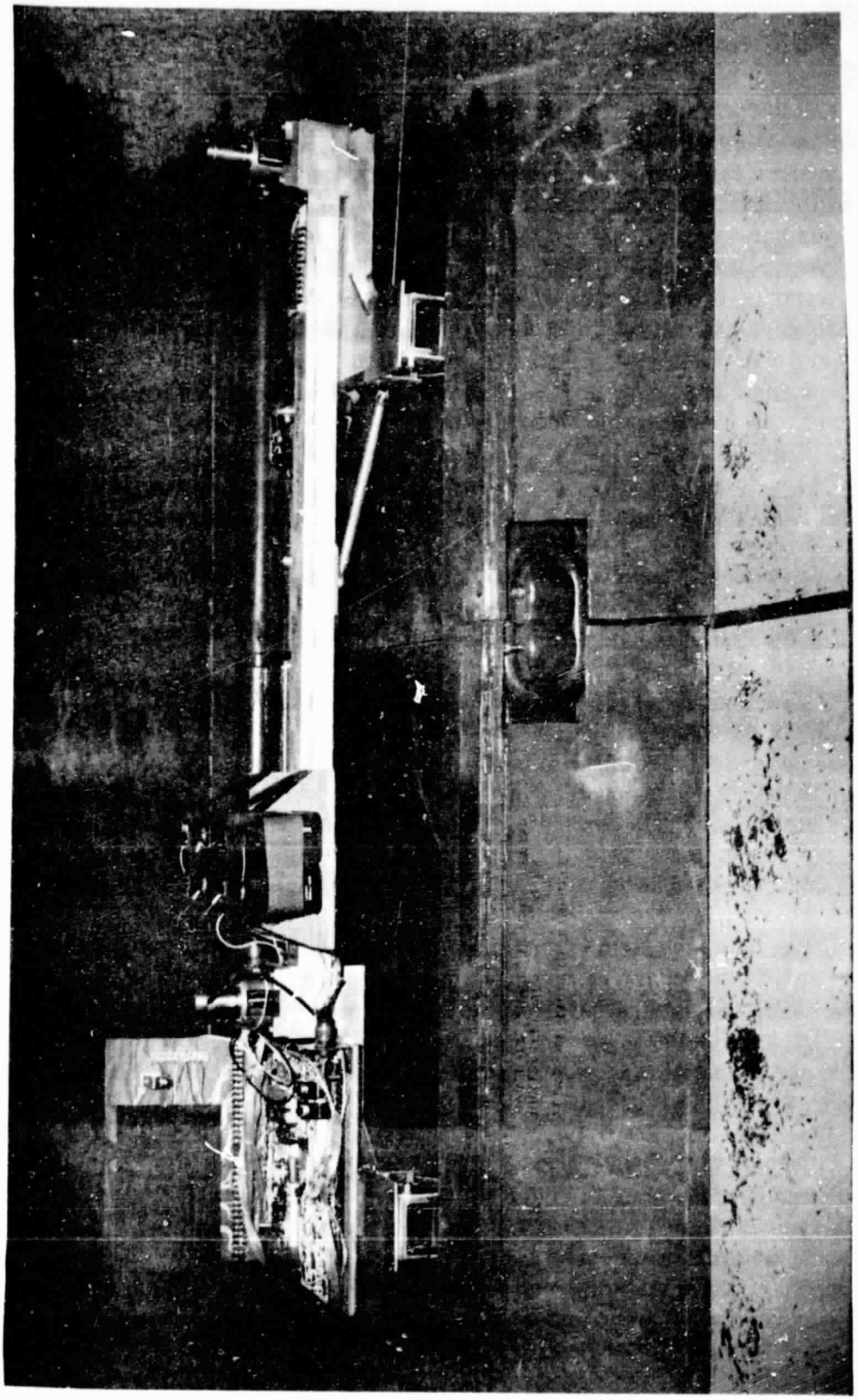

Figure 90. Yaw angle cart.

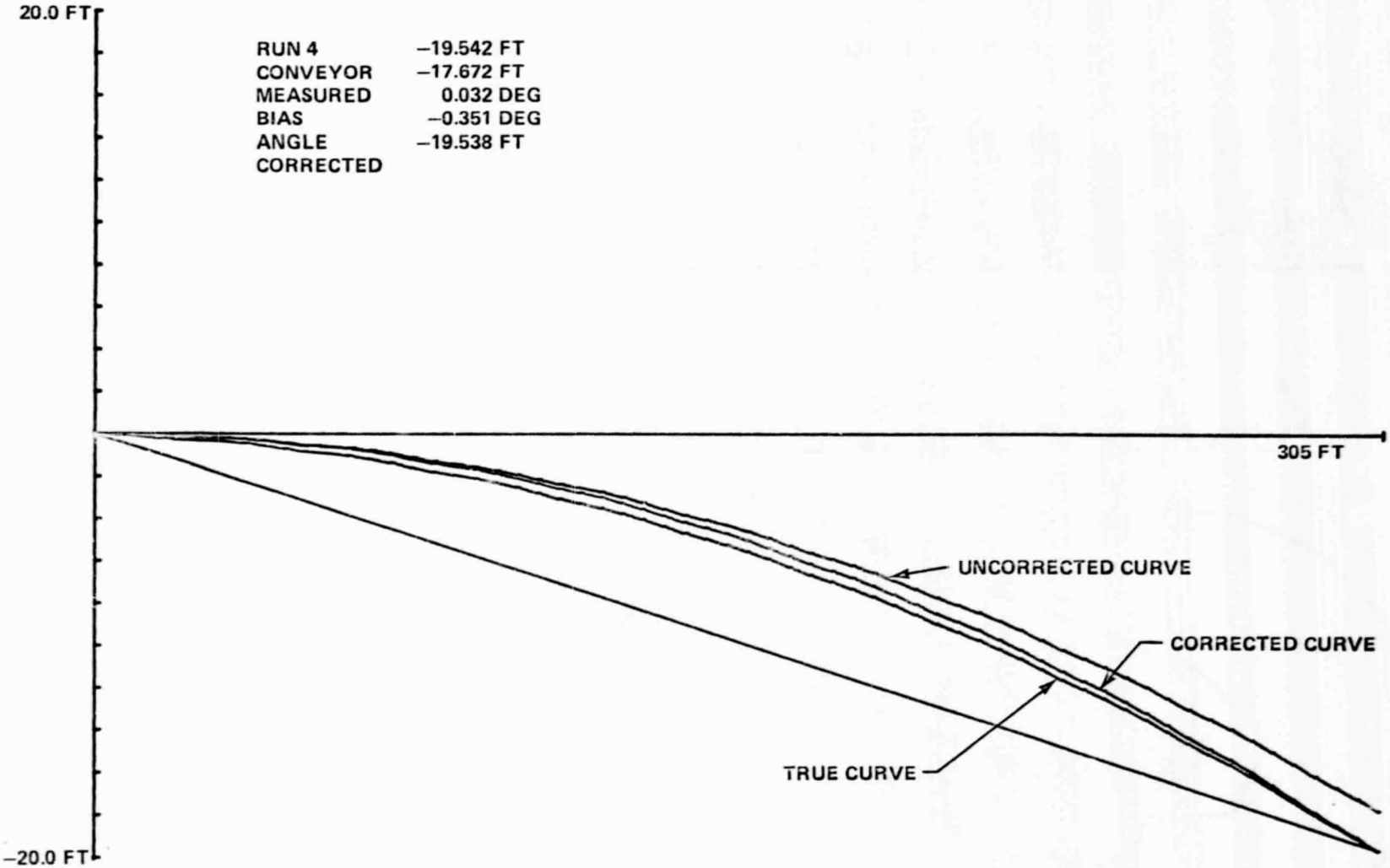

Figure 91. Simulated coal face measurement.

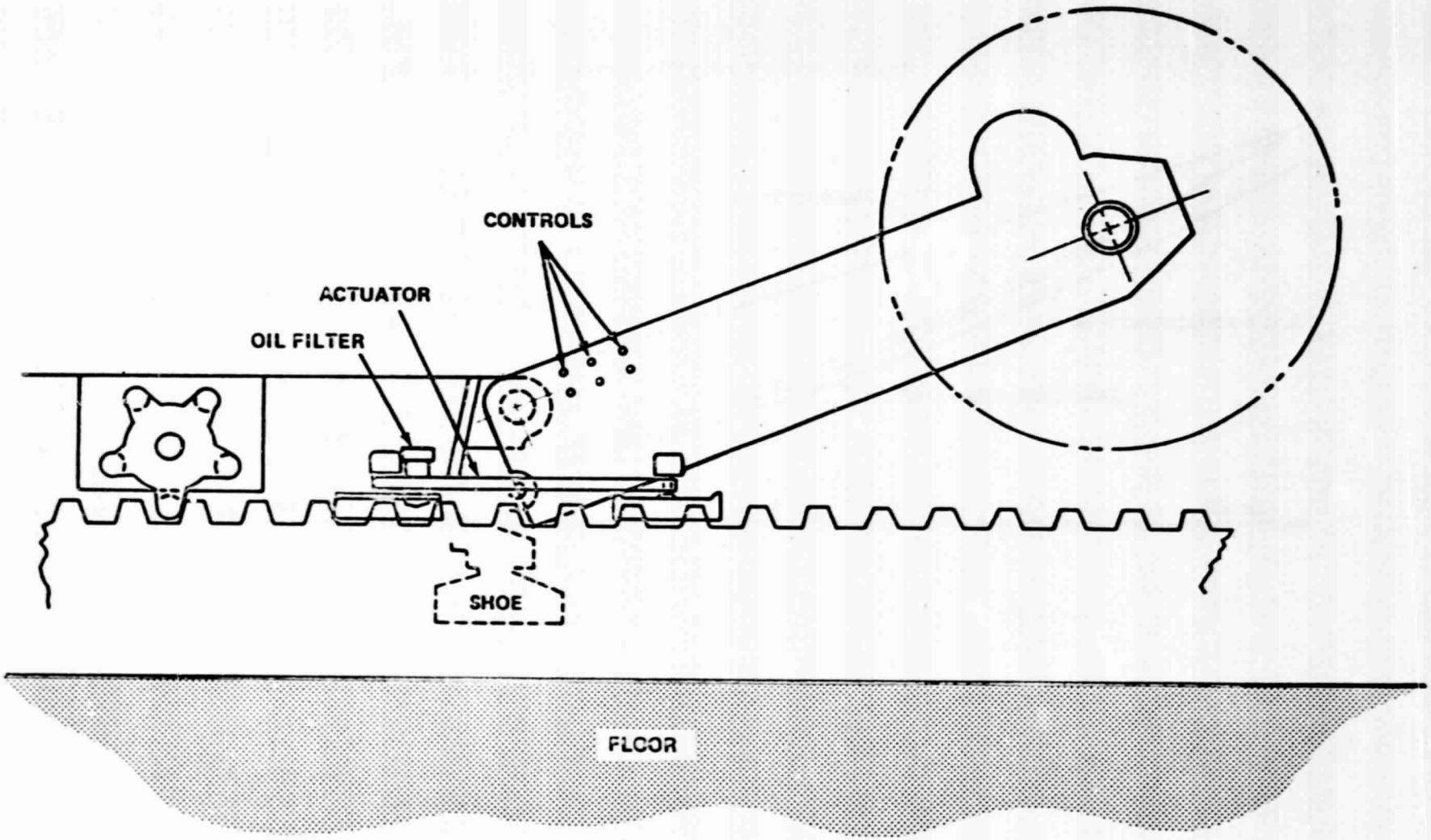

Figure 92. Mechanical hardware attachment concept.

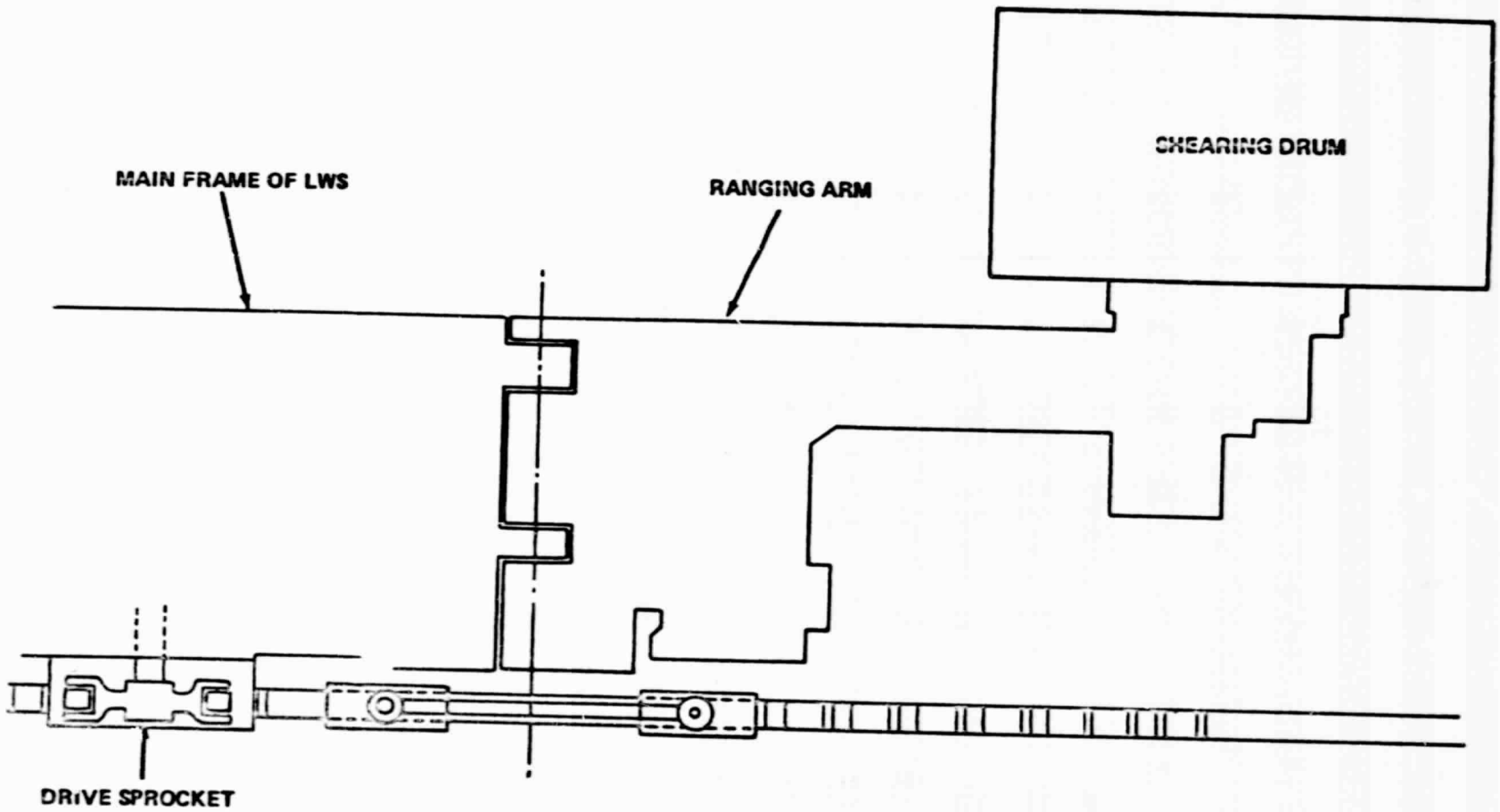

Figure 93. Drive sprocket and shearing drum attachment concept.

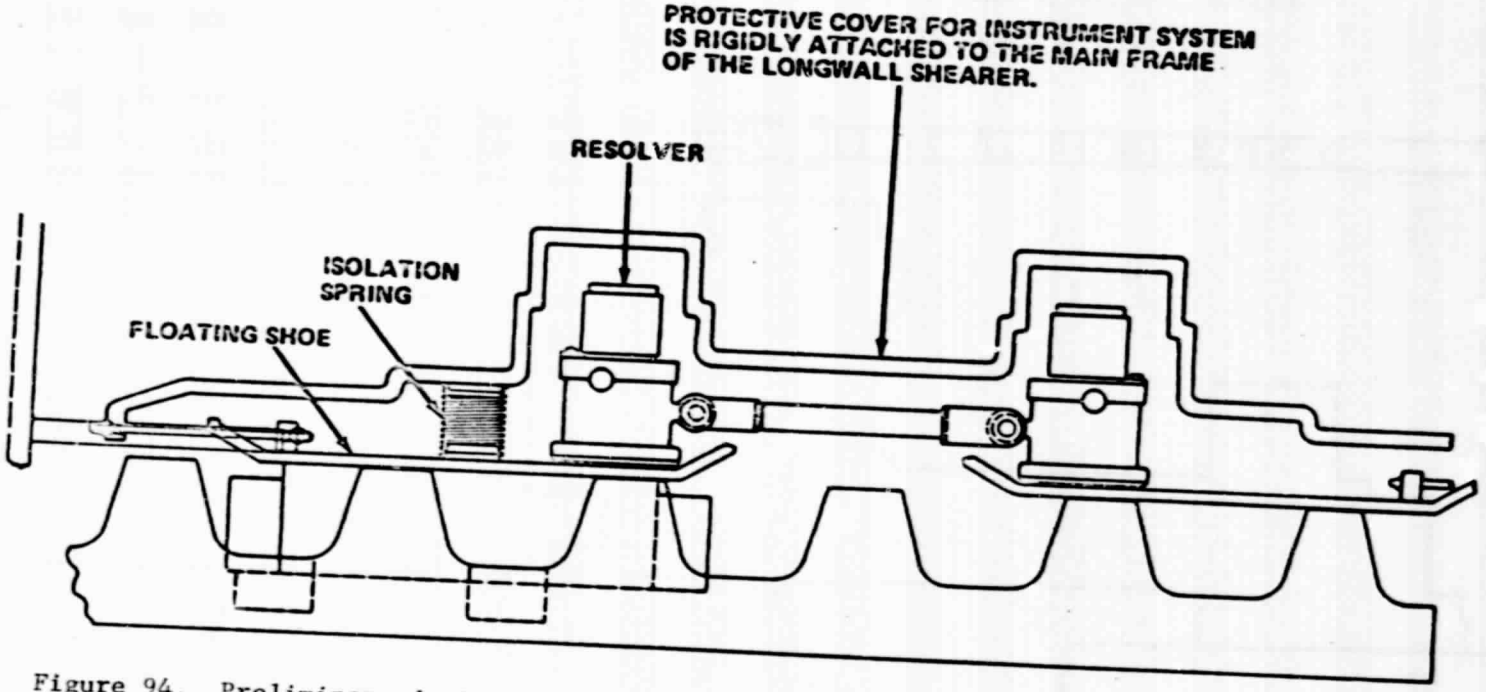

Figure 94. Preliminary design: method to integrate face measuring (angle cart) and shearer.

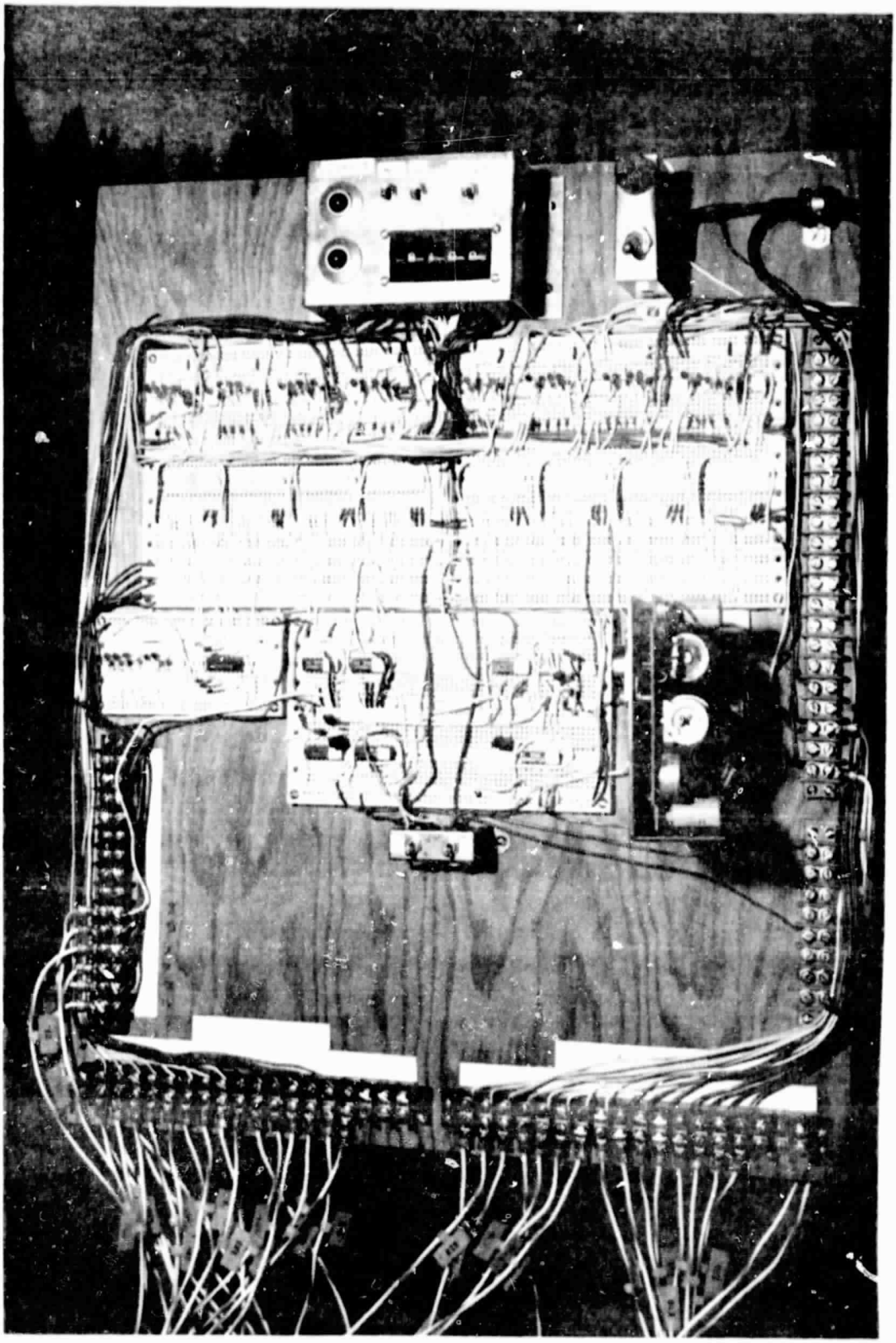

Figure 95. Breadboard control electronics.

4.3.2 Requirements. The yaw measuring device will be designed to meet the following specifications:

(a) Accuracy — The overall system should be able to calculate the true curve of a 600 ft coal face within ±1 ft of the true position.

(b) Operating Speed — The yaw angle measuring device should be able to take data while moving along the coal face at speeds between 0 to 40 ft/min.

(c) Sample Linearity — The angle samples must be evenly distributed over a distance of 1 ft.

(d) Input Data — Provisions must be made to input and store the following data:

(1) End points A and B.

(2) Number of runs using the same end points.

(3) Number of sections.

(e) Output Information — The machine should be able to display input data on request and should also be able to request data update with lights or equivalent.

(f) Measurement Direction — The yaw measurement is to be made in one direction only. This will probably be made when the machine is traveling toward the entry containing the display panel.

(g) Calculation Time — The microprocessor should be able to calculate the correct displacement curve within 2 min after the last angle is measured.

(h) Equipment Location — The measuring equipment should be located on the Joy machine. The processor can be located on the machine. The input and output terminals, display panel, and panel driver will be located in the entry tunnel.

(i) Data Transmission — Data can be transmitted from the machine to the display panel and input terminal over a 500 ft coaxial cable.

(j) Mine Permissible — This first model does not have to meet the Mine Permissible Specification.

(k) Power Available — 115 V, 60 Hz, ±20 V.

(l) Abort a Run — Provision should be made to abort a run.

(m) Start a Run — A push-button switch may be used to start a run.

Operating Environment of Apparatus Delivered Under This Action.

(n) Water Spray — System must operate in water spray continuously.

(o) Coal Dust — System is exposed to coal dust.

(p) Air Temperature — 50° to 90°F.

(q) Shock and Vibration — Must be able to operate while Joy machine is operating.

4.4 Roll Measuring

A requirement exists in the Automated Longwall system for an instrument that will measure the roll angle of the shearing machine about its longitudinal axis. This measurement will be used to control actuators that adjust the in-seam tilt of the cutting drum. A Moog Model 86-121 level sensor has been tested in the laboratory to verify its specified measuring accuracy of 1 arc min and linearity of 0.5 percent of full scale (Fig. 96). Plans for the roll sensor include the construction of a protective case which will permit its mounting on the Joy shearer at Bruceton, where further tests will be performed.

C-3

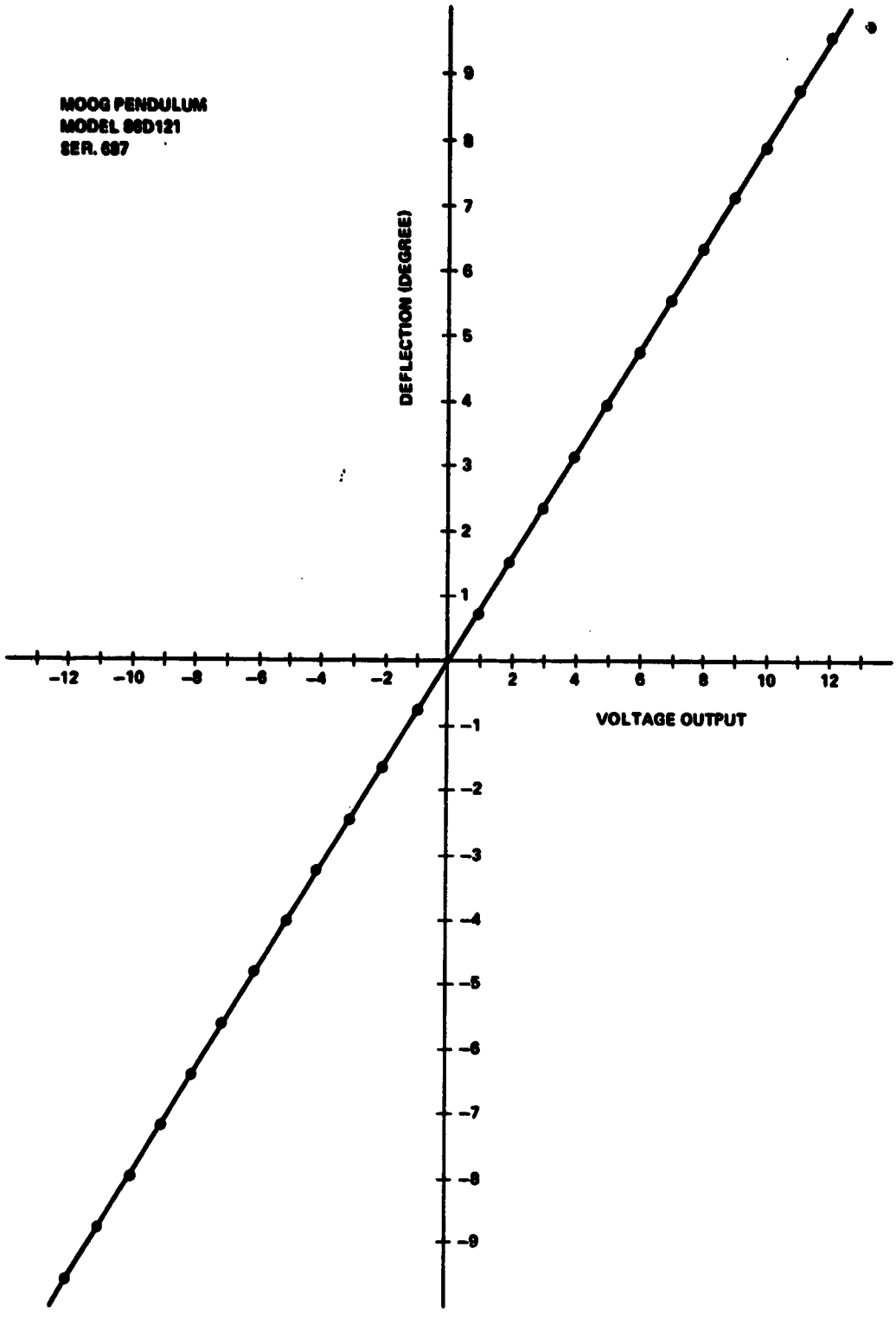

Figure 96. Linearity curve.

5.0 TECHNICAL SUMMARY

5.1 Nucleonic CID

Work on the backscatter gamma ray nucleonic CID has progressed with the design and manufacture of the two-point contact, independent floating head instrument and its mating control and display box. The independent and floating heads were chosen to minimize the coal depth measuring errors which are induced by the presence of air gaps between the instrument and the coal surface. It is anticipated that this experimental CID will have 0 to 8 in. depth measuring capabilities with ±1/2 in. accuracy. This instrument will be tested on the MSFC CID simulator and in the Bruceton experimental mine before it is incorporated into the Mock Longwall VCS at Bruceton.

5.2 Radar CID

Because of its great potential, considerable effort has been expended on testing, evaluating, and improving the FM-CW radar. The present design operates over a frequency range of 2.2 to 4.3 GHz and has a measuring range of 2 to 5.5 in. with an accuracy of ±0.5 in. Studies have been conducted to identify the magnitude of the radar's signals attenuation as a function of the moisture in the coal and the masking of the coal/rock interface by the strong first return of the coal/air interface, and to improved signal processing algorithms. Plans for the radar CID in FY78 include preparing and providing the 2.2 to 4.3 GHz radar for inclusion in the Mock Longwall VCS test program and the building and evaluation of an improved FM-CW radar which operates at 0.7 to 4.3 GHz and one which operates at 0.7 to 8 GHz and has a theoretical measuring range of 1 to 12 in. in coal having an attenuation of 3 dB/in. (Bruceton Mine).

5.3 Sensitized Pick CID

A program was initiated this year for the design, manufacture, and mine test of a sensitized pick CID. The design consists of a standard pick mounted in a modified block, where the block is instrumented with a strain gage and accelerometer to measure the pick's cutting forces. The force measurements will be transmitted from the rotating drum to a receiver mounted on the shearer chassis, where the data will be recorded on magnetic tape. Following the mine test, scheduled for early November 1977, the recorded data will be analyzed by MSFC for determination of a signal processing algorithm. The sensitized pick hardware will be transferred to the Bureau for mounting on their Joy shearing machine following the mine tests.

5.4 Surface Recognition CID

The design of an experimental surface recognition CID has been completed, and manufacture of the instrument is 95 percent complete. Performance evaluation tests will be made at MSFC using the CID simulator and then at the Bruceton experimental mine in early FY78.

5.5 Natural Radiation

Studies were undertaken this year to determine the potential for using the natural emission gamma rays from shale as a CID. This concept is similar in principle to the backscatter gamma ray CID, but does not require a radioactive source and does not have to be in immediate contact with the surface. The coal depth is determined by the number of photons counted in a specified time interval. The same sodium iodide crystal detector that is used in the backscatter nucleonic CID is also used in this concept. Tests were performed in several mines using several different detector shielding configurations. The test results indicated that this concept has considerable CID potential as a depth measuring sensor with 0 to 6 in. range and ±0.5 in. accuracy. FY78 plans include fabrication and further mine testing of an experimental natural radiation CID.

5.6 Magnetic Resonance CID (Late)

A study has been made to ascertain the feasibility of using the magnetic resonance phenomena to measure coal seam thickness. Laboratory measurements of coal and shale samples have established that there is a significant difference in the number of free hydrogen electrons in these materials, thereby making coal thickness measurements possible. Also, an analytical model of an idealized magnetic resonance CID was developed to determine instrument size and performance. Computer simulations have shown that a 12 by 12 by 6 in. instrument could measure 20 in. thick coal with an estimated accuracy of ±0.3 in. FY78 plans include the design, manufacture, and test of an experimental magnetic resonance CID.

5.7 Hydraulic Drill CID

The concept of locating the coal/rock interface by measuring the depth of a slot which has been cut through the coal to the rock interface by a high pressure water jet will be investigated in FY78 by the University of Missouri at Rolla.

5.8 Infrared CID

Infrared measurements in the 8 to 12 m wavelength range were made on wet and dry coal and shale. The overlapping in data makes surface identification by this method impossible. No further activities are planned.

5.9 Electrical Properties CID

Laboratory tests were performed to determine whether coal and shale could be differentiated by resistance and/or capacitance measurements. An overlap in the coal and shale measurements when the surfaces were wet makes discrimination by this concept impossible. No further activities are planned.

5.10 Thermal Sensitized Pick CID

Monitoring of the cutting bit's temperature by means of thermistors implanted into the tip to identify the rise in temperature associated with cutting rock does not appear feasible because of the massive thermal inertia of cutting bit, measuring response time of thermistor, and the bit cooling effect due to the water spray. No further activities are planned.

5.11 Mechanical Drill CID

The concept of locating the coal/rock interface by instrumenting a mechanical drill to measure torque and/or the drill cutting chips via a reflectometer was investigated by three independent organizations: NASA, Foster-Miller, and Bendix. While the conclusions were not unanimous, NASA believes that for nonlongwall applications the mechanical drill concept does have sufficient potential to warrant its development into an engineering model for further testing. NASA, however, is not planning to continue this effort in FY78, based on discussions with the Bureau.

5.12 Acoustic CID

Laboratory tests performed under ideal conditions within 0.25 and 0.50 MHz ultrasonic transmitter and receiver have shown that the signal attenuation in coal is approximately 6 dB/in. This value is approximately two times greater than radar signal attenuations and would limit the depth measuring capability of an acoustic CID to approximately 2 in. In FY78 further investigations are planned to include use of a lower frequency transducer to improve the instrument's depth measuring capabilities and methods of coupling the signals to coal.

5.13 Artificial Material Test

Samples of artificial coal and rock materials which are planned for use in the Mock Longwall test facilities were provided by the Bureau of Mines for CID operational verification tests. Neither the radar, nucleonic, nor surface recognition CID's would function properly with these samples. However, recommendations were provided for correcting the deficiencies. Additional tests are also planned to investigate the possibility of placing 0 to 2 in. segments of steel wire in the artificial rock material for interface bonding and radar signal reflections.

5.14 Vertical Control System (VCS)

Evaluation and refinement of the baseline VCS simulation model has continued this year. Several major changes in the model were required to reflect the latest configuration of the Joy shearing machine, namely the new location of the trapping shoe and the longer boom arms. Refinements to the model involve statistical CID error models, more accurate determination of boom actuator controls, smoothing of the cut surface by modeling the full circumferential drum cutting action, CID to drum top/bottom distance indicator, and multipass simulation capabilities.

The simulation results indicate that the baseline VCS, which consists of a drum trailing depth measuring CID, sensitized picks and last-cut follower can mine greater than 95 percent of the desired coal with 1.25 percent of the total extracted materials being rock when operating at 20 ft/min and employing a CID with a 3σ error of 2 in.

The simulation model will continue to be studied and refined during this coming year. One of the most important refinements will be inclusion of the hydraulic boom actuator dynamic model.

5.15 Alternate VCS Studies

In addition to the baseline VCS which is being analyzed, studies were also initiated to investigate the relative merits of an alternate VCS which employs various forms of predictive control laws. These studies were performed using a simplified math model of the system. Evaluation of the performance data indicates that the baseline VCS provides equal or better performance than investigated predictive control laws, when the system's CID has a 1σ measuring accuracy of 0.4 in. or less. For systems employing less accurate CID's, the VCS performance can be increased by using a control law that uses stored CID measurements from the previous cut and present cut CID measurements.

However, it is NASA's opinion that CID's will be available that have a 1σ accuracy of 0.5 in. or less and that switching from the baseline VCS to the predictive control law with its increased complexity is not warranted at this time.

5.16 Joy Boom Actuator Transfer Function

During the past year, a series of tests were conducted to determine the dynamic characterization of the Joy shearing machine hydraulic boom actuator control system. Following the test, the recorded data were analyzed and a mathematical model of the system was generated. This mathematical model will now be incorporated into the baseline VCS simulation to replace the kinematic model of the actuator now being used.

5.17 Yaw Measuring Instrument

The angle measuring cart, which was built in FY76 to verify the concept which determines the face profile by measuring the relative angular change between successive conveyor sections, was modified this year by shortening the distance between the two angle measuring resolvers. This modification enables a new algorithm to calculate and remove steady-state bias error from the measurement. The angle measuring instrument can now measure the face profile to within ±6 in. of its true position by knowing only the location of the two end points. A concept design has been completed for this instrument which can be attached to the Joy machine, using the conveyor's gear rack for its measuring reference. Plans have been made to manufacture and test the angle measuring instrument on the Joy shearer, at Bruceton, in 1978.

5.18 Roll Measuring Instrument

The roll measuring instrument has been laboratory tested for linearity and accuracy. The FY78 plans include mounting the instrument on the Joy machine at Bruceton for operational/environmental tests.

5.19 Joy Shearer In-Mine Environmental Data

The task of measuring and recording the acceleration and acoustic level on the Joy shearing machine while operating in the mine was completed. These data were acquired from Joy LW-300 operating in the Kopperstone No. 2 mine. Analysis of these data identified natural frequencies occurring in the machine's structure at 8, 20, 38, 90, 162, 334, 502, 256, and 892 Hz, with a peak acceleration of 4.3 g occurring on the boom. A recommended vibration test criterion was formulated from these data for VCS instruments that are to be mounted on the Joy machine.

6.0 SPECIAL STUDIES

6.1 Effects of Automation on Production and Cost

A limited study was initiated to obtain a better perspective of the potential benefits and limitations of automating the longwall shearing process, particularly with respect to face production potential and cost. Some objectives of the study were to determine:

(a) Face production rate potential and limitations

(b) Effect on cost of coal (minimum selling price)

(c) Effect on shearer guidance and control system technical requirements and cost of guidance and control.

The preliminary results and conclusions reached from this study at this point are summarized as follows:

(a) With an automated system which includes drum vertical control, face advancement and alignment (yaw and roll), face production rates on the order of 2500 tons/shift would be routinely possible (for the methods and conditions assumed for the study) within the limits of current equipment capabilities (Note: Higher face production rates have actually been achieved for short periods as evidenced at Consol's Robinson Run Mine, when 12 395 tons were mined in a 24 hr period in January 1976).

(b) At this time there appears to be no particular limitation from the guidance and control system or available shearer haulage, shearer power and speeds up to 30 or 40 ft/min. Since control of the drums and face advance will be automated, the operators will not have to keep up with the shearer or manually advance the roof supports at high rates. A support must advance each 10 sec for shearer speeds of 30 ft/min. Conveyor systems are currently limited to approximately 20 tons/min, which equates to a maximum shearer speed of 30 ft/min and approximately 2500 tons/shift for a full face cutting method (see Model B) in a 72-in. seam. Figures 97, 98, and 99 describe production models used in the study and the effect of shearer speed on face production for various conditions. Also the capability of the shearer to attain the necessary cutting rates does not appear to be a problem because available production units have the horsepower and speed range to meet these conditions.

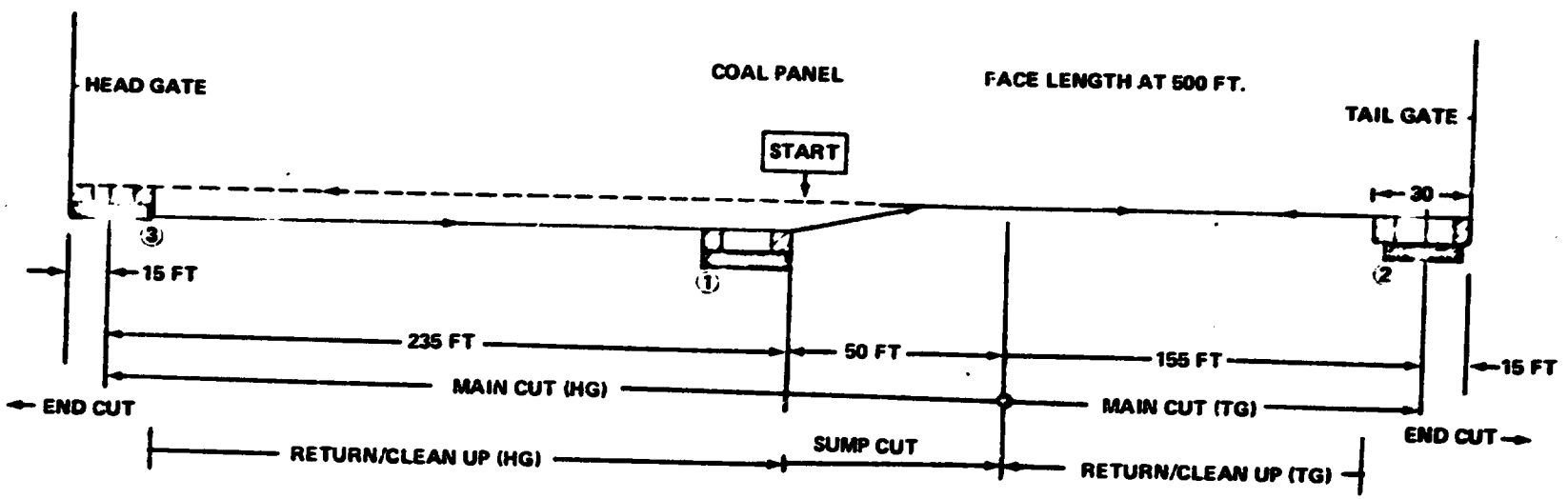

OPERATIONS SEQUENCE (ONE SHEAR)

- SHEARER CHECKOUT/START–UP
- SUMP CUT = 80 FT AT 10 fpm
- MAIN CUT TO TG = 155 FT/Vh
- END CUT AT TG = 15 FT AT 5 fpm
- TURNAROUND – TG (2 DRUMS)
- RETURN/CLEAN–UP (TG) = 2 (170 FT – 30 FT)/Vh + 50 = 280/Vh + 50
- MAIN CUT TO HG = 315 FT/Vh
- END CUT AT HG AT 15 FT AT 5 fpm
- TURNAROUND – HG (2 DRUMS)
- RETURN/CLEAN–UP (HG) = (250 FT – 30 FT)/Vh + 50 = 440/Vh + 50

Figure 97. Longwall Model A (half-face or single-shear method).

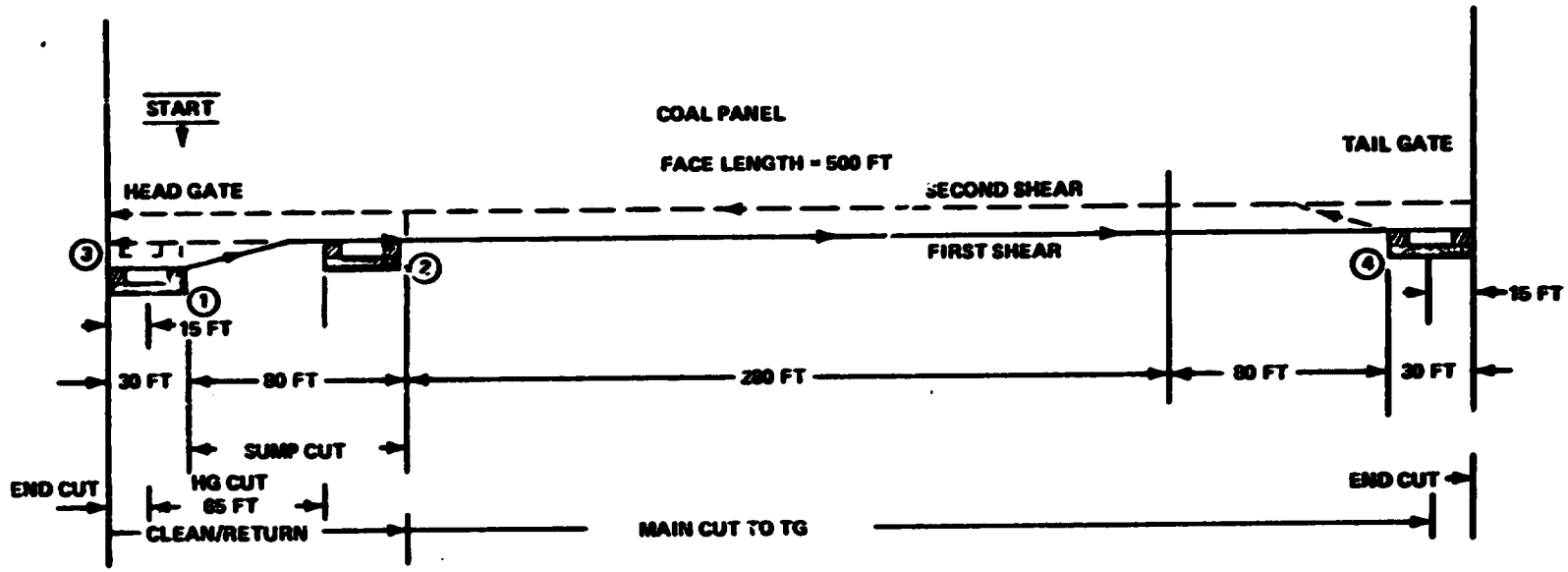

OPERATIONS SEQUENCE (ONE SHEAR)

- SHEARER CHECKOUT AND START-UP
- SUMP CUT AT HG = 80 FT AT 10 fpm
- TURNAROUND – SUMP (2 DRUMS)
- HG CUT = 65 FT/Vh
- END CUT AT HG = 15 FT AT 5 fpm
- TURNAROUND – HG (2 DRUMS)
- CLEAN AND RETURN = 2 280 FT/Vh + 50 = 160/Vh + 50
- MAIN CUT TO TG = 375 FT/Vh
- END CUT AT TG = 15 FT AT 5 fpm
- TURNAROUND – TG (2 DRUMS)
- REPEAT ABOVE OPERATIONS BUT IN OPPOSITE DIRECTION FOR NEXT SHEAR, STARTING WITH "SUMP CUT AT TG"

Figure 98. Longwall Model B (full-face or double-shear method).

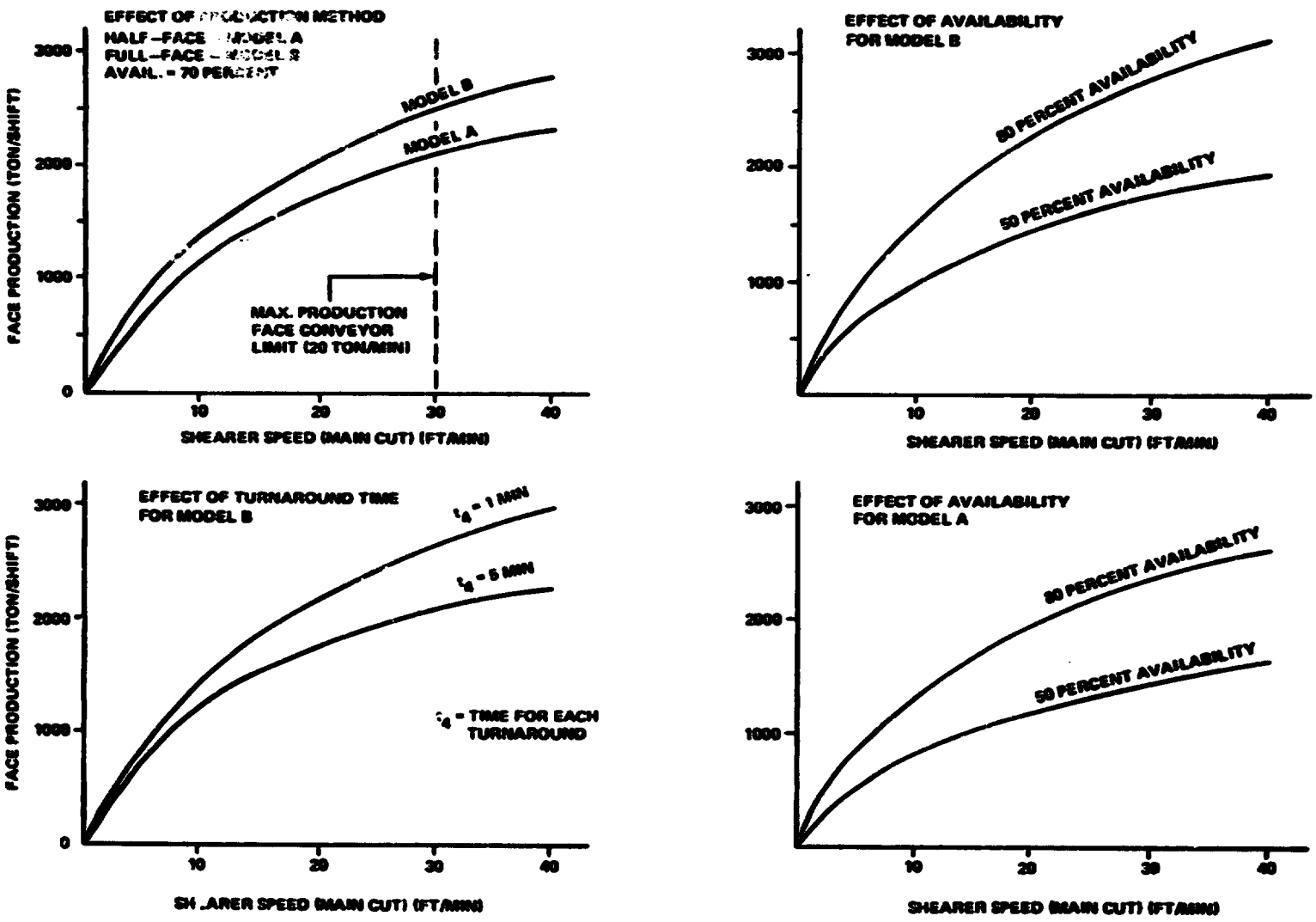

Figure 99. Longwall face production versus shearer speed.

(c) The face production and cost models further indicate the necessity of high equipment reliability and the importance of minimizing down time. For example, the 2500 tons/shift rate utilized in this study is obtainable on a routine basis only if equipment availability of 70 percent can be realized. This equates to a shearer utilization (percent of available work time on face when shearer is actually cutting coal) factor of 52 percent versus 40 percent or less now commonly encountered. The effect of machine availability (time when equipment is not down for maintenance or repair) can be seen in Figure 97. Automation in itself may be able to eliminate some of this down time caused by such problems as misaligned face, inadequate roll control (where shearer tends to climb up and out of seam during advance) and high pick maintenance. However, this will require a guidance and control system which is reliable, does not require much maintenance and is easy to operate.

(d) Figure 99 also shows the effect of shearer turnaround time on face production. A turnaround time of 2 min at each end of the cut was assumed for the baseline case. By further reducing turnaround time, additional gains could be made in production rate. Automating the turnaround might accomplish this; however, trade-off studies will be necessary to further assess this potential versus additional cost or complexity.

(e) For a face production rate of 2500 tons/shift, the cost per ton of coal could be reduced by approximately 20 percent, as shown in Figure 100. The reduction comes from (1) with a 2500 ton/shift/face capability only one-half

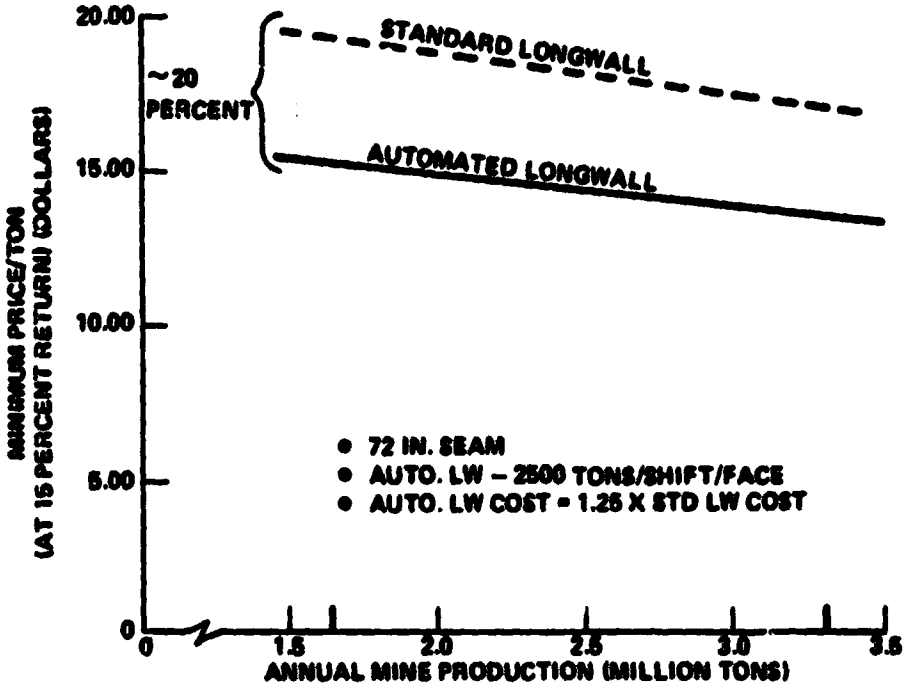

Figure 100. Potential reduction in cost of prepared coal with automated longwall face.

the number of operating longwall faces would be required to achieve the same annual mine output (million tons/year), (2) lower overall percentage of waste material in the coal, and (3) some increased recovery of coal from the seam. Cost calculations were based on the data presented in Bureau of Mines publications 1C8715 and 8720 and information supplied by the Jet Propulsion Laboratory. For this example, the net difference in the cost of coal was approximately $4/ton of processed coal or approximately $2/ton for the ROM (run-of-the-mine) output. Most of the savings in ROM coal came from a reduction in the initial and deferred capital required with less number of longwall faces. Of the factors affecting the net price per ton for processed coal, the effect of the percentage of rock or waste in the coal is quite significant. The assumptions as to the longwall contribution to ROM contamination levels used in this study were based upon the field survey data by Arthur D. Little, Inc., June 1977, for the Bureau of Mines, available literature, and MSFC's VCS simulation studies. This information indicates that it should be possible to reduce rock contamination levels currently experienced with the use of automated drum control and that control system requirements to produce cleaner coal should be further emphasized. Improvement in contamination levels will require further study. However, even if there were no improvement in current contamination levels, a significant price reduction on the order of 15 percent is still realizable from the other factors.

(f) Figure 101 shows that beyond a rate of 2500 tons/shift, there appears to be a decreasing cost advantage as the curve tends to flatten around 3000 tons/shift; therefore, for the 72 in. seam case, it would appear that most of the benefits from increasing face production can be realized with the capacities of currently available equipment.

(g) The increased equipment cost associated with automating and improving the reliability of the longwall equipment and its effect on the price of coal were considered. The specific costs of the guidance and control system or other longwall modifications required are not currently known; however, for these studies a factor of 1.25 times a standard longwall cost[7] was used for the cost of an automated longwall system, which equates to a 1.1 percent increase in price/ton at 2500 tons/shift/face or a 2.5 percent increase at 890 tons/shift/face. It can be seen from Figure 102 that the additional costs for automation would have to be considerably higher than this before significantly off-setting economic gains from increased production and cleaner coal. This also suggests that additional cost to obtain better equipment reliability and lower maintenance schedules would be quite cost effective at the higher production rates for many situations. A detailed cost optimization or a trade-off analysis would be required for any given mine situation.

7. Standard longwall cost used for a 72 in. seam was approximately $3 270 000/face.

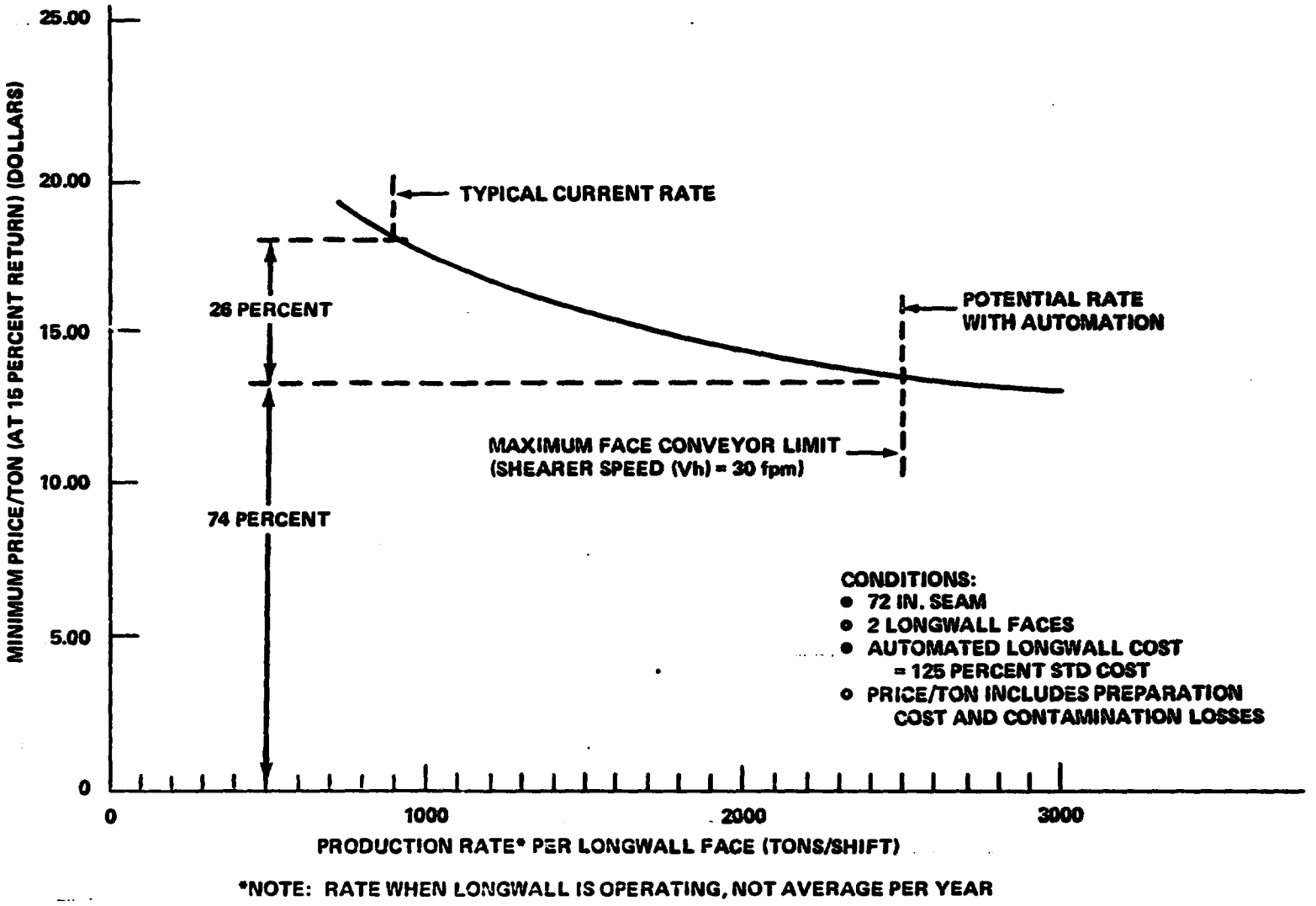

Figure 101. Automated longwall shearer — effect of increasing face production rate on cost of coal.

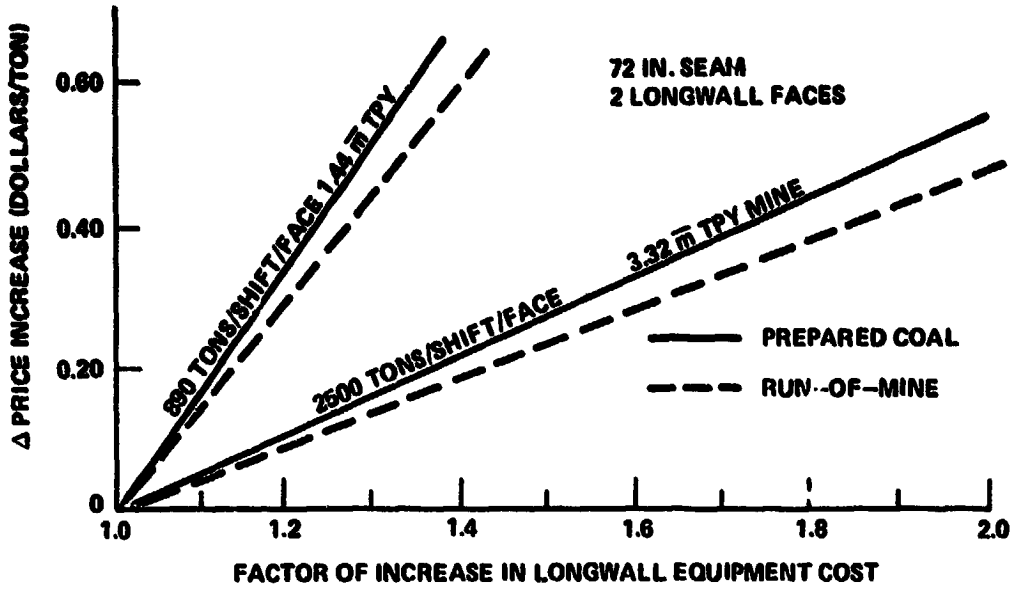

Figure 102. Effect of increasing longwall equipment cost on cost of coal.

Further results and details of these studies will be available under separate cover, when completed.

6.2 Floor Cut Control

The development of a roof CID has received the most attention in this program, principally because it is used in a simpler situation than the floor CID, i.e., less water and debris. Because of these complications to floor sensing, an alternative to direct floor sensing has been under investigation. A preliminary investigation was conducted on the feasibility of cutting coal to a constant height, with the height being measured from the cut roof. That is, a roof CID is used to cause the lead drum to cut within a prescribed distance of the roof interface and then the following drum is made to cut a constant distance from the roof cut.

One way this can be done is to store the lead drum elevation as a function of downface distance so that when the floor drum is at a given distance down the face, its elevation is determined by that which the roof drum had at that distance. This technique requires the measurement and storage of position and elevation data.

Another, and possibly simpler, way is to sense the distance from the rear drum to the roof cut, and control the rear drum accordingly. If the distance is sensed from the chassis to the cut roof, an error can arise if the shearer has changed its pitch attitude during the time it takes for the rear drum to occupy the corresponding position.

This error can be avoided if the distance is measured from the drum hub to the cut roof. In this case, the pitch attitude of the chassis has no effect.

The next problem is how to measure the distance from the drum hub (or in that vicinity) to the present cut. Mechanical and noncontact devices have been considered; either one will have to be offset laterally so that the present roof cut is accessible.

If radar (or acoustics) is used, there seems to be little problem in determining the reflection off the present cut and therefore the distance from the hub to the present cut. The radar unit will be mounted near the end of the ranging arm and therefore will be subjected to a harsh environment. Isolation is possible, however.

While the severity of the mine environment is recognized, a mechanical device has not been ruled out; in fact, in many respects, it is superior to non-contacting devices. If made sufficiently sturdy, it could be mounted in the vicinity of the hub (on the ranging arm near the hub) and could be made deployable. The probe could be made telescoping and the relative displacement between the sliding members used as a control signal. The form of the signal could be electrical as in a linear potentiometer, or it could be a hydraulic system.

An error is incurred if no provision is made to maintain the measuring probe at right angles to the cut roof, i.e., the probe maintains a fixed angle with the ranging arm. (Elevation or depression of the ranging arm changes the angle the probe makes with the present cut surface.) However, simulation shows that the error is insignificant.

In the simulation it was assumed that a mechanical probe was used that had a plate which pressed against the present cut, and that the response of the ranging arm was instantaneous. The results showed that suitable slaving of the rear drum was achievable.

The present-cut follower could also be used as a last-cut follower by appropriate positioning (probably a rotation and retraction).

6.3 Radar Use for Fault Detection

An investigation was undertaken during the course of testing the monocycle radar. This investigation was an experimental determination of the effects of cracks in an otherwise homogeneous medium. The set-up consisted of illuminating a cinderblock wall with the radar. The cinderblock wall was 9.3 cm thick. A second cinderblock wall was constructed parallel to, and directly behind, the first and could be moved from a position directly adjacent to the front wall to any desired position behind it (Fig. 103).

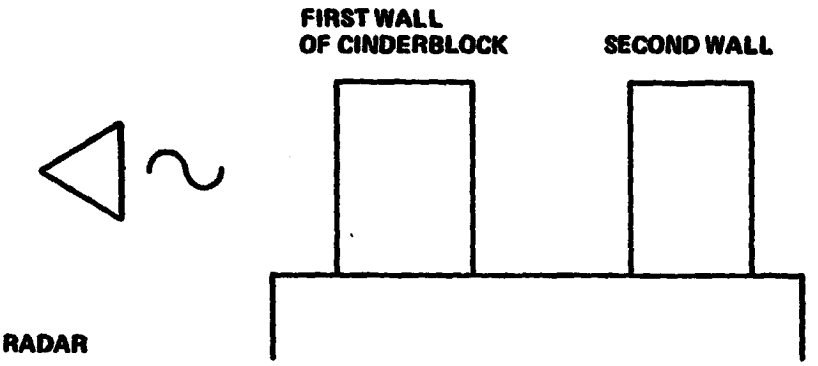

Figure 103. Test arrangement.

Figure 104 shows a radar signal consisting of the transmit pulse, A; the reflection from the front face of the cinderblock, B; and the reflection from the backface of the cinderblock, C, of a single wall. To verify the identification of these locations, the second wall was shoved against the first wall, with the result shown in Figure 105. Note that the signal at C is no longer at the same position, but has shifted to the right to a position twice the distance from B, indicating the double thickness. The interface of the two cinderblocks is not discernible with any confidence.

Figure 106 shows the cinderblocks separated by approximately 3 mm. It is apparent that the interface between the two blocks is now emerging. Figure 107 shows this more strongly for a 6 mm separation, where the backside of each block is shown at C and D. Figure 108 shows a 2 cm separation. The predominance of the signal at C remained for all separations greater than 2 cm. Figure 109 shows the return for a separation of 4 cm.

These results suggest the possibility of using monocycle radar for fault detection.

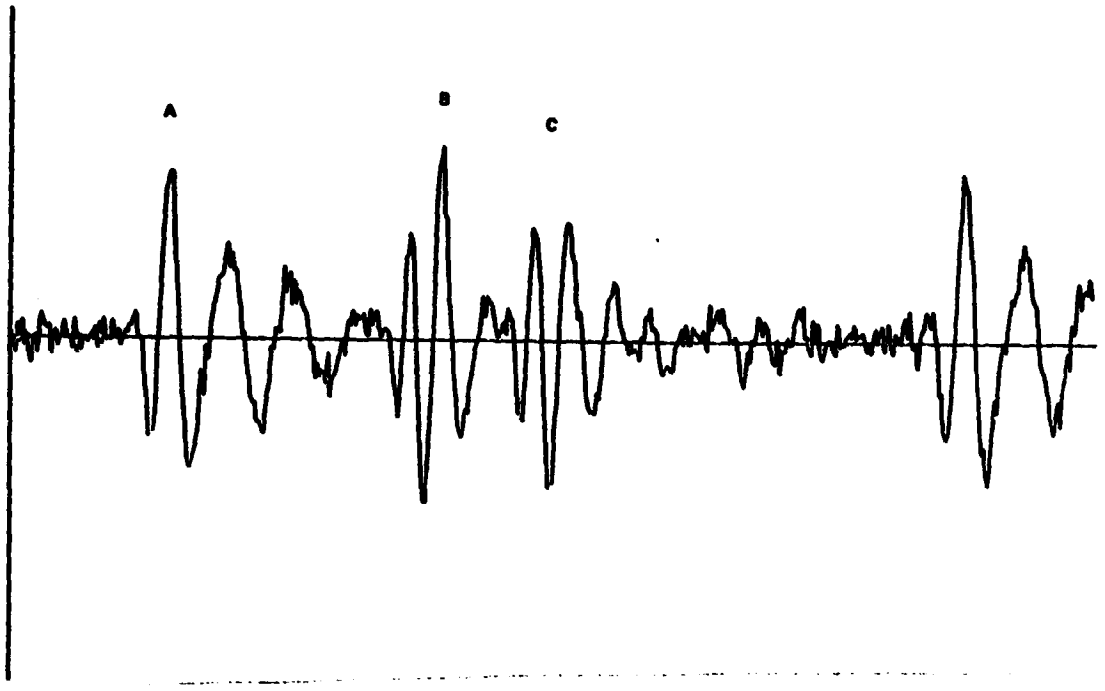

Figure 104. Radar signal return from single cinderblock target (9.3 cm thick).

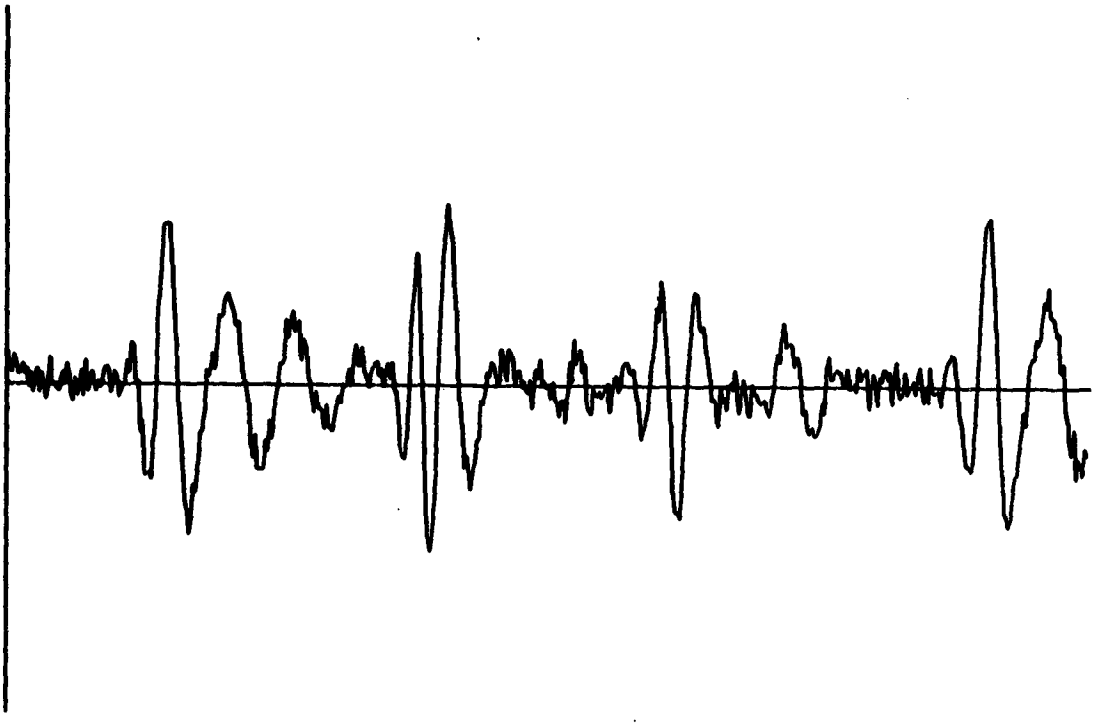

Figure 105. Radar return signal, two adjacent cinderblock targets.

Figure 106. Radar return signal, two cinderblock targets (separation: 4 cm).

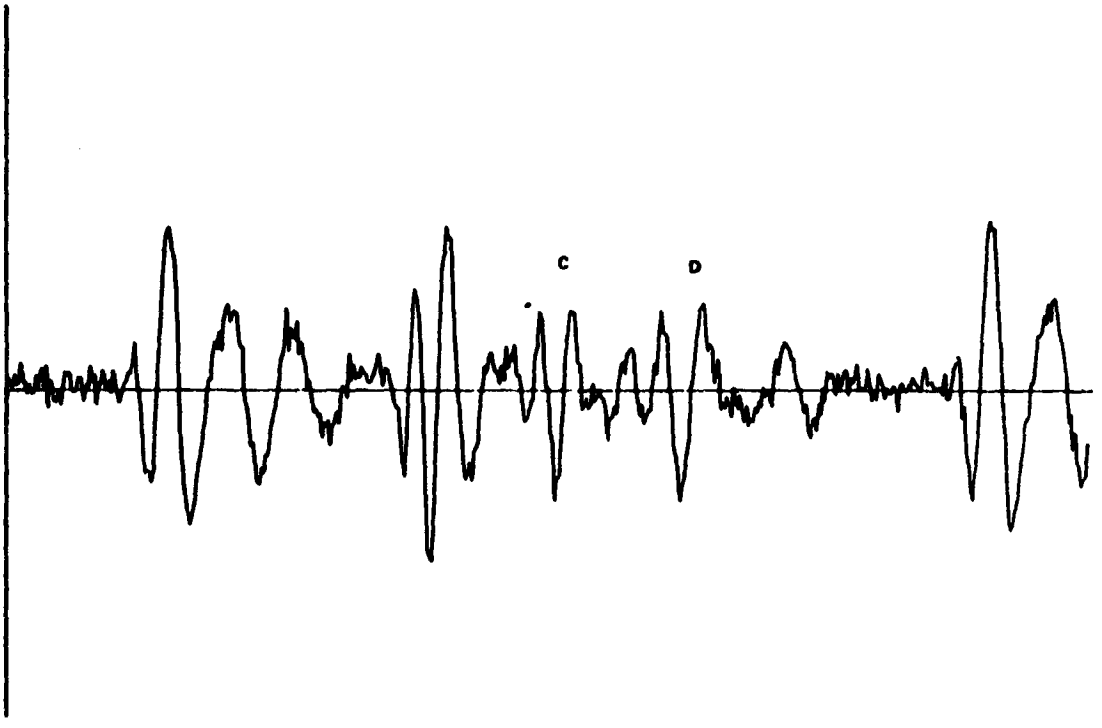

Figure 107. Radar return signal, two cinderblock targets (separation: 6 mm).

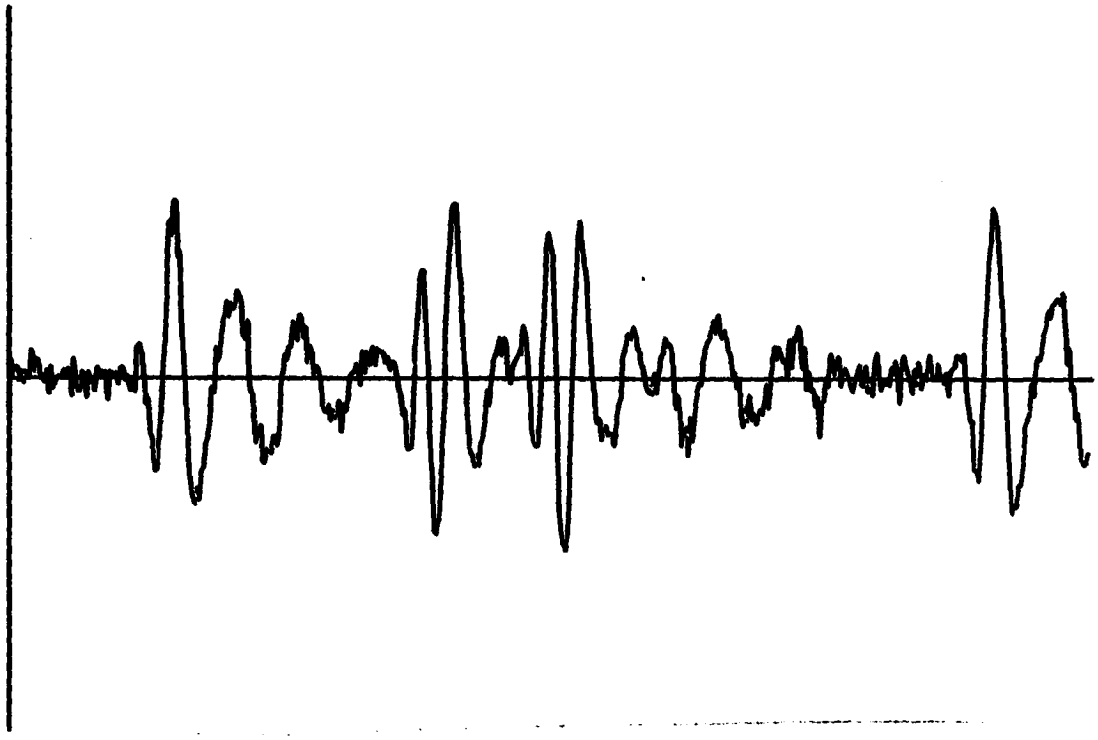

Figure 108. Radar return signal, two cinderblock targets (separation: 2 cm).

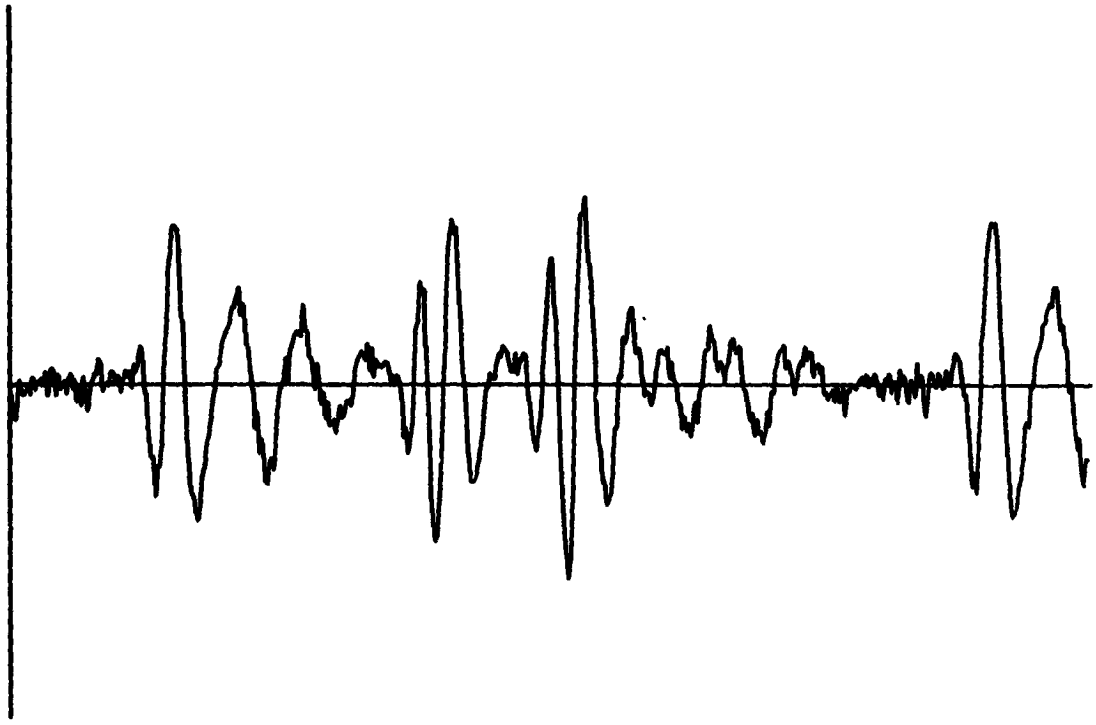

Figure 109. Radar return signal, two cinderblock targets (separation: 4 cm).

APPENDIX

ANALYSIS OF OCTOBER 1977 BRUCETON MINE DATA OF NATURAL RADIATION

RESULTS OF NATURAL RADIATION TESTS

The test data were analyzed to determine their statistical characteristics; however, because of the large amount of data, only a few configurations were analyzed extensively. These statistical analyses included histogram, chi-square goodness-of-fit tests, calculation of means and standard deviations, and tests for randomness.

STATISTICAL CHARACTERISTICS

Figure A-1 presents a histogram constructed from 300 readings. Superimposed is the corresponding normal distribution. A chi-square test of these data with both a Poisson and normal distribution showed that a better fit would have been obtained 40 percent of the time if sampled from a Poisson population and a better fit would have been obtained 60 percent of the time from a normal population. Other histograms showed this typical shape.

Since radioactive decay has long been used to illustrate Poisson processes in which the standard deviation is equal to the square root of the mean, the standard deviations for 31 tests (300 points per test) were plotted against their corresponding sample means (Fig. A-2). The trend is clear: the larger the mean number of counts, the greater the standard deviation.

A series of standard tests for randomness were run on some of the tests. In one such test, the 300 readings (in the sequence in which they were taken) were analysed for runs up and down, runs above and below the median, and the mean square successive difference. These tests are sensitive to lack of randomness in successive readings [11]. Table A-1 shows a comparison of the theoretical and actual number of runs up and down for 100 data points. Table A-2 presents a comparison of the actual results with theoretical results for runs above and below the median. Agreement is acceptable in both tests, with the actual number of runs of all length lying within one standard deviation of the theoretical average number of runs of all length.

Finally, the mean square successive difference test was applied to the data, and the agreement between actual and theoretical was good.

To further test independence of successive readings, 127 one second counts were made in the laboratory (Table A-3) where there was virtually no lapse between the intervals (2.2 μsec dead time between channels). The test was repeated using one-half second intervals (Table A-4). The results shown

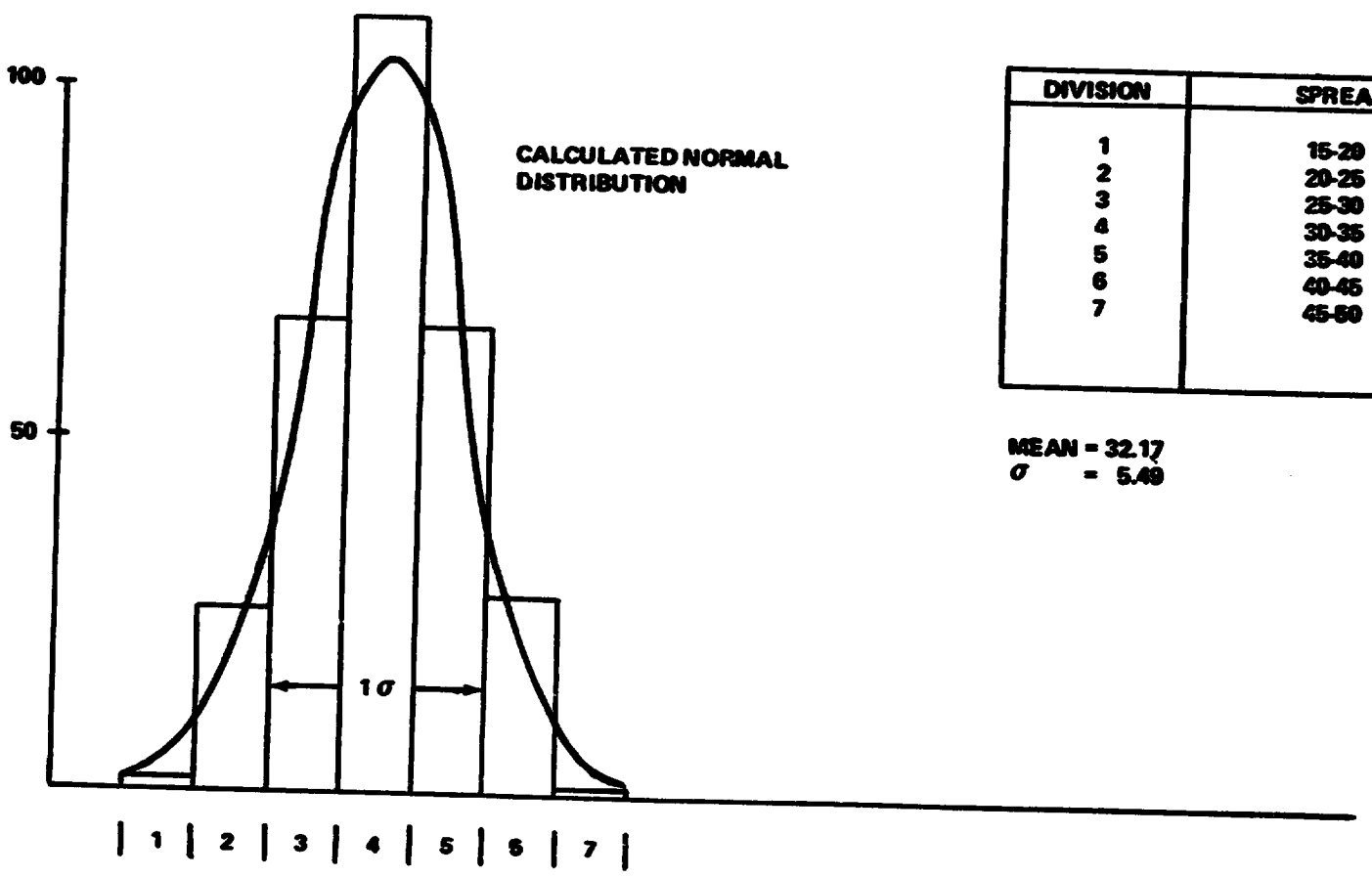

DIVISION	SPREAD
1	15-20
2	20-25
3	25-30
4	30-35
5	35-40
6	40-45
7	45-50

MEAN = 32.17
σ = 5.49

Figure A-1. Natural radiation histogram measurements of 8 1/2 in. of coal, illustrating normal distribution of data.

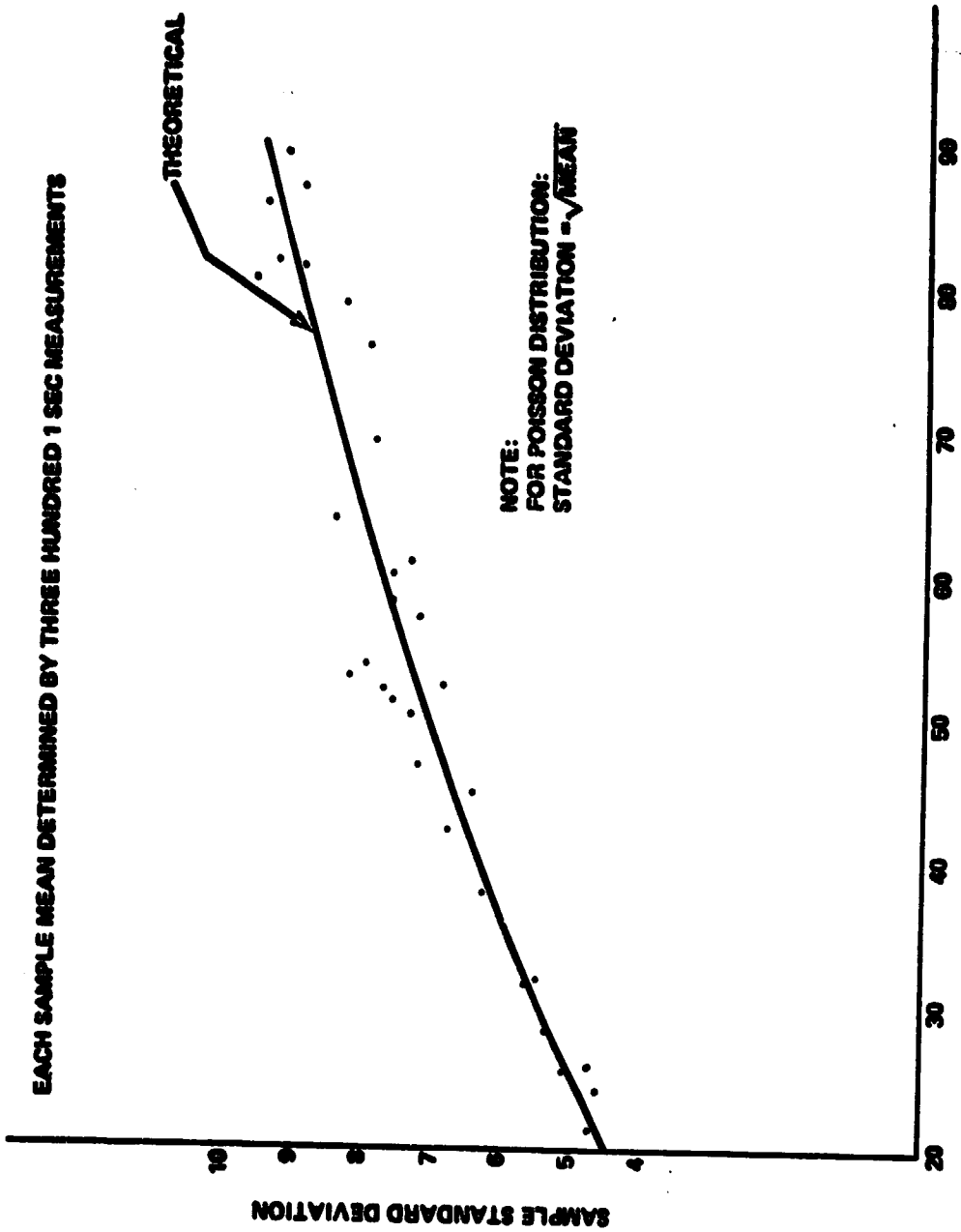

Figure A-2. Sample standard deviation versus sample mean.

TABLE A-1. COMPARISON OF RESULTS FOR RUNS UP AND DOWN

Measurement	Values	
	Actual	Theoretical
Runs of All Length	62	66.3
Runs of Length One	38	41.92
Runs of Length Two	17	17.6
Runs of Length Three	6	5.77
Runs of Length Four or More	1	1.33
Standard deviation of 12 runs of all length = 3.29		

TABLE A-2. COMPARISON OF RESULTS FOR RUNS ABOVE AND BELOW THE MEDIAN

Number of Runs of All Length		Values	
		Actual 46	Theoretical 51
Test 1	Length 1	11	12.5
	Length 2	4	6.25
	Length 3	4	3.12
	Length 4	1	1.56
	Length 5	3	1
Test 2	Length 1	12	12.5
	Length 2	3	6.6
	Length 3	3	3.12
	Length 4	2	1.56
	Length 5	3	1
Standard deviation of runs of all length = 4.97			

TABLE A-3. TEST RESULTS OF 127 ONE SECOND COUNTS IN LABORATORY (RUNS UP AND DOWN)

Measurements		Values	
		Actual	Theoretical
Runs of All Length	Test 1	92	84.33
	Test 2	88	
	Test 3	87	
Runs of Length 1	Test 1	64	53
	Test 2	56	
	Test 3	58	
Runs of Length 2	Test 1	24	23.05
	Test 2	22	
	Test 3	23	
Runs of Length 3	Test 1	3	6.57
	Test 2	9	
	Test 3	4	
Runs of Length 4	Test 1	1	1.42
	Test 2	1	
	Test 3	0	

Standard Deviation of Runs of All Length = 4.71
Three tests each comprising 127 consecutive 1 second intervals

TABLE A-4. TEST RESULTS OF 127 ONE-HALF SECOND COUNTS IN LABORATORY (RUNS UP AND DOWN)

Measurements	Values	
	Actual	Theoretical
Runs of All Length	81	84.33
Runs of Length 1	45	53.00
Runs of Length 2	29	23.05
Runs of Length 3	6	6.57
Runs of Length 4	1	1.42

Standard deviation for Runs of All Length = 4.71
127 consecutive 1/2 second readings

in Figures A-3 and A-4, show no indication of dependence of one value on the preceding value. The mean square successive difference tests showed entirely reasonable values for the test statistic (approximately a 23 percent chance that the statistic would have had a greater deviation for a random process).

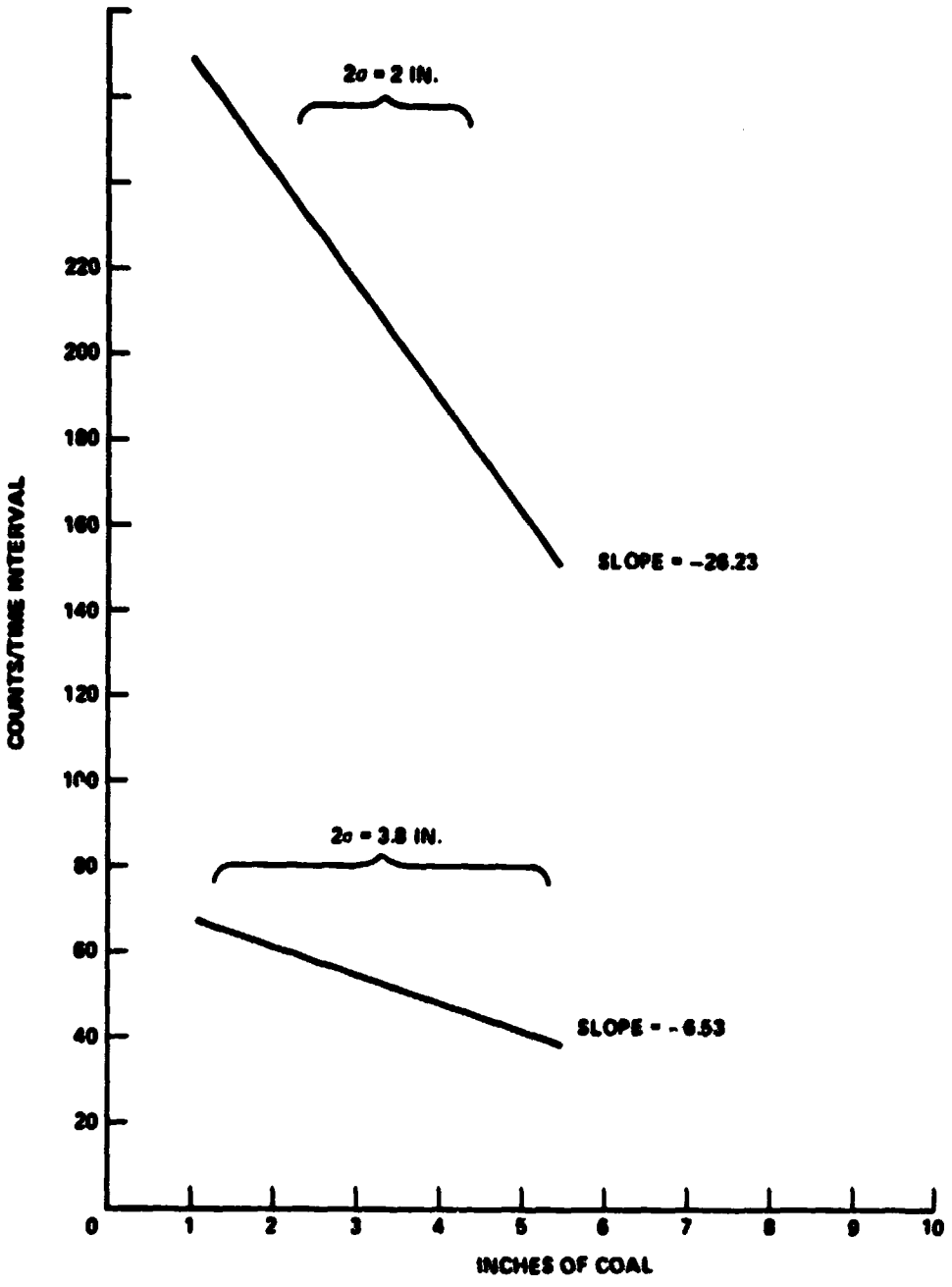

Figure A-3. 2σ limits for measuring 3 1/4 in. coal using 1 sec counts and 4 sec counts.

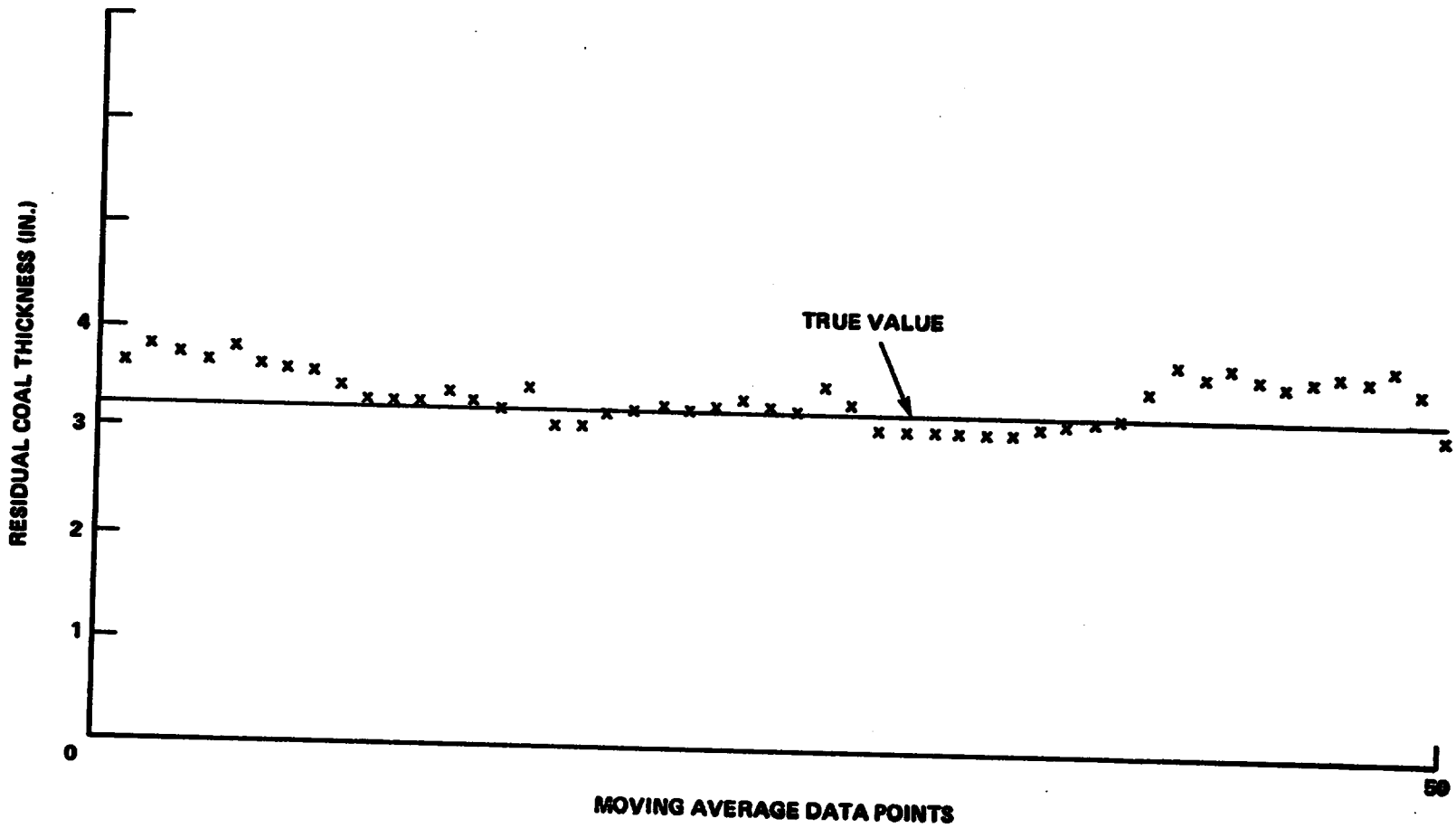

Figure A-4. Natural radiation measurements moving average of 10 points showing variations around a true measurement of 3 1/4 in. of coal.

COAL DEPTH MEASUREMENTS USING NATURAL RADIATION

Surfaces were prepared on the roof and floor of the Bruceton test area. At each prepared surface, a total of 300 one second counts were made. As explained earlier, the coal thickness was measured in a shielded and unshielded configuration. Figure 16 shows the average of 300 readings taken at each coal thickness on the ceiling. The solid line is a least square quadratic fitted to these points for both cases.

Figure 17 shows the tests performed on the floor. Except for the unshielded case on the floor, the curves are close to each other in shape as judged by the coefficients of the first and second powers of X.

The large number of measurements taken for each coal depth allows close estimates to be made of the population mean and standard deviation. The 99 percent confidence limits are shown in Table A-5.

TABLE A-5. 99 PERCENT CONFIDENCE LIMITS FOR ROOF MEASUREMENTS, SHIELDED

Inches of Coal	Sample Mean	Sample Standard Deviation	Population Mean, μ	Population Standard Deviation, σ
0	86.51	9.25	$85.12 = \mu = 87.89$	$8.36 = \sigma = 10.32$
2 3/4	60.21	7.59	$59.07 = \mu = 61.35$	$6.86 = \sigma = 8.48$
3 1/4	52.30	6.91	$51.26 = \mu = 53.34$	$6.24 = \sigma = 7.72$
4 1/2	44.67	6.47	$43.7 = \mu = 45.64$	$5.85 = \sigma = 7.22$
6 1/4	32.72	5.62	$31.87 = \mu = 33.56$	$5.08 = \sigma = 6.275$
8 1/2	32.17	5.49	$31.35 = \mu = 32.99$	$4.96 = \sigma = 6.13$
10 1/4	25.77	4.72	$25.06 = \mu = 26.48$	$4.27 = \sigma = 5.27$
11	28.49	5.32	$27.69 = \mu = 29.29$	$4.81 = \sigma = 5.94$

Accuracy can be increased by increasing the number of counts. It can be shown that if the counts, for a given coal depth, are increased by a factor K, then the standard deviation of the depth of coal being measured is decreased by a factor of 1/K. This is based on a straight line approximation to the curve over a small region. This reduction in coal depth error is illustrated in Figure A-3

for a measurement of 3 1/4 in. of coal based on 1 sec and 4 sec counts of data in Figure A-4. Note that while the standard deviation of the 4 sec count point is greater than that of the 1 sec count curve, a reduction in error is achieved because the slope of the former is steeper than that of the latter (-26.43 versus -6.52).

In an effort to reduce the dispersion of the coal depth measurements, a moving average was calculated for the shielded ceiling data for a coal depth of 3 1/4 in. This is equivalent to an experiment wherein a 3 1/4 in. slab of coal is being measured by a moving sensor at the rate of one measurement per second. Each point (1 sec separation between points) shown is the average of the last 10 data points. It can be seen that the error in coal depth measurement does not exceed 1/2 in. when using this method (Fig. A-4).

REFERENCES

1. The Development of Automated Longwall Shearer: Final Report — March 1975 through September 30, 1976. ALW-7, U.S. Department of Interior, Bureau of Mines.

2. Quarterly Progress Report, January — March 1977. ALW-9, U.S. Department of Interior, Bureau of Mines.

3. Nucleonic Coal Detector with Independent, Hydropneumatic Suspension. Final Report for MSFC/NASA Contract No. NAS8-32214.

4. Ferrier, E. J. and Field, J. D.: An Automatic Sensing and Guiding System for Coal Extraction Machines. EMI Electronics, Limited, Middlesex, England.

5. Roepke, W., Lindroth, D. P., and Myren, T. A. A.: Reduction of Dust and Energy During Coal Cutting Using Point-Attack Bits. Bureau of Mines, RI 8185, 1976.

6. Warner, E. M.: Cable and Wireless Remote Control of Continuous Miners. Joy Manufacturing Company, published in Mining Congress Journal, October 1974.

7. Cook, John C.: Radar Transparencies at Mines and Tunnel Rocks. Ensco, Inc., Springfield, Virginia, November 12, 1974.

   Cook, John C.: A Study of Radar Exploration of Coalbeds. Technical Report 71-8, June 1971.

8. Swindall, Paul: Dielectric Measurements of Coal, Brick and Cement Block at 3 and 5 GHz. Marshall Space Flight Center, Alabama, Internal Note, September 1975.

9. Lundien, J.: Terrain Analysis by Electromagnetic Means: Laboratory Measurement of Electromagnetic Propagation Constants in the 1.0 to 1.5 GHz Microwave Spectrum. Technical Report 3-693, February 1971.

10. Von Hipple, A.: Dielectric Materials and Applications. Technology Press of MIT and John Wiley and Sons, New York, 1954.

11. Hald, A.: Statistical Theory with Engineering Applications. John Wiley and Sons, New York, 1952.

☆ U.S. GOVERNMENT PRINTING OFFICE 1979—640-081/365 REGION NO. 4